CHEMISTRY HALL LIBRARY

BULLETIN
OF THE
CHEMICAL SOCIETY OF JAPAN

Vol. 33 No. 7 July 1960

OHIO STATE UNIVERSITY
AUG 26 1960
LIB... ...Y

CONTENTS

General and Physical

C. MIYAKE: Magnetic and Spectrophotometric Studies on Decoloration of Thiocyanato Iron(III) Complexes in Solutions. I. 867

M. EBATA: Effect of Temperature on the Viscosity and the Optical Rotation of Poly-ε-aminocaproyl-α-alanine 899

T. KOBAYASHI, Y. TANIZAKI and N. ANDO: Absorption Spectra of Dyes. VI. Steric Effects in Conjugated Systems of Benzidine Disazo Dyes and their Copper Derivatives 913

A. KUBOYAMA: π-Electronic Structure of Diphenoquinone 917

H. SHIMIZU and S. FUJIWARA: Harmonic Oscillator Model for the Analysis of NMR Spectra of Di-substituted Benzenes 920

Y. KUBOKAWA: Chemisorption of Hydrogen on Zinc Oxide. III. The Effect of Additions of Foreign Ions to Zinc Oxide 936

H. SUZUKI: The Ultraviolet Absorption Spectra of Stilbene and Some Related Compounds in the Solid State Measured by the Pressed KCl Disk Technique 944

K. MORIGAKI, K. KUWATA and K. HIROTA: Paramagnetic Resonance of Radicals of Some Aromatic Vinyl Compounds. I 952

K. MORIGAKI, K. KUWATA and K. HIROTA: Paramagnetic Resonance of Radicals of Some Aromatic Vinyl Compounds. II 958

K. FUKUI, K. MOROKUMA, T. YONEZAWA and C. NAGATA: A Further Study of Simple LCAO MO Perturbation Treatment of Conjugated Molecules 963

Y. HORIKI: The Adsorption of Dye Mixtures by Cellophane Sheet. II. A Quantitative Discussion of the Adsorption of Dyes 974

Y. TANIZAKI: Dichroism of Dyes in the Stretched PVA Sheet. III. Direction of Absorption of Pinacyanol Iodide. 979

A. KISHIMOTO, E. MAEKAWA and H. FUJITA: Diffusion Coefficients for Amorphous Polymer and Water Systems 988

A. MIYAKE: On the Assignment of a Band at 727 cm^{-1} in Polyethylene Terephthalate 992

K. ISHIDA: Application of the Theory of Regular Solutions to Binary Phase Equilibria. I. Method of Application to Binary Liquid Equilibria 998

K. ISHIDA: Application of the Theory of Regular Solutions to Binary Phase Equilibria. II. Dependency of the Interchange Energy upon Temperature 1002

K. KAWAI and H. MURATA: Normal Vibrations and Thermodynamic Properties of Chromium and Molybdenum Hexacarbonyls. 1008

Analytical and Inorganic

S. K. DATTA: Rapid Determination of Thorium by Fluoride Titration Using Some Chromotropic Azo Dyes. 882

K. SAITO, S. IKEDA and M. SAITO: Separation of Radioactive Arsenic from Germanium Irradiated with Protons 884

S. TOBISAWA: Magnetic Susceptibilities of Sulfur, Selenium and Tellurium from Room Temperature to 1100°C 889

(Continued on inside cover)

Published by the Chemical Society of Japan

THE CHEMICAL SOCIETY OF JAPAN
(NIPPON KAGAKUKAI)

Founded in 1948

Successor to the former Chemical Society of Japan founded in 1878 and to the Society of Chemical Industry, Japan founded in 1898.

OFFICERS

Shoichiro NAGAI, *President*, Nihon University, Tokyo
Eiichi IWASE, *Vice-President*, Institute of Physical and Chemical Research, Tokyo
Wasaburo KIMURA, *Vice-President*, Nagoya University
Sojiro OKA, *Vice-President*, The University of Tokyo
Ichiro SAKURADA, *Vice-President*, Kyoto University
Hiroshi SOBUE, *Vice-President*, The University of Tokyo

BULLETIN OF THE CHEMICAL SOCIETY OF JAPAN

Editor: Yoshiyuki URUSHIBARA, The University of Tokyo, Tokyo
Assistant Editor: Saburo NAGAKURA, The University of Tokyo, Tokyo
Editorial Board:

Toshio ANDO	Ichiro MIYAGAWA	Tadashi SUEHIRO
Yoshié BANSHO	Masazumi NAKAGAWA	Kenzi TAMARU
Hidehiro GOTÔ	Koji NAKANISHI	Takeo WATASE
Yoshimasa HIRATA	Shigeo OKUMURA	Iwao YASUMORI
Kenichi HONDA	Kazuo SAITO	Tsuneo YOSHINO
Sunao IMANISHI	Naoyasu SATA	Koshiro YOSHIOKA

(*Continued from outside cover*)

K. NUKADA, K. NAITO and U. MAEDA: On the Mechanism of the Extraction of Uranyl Nitrate by Tributyl Phosphate. II Infrared Study 894

H. HAMAGUCHI, R. KURODA and R. NEGISHI: Quantitative Spectrochemical Analysis of Minor Elements in Silicates with Double Internal Standards 901

S. YAMADA, H. NISHIKAWA and R. TSUCHIDA: Spectrochemical Study of Microscopic Crystals. XXI. The Structure and Absorption Spectra of the Red and the Black Form of Nitrosopentammine-cobalt Salts. 930

M. MORI: On Some Dark-colored Chlorocuprates(I, II) and Related Compounds. I. The Method of Preparation and Some Properties 985

Organic and Biological

S. KIMURA: Synthesis of Dyes with the Neocyanine Structure Presented by Brooker, and Related Dyes. III. Condensation of 3-Ethyl-2-methylbenzothiazolium Iodide and Nitrosobenzene, and the Dyes Obtained from its Condensates. 872

S. KIMURA: Synthesis of Dyes with the Neocyanine Structure Presented by Brooker, and Related Dyes. IV. Structure of the Dyes Obtained by the Condensation of 3-Ethyl-2-methylbenzothiazolium Iodide with Nitrone or Anil Derivatives 875

S. KIMURA: Synthesis of Dyes with the Neocyanine Structure Presented by Brooker, and Related Dyes. V. Synthesis of the Brooker-type Dyes from the Anil of 3-Ethyl-2-formylbenzothiazolium Iodide 879

K. DOI: The Synthesis of 4-Aminotropone 887

S. ISHIDA: Polyethers. III. Polymerizations and Polymers of Some Substituted Ethylene Oxides. 924

E. MAEKAWA und Y. SUMIMOTO: Zur Darstellung von 3-Methylpolymethoxyphthaliden 941

Applied

N. OGATA: The Transition Polymerization of Acrylamide. I. On the Polymerization Condition and the Property of Polymer 906

Short Communications

M. INOUE, H. HITOMI, K. MIZUNO, M. FUJINO, A. MIYAKE, K. NAKAZAWA, M. SHIBATA and T. KANZAKI: Glumamycin, A New Peptide-type Antibiotic 1014

T. MATSUMOTO und A. ICHIHARA: Eine Neue Synthese des *cis*- und *trans* D, L-Desmethylmuscarins 1015

S. UMEZAWA and S. ZEN: Formation of Isoxazolecarboxylic Acids from α, β-Unsaturated α-Nitroesters 1016

T. ARAI and T. OGURI: Electrolytic Reduction of Benzaldehyde at a Mercury Cathode—Preparation of Dibenzyl Mercury. 1018

I. IWASAKI and T. OZAWA: Genesis of Sulfate in Acid Hot Spring 1018

K. HIROTA and T. HISANO: A Research on Isotopic Composition of Evolved Hydrogen Molecules with Special Reference to the Mechanism of Nickel Cathode 1019

Magnetic and Spectrophotometric Studies on Decoloration of Thiocyanato Iron(III) Complexes in Solutions. I

By Chie MIYAKE*

(Received August 20, 1959)

The reaction between iron(III) and thiocyanate ions has been studied in detail by many authors for more than 30 years. Despite the vast experimental data thus accumulated, no decisive conclusion seems to have been drawn as to the nature of the species which exist in the solutions. In 1953, reviewing all the reports ever published, S. Z. Lewin et al.[1] have shown the following series of equilibria as the basis upon which all of the experimental evidences can be correlated.

$$Fe^{3+} + SCN^- \rightleftharpoons FeSCN^{2+} \quad (1)$$

$$FeSCN^{2+} + SCN^- \rightleftharpoons Fe(SCN)_2^+ \quad (2)$$

$$Fe(SCN)_2^+ + SCN^- \rightleftharpoons Fe(SCN)_3 \text{ or } [1/2Fe_2(SCN)_6] \quad (3)$$

$$Fe(SCN)_3 + SCN^- \rightleftharpoons Fe(SCN)_4^- \quad (4)$$

and probably also:

$$Fe(SCN)_4^- + SCN^- \rightleftharpoons Fe(SCN)_5^{2-} \quad (5)$$

$$Fe(SCN)_5^{2-} + SCN^- \rightleftharpoons Fe(SCN)_6^{3-} \quad (6)$$

On the other hand, in the field of chemical analysis the color reaction between iron(III) and thiocyanate ions has long been used as a proof of the existence of iron(III) ions, as well as being used as the procedure of its quantitative determination. However, in the above-mentioned solutions there exists a gradual color change with time, which makes the quantitative measurements somewhat difficult. And indeed the explanation of this change itself is still in question. In 1952, Hiraki et al.[2] from the spectrophotometric measurements with a Dubosk spectrophotometer, reported that the fading of color is caused by the reduction of iron(III) to iron(II) by thiocyanate ions. If this reaction did exist, there should be a change of magnetic susceptibility of the solutions as the fading of color proceeds. Thus, the decoloration mechanism of the solutions is one of the most interesting subjects to be clarified in the field of magnetochemistry. In this paper were summarized the measurements of the magnetic susceptibility and the visible absorption spectra during the decoloration.

Experimental

Materials.—Iron solution: A given amount of Mohr's salt was dissolved in distilled water containing several drops of conc. sulfuric acid. Adding a small amount of hydrogen peroxide (30%) in order to oxidize iron(II) to iron(III), the solution was heated on a water bath to expel the excess of hydrogen peroxide. After cooling, the solution was diluted to exactly 0.05 M with distilled water.

Potassium thiocyanate: The reagent of analytical grade was dissolved and diluted to 0.5 M with distilled water. The solution obtained was completely colorless and its test by $\alpha\cdot\alpha'$-dipyridyl was also negative. Therefore, neither iron(III) nor iron(II) ions can exist in our prepared solution.

Hydrochloric acid: The hydrochloric acid was purified by distillation until it gave a negative test for iron.

Sample solution: The solution to be measured was prepared by adding a given amount of hydrochloric acid and potassium thiocyanate to the iron stock solution and then was diluted to the desired concentrations.

Measurements.—The magnetic susceptibility of the solutions was measured from time to time during the decoloration by the torsion magnetometer with fused silica[3].

Absorption spectra were determined by a Beckman Model DU Spectrophotometer. Matched 10 mm. silica cells with quartz 9.5 mm. thick were used; this gave an effective optical path of 0.5 mm.

Experimental Results

Magnetic Data.—The magnetic moments in Bohr magnetons for total iron in the solutions of thiocyanato iron(III) and thiocyanato iron(II) complexes are shown in Table I. The magnetic moment is calculated from the formula $\mu = 2.84\sqrt{\chi \times T}$ where χ is the susceptibility per gram atom of total iron in the solutions and T the absolute temperature[4]. Here, any magnetic interaction is neglected, since all of the solutions are magnetically dilute. Fig. 1 shows

* Present address, Nuclear Engineering Department, College of Engineering, Osaka University, Higashinoda, Miyakojima, Osaka.

1) S. Z. Lewin and R. S. Wagner, *J. Chem. Educ.*, **No. 9**, 445 (1953).

2) Y. Hiraki, K. Tamura and M. Katumi, *Sci. Repts. Saikyo Univ.*, **I**, 19 (1952).

3) H. Takaki, N. Kawai, C. Miyake and T. Morita, *J. Phys. Soc. Japan*, **13**, 629 (1958).

4) J. H. Van Vleck. "The Theory of Electric and Magnetic Susceptibilities", Oxford University Press, Oxford (1932), p. 282.

TABLE I. MAGNETIC MOMENTS OF IRON IN BOTH THIOCYANATO IRON(III) AND THIOCYANATO IRON(II) COMPLEXES N HYDROCHLORIC ACID SOLUTIONS*,**

Magnetic moment(Bohr magneton)	
Iron(III)	Iron(II)
5.92	5.45
5.91	5.46
5.91	5.44

* 0.05 M thiocyanato iron(III) complex, 0.12 N hydrochloric acid solution.
** All of the measurements were made fifteen minutes after the solutions were prepared.

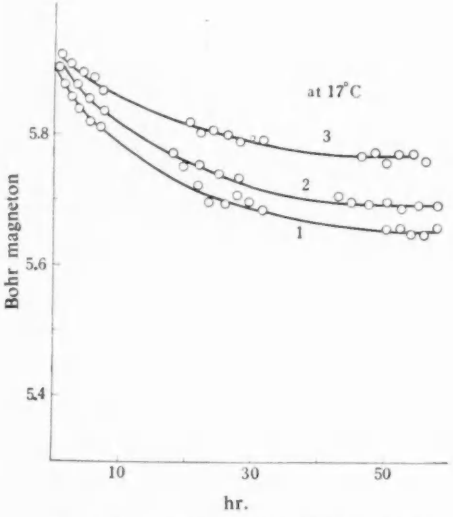

Fig. 1. Dependency of decrease in magnetic moment of iron upon concentration of hydrochloric acid. (0.005 M iron(III), 0.05 M thiocyanate ion solutions).
1: 0.012 N HCl 2: 0.12 N HCl
3: 1.2 N HCl

the decrease in magnetic moment of the solutions with varying concentrations of hydrochloric acid, when the amount of thiocyanate ions in the solutions are held constant. Fig. 2 represents the similar decrease with varying concentrations of thiocyanate ions.

Spectrophotometric Data.—Fig. 3 shows the spectral curve of thiocyanato iron(III) complexes and that of thiocyanato iron(II) complexes in hydrochloric acid solutions. Of all the present absorption measurements, some representative curves of thiocyanato iron(III) complexes with varying concentrations of thiocyanate ions are shown in Fig. 4. The maxima of the absorbance at about 470 mμ due to thiocyanato iron(III) complexes shift to the region of longer wave length. This bathochromic effect may be attributed to the increase

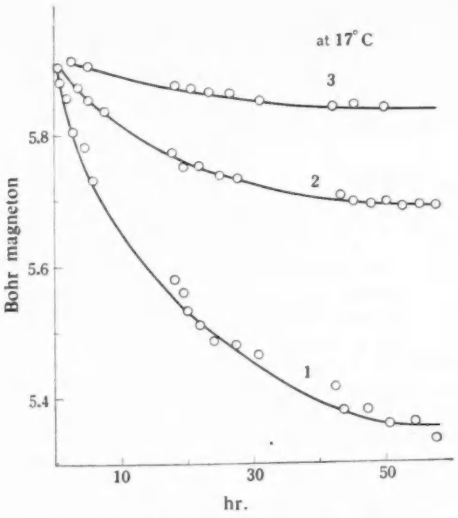

Fig. 2. Dependency of decrease in magnetic moment of iron upon concentration of thiocyanate ions. (0.005 M iron(III), 0.12 N hydrochloric acid solutions).
1: [Fe(III)]/[NCS⁻]=1:100
2: 〃 =1:10
3: 〃 =1:0.14

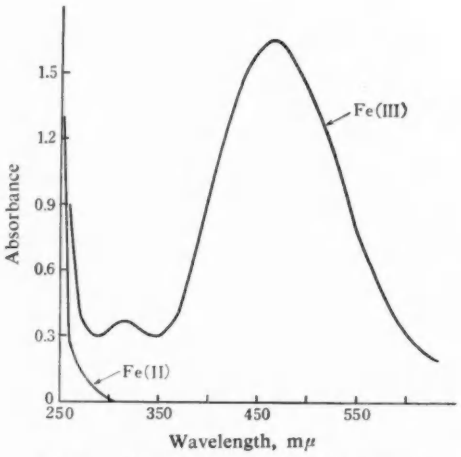

Fig. 3. Absorption spectra of thiocyanate iron(III) and thiocyanato iron(II) complexes in hydrochloric acid solutions.

in ratio of the number of coordinated thiocyanate ions to that of coordinated chloride ions. At the same time, the absorbances at the maxima increase with increasing concentrations of thiocyanate ions. The other absorption maxima at about 320 mμ are probably due to chloro iron(III) complexes as shown

TABLE II. EFFECTS OF CONCENTRATIONS OF BOTH HYDROCHLORIC ACID AND THIOCYANATE IONS TO ABSORBANCES AT ABOUT 470 mμ AND 320 mμ

	Increase of [NCS^-]	Increase of [HCl]
	Absorbance at about 470 mμ	
Wavelength of max. absorbance	bathochromic	constant*
absorbance	increase	decrease*
Rate of decrease in absorbance	increase	decrease
	Absorbance at about 320 mμ	
Wavelength of max. absorbance	bathochromic*	bathochromic
absorbance	decrease*	increase
Rate of decrease in absorbance	constant*	decrease

* The absence of notable effect.

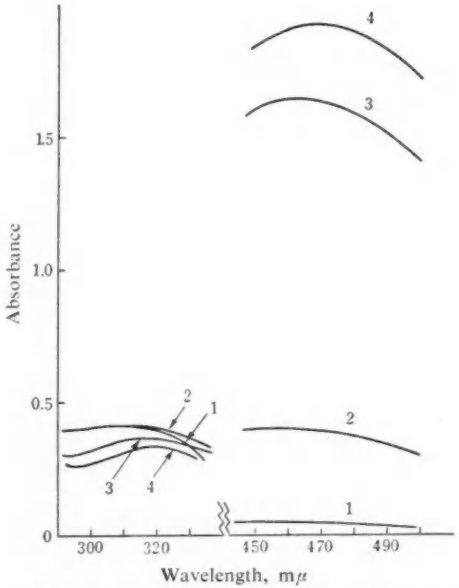

Fig. 4. Absorption spectra of thiocyanato iron(III) complex solutions with varying concentration of thiocyanate ions. (0.005 M iron(III), 0.12 N hydrochloric acid solutions).
1 : 0.0005 M, 2 : 0.005 M, 3 : 0.05 M, 4 : 0.7 M

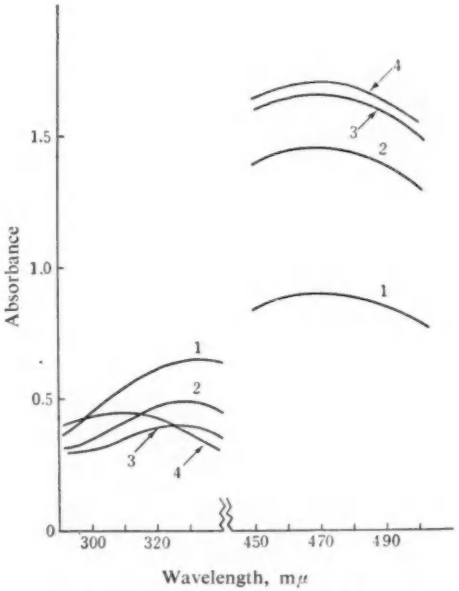

Fig. 5. Absorption spectra of thiocyanato iron(III) complex solutions with varying concentration of hydrochloric acid. (0.005 M iron(III), 0.05 M thiocyanate ion solutions).
1 : 3.6 N, 2 : 1.2 N, 3 : 0.6 N, 4 : 0.12 N

in Fig. 5.[5] In Table II, the results of spectrophotometric measurements are summarized. Here, it seems to be of importance for the following discussion to compare the time-change in magnetic moment (already shown in Figs. 1 and 2) and the similar change in absorbance at about 470 mμ (shown in Fig. 6).

Discussion

Before going directly into the discussion, the following remarks seem to be necessary.

The magnetic measurement is quite useful and important for determining the electronic spatial configuration in the complex containing transition element. For example, if the complex be assumed to have the inner orbital type of binding, then the 3d-electrons of iron(III) ion are necessarily paired, leaving only one residual electron to be unpaired, giving 1.7 Bohr magnetons (theoretical) to the complex. But on the other hand, when the complex has a binding of the so-called outer orbital type, all of the 3d-electrons of iron(III)

5) M. Ishibashi, T. Shigematsu, Y. Yamamoto, M. Tabushi and T. Kitagawa, This Bulletin, 30, 433 (1957).

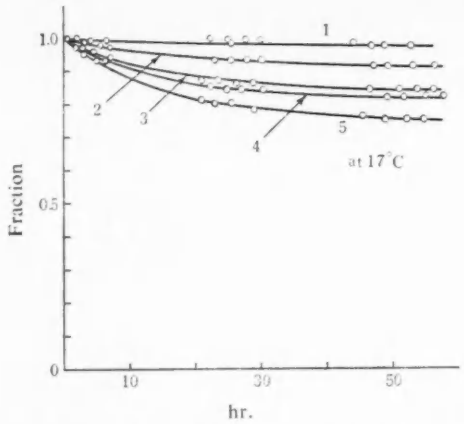

Fig. 6. Decrease of absorbances with time at about 470 mμ of ferric thiocyanate solutions.
1: corresponds to 3 in Fig. 2
2: 3 in Fig. 1
3: 2 in Figs. 1 and 2
4: 1 in Fig. 1
5: 1 in Fig. 2

ion are left unpaired, thus giving 5.9 Bohr magnetons (theoretical). In case of iron(II), the complex with the inner orbital type has no magnetic moment and that with the outer orbital type has 4.8 Bohr magnetons (theoretical), respectively. The number of unpaired electrons n of complex can generally be calculated from the magnetic measurements by the formula $\mu=\sqrt{n\times(n+2)}$.

The present magnetic observations which are shown in the preceding section and tabulated in Table I, show that thiocyanato iron(III) complex has five unpaired electrons and thiocyanato iron(II) complex four unpaired electrons, both belonging to the outer orbital type of binding. If the decoloration depends upon the simple reduction of iron(III) to iron(II) by thiocyanate ions, it is required that the magnetic moment decreases by 0.47 Bohr magneton and completely reduced solutions become colorless. This is evident from Fig. 3 in which it is shown that the iron(II) has no absorption in the region of visible light.

Although the magnetic data in Figs. 1 and 2 seem to support the idea that the above-mentioned simple reduction had actually been taking place, the spectrophotometric data are not favourable, because the absorbances at 470 mμ are still greater even after the decrease of the magnetic moment. In order to harmonize the above-mentioned discrepancy there must be another scheme by which all of the obtained data can be consistent. If we assume that the iron(II) ion already reduced in the solutions and the iron(III) ion still remaining were combined through the bridges of hydroxo ions, chloride ions or thiocyanate ions, and also that they were formed in the so-called "binuclear complex" or "dimer", whose unpaired electron is single, the reduction of the magnetic moment in solution and the amount of the remaining color may be plausible, despite the fact that a question still remains whether or not the free iron(III) ion and that combined into the dimer have the same absorbance character in the region of visible light.

The probable formula of the dimer is considered to be one of the following three types:

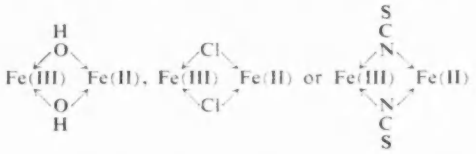

The study of the problem concerning the determination of the actual type existing in the present solutions must be continued. However, a series of reactions up to the above-mentioned formation of dimer, seems to be initiated in any way by the partial reduction of iron(III) to iron(II) as has already been stated. This argument is directly proved in Figs. 1, 2 and 6, which indicate that the solution with greater decrease in magnetic moment shows a greater decreases in absorbance. At the same time, we can say from the figures that both the decoloration and demagnetization with time proceed almost proportionally to the concentration of thiocyanate ions and inversely proportionally to the acidity of the solutions (hydrochloric acid). The acidity is generally considered to suppress the power of reduction of thiocyanate ions[6]. These tendencies are shown in Table II.

On the basis of the formation of the dimer which the present author has proposed, both the magnetic and spectrophotometric data are summarized in the following way. In the formation of the dimer which we supposed to have the inner orbital type of binding, five unpaired electrons of the original iron(III) ion and six electrons of iron(II) ion are paired with each other, leaving in the dimer only one unpaired electron. The number of the unpaired electrons thus reduced, hence the reduction of magnetic moment, is quite large. Therefore, we can say that the number of the originally unpaired electrons of $2\times$Fe(III),

6) G. Charlot, "L'analyse qualitative et les réactions en solution", Masson et Cie (1957), p. 334.

ten, are reduced and finally only one unpaired electron is left in the dimer.

Supposing that α-fractions of iron(III) in the original solutions are reduced to iron(II) and converted into the 1:1 dimer with iron(III), the final number of the unpaired electrons in the dimer is given by

$$5\times(1-2\alpha)+\alpha=5-9\alpha \qquad (1)$$

and the corresponding theoretical magnetic moment by

$$\{5.92^2\times(1-2\alpha)+1.73^2\times\alpha\}^{1/2} \qquad (2)$$

In the above relation only the spin contribution to the magnetic moment is taken into consideration and at the same time for simplicity's sake, the true equilibrium conditions in the formation of the dimer is ignored.

On the other hand, the spectrophotometric fractional absorbances of the solutions can be expressed by

$$\varepsilon\times(1-\alpha) \qquad (3)$$

where ε is the molar extinction coefficient. Here, the difference of the extinction coefficient between free iron(III) and iron(III) in the dimer are again neglected. The present results of measurements so far obtained seem to show a good agreement with the above relations (2) and (3).

Werbel et al.[7], in their results for the same substance using 0.06 M thiocyanato iron(III) complex in 1.9 M perchloric acid solution, have reported that the magnetic moment of 5.88 Bohr magnetons was obtained about one hour after its preparation and that about one percent of the total amount of iron(III) originally present was converted into iron(II). They have also pointed out that the magnetic moment of thiocyanato complex is too small to account for the reaction due to simple reduction from iron(III) to iron(II), because of the too small difference in magnetic moment between them. The result obtained by Werbel et al. seems, however, to be quite reasonably explained on the present consideration of the existence of dimer.

7) B. Werbel, V. H. Debeler and W. C. Vosborgh, *J. Am. Chem. Soc.*, 65, 2329 (1943).

Summary

The decoloration mechanism of thiocyanato iron(III) complex solutions was investigated by means of both the magnetic and spectrophotometric methods. The data for the magnetic measurements supported that the decoloration was caused by the simple reduction of iron(III) to iron(II) by thiocyanate ions. But such a simple model of the reduction was not favourable for the observed decoloration, because the decrease in the absorbance was too small, being only about twenty percent. In order to eliminate this discrepancy, another scheme was proposed, which ascribes the magnetic and spectral observations to the formation of a binuclear complex of iron(III) and iron(II), a so-called dimer, during the decoloring reaction. This dimer possesses only one unpaired electron and accordingly very small magnetic moment, but possesses the significant absorbance due to iron(III). On this model, the greater decrease in magnetic moment and the rather smaller decrease in absorbance which we obtained, were quite satisfactorily clarified.

The author wishes to express her sincere thanks first to Professor H. Takaki for his continuous encouragement and interest throughout the present work. She wishes to convey her sincere thanks to Dr. Y. Yamamoto whose advice and discussions were very fruitful in this experiment. The author's thanks are also tendered to professor M. Ishibashi, whose kind permission to use the Beckman spectrophotometer gave added value to her study.

Department of Chemistry
Faculty of Science
Kyoto University
Sakyo-ku, Kyoto

Synthesis of Dyes with the Neocyanine Structure Presented by Brooker, and Related Dyes. III. Condensation of 3-Ethyl-2-methylbenzothiazolium Iodide and Nitrosobenzene, and the Dyes Obtained from its Condensates

By Shiro KIMURA

(Received November 17, 1959)

The synthetic process for the "Brooker-type dyes" described in the preceding paper[1] could possibly be improved with regard to the yield and by-product formation. The present series of experiments was carried out in order to obtain some fundamental concept of this reaction. An attempt was first made to prepare the 2-aldehyde anil derivative I of 3-ethyl-2-methyl-benzothiazolium iodide by the condensation of 3-ethyl-2-methylbenzothiazolium iodide and nitrosobenzene. In accordance with the report Katayanagi[2], the condensation of 3-ethyl--2-methylbenzothiazolium iodide and nitrosobenzene was carried out in ethanol with piperidine as a condensation agent. The product of this reaction was obtained as dark purple-needle crystals, m. p. 213–214°C (decomp.) λ_{max} 390 mμ which became bluish purple prisms, m. p. 215°C (decomp.), when recrystallized from acetic anhydride. But this was not the expected anil I and was found to be a nitrone II.

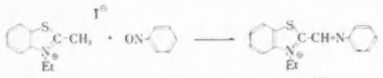

(I)

The basic condensation reactions of active methyl and nitroso compounds in general has been known from olden times as the Ehrlish-Sachs reaction[3]. It has been clarified in recent years that this reaction is accompanied by an oxidative reaction to form a nitrone as a by-product, besides the anil. It is also known that these two products are difficult to separate. The nitrone obtained in the present series of experiments was not completely pure and rather difficult to separate. When the impure nitrone was boiled with nitrosobenzene in ethanol, a dark purple substance was obtained which crystallized in reddish brown needles, m. p. 219°C (decomp.). Its analytical values were closer to those of the phenylnitrone. Then a mixture of 1 mol. of 3-ethyl-2-methyl-benzothiazolium iodide and 3 mol. of nitroso-benzene in ethanol was reacted with the addition of piperidine and reddish brown needles, m. p. 219°C (decomp.) were obtained. This was found to be pure nitrone II from its analytical values. The mechanisms of this reaction were shown by the following scheme:

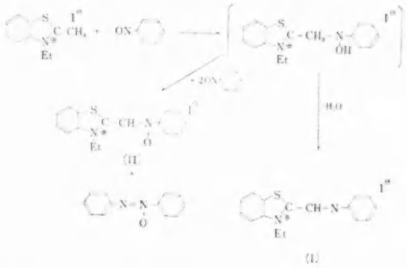

(II)

(I)

Synthesis of the phenylnitrone was also attempted with reference to the general method of synthesis by Kröhnke and others[4] for the phenylnitrone of 1-methyl-2-formylpyridinium iodide, and preparation of *N*-(3-ethyl-1-thia-3-azoniainden-2-ylmethyl) pyridinium diiodide was undertaken, but the product seemed to be labile and the objective was not attained.

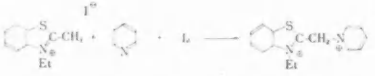

A purely synthetic preparation of the anil from heterocyclic ammonium salts has recently been reported by Mcgookin[5]. This process was applied to 3-ethyl-2-methylbenzothiazolium iodide and pure anil I of 3-ethyl-2-formyl-benzothiazolium iodide was obtained. In this case, equimolecular amounts of 3-ethyl-2-methylbenzothiazolium iodide and nitroso-benzene were reacted in absolute ethanol, with anhydrous potassium carbonate as the condensation agent, and red needles, m. p. 199°C (decomp.) were obtained.

(I)

1) S. Kimura, *Bull. Soc. Sci. Phot. Japan*, **9**, 45 (1959).
2) M. Katayanagi, *J. Pharm. Soc. Japan*, **69**, 38 (1949).
3) P. Ehrlich and F. Sachs, *Ber.*, **32**, 2341 (1899).
4) F. Kröhnke and H. Leister, ibid., **71**, 2583 (1938).
5) A. Mcgookin, *J. Appl. Chem.*, **5**, 65 (1955).

Similarly, condensation, of 3-ethyl-2-methylnaphtho[2, 1-*d*]-thiazolium iodide and nitrosobenzene afforded the anil III of 3-ethyl-2-formylnaphtho[2, 1-*d*]thiazolium iodide.

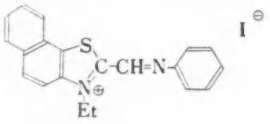

(III)

We then attempted the synthesis of 3, 3′-diethyl-2, 2′-vinylidendibenzothiazolium diiodide as a clue to the synthesis of "Brooker-type dyes", by the condensation of 3-ethyl-2-methylbenzothiazolium iodide with these nitrone derivative obtained above. Unexpectedly, however, this reaction was found to be much more complicated than was anticipated.

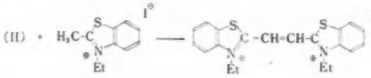

By refluxing an equimolar mixture of this phenylnitrone of 3-ethyl-2-formylbenzothiazolium iodide and 3-ethyl-2-methylbenzothiazolium iodide in pyridine for 30 min., a mixture of four kinds of dyes was obtained: the dyes were purified by fractional crystallization from acetone according to the scheme shown:

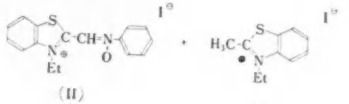

(II)

refluxed in pyridine for 30 min.
Et_2O added, and washed with water

Dark pinkish purple needles m. p. 141~150° with decomp. p. 181°C

Waste liquor

recrystallized from acetone

Tan needles with copper luster m. p. 255~256°C (decomp.)

Filtrate

concn.

Dark green crystals m. p. 243~245°C (decomp.)

Filtrate

concn.

recrystd. from MeOH

recrystd. from MeOH, then from acetone

Filtrate

recrystd. from MeOH

Copper-colored crystals. m. p. 265°C (decomp.) λ_{max} 580 mμ (VI)

Green needles m. p. 266°C (decomp.) λ_{max} 580 mμ (V)

Filtrate

concd.

Solid

recrystd. from MeOH

Bluish violet needles, m. p. 265°C (decomp.) λ_{max} 560 mμ (IV)

Dark tan crystal with copper luster, m. p. 187~194°C (decomp.)

Waste liquor

recrystd. from acetone then twice from MeOH

Dark brown crystals, m. p. 218°C (decomp.) λ_{max} 457 mμ (VII)

These dyes were also examined by paper chromatography and exactly the same four kinds of dyes were found to have been formed.

The structures of these four kinds of dyes

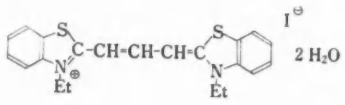

(IV)

were examined from their analytical values and absorption spectra and IV was identified with the known 3,3′-diethylthiacarbocyanine iodide dihydrate by comparison with the dyes prepared by a known route.

The analytical values of V were very close to those of the known trinuclear carbocyanine, 3, 3′-diethyl-9-(3-ethyl-2-benzothiazolinylidenemethyl)thiacarbocyanine iodide, but the absorption spectra and physical characteristics were entirely different and no presumption could be made of its structure. The analytical

values of VI suggested it to be a diiodide, and accordingly a trinuclear carbocyanine, 3,3'-dietyl-9-(3-ethyl-1-thia-3-azoniainden-2-yl)-thiacarbocyanine diiodide, was presumed. The dye with this structure had earlier been synthesized by Tanabe[6] who recorded the melting point of 85°C and λ_{max} 545 mμ, but these data are entirely different from those of VI and definite conclusion can be drawn. Its 8-substituted isomer was synthesized by Anish[7] and shwos entirely different physical properties.

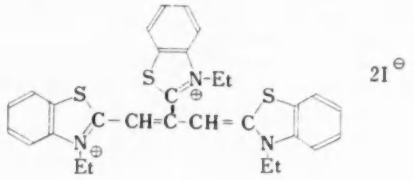

(VI)

VII was assumed to be a monomethine from its absorption spectrum and analytical values suggested the structure of a trinuclear monomethinecyanine, 3,3'-diethyl-8-(3-ethyl-2-benzothiazolinylidenemethyl)thiacyanine iodide monohydrate.

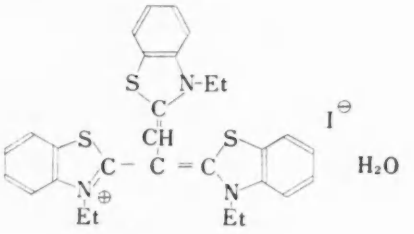

(VII)

Chemical evidences for the structure of these four dyes will be discussed in the following paper.

Experimental

Preparation of the Phenylnitrone II of 3-Ethyl-2-formylbenzothiazolium Iodide.—A solution of 50 g. of 3-ethyl-2-methylbenzothiazolium iodide and 18 g. of nitrosobenzene dissolved in 500 ml. of ethanol with warming on a water bath, added with 7 drops of piperidine, was stirred thoroughly and allowed to stand for about 2 hr. The dark purple crystals that separated out were collected by filtration, washed with water and methanol, and 21 g. (yield, 33%) of a dye, m. p. 156~164°C (decomp. at 174°C), was obtained. Recrystallization of this dye from 200 ml. of methanol afforded 7 g. (yield, 11%) of dark purple needles, m. p. 213~214°C (decomp.). Approximately the same result was obtained on repeating this experiment several times.

These dyes were boiled with about 40 volumes of acetic anhydride for 30 min. and the dark bluish purple prismatic crystals thereby formed were collected by filtration. After washing with ether the dye melted at 215°C with decomposition and its analytical value supported the nitrone structure.

Found: C, 46.56; H, 4.07; N, 6.62; I, 29.93. Calcd. for $C_{16}H_{13}ON_2IS$: C, 46.82; H, 3.66; N, 6.83; I, 30.98%.

Condensation of the Phenylnitrone II of 3-Ethyl-2-formylbenzothiazolium Iodide and 3-Ethyl-2-methylbenzothiazolium Iodide.—A solution of 6 g. of the phenylnitrone II of 3-ethyl-2-formylbenzothiazolium iodide and 4.8 g. of 3-ethyl-2-methylbenzothiazolium iodide in about 100 ml. of pyridine was refluxed for 30 min. and the major part of pyridine was distilled off under reduced pressure. About 100 ml. of ether was added to the residue, the dark purple crystals that precipitated out were washed with several 300 ml. portions of ether. The residue was mixed with 50 ml. of water, filtered, and the precipitate on the filter was washed with water. The dark pinkish violet crystals, m. p. 141~150°C (decomp. at 181°C) so obtained were dissolved in ca. 1 l. of acetone, concentrated to 400 ml., and 0.5 g. of dark tan crystals with copper luster, m. p. 255~256°C (decomp.) was obtained. Concentration of its mother liquor afforded 0.3 g. of dark green crystals, m. p. 243~245°C (decomp.). Further concentration of its mother liquor to about 50 ml. separated an oily substance which crystallized upon addition of ca. 50 ml. of ether. The crystals were collected by filtration and washed with ca. 30 ml. of ether, affording 0.4 g. of dark tan crystals with copper luster, m. p. 187~197°C (decomp.). These three kinds of crude dyes were purified through fractional crystallization and four kinds of pure dyes were isolated.

Purification of the Dark Tan Crystals, M. P. 255~256°C (Decomp.).—A solution of 0.5 g. of the crude dye dissolved in 50 ml. of methanol was concentrated to about 30 ml. and 0.35 g. of green needles, m. p. 260~262°C, separated. This substance was recrystallized twice from methanol to 0.18 g. of green needles V m. p. 266°C (decomp.) λ_{max} 580 mμ.

Found: C, 53.31; H, 4.06; N, 6.95; I, 20.53. Calcd. for $C_{28}H_{24}N_3IS_3$: C, 53.75; H, 3.84; N, 6.72; I, 20.25%.

The initial filtrate left after separation of the green crystals was concentrated and the copper-colored crystals m. p. 258°C (decomp.), so formed were recrystallized from methanol to clustered crystals VI m. p. 265°C (decomp.) λ_{max} 580 mμ.

Found: C, 45.80; H, 4.29; N, 5.22. Calcd. for $C_{30}H_{29}N_3I_2S_3$: C, 46.10; H, 3.70; N, 5.38%.

Purification of Dark Green Crystals, M. P. 243~245°C (Decomp.).—A solution of 0.3 g. of the crude dye dissolved in 60 ml. of methanol was concentrated to about 30 ml. and a mixture of green and bulish purple needle crystal was obtained. The green crystals were comparatively sparingly soluble in acetone and, therefore, the bluish purple crystals

6) Y. Tanabe, *J. Pharm. Soc. Japan*, **74**, 814 (1954).
7) A. W. Anish, U. S. Pat. 2,427,177 (1944).

dissolved out with 100 ml. of acetone, leaving 0.1 g. of green needles, m. p. 262°C (decomp.). The acetone solution was concentrated to 80 ml. and 0.05 g. of the same green crystals, m. p. 265°C (decomp.) separated. These green crystals were found to be identical with the dye V described above. The acetone mother liquor was concentrated to 20 ml. and 0.04 g. of bluish purple needles, m. p. 260°C (decomp.), was obtained. This was recrystallized from a small amount of methanol to 0.01 g. of bluish purple needles IV m. p. 265°C (decomp.) λ_{max} 560 mμ.

Found: C, 48.03; H, 4.55; N, 5.52; I, 25.61. Calcd. for $C_{21}H_{21}N_2IS_2 \cdot 2H_2O$: C, 47.70; H, 4.73; N, 5.31; I, 24.03%.

Purification of the Dark Tan Crystals with Copper Luster, M. P. 187~194°C (Decomp.).—A solution of 0.4 g. of the crude dye dissolved in 300 ml. of acetone was concentrated to 50 ml. and 0.3 g. of dark brown needles, m. p. 210~211°C (decomp.) was obtained. This was mixed with a small amount of bluish purple crystals which were removed and the rest was recrystallized twice from methanol to 0.12 g. of dark brown needles, VII, m. p. 218°C (decomp.) λ_{max} 457 mμ.

Found: C, 52.25; H, 4.55; N, 6.c9; I, 19.65. Calcd. for $C_{29}H_{25}N_3IS_3 \cdot H_2O$: C, 52.80; H. 4.55; N, 6.37; I, 19.28%.

Separation of Dye Mixture by Chromatography.—Instead of the fractional crystallization as described above, the precipitate obtained from the pyridine reaction mixture was purified through chromatography. A solution of 2 g. of this mixture was dissolved in ca. 200 ml. of acetone concentrated to about 100 ml. and allowed to stand overnight. About 400 ml. of acetone was added to this mixture to dissolve the crystals but sparingly soluble crystals V remained undissolved. The green crystals were removed by filtration, the filtrate was concentrated about 200 ml., and the solution was passed through a column of alumina (Merck), requiring about 1.5 hr., the adsorbed layers separated into pale orange, violet, and pink bands. Each of these bands was eluted with acetone, the acetone elute was concentrated, and separated crystals were recrystallized from methanol. Dark brown needles VII m. p. 216°C (decomp.) λ_{max} 457 mμ. were obtained from the pale orange band, green needles V m. p. 260°C (decomp.), λ_{max} 580 mμ, from the violet band, and bluish purple needles IV m. p. 267~268°C (decomp.), λ_{max} 560 mμ, from the pale pink band. The dye VI obtained by fractional crystallization, was not isolated from this chromatographic separation.

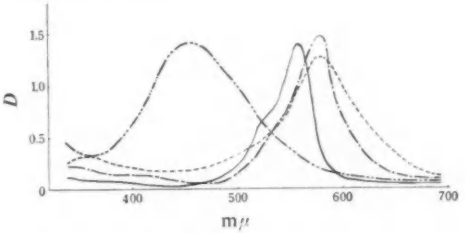

Fig. 1. Absorption spectral curves of IV, V, VI and VII (in ethanol).
—— (IV) —— (V) ---- (VI)
—— (VII)

Chemical evidences for the structure of these four dyes will be discussed in the following paper.

Research Laboratory
Fuji Photo Film Co. Ltd.
Minami-Ashigara-machi
Kanagawa-ken

Synthesis of Dyes with the Neocyanine Structure Presented by Brooker, and Related Dyes. IV. Structure of the Dyes Obtained by the Condensation of 3-Ethyl-2-methylbenzothiazolium Iodide with Nitrone or Anil Derivatives

By Shiro KIMURA

(Received November 17, 1959)

It has been shown in the preceding paper[1] that the condensation of phenylnitrone of 3-ethyl-2-formylbenzothiazolium iodide and 3-ethyl-2-methylbenzothiazolium iodide in pyridine gave four kinds of dyes and their structures were deduced from analytical values and absorption spectra.

In order to examine the formation process of these dyes, the anil I and 3-ethyl-2-methylbenzothiazolium iodide were reacted by refluxing for a short time (8~15 min.) in pyridine and, in this case, 3, 3-diethyl-9-(3-ethyl-1-thia-3-azoniainden-2-yl)thiacarbocyanine diiodide (VI) alone was obtained. This result shows that

1) S. Kimura, This Bulletin, 33, 872 (1960).

this dye VI is initially formed in the early stage of this reaction and its formation mechanism is considered to be as follows:

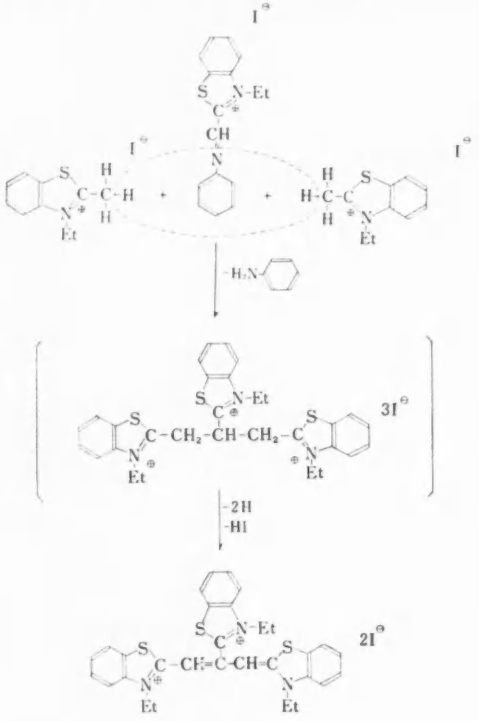

(VI)

Dehydrogenation of cyanines in pyridine had been observed already by Mills[2] and the present reaction was considered to be of similar mechanism. The dye VI obtained earlier was isolated as an anhydrous salt, but the same dye obtained in the present series of experiments possessed 2 mol. of water of crystallization. The same dye VI was also obtained on replacing the anil I with the nitrone II but the yield of the dye was better when the anil was used.

Tanabe synthesized dyes of this structure and reported the formation of 3-ethyl-2-trichloromethylbenzothiazolium chloride as an intermediate during the reaction of 3-ethyl-2-methylbenzothiazolium iodide and thionyl chloride. On following this reaction, a substance of m. p. 124°C (decomp.), identical with that reported in the literature, was obtained in a good yield. The elemental analytical values, however, did not correspond to those of the objective intermediate and further, iodine was detected besides the chlorine atom. Therefore, this product was not considered to be 3-ethyl-2-trichloromethylbenzothiazolium chloride as reported in the literature. Further, an attempt was made to prepare a dye with this intermediate but a single dye of m. p. 85°C as given in the literature was not obtained and in its stead, a crude dye of m. p. 185°C (decomp.) was obtained. This dye was submitted to paper chromatography and dye spots of yellow, magenta, and purple were separated on the chromatogram, showing the dye to be a mixture. Although further examination of this crude dye mixture was not made, it is certain that the dye VI obtained in the present series of experiments is not the same as the dye obtained by Tanabe.

This dye VI was heated at 130°C for about 12 hr. in the Abderhalden apparatus for the purpose of determining the water of crystallization and the loss in weight was more than that calculated. Therefore, the dried sample was examined by paper chromatography and it was found that the dye VI had changed into the structurally unknown dye V described in the preceding paper. Consideration of this phenomenon showed the necessity of assuming the liberation of ethyl iodide and analytical results supported this assumption. Therefore, the structure of this dye V must be 3, 3′-diethyl-9-(2-benzothiazolyl)thiacarbocyanine iodide.

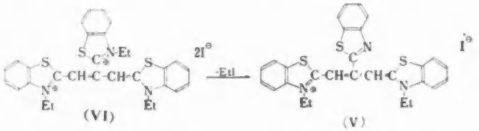

(VI) (V)

In order to clarify the structure of this dye V an attempt was made to synthesize it by a different route. With reference to the report of Ried and others[3], iodine was applied to 2-methylbenzothiazole in pyridine, and the *N*-(benzothiazol-2-ylmethyl)pyridinium perchlorate obtained therefrom was reacted with nitrosobenzene to form the phenylnitrone VIII of 2-formylbenzothiazole. Condensation of VIII with 2 mol. of 3-ethyl-2-methylbenzothiazolium iodide in pyridine afforded the same dye as V. This fact proves the correctness of the structure of 3, 3′-diethyl-9-(2-benzothiazolyl)thiacarbocyanine iodide for V.

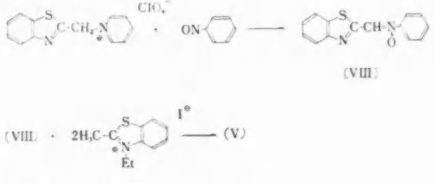

(VIII)

2) W. H. Mills, *J. Chem. Soc.*, **121**, 455 (1922).

3) W. Ried and H. Bender, *Ber.*, **89**, 1893 (1956).

With the identification of the structure of the dye V, the structure of the dye VI also became certain and conversion of this dye VI into V was experimentally proved by refluxing in pyridine for about 2 hr.

Condensation of the anil III of 3-ethyl-2-formylnaphtho-[2, 1-*d*]thiazolium iodide with 2 mols. of 3-ethyl-2-methylbenzothiazolium iodide in pyridine afforded, as anticipated, 3,3′-diethyl-9-(3-ethyl-1-thia-3-azoniacyclopenta-[*a*]naphth-2-yl)thiacarbocyanine diiodide (IX). It was thereby found that this process can be recommended as a general method for the synthesis of dyes of this type.

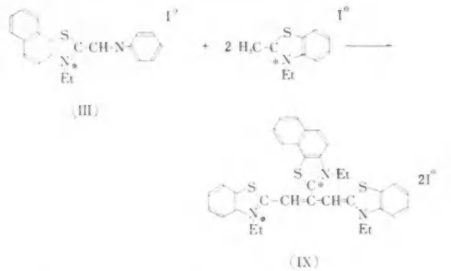

(III) (IX)

The foregoing experiments have revealed the course of formation of the dyes V and VI in the reaction described in the preceding paper and, consequently, formation of the dyes thought to be 3, 3′-diethylthiacarbocyanine iodide (IV), and 3, 3′-diethyl-8-(3-ethyl-2-benzothiazolinylidenemethyl)thiacyanine iodide (VII) was found to occur through the reaction of 3-ethyl-2-methylbenzothiazolium iodide with 3, 3′-diethyl-9-(3-ethyl-1-thia-3-azoniainden-2-yl)-thiacarbocyanine diiodide (VI) in pyridine.

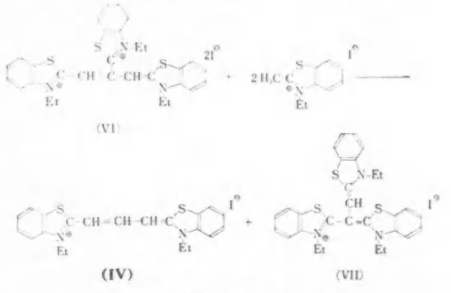

(VI) (IV) (VII)

The structure of the dye VII was merely presumed from its analytical values and absorption spectrum, and unequivocal establishement of this structure has not succeeded as yet, but it is certain that the dye VI is cleaved at the 9-position to liberate the substituent group to form the dye IV. In order to ascertain this cleavage reaction, the dye VI was refluxed with 3-ethyl-2-methylnaphtho[2, 1-*d*]thiazolium iodide in pyridine and the same dye (IV) was found to be formed. Whether the dye X formed at the same time is the anticipated 3, 3′-diethyl-8-(3-ethyl-2-naphtho[2, 1-*d*]thiazolinyl-idenemethyl)-6′, 7′-benzothiacyanine iodide or not is still uncertain since, although the analytical values of the dye X are comparatively close to the theoretical values, its absorption maximum is in a longer wavelength region (650 mμ), and this is unthinkable in the case of monomethine dyes.

Therefore, structural determination of these dyes VII and X must await further studies.

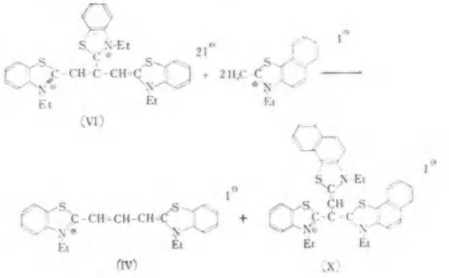

(VI) (IV) (X)

Experimental

Reexamination of Synthetic Method Tanabe's for the So-called 3, 3′-Diethyl-9-(3-ethyl-1-thia-3-azoniainden-2-yl)thiacarbocyanine Diiodide.—The experiments followed Tanabe's report[4]. To 6.1 g. (0.02 mol.) of 3-ethyl-2-methylbenzothiazolium iodide, 24 ml. of thionyl chloride was added dropwise with cooling, by which the iodide turned black and dissolved gradually. Ether was added to this reaction mixture and the yellow precipitate thereby formed was collected to 7 g. of a solid, m. p. 100°C. This was dissolved in thionyl chloride, reprecipitated with ether, and 5 g. (yield, 79%) of yellow powder, m. p. 124°C (decomp.), was obtained. This substance agrees with the so-called 3-ethyl-2-trichloromethylbenzothiazolium chloride, m. p. 125°C (decomp.), reported by Tanabe, but he had assumed this structure from the analytical value of the chlorine alone, and elemental analyses in the present series of experiments gave results which were inconsistent with this structure.

Found: C, 30.81; H, 3.43; N, 3.70. Calcd. for $C_{10}H_9NCl_4S$: C, 37.85; H, 2.84; N, 4.42%.

A solution of 1 g. (0.0032 mol.) of this intermediate product and 2 g. (0.0057 mol.) of 3-ethyl-2-methylbenzothiazolium iodide dissolved in 2.5 ml. of acetic anhydride, added with 1 g. of anhydrous potassium acetate, was heated in an oil bath at 120~130°C for 10 min., cooled, and ether was added to this reaction mixture. The crude dye that precipitated out was collected by filtration washed with water, and the powdery dye so obtained was recrystallized from acetone to 0.5 g. of pale purplish brown powder, m. p. 185°C (decomp.). This dye

4) Y. Tanabe, *J. Pharm. Soc. Japan*, **74**, 814 (1954).

is different from that of m. p. 85°C reported in the literature and was found to be a mixture of three kinds of dyes, giving spots colored violet, pink, and yellow by paper chromatography. R_f values were 0.54 (violet), 0.72 (pink), and 0.81 (yellow) (butanol : water = 6 : 1). This dye was also different from the dye VI obtained in the present series of experiments.

Results of this reexamination indicated that there is some doubt about the structure of this intermediate and the dye produced in the present series of experiments was never identical with that reported in the literature. Therefore, this examination was not followed further.

Formation of 3, 3'-Diethyl-9-(2-benzothiazolyl)-thiacarbocyanine Iodide (V) by Liberation of Ethyl Iodide from 3, 3'-Diethyl-9-(3-ethyl-1-thia-3-azonia-inden-2-yl)thiacarbocyanine Diiodide (VI).—The dye VI was heated in the abdelhalden apparatus at 120~130°C in 20 mmHg for 12 hr. and the loss in weight amounted to 12.22%. The values calculated for 2 mol. of water of crystallization is 4.41%. This dried dye was developed by paper chromatography by which it separated into two kinds of dyes: one a violet zone of R_f 0.44 and the other of reddish violet zone of R_f 0.89 (butanol : water = 6 : 1). The violet zone was that of the starting dye VI and the reddish violet zone agrees with R_f 0.89 of the dye V.

On boiling this dye VI in pyridine for 2 hr., the dye VI completely changed into V and the unity of this dye was proved by the reddish violet single zone of R_f 0.90 in the paper chromatogram.

The fact that the chromatographic purification of the mixture of four kinds of dyes through alumina column only afforded three kinds of dyes, IV, V and VII, as described in the preceding paper, indicates that VI had transited into V.

Preparation of the Phenylnitrone VIII of 2-Formylbenzothiazole.—To a solution of 6.52 g. (0.02 mol.) of *N*-(benzothiazolyl-2-methyl)-pyridinium perchlorate and 2.14 g. (0.02 mol.) of nitrosobenzene dissolved in 40 ml. of pyridine, 20 ml. of 2 N sodium hydroxide solution was added and the mixture was stirred, by which process exothermic reaction took place. The mixture was allowed to cool and crystals separated out after 2 hr. The crystals were collected by filtration, washed with ethanol, and 3 g. of yellowish brown needles, m. p. 160~167°C, was obtained. Recrystallization from ethanol afforded 1.1g. (yield, 21.6%) of pale yellowish brown needles, m. p. 163~164°C.

Found: C, 66.28; H, 4.17; 10.82. Calcd. for $C_{14}H_{10}ON_2S$: C, 66.15; H, 3.98; N, 11.02%.

Preparation of 3, 3'-Diethyl-9-(2-benzothiazolyl)-thiacarbocyanine Iodide (V).—A solution of 0.254 g. (0.001 mol.) of the phenylnitrone VIII of 2-formylbenzothiazole and 0.61 g. (0.002 mol.) of 3-ethyl-2-methylbenzothiazolium iodide in 3 ml. of pyridine was refluxed in an oil bath of 120°C for 10 min. The color of the reaction mixture changed from the initial yellow through green to purple. Ether was added to the reaction mixture to precipitate the dye formed which was collected by decantation and washed with wather to 0.4 g. of crystalline powder, m. p. 192~195°C (decomp.). Recrystallization from ethanol afforded 0.1 g. (yield, 16%) of green needles, m. p. 266°C (decomp.): λ_{max} 580mμ. Paper chromatogram: R_f 0.89 (butanol : water = 6 : 1): single spot of violet, indicating the substance to be identical with dye V among the four kinds of dyes isolated from a mixture.

Synthesis of 3, 3'-Diethyl-9-(3-ethyl-1-thia-3-azoniacyclopenta[*a*]naphth-2-yl)thiacarbocyanine Diiodide (IX).—A mixture of 2.2 g. of the anil III of 3-ethyl-2-formylnaphtho[2, 1-*d*]thiazolium iodide and 3.0 g. of 3-ethyl-2-methyl-benzothiazolium iodide in 30 ml. of pyridine was heated in an oil bath of 130°C for 25 min., cooled, and ether was added to this mixture. The precipitate thereby formed was separated by decantation, washed with ether and water, and warmed with a small amount of ethanol. On allowing this solution to cool, navy-blue crystalline powder was obtained which melted once at 185°C, resolidified, and again melted with decomposition at 245°C. Two recrystallizations from ethanol failed to change this mode of melting. Paper chromatogram exhibited a single zone of bluish purple color at R_f 0.51, λ_{max} 585 mμ. The analytical values agreed with those calculated as a monohydrate.

Found: C, 48.06; H, 4.07; N, 5.08; I, 29.54. Calcd. for $C_{34}H_{31}N_3I_2S_3 \cdot H_2O$: C, 48.06; H, 3.89; N, 4.95; I, 29.95%.

Formation of 3,3'-Diethylthiacarbocyanine Iodide (IV) and 3, 3'-Diethyl-8-(3-ethyl-2-benzothiazolinyl-idenemethyl)thiacyanine Iodide (VII) from the Dye VI and 3-Ethyl-2-methylbenzothiazolium Iodide.—A mixture of 0.1 g. of VI and 0.075 g. of 3-ethyl-2-methylbenzothiazolium iodide in 30 ml. of pyridine was boiled and an aliquot of this reaction mixture was periodically examined by paper chromatography (butanol : water = 6 : 1) to find the formation of dyes. After 30 min., the starting dye still appeared as a spot at R_f 0.35, but this disappeared after 60 min., and the reaction solution contained three kinds of dyes, one of reddish pink zone at R_f 0.75 (dye IV), one of violet zone at R_f 0.86 (dye V), and one of brown zone at R_f 0.93 (dye VII).

Formation of 3,3'-Diethylthiacarbocyanine Iodide (IV) and 3, 3'-Diethyl-8-(3-ethyl-2-naphtho[2, 1-*d*]-thiazolinylidenemethyl)-6', 7'-benzothiacyanine Iodide (X) from the Dye VI and 3-Ethyl-2-methyl-naphtho[2, 1-*d*]thiazolium Iodide.—A mixture of 1 g. of IV and 0.9 g. of 3-ethyl-2-methylnaphtho[2, 1-*d*]-thiazolium iodide in 300 ml. of pyridine was boiled at 130°C for 4 hr., pyridine was removed under a reduced pressure, and the residue was washed with 2 portions of ether. The residue was dissolved in acetone and the solution was developed through an alumina column by which the product separated into three bands of greenish black, reddish pink, and violet, from bottom to top. The reddish pink band was eluted with acetone, acetone solution was evaporated, and the residue was treated with ether, affording 0.1 g. of a crude dye, m. p. 200°C (decomp.): λ_{max} 580 mμ: paper chromatogram: R_f 0.74 (butanol : water = 6 : 1). This was identified with the dye IV.

The greenish black zone was eluted with acetone and the residue obtained on evaporation of acetone was treated with ether, affording greenish black

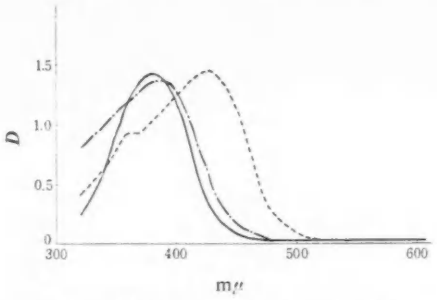

Fig. 1. Absorption spectral curves of I, II and III (in ethanol).
—·— (I), —— (II), ---- (III)

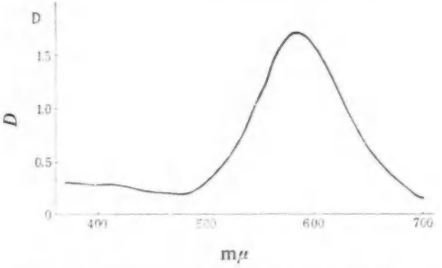

Fig. 2. Absorption spectral curve of IX (in ethanol).

crystalline powder, m. p. 192°C (decomp.). Recrystallization from methanol gave 0.5 g. of a dark green crystalline powder, m. p. 195°C (decomp.): λ_{max} 470 and 650 mμ. Paper chromatogram: a single spot of dark green color at R_f 0.94 (butanol: water = 6 : 1).

Found: C, 59.75; H, 4.56; N, 6.00. Calcd. for $C_{37}H_{32}N_3IS_3$: C, 59.90; H, 4.32; N, 5.67%.

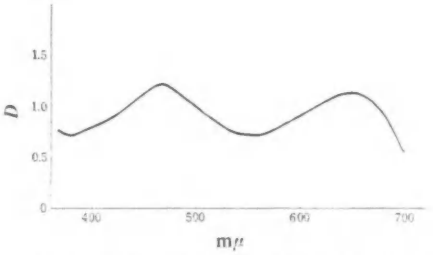

Fig. 3. Absorption spectral curve of X (in ethanol).

Research Laboratory
Fuji Photo Film Co. Ltd.
Minami-Ashigara-machi
Kanagawa-ken

Synthesis of Dyes with the Neocyanine Structure Presented by Brooker, and Related Dyes. V. Synthesis of the Brooker-type Dyes from the Anil of 3-Ethyl-2-formylbenzothiazolium Iodide

By Shiro KIMURA

(Received November 17, 1959)

Synthesis of the Brooker-type dye, 3, 3′-diethyl-9-[2-(3-ethyl-1-thia-3-azoniainden-2-yl) vinyl] thiacarbocyanine diiodide (II) in a good yield from the anil I of 3-ethyl-2-formylbenzothiazolium iodide and 3, 3′-diethyl-9-methylthiacarbocyanine iodide is discribed in this paper and this is the reverse of the reaction given in Part II of this series[1] for synthesis of the Brooker-type dyes from the nitrone of 3, 3′-diethyl-9-formylthiacarbocyanine bromide. At the same time, properties of the dye and synthetic process for similar dyes are described.

Pure synthetic process for the anil I was described in the preceding paper[2]. An equimolar mixture of this anil and 3, 3′-diethyl-9-methylthiacarbocyanine iodide was warmed in piperidine at 80~100°C for 5 min. and the dye II was obtained as brownish black leaflet crystal with copper luster, m. p. 257°C (decomp.).

It was shown in II that, during the course of the synthesis of this dye, heating of the mixture in a basic solvent for a long period of time or development of the product through alumina column afforded a dye of m. p. 219°C (decomp.). It was assumed that, similar to the case of 3, 3′-diethyl-9-(3-ethyl-1-thia-3-azonia-

1) S. Kimura, *Bull. Soc. Sci. Phot. Japan*, **9**, 45 (1959).

2) S. Kimura, This Bulletin, **33**, 872 (1960).

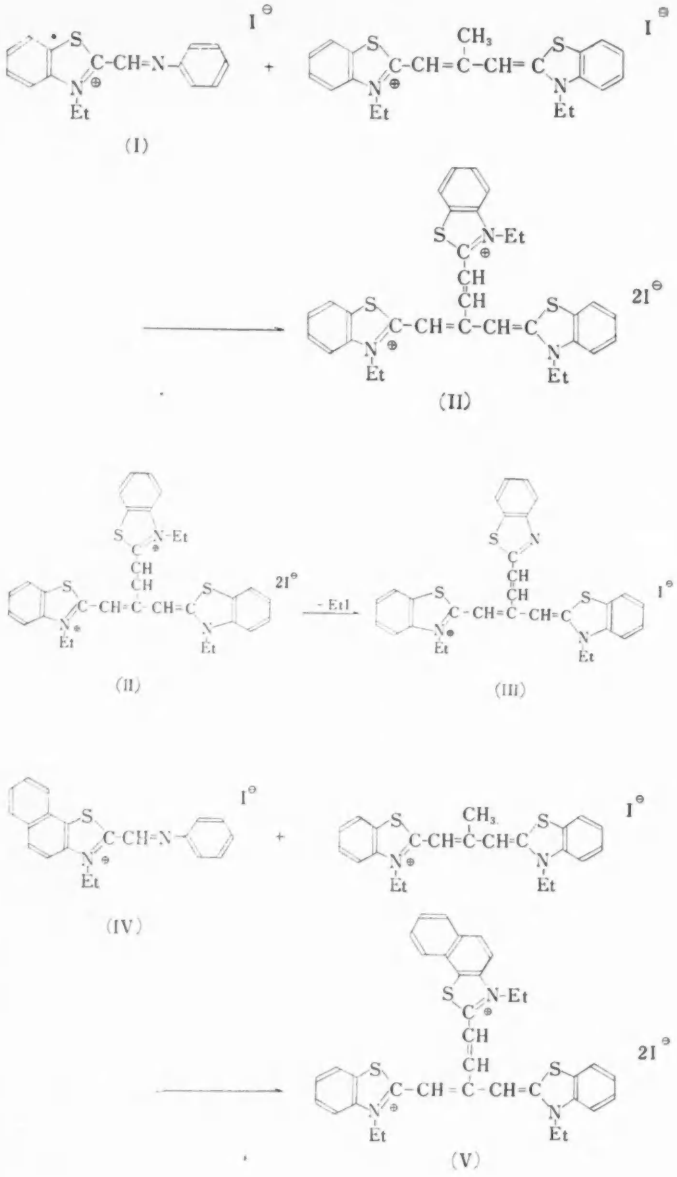

inden-2-yl)thiacarbocyanine diiodide described in the preceding paper, this dye II might also have undergone liberation of ethyl iodide to form 3, 3′-diethyl-9-[2-(2-benzothiazolyl) vinyl] thiacarbocyanine iodide (III). This dye III had already been synthesized by Hamer[3] and examination of her synthetic process showed that they are identical dyes.

Condensation of 3-ethyl-2-formylnaphtho-[2, 1-*d*] thiazolium iodide (IV) and 3, 3′-diethyl-9-methylthiacarbocyanine iodide in pyridine similarly afforded 3, 3′-diethyl-9-[2-(3-ethyl-1-thia-3-azoniacyclopenta[*a*] naphth-2-yl)vinyl] thiacarbocyanine diiodide (V) as purplish black crystalline powder of m. p. 257°C (decomp.): λ_{max} 650 mμ.

3) F. M. Hamer, *J. Chem. Soc.*, **1952**, 3197.

This synthetic process for the Brooker-type dyes from anils gives the product in comparatively good yield and can be recommended as a general method of synthesis of this type of dyes.

Experimental

Preparation of 3, 3'-Diethyl-9-[2-(3-ethyl-1-thia-3-azoniainden-2-yl) vinyl] thiacarbocyanine Diiodide (II).—A solution of 0.95 g. of the anil I of 3-ethyl-2-formylbenzothiazolium iodide and 1 g. of 3, 3'-diethyl-9-methylthiacarbocyanine iodide in 80 ml. of pyridine was heated at 80~100°C for 5 min. and cooled; ether was added to the reaction mixture to precipitate the dye formed. The precipitate was collected by filtration, washed with water, and 1.2 g. of the crude dye was obtained as purplish black powder, m.p. 180~190°C (decomp.). Recrystallization from methanol afforded 0.045 g. (yield, 2.8%) of brownish black leaflets, m. p. 257°C (decomp.). Paper chromatogram showed a single zone of violet color at *Rf* 0.37 (butanol : water=6 : 1), λ_{max} 560 mμ. This was identified with the dye II whose preparation was described in Part II of this series[1].

Found: C, 47.48; H, 3.91; N, 5.48; I, 30.94. Calcd. for $C_{32}H_{31}N_3I_2S_3$: C, 47.60; H, 3.81; N, 5.21; I, 31.50%.

Formation of 3, 3'-Diethyl-9-[2-(2-benzothiazolyl) vinyl] thiacarbocyanine Iodide (III) by Liberation of Ethyl Iodide from the Dye II.—Examinations were made on elementary analytical values of the green needles, m. p. 219°C (decomp.), isolated during alumina chromatography of the product obtained from preparation of the dye II, described in Part II[1], and the values were found to be close to those calculated for III.

Found: C, 55.60; H, 4.82; N, 6.44. Calcd. for $C_{30}H_{26}N_3IS_3$: C, 55.29; H, 4.02; N, 6.45%.

The dye of m. p. 218°C (decomp.), obtained on following the synthetic process of Hamer, exhibited the same absorption curve as this dye III with λ_{max} at 563 mμ, proving these dyes to be identical.

Preparation of 3' 3'-Diethyl-9-[2-(3-ethyl-1-thia-3-azoniacyclopenta [*a*] naphth - 2 - yl) vinyl] thiacarbocyanine Diiodide (V).—A mixture of 1 g. of the anil IV of 3-ethyl-2-formylnaphtho[2, 1-*d*]thiazolium iodide and 1 g. of 3, 3'-diethyl-9-methylthiacarbocyanine iodide in 80 ml. of pyridine was heated in an oil bath of 115~120°C for 10 min. Insoluble matter was filtered off, ether was added to the filtrate to precipitate the dye formed, and the mixture was allowed to stand over night. The precipitate was collected by filtration, washed with ether, and 0.8 g. of crude dye, m. p. 185~195°C (decomp.), was obtained. Recrystallization from 50 ml. of methanol afforded, as the first crop, the starting dye as indigo prisms, m. p. 275°C (decomp.), and concentration of this mother liquor to one-half the original volume afforded 0.17 g. of crystals of m. p. 195°C (decomp.). Recrystallization of this second crop of crystals from 30 ml. of methanol gave 0.05 g. of purplish black crystalline powder, m. p. 257°C (decomp.): λ_{max} 650 mμ.

Found: C, 50.00; H, 3.94; N, 5.00. Calcd. for $C_{36}H_{33}N_3I_2S_3$: C, 50.40; H, 3.86; N, 4.90%.

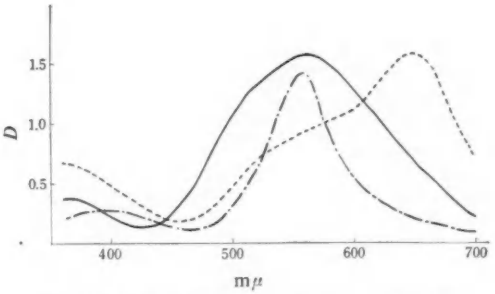

Fig. 1. Absorption spectral curves of II, III and V (in ethanol).

—— (II) —— (III) ---- (V)

Research Laboratory
Fuji Photo Film Co. Ltd.
Minami-Ashigara-machi
Kanagawa-ken

Rapid Determination of Thorium by Fluoride Titration Using Some Chromotropic Azo Dyes

By Sachindra Kumar DATTA

(Received January 8, 1960)

Thorium nitrate has been employed by many workers as a reagent for the volumetric analysis of fluoride. Willard and Winter[1] used alizarin sulfonate as indicator in the titration of fluorine with thorium nitrate. This method for the determination of fluorine in minerals and rocks has undergone many modifications in the hands of many workers[2]. Menis and co-workers[3] used alizarin red-S for the titration of fluoride by an automatic spectrophotometric device. Gurev and Ioffe[4] employed the thorium-alizarin red-S lake for the photometric determination of fluorine in zinc concentrates and electrolytes. This dye found application in the determination of this halogen by column chromatography with cellulose supported with alizarin red-S[5]. This thorium-alizarin sulfonate method has also been used by Guntz and Arene[6] for the colorimetric determination of fluorine in waters. Organic fluorine has also been determination by this method by Musgrave and Smith[7] and later the method was modified by Stross and coworkers[8] and also by Ellis and Musgrave[9]. Milton and Liddel[10] employed solochrome Brilliant Blue B. S. as indicator for the estimation of fluorine. Willard and Horton[11] made a comparative study on the use of many indicators for the titration of fluoride with thorium nitrate and showed that purpurin sulfonate and alizarin red-S gave reproducible results. Banerjee[12] used his dye SPADNS as indicator for such titration. The present author employed three dyes: SNADNS-4, di-SNADNS-4 and nitroso-SNADNS-4 for the determination of fluorine present in fluorides and rocks[13].

The reversed procedure, i. e., titration of thorium with a soluble fluoride in presence of a metal indicator is also feasible. Banerjee[14] carried out such a titration using SPADNS dye. The present paper describes a method for the titrimetric determination of thorium with sodium fluoride using three chromotropic azo dyes: nitroso-SNADNS-4, SNADNS-6[15] and CHPADNS[16], prepared from 1-naphthylamine-4-sulfonic acid, 1-naphthylamine-6-sulfonic acid and *p*-aminosalicylic acid respectively. The dyes form pink to violet complexes with thorium, which are decomposed by the addition of a standard fluoride solution resulting in the liberation of the free dyes showing a marked color change at the end point.

Experimental

Reagents and Chemicals.—*Sodium Fluoride.*—A stock solution was prepared from Merck's analytical grade sodium fluoride, previously dried at 120°C to constant weight.

Thorium Nitrate.—A thorium nitrate solution of strength 0.0128 M was prepared from thorium nitrate tetrahydrate (E. M.) by standardising gravimetrically with oxalic acid and phenyl acetic acid.

Dye Solution.—The dyes were prepared by following methods previously described[15,16]. A 0.1% solution of the dyes was used.

TABLE I. EFFECT OF pH ON THE TITRATION
NaF = 0.0526 M

Th taken mg.	pH	Th found (mg.) with the dyes		
		Nitroso-SNADNS-4	SNADNS-6	CHPADNS
14.85	1.81	13.20	12.81	12.63
	2.01	13.51	13.45	13.52
	2.25	13.92	13.86	13.94
	2.43	14.84	14.82	14.83
	2.62	14.86	14.83	14.84
	2.83	14.84	14.86	14.86
	3.22	14.75	14.72	14.74

1) H. H. Willard and O. B. Winter, *Ind. Eng., Chem., Anal. Ed.*, 5, 7 (1933).
2) G. Bruinisholz and J. Michod, *Helv. Chim. Acta*, 37, 874 (1954); F. Grimaldi and F. Cutta, *Anal. Chem.*, 27, 918 (1955); G. Pletzka and P. Ehrlich, *Angew. Chem.*, 65, 131 (1953); D. S. Reynolds and W. L. Hill, *Ind. Eng. Chem., Anal. Ed.*, 11, 21 (1939); H. R. Shell and R. L. Craig, *Anal. Chem.*, 26, 996 (1954).
3) O. Menis, D. L. Manning and R. G. Ball, *Anal. Chem.*, 30, 1772 (1958).
4) S. D. Gurev and V. P. Ioffe, *Anal. Abstr.* 6, 159 (1959).
5) S. K. Yasuda and J. L. Rambert, *Anal. Chem.*, 30, 1489 (1958).
6) A. A. Guntz and M. Arene, *Chim. Anal.*, 40, 453 (1958).
7) W. K. R. Musgrave and J. Smith, *J. Chem. Soc.*, 1949, 3026.
8) Stross et al., *Metallurgia*, 36, 346 (1947).
9) J. F. Ellis and W. K. R. Musgrave, *J. Chem. Soc.*, 1950, 1969.
10) R. F. Milton, H. F. Liddel and J. E. Chivers, *Analyst*, 72, 43 (1947).
11) H. H. Willard and C. A. Horton, *Anal. Chem.*, 22, 1190 (1950).
12) G. Banerjee, *Anal. Chem. Acta*, 13, 409 (1955).
13) S. K. Datta, *Z. anal. Chem.* 149, 333 (1956).
14) G. Banerjee, ibid., 146, 417 (1956).
15) S. K. Datta, ibid., 149, 270 (1956).
16) S. K. Datta, ibid., 167, 105 (1959).

TABLE II. DETERMINATION OF THORIUM WITH FLUORIDE

Th taken mg.	Volume of 0.0263 M NaF: Theoretical ml.	Actually required using the dyes: Nitroso-SNADNS-4 ml.	SNADNS-6 ml.	CHPADNS ml.	Alizarin-S ml.
43.07	28.24	28.19	28.17	28.18	28.17
31.19	20.45	20.42	20.40	20.43	20.41
29.70	19.47	19.48	19.45	19.47	19.43
23.76	15.58	15.60	15.59	15.61	15.57
11.88	7.79	7.78	7.76	7.80	7.80
2.97	1.95	1.98	1.94	1.96	1.93
1.49	0.98	0.96	1.00	0.94	0.95

Buffer Solution.—Standard acetate buffer mixtures of different pH were prepared as usual.

Starch Solution.—A 5% starch solution was prepared when required.

Optimum Conditions for the Determination of Thorium.—*Hydrogen Ion Concentration.*—Titration of thorium was carried out in solutions having different pH, adjusted by 0.01 N hydrochloric acid, sodium hydroxide or acetate buffer. It was observed that a pH range from 2.4 to 2.8 was more or less suitable for estimation with these dyes. (Table-I).

Concentration of the Dyes.—A. half ml. of 0.1% dye solution was sufficient to give good end points with smaller amounts thorium in 50 ml. volume.

Concentration of Thorium Solution.—Reproducible results were obtained when very dilute solutions of thorium were titrated. The end point becomes obscure and a considerable amount of the indicator is absorbed by the increased amount of thorium fluoride precipitate. The quantity of thorium present should not be more than 50 mg. per 50 ml.

Starch Solution.—A 5 ml. portion of 5% freshly prepared starch solution should be added per 50 ml. solution to reduce the precipitation of thorium fluoride, acting as a protective colloid[5].

Volume of Titrating Solution.—In order to find out the effect of dilution of the volume of the titrating solution on the end point, titrations were carried out by varying the final volume of the solution keeping all other things constant. It was found that titration was best done in 40~50 ml. volume.

Temperature.—The titration is to be carried out at room temperature. At higher temperature the end point became indistinct.

Analytical Procedure.—An aliquot quantity of thorium nitrate solution was taken in a 250 ml. Erlnmeyer flask to which was added 0.5 ml. of the indicator, the mixture was diluted to 40 ml. the pH was adjusted to 2.5 with 0.01 N sodium hydroxide or hydrochloric acid, 5 ml. of starch solution were added and the volume was finally made up to 50 ml. The titration was carried out rapidly with the standard sodium fluoride solution till the end point was attained. Blank titrations were also carried out side by side. Titration should be completed quickly as the efficacy of the starch solution is soon lost. At the end point the color of the solution with nitroso-SNADNS-4, changed from reddish-pink to yellow, with SNADNS-6 the change was from pinkish-blue to pink and with CHPADNS the color changed from pinkish-violet to red. The end point with nitroso-SNADNS-4 was very sharp and distinct. Some of the representative data given in Table II, show that the method is stoichiometric up to about 50 mg. of thorium, within the limits of experimental error. The results have been compared with those obtained by the use of alizarin red-S indicator at pH 2.9~3 and the results were found to agree favorably.

Determination of Thorium in Micro Quantities. The procedure for titrating microgram amounts of thorium was the same as before, excepting that a micro-burette, more dilute solutions of the fluoride and thorium nitrate and 0.5 ml. of 0.05% dye solution per 50 ml. final volume, were used. The end points were sharper in this titration as the bulk of thorium fluoride formed was small. The data recorded in Table III, indicate that as low as 3.8 μg. of thorium per 50 ml. may be determined using these dyes with fair accuracy.

TABLE III. MICRO-TITRATION OF THORIUM WITH FLUORIDE

Th taken μg.	Th found in μg. (NaF=0.0013 M): Nitroso-SNADNS-4	SNADNS-6	CHPADNS
22.88	22.90	22.86	22.89
15.26	15.22	15.19	15.21
11.44	11.41	11.40	11.38
7.63	7.60	7.60	7.62
3.81	3.78	3.74	3.76

Effect of Various Ions on the Determination.—Possible interference in this determination was investigated. The ions that complex thorium or the dyes and also those which react with fluoride, interfere strongly. The elements which caused interference are as follows: lead, mercury(I), alkaline earth metals, iron, tin, manganese, magnesium, cerium, rare earth elements, zirconium, phosphate, borate, oxalate, tartrate and citrate. Determination could be carried out in the presence of other elements like copper, cadmium, aluminum, beryllium, zinc, mercury(II), cobalt, nickel, sodium and potassium. The results have been placed in Table IV.

Table IV. Determination of thorium in presence of diverse ions

Th taken=8.91 mg.=5.84 ml. of 0.0263 M NaF

Elements	Amount mg.	Titre value (ml.) with Nitroso-SNADNS-4	SNADNS-6	CHPADNS
Na	12.84	5.88	5.81	5.89
K	13.16	5.87	5.88	5.86
Cu	5.21	5.80	5.79	5.80
Cd	9.32	5.89	5.80	5.88
Al	6.03	5.81	5.78	5.80
Be	5.71	5.80	5.79	5.79
Zn	8.72	5.82	5.88	5.81
Hg(II)	4.32	5.83	5.80	5.86
Co	8.13	5.80	5.81	5.78
Ni	6.04	5.81	5.79	5.80

Summary

The thorium-chromotropic azo dye complexes are found to be fast-reacting with fluorides, in which exchange of dye molecule for fluoride ion takes place. The colored thorium-dye complexes are thereby decomposed with the liberation of the free dye and formation of thorium fluoride. The color changes at the end point enable visual comparison. Three dyes: nitroso-SNADNS-4, SNADNS-6 and CHPADNS have been used here as thorium complexing agents or indicators. The color change with the nitroso-SNADNS-4 at the end point is very sharp. Titrations are best carried out at pH range 2.4~2.8 and thorium present should not be more than 50 mg. per 50 ml. solution. With the increased precipitation of thorium fluoride the dyes are adsorbed in the precipitate and the end point becomes more obscured. Microgram amounts of thorium may also be determined by this method. A large number of cations and anions interfere in the process, of which the most important are: iron, cerium, rare earth elements, alkaline earth elements, phosphates, borates, oxalates, tartrates and citrates. This method is best applicable to thorium solutions from which the interfering elements have been removed.

Chemical Laboratory
Victoria (Government) College
Coochbehar, India

Separation of Radioactive Arsenic from Germanium Irradiated with Protons

By Kazuo Saito, Shigerô Ikeda and Makoto Saito

(Received January 26, 1960)

Concerning the preparation of radioactive arsenic including ^{70}As, ^{71}As, ^{72}As and ^{74}As, from a germanium target irradiated with protons, a little information is available. Green et al.[1] extracted germanium tetrachloride with benzene and left arsenic in the aqueous phase consisting of 11 N hydrochloric acid. Irvine[2] distilled off germanium tetrachloride in an oxidative atmosphere in the presence of carrier arsenic and hydrochloric acid. These reports, however, give only insufficient information on the preparation of radioactive arsenic of a very high specific activity (e. g. 1 mc in 0.05 ml. of aqueous solution containing less than 10 μg. of arsenic).

With the aims of measuring the accurate energy of the gamma rays of arsenic −74 by the internal conversion method and using the product for a tracer of a high specific activity, the present authors examined the separation of almost carrier-free arsenic by distillation with reference to the rate of distillation; they also applied the solvent extraction method[3] with diethyldithiocarbamate to the present purpose. Since commercial germanium of a high purity contains a very small amount of arsenic (e. g. less than 0.0001%), the product can not be called carrier-free. However this is regarded as practically carrier-free from either a nuclear spectroscopic or a radiochemical viewpoint; never-the-less the term "carrier-free" is not used in this paper.

It was elucidated that the distillation of arsenic trichloride in the absence of germanium, is completed within 5 min. (Table I.) and the

1) M. Green and J. A. Kafalas, *J. Chem. Phys.*, 22, 760 (1954).
2) W. Irvine Jr., *J. Applied Phys.*, 13, 910 (1942).
3) N. Stanford, P. F. Wyatt and F. G. Kershaw, *Analyst*, 70, 232 (1945).

distillate contains no appreciable amount of solute other than hydrogen chloride, hydrogen bromide and radioactive arsenic in an almost carrier-free state. It is often seen that the distillation of a substance is retarded on a micro scale, but this is not the case. It remains uncertain, however, whether the rapid distillation is due to the possible presence of a very small amount of carrier or to the fact that a large amount of hydrogen chloride simultaneously distils out. The distillate can be used as a tracer for arsenic. It was found, however, more convenient to extract arsenic into an organic phase and extract it back into an aqueous layer, for the product to be submitted to conversion electron measurement in a beta-ray spectrometer.

The extraction of diethyldithiocarbamate with carbon tetrachloride provides satisfactory results on such a micro scale, provided that a sufficient amount of the reagent is present. (Fig. 1) The use of an acetate buffer, which is generally involved in the analytical use of this reagent, was not found essential for a quantitative extraction, whenever the pH is duely adjusted. It appears as if the use of a buffer causes the presence of a salt-like substance in the final product, which vitiates the specific activity and hence the conversion electron spectrum. Although the presence of germanium does not interfere with the extraction, most satisfactory results were obtained by the application of the extraction method to the distillate of almost carrier-free arsenic trichloride. Retardation of the extraction, which is often involved in the case of carrier-free separation, was not recognized. The reason is uncertain, but it must be noticed that a large excess of diethyldithio carbamate is essential for a rapid extraction and that a very small amount of the reagent is extracted into the organic phase at the given pH.

When relatively short-lived arsenic-69, 70, 71, 72 and 76 decay after one week, the redioactivity consists of arsenic-74 (half-life, 17.5 days) and arsenic-73 (76 days); the latter gives only two gamma rays of 14 and 54 keV. and does not interfere with the measurement of gamma-rays of arsenic-74 having higher energies, by the scintillation method. Hence the product is satisfactorily used for the study of the decay scheme of ^{74}As and as a tracer of arsenic having an apparent half-life of 17.5 days. The result of the study of the decay scheme was published elsewhere[5]. A part of the spectrum is shown in Fig. 2, which clearly shows that the source is thin enough to give a resolution of $\pm 0.8\%$. The amount of miscellaneous substances in the final product, including carrier arsenic is less than 10 μg. for 0.4 mc, the specific activity for ^{74}As being about 1 mc per 25 μg. immediately after preparation. The overall yield for ^{74}As is about 70%.

Experimental

Target and Irradiation.—Elementary germanium of a purity more than 99.99999999% (measured by the Hole effect) (possible chemical purity more than 99.999%) and germanium dioxide (purity more than 99.999%) were used as target. The germanium was placed on a water-cooled detachable stem and covered with a thin (20 μ) foil of aluminum. The oxide was mixed with a dilute solution of glycerin phthalate resin (glyptal) in ethylacetate, mounted on an aluminum plate and dried at 250°C; the plate was fixed on the head of the stem.

Irradiation was made in INS cyclotron (diameter of the magnet pole piece, 163 cm.) with protons of various energies ranging from 10 to 14 MeV. for 2 to 5 hr., the intensity of the beam current being 10 to 20 μA. The irradiated target was set aside in the vacuum chamber for 1 hr., the head of the stem taken out and the target submitted to chemical separation.

The irradiated unit contained arsenic-70, 71, 72, 73, 74 and 76, germanium-69 and 71 (produced by (p, pn) reaction) and probably a small amount of gallium-67, 68, 70 and 72 (produced by (p, 2p) and (p, α) reaction) as radioactive nuclides. The total amount of radioactive substance was of the order of several ten mc immediately after irradiation, when the beam current was 15 μA and the duration of irradiation was 5 hr.; the amount of arsenic-74 appeared to be 1 mc or a little less. Irradiation was made five times altogether. Chemical behavior of the produced nuclides was carefully checked. Essential parts are described as follows.

Distillation.—The elementaryger manium (10 g., in four pieces) was placed in a Clysen-type flask, dissolved in aqua regia (30 ml.) and germanium tetrachloride distilled in a current of chlorine with the addition of 6 N hydrochloric acid (50 ml.) until the volume of the residue is less than 1 ml. The addition of hydrochloric acid and the distillation were repeated three times. Germanium oxide taken off the plate was placed in the flask and similarly distilled. The remaining charred resin did not interfere with the subsequent distillation of arsenic. The removal of germanium was almost complete. The chlorine being removed in a current of nitrogen, the arsenic trichloride was distilled in the presence of 10 N hydrochloric acid (10 ml.) and 9 N hydrobromic acid (5 ml.), into an ice-cooled adapter containing water (10 ml.). The arsenic was found in the first a few milliliters' portion. This fact was clearly demonstrated by a small-scaled distillation

4) C. L. Luke, and M. E. Campbell, *Anal. Chem.*, **25**, 1588 (1953); H. Goto and Y. Kakita, *J. Chem. Soc. Japan, Pure Chem. Sec. (Nippon Kagaku Zasshi)*, **77**, 739 (1956).

5) T. Yamazaki et al., *J. Phys. Soc. Japan*, in press. After the completion of the present study, the following two papers have appeared. They concern the decay scheme of ^{74}As, but not the chemical procedures. E. P. Gligoriev et al., *Izvestia Akad. Nauk, SSSR, Ser. Phys.*, **22**, 831, (1958); D. J. Horen et al., *Phys. Rev.*, **113**, 875 (1959).

Table I. Distillation of arsenic trichloride*

Fraction	Distilled ml.	Time of distil. min.	Relative counting rate, c.p.m.	Remarks
1	5	5	10863	**
2	4	8	241	
3	5	13	88	
4	5	20	56	
5	5	24	45	
6	5	30	7	+HCl 10 ml. +HBr 5 ml.
7	5	35	23	
8	7	42	16	

* The amount of the radioactive As is much smaller than that in the practical separation, but the volume of the aq. soln. is almost the same.

** Initial vol. of the aq. soln. 0.5 ml.; the counting rate, 12100 c.p.m.

shown in Table I. The total recovery was about 94%; most of the remaining radioactive arsenic was found on the surface of the rubber stoppers.

Solvent Extraction.—The experimental procedure shown in the original paper[3] was followed.

Since this method has been examined for use in micro analysis of arsenic[4], the following experiments were centered around the rate of extraction on such an ultra-micro scale. The distillate was heated to dryness with sulfuric acid (1 N, 2 ml.) and nitric acid (15 N, 5 ml.), mixed with hydrochloric acid (12 N, 1 ml.) and water (15 ml.) and again heated to 50°C. The product is treated with potassium iodide solution (10%, 3 ml.) and sodium sulfite (1 g.), made pH 5 with sodium acetate (10%, 5 ml.) and aqueous ammonia solution and shaken with carbon tetrachloride for 1 min. (equal volume to the aqueous layer) in the presence of variable amounts of sodium diethyldithiocarbamate solution (0.1%, in water). The results are shown in Fig. 1.

It is clearly seen that the extraction largely depends on the amount of the reagent. No appreciable adsorption of radioactive arsenic was observed on the surface of the glass wares, not excepting the ground parts. A similar extraction curve was obtained in the presence of germanium. A satisfactory extraction of arsenic was also effected in the absence of any buffer, provided that the pH was duely adjusted. Back-extraction of radioactive arsenic was substantiated from the carbon tetrachloride solution, by the use of 8 N nitric acid, 6 N hydrochloric acid or aqueous ammonia solution. Single extraction suffices for the recovery of more than 90% of the radioactive arsenic.

Measurement of Radioactivity.—For checking the procedures for separation, a G. M. counter was used, the sample being placed at a reproducible geometry. Since one series of experiments is completed within a few hours, the radiochemical composition of the sample can be regarded as identical, although the sample solution contains, especially at the early stage of separation, several radioactive nuclides. Hence the counting rate was shown in c. p. m. on an arbitrary scale in the figures and tables.

For the measurement of the conversion electron spectrum, the back-extracted arsenic in nitric acid solution was mounted on a trace of insulin on a thin polyvinylchloride foil lined with a thin layer (several μg. per cm^2) of vacuum-evaporated aluminum, dried up under an infrared lamp or in vacuo and attached to a beta-ray spectrometer. (INS-III, $\rho = 18$ cm.)

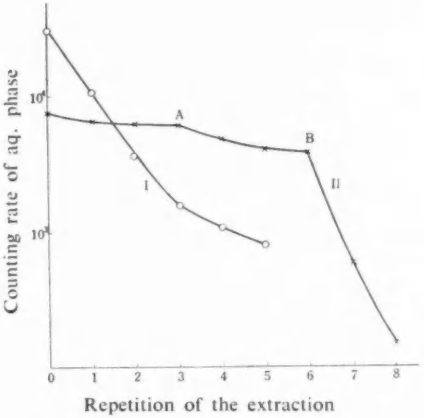

Fig. 1. Extraction of arsenic with carbontetrachloride in the presence of diethyldithiocarbamate.

Curve I. Extraction in the presence of 3 ml. of 0.1% reagent soln.; vol. of the aq. phase, 6 ml.; time of shaking 1 min. each.

Curve II. Extraction in the presence of a less amount of reagent; initial, 0.5 ml.; vol. of the aq. phase, 6 ml.; time of shaking, 1 min. At point A and B, 0.5 ml. and 1.0 ml. of 0.5% reagent soln. were respectively added.

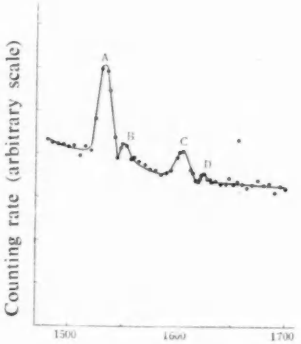

Fig. 2. Conversion electron spectrum of aresenic-74.

A, 596 keV.-K; B, 596 keV.-LM; C, 635 keV.-K; D, 635 keV.-LM.

The experiments were carried out co-operatively by the members of the beta- and gamma-ray group of the Institute for Nuclear Study (Dr. Mitsuo Sakai, Messers. Hidetsugu Ikegami and Toshimitsu Yamazaki), to whom the authors thanks are due. They are also indebted to Professor Hidehiro Goto of Tohoku University for his encouragement. A part of the expenses was defrayed from the Ministry of Education.

Institute for Nuclear Study
The University of Tokyo
Tanashi, Tokyo (K. S.)

Institute for Iron,
Steel and other Metals
Tohoku University
Katahira-cho, Sendai
(S. I. and M. S.)

The Synthesis of 4-Aminotropone

By Kozo Doi

(Received November 17, 1959)

Tropolone[1] (I) and its isomers, 3-hydroxytropone[2] (II) and 4-hydroxytropone[3] (III) have been synthesized and their reactions have also been investigated. The amino homologues, of tropolones, 2-aminotropone[1] (IV) and derivatives, have already been synthesized and their reactions have been studied in detail. The isomeric 3-aminotropone (V) and 4-aminotropone (VI), on the other hand, have sofar not been prepared. The present communication deals briefly with the synthesis of the 4-isomer VI starting from 4-aminotropolone[1] (VII).

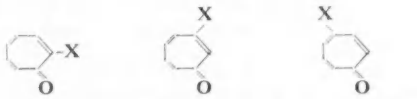

I: X=OH II: X=OH III: X=OH
IV: X=NH_2 V: X=NH_2 VI: X=NH_2

Reaction of 4-aminotropolone sulfate and *p*-toluenesulfonyl chloride in pyridine afforded, with company of a di-*p*-toluenesulfonate (VIII), 4-amino-2-*p*-toluenesulfoxytropone (IX), of which hydrogenolysis[5] over 5% palladized charcoal gave easily 4-aminotropone (VI).

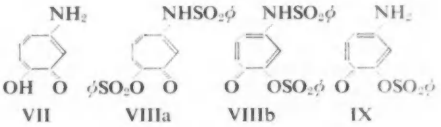

VII VIIIa VIIIb IX

The ultraviolet absorption of the aminotropone VI shows an tropone type of spectrum[6], having maxima at 228 mμ (log ε 4.35), 260 (3.89) and 365 (4.38) (Fig. 1).

The structure of the aminotropone VI is more reasonably assumed from the fact, that its infrared spectrum has two absorption bands,

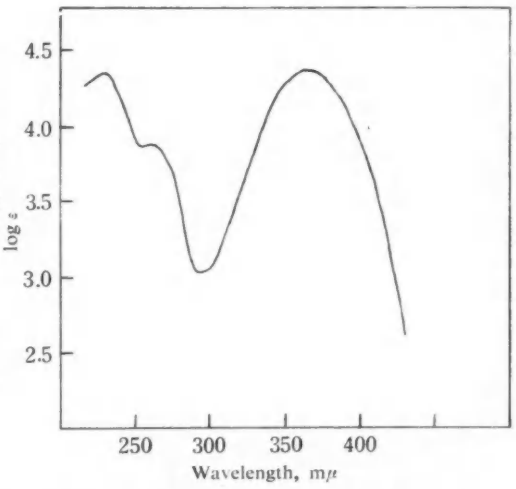

Fig. 1. Ultraviolet absorption spectrum of 4-aminotropone (VI) in methanol.

1) cf. P. L. Pauson, *Chem. Revs.*, **55**, 9 (1955).
2) R. B. Johns, A. W. Johnson and M. Tisler, *J. Chem. Soc.*, **1954**, 4605; A. W. Johnson and M. Tisler, ibid., **1955**, 1841.
3) T. Nozoe, T. Mukai, Y. Ikegami and T. Toda, *Chem. & Ind.*, **1955**, 66; R. B. Johns, A. W. Johnson, A. Langemann and J. Murray, *J. Chem. Soc.*, **1955**, 309.
4) K. Doi, Abstracts of the 12th Annual Meeting of the Chemical Society of Japan, p. 230 (1959).
5) T. Nozoe, S. Seto, T. Sato and S. Ninagawa (to be published) have found the formation of tropones from 2-*p*-toluenesulfoxytropones with a similar hydrogenolysis procedure.
6) M. Tsuboi, This Bulletin, **25**, 369 (1952).

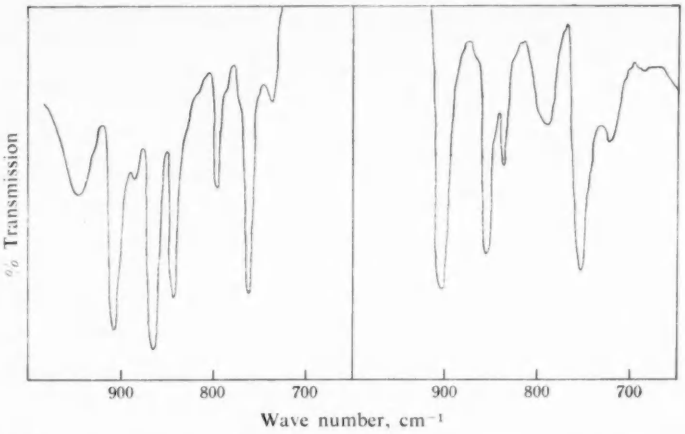

Fig. 2. Infrared absorption spectra of 4-aminotropone (VI, right) and 4-hydroxytropone (III, left).

790 and 903 cm^{-1}, which have been assigned[7] to the bands based on the CH out-of-plane vibrations of 4-substituted tropones. It may support the structural assignment above described, that the infrared spectrum of 4-hydroxytropone[7] (III) has two absorption bands, 797 and 865 cm^{-1}, and the features of the absorption in this region are closely ressembling to that of the aminotropone VI (Fig. 2).

Experimental

4-Amino-2-*p*-toluenesulfoxytropone (IX).—To a stirred solution of 4-aminotropolone sulfate[4] (2 g.) and pyridine (3 cc.), was added *p*-toluenesulfonylchloride (1.9 g.) for 3 min. at room temperature. After 30 min., dilution with water (20 cc.) and subsequent filtration afforded a pale yellow solid (2.6 g.), m. p. 199~200°C (decomp.), of which fractional recrystallization from methanol gave a less soluble product, a di-*p*-toluenesulfonate (VIII, 1.8 g.), m.p. 213°C (decomp.),

Found: C, 56.37; H, 4.54; N, 3.56. Calcd. for $C_{21}H_{19}O_6NS_2$: C, 56.61; H, 4.30; N, 3.14%.

and more soluble product IX (0.12 g.), yellow needles, m. p. 194°C (decomp.).

Found: C, 57.67; H, 4.41; N, 5.00. Calcd. for $C_{14}H_{13}O_4NS$: C, 57.73; H, 4.50; N, 4.82%.

4-Aminotropone (VI).—A mixture of IX (0.3 g.), sodium acetate trihydrate (0.15 g.), 5% palladized charcoal (50 mg.) and methanol (100 cc.) was shaken in the hydrogen atmosphere until absorption of hydrogen ceased. After 8 hr., the catalyst was removed and the filtrate was concentrated in vacuo. The residual solid, after chromatographic purification (ethyl acetate-alumina) followed by crystallization from ethyl acetate, afforded 4-aminotropone (VI, 20 mg.), yellow prisms, m. p. 218°C (decomp.).

Found: C, 69.08; H, 5.83; N, 11.63. Calcd. for C_7H_7ON: C, 69.40; H, 5.83; N, 11.56%.

The author thanks Professor Yoshio Kitahara very much for his unfailing guidance, also Mr. Yusaku Ikegami for the infrared spectral analysis and Messrs. Shinichi Ohyama and Yoko Endo for the microanalyses.

The Chemical Research Institute of Non-Aqueous Solutions
Tohoku University
Katahira-cho, Sendai

7) Y. Ikegami *Kagaku-no-Ryoiki (J. Japanese Chem.)*, Extra No. 38, p. 33, Nankodo Co., Tokyo (1959).

Magnetic Susceptibilities of Sulfur, Selenium and Tellurium from Room Temperature to 1100°C

By Shōtarō Tobisawa

(Received August 18, 1959)

The temperature-dependences of magnetic susceptibilities of sulfur, selenium and tellurium have, hitherto, been investigated by many workers. Some different results can, however, be found among their data. The magnetic susceptibilities of the three elements have, therefore, been measured with the recording magnetic balance to compare the present results with those reported by other investigators and to compare the present results with experimental results observed on the physical properties such as viscosity, specific heat, electrical conductivity and so on.

Experimental

Materials.—*Sulfur.*—Guaranteed sulfur, Kanto Chemical Co. Ltd., was purified by Bacon and Fanelli's procedure[1], and then was treated by Gardner and Fraenkel's method[2] to eliminate magnetic impurities.

Selenium.—Guaranteed selenium, Junsei Chemical Co. Ltd., was distilled several times under high vacuum to obtain selenium of spectro grade. A glassy solidified black-selenium (glassy selenium) was prepared by quenching a sample of molten selenium under vacuum of 10^{-5} mmHg. This sample was confirmed to have diffused rings without diffraction patterns by X-ray analysis. Hexagonal selenium was obtained by heating a sample of glassy selenium at about 130°C for 48 hr. under vacuum of 10^{-5} mmHg. This sample was found to have hexagonal patterns.

Tellurium.—Tellurium of Merck (sample A) and a specimen produced by Mitsubishi Ōsaka Refinery (sample B) were distilled three and five times, respectively, to obtain tellurium of spectro grade. Both the samples were crystallized by cooling very slowly from the molten state under vacuum of 10^{-5} mmHg. It was ascertained by X-ray examinations that both the samples had hexagonal patterns.

Measurements.—Measurements were carried out by using the recording magnetic balance described in detail in the previous report[3]. The dimension of the sample bulb was the same as the previously reported one. The apparatus, which was operated by the Faraday method, was modulated on a recording chart to be able to indicate the changes of

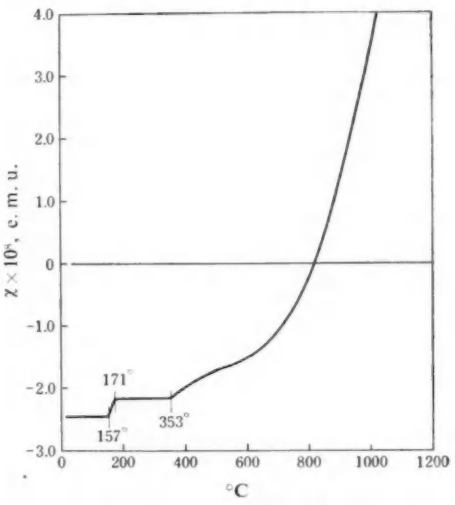

Fig. 1. Magnetic susceptibility-temperature curve for sulfur (50.2 mg. in weight).

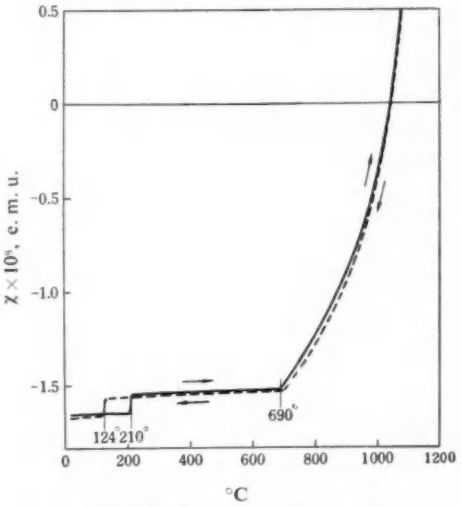

Fig. 2. Magnetic susceptibility-temperature curve for glassy selenium (50.0 mg. in weight).
—— heating ---- cooling

1) R. F. Bacon and R. Fanelli, *J. Am. Chem. Soc.*, **65**, 639 (1943).
2) D. M. Gardner and G. K. Fraenkel, ibid., **76**, 5891 (1954); ibid., **78**, 3279 (1956).
3) S. Tobisawa, This Bulletin, **32**, 1173 (1959).

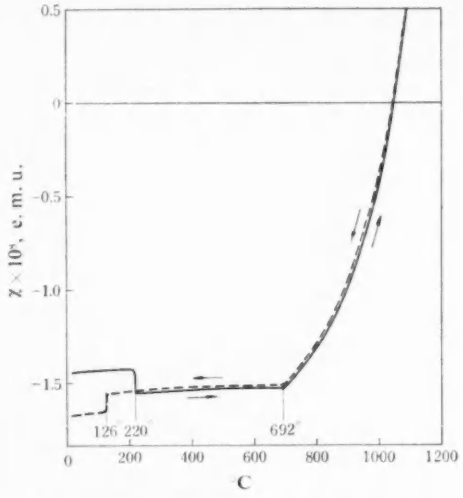

Fig. 3. Magnetic susceptibility-temperature curve for hexagonal selenium (50.2 mg. in weight).
—— heating ---- cooling

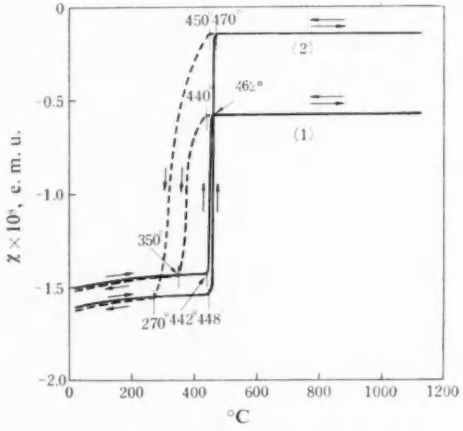

Fig. 4. Magnetic susceptibility-temperature curves for hexagonal tellurium.
(1) sample A (50.0 mg. in weight).
(2) sample B (50.1 mg. in weight).
—— heating ---- cooling

0.1 mA, which corresponded to -1.3×10^{-9} e.m.u. in magnetic susceptibility. In each experiment, a sample of about 50 mg. was charged into a fused quartz bulb. This bulb was sealed carefully, after having been evacuated to about 10^{-5} mmHg. The measurements were made with heating or cooling rates of 300°C per hour, at constant field, 8250 Oersteds. The results obtained are shown in Figs. 1—4.

Results

Comparison with the Results Obtained by other Investigators.—*On the Solid State.*—The magnetic susceptibilities of the three elements obtained at room temperature are given in Table I. The susceptibility of sulfur scarcely changes with temperature, while those of selenium and tellurium change slightly with temperature.

Table I. The magnetic susceptibilities of the three elements

Sample	$\chi\times10^6$ (per g.)
Sulfur	−0.49
Glassy selenium	−0.33
Hexagonal selenium	−0.29
Hexagonal tellurium	−0.30 (Sample A) −0.32 (Sample B)

On the Behavior of Susceptibilities at the Melting Points and their Neighborhood.—(1) The susceptibility of sulfur showed no particular changes at the melting point and its neighborhood. It began to decrease from 157°C, and reached -0.43×10^{-6} per g. at 171°C. Ishiwara[4] reported that the susceptibility of sulfur decreased at about 160°C, while Honda[5] showed that the susceptibility of sulfur had a minimum value at the melting point.

(2) Busch et al.[6] reported that the volume susceptibility of hexagonal selenium increased on fusion. In Figs. 2 and 3, the susceptibility of glassy selenium decreased slightly at 210°C, while that of hexagonal selenium increased slightly at 220°C. On cooling, both kinds of liquid selenium turned to glassy selenium, showing slight increases in susceptibilities at about 125°C under the present experimental condition. Busch et al. reported that the volume susceptibility of glassy selenium had no abrupt changes despite the fast cooling of molten selenium.

(3) The susceptibility of hexagonal tellurium of sample A began to decrease at 442°C and reached the value of -0.12×10^{-6} per g. at 462°C. The susceptibility of sample B began to decrease at 448°C and reached the value of -0.03×10^{-6} per g. at 470°C. The susceptibility-temperature curve for hexagonal tellurium deflected toward sides opposite to that for hexagonal selenium, as shown in Figs. 3 and 4. Under the present experimental condition, sample A was supercooled to 350°C, while sample B was supercooled to 270°C.

In the Liquid State.—(1) The susceptibility

4) T. Ishiwara, *Science Repts. Tōhoku Imp. Univ.*, **9**, 233 (1920).
5) K. Honda, ibid., **1**, 1 (1911).
6) G. Busch and O. Vogt, *Helv. Phys. Acta*, **30**, 224 (1957).

of liquid sulfur scarcely changed until 353°C (-0.43×10^{-6} per g.).

(2) The susceptibility of fused selenium, -0.31×10^{-6} per g. at 220°C, decreased slightly with temperature. The values reported as the susceptibility of fused selenium are as follows: -0.31×10^{-6} [7], -0.304×10^{-6} [8] and -0.32×10^{-6} per g.[9] Busch et al.[6] showed that the volume susceptibility of fused selenium was -1.347×10^{-6} per cc. at the melting point. Taking 3.987 g. per cm^3 [10] as the density of fused selenium at 220°C, Busch's value corresponded to -0.338×10^{-6} per g. in mass susceptibility. This value is greater than the present experimental value at 220°C.

(3) The value of liquid tellurium from sample B at 470°C, -0.03×10^{-6} per g., consistent with the values of liquid tellurium obtained by Honda[11] and Endo[12], was smaller than that of sample A. On the other hand, values reported as the volume susceptibility of liquid tellurium by the other authors were -0.3×10^{-6} [13] and -0.767×10^{-6} [6] per cc.

In the Higher Temperature Range.—(1) The curve in Fig. 1 deflected toward paramagnetic sides above 353°C. Néel[14] and Scott[15] reported that the diatomic sulfur molecule produced by the dissociation of sulfur at high temperature, was paramagnetic. On the assumption that the deflection toward paramagnetic sides above 353°C is due to the paramagnetism of the diatomic sulfur molecule, an attempt was made to estimate the weight of the diatomic sulfur molecule at every temperature by comparing the experimental value of paramagnetic susceptibility with the value calculated from Van Vleck's equation[16]. The ratios of the weight of the diatomic sulfur molecule to the total weight of sulfur at every temperature, are shown in Fig. 5.

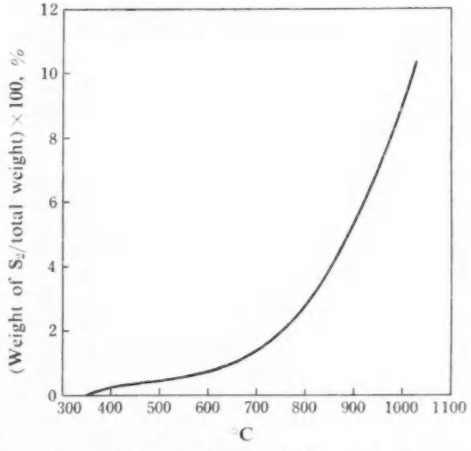

Fig. 5. (Weight of S_2/total weight)-temperature curve for sulfur.

(2) From Figs. 2 and 3, it is clear that selenium shows paramagnetism above 690°C and that the paramagnetic change occurs reversibly with temperature. Bhatnagar et al.[17] found that selenium vapor as well as sulfur vapor was paramagnetic. The ratio of the weight of the diatomic selenium molecule to the total weight of selenium was estimated in the same way as that used for sulfur. The results are given in Fig. 6.

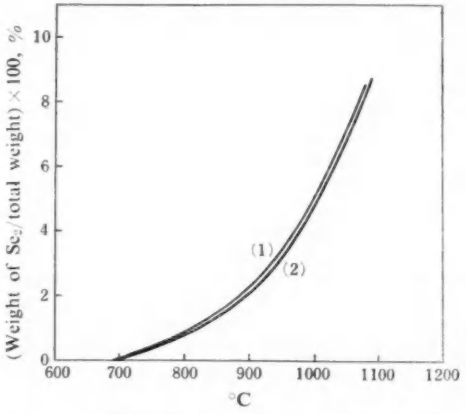

Fig. 6. (Weight of Se_2/total weight)-temperature curve for selenium.
(1) for glassy selenium.
(2) for hexagonal selenium.

(3) In contrast with sulfur and selenium, tellurium showed no paramagnetic changes until 1100°C under the present experimental condition. On the other hand, Busch et al. reported that tellurium was paramagnetic above 980°K.

Reference to Experimental Results Observed on the Physical Properties such as Viscosity, Specific Heat, Electrical Conductivity and so on.—*Sulfur.*—It is well known that liquid sulfur

7) P. Curie, *Ann. de Chem. et Phys.*, **5**, 289 (1895).
8) K. Honda and T. Sone, *Science Repts. Tōhoku Imp. Univ.*, **2**, 25 (1913).
9) M. Owen, *Ann. Physik*, **37**, 657 (1912).
10) S. Dobinski and J. Wesolowski, *Bull. intern. acad. polon. sci., Classe sci. math. nat.* **No. 8-9A**, 446 (1936).
11) K. Honda, *Ann. Physik*, **32**, 1027 (1910).
12) H. Endo, *Science Repts. Tōhoku Imp. Univ.*, **16**, 206 (1927).
13) S. R. Rao and S. R. Govindarajan, *Proc. Indian Acad. Sci.*, **10A**, 235 (1939).
14) L. Néel, *Compt. rend.*, **194**, 2035 (1932).
15) A. B. Scott, *J. Am. Chem. Soc.*, **71**, 3145 (1949).
16) J. H. Van Vleck, "Electric and Magnetic Susceptibilities", Oxford University Press, Oxford. London (1937), p. 266.
17) S. S. Bhatnagar, H. Lessheim and M. L. Khanna, *Proc. Indian Acad. Sci.*, **6A**, 155 (1937); *Nature*, **140**, 152 (1938).

has anomalies in regard to the physical properties such as viscosity[1,18,19], specific heat[20] and others[19,21] in the vicinity of 160°C. Gee[22] has interpreted these anomalies from the standpoint of the equilibrium between eight-membered sulfur rings and long chain polymers. Gee and his colaborators[23] measured the susceptibility of sulfur to investigate the existence and concentration of free radicals. They could not find any paramagnetic contribution from free radicals. On the other hand, Gardner et al.[2] confirmed the paramagnetism due to free radicals by the paramagnetic resonance absorption measurements over the range from 189° to 414°C, and stated that the paramagnetism increased reversibly with temperature. From the comparison of the present results with various results mentioned above, it can be concluded that the change in susceptibility of liquid sulfur at 157 ~171°C suggests the formation of free radicals due to the scission of the eight-membered sulfur rings. Therefore, it is reasonable to suppose from the curve in Fig. 1 that there occurred no scission of the eight-membered sulfur rings from the melting point to 157°C. Also no scission was acceptable in the temperature range from 171° to 353°C, because the curve in Fig. 1 showed no change in this range. The results mentioned above are supported by the fact that the maximum viscosity of liquid sulfur decreased rapidly with temperature in the corresponding range.

Selenium.—The change in susceptibility of hexagonal selenium at 220°C is due to phase transition on fusion, because the melting point of hexagonal selenium reported in the literature is 217.4°[24] or 220.2°C[25]. On the contrary, it is known that glassy selenium has no definite melting point. By X-ray investigations Lark-Horovitz[26] has concluded that glassy selenium consists of supercooled liquid, and that the chain structure was preserved in the liquid states. On the other hand, from X-ray analysis Krebs[27] insists that about one-third of glassy selenium is in the form of eight-membered selenium ring and the rest in poly-membered ring with about one thousand selenium atoms. From the electrical measurements on selenium, glassy selenium is an insulator and liquid selenium is a semiconductor with predominant hole conduction[28]. According to Krebs' interpretation, this difference between the electrical properties for glassy and liquid selenium can be ascribed to the difference between ring structure of glassy selenium and the chain structure of liquid selenium. It is reasonable to conclude that the decrease in susceptibility of glassy selenium at about 210°C can be attributed to the scission of selenium rings similar to the scission of sulfur at 157~171°C, and that the increases in susceptibilities of liquid selenium at about 125°C on cooling are related to the reclosing of chains into rings. No scission was acceptable in the temperature range from 220° to 690°C, because the susceptibility-temperature curves for selenium in Figs. 2 and 3 showed no abrupt changes in this temperature range. This interpretation is supported by the fact that the viscosity of liquid selenium decreases smoothly with temperature, showing no scission of rings[29].

Tellurium.—Umino[30] reported an anomaly in specific heat of solid tellurium. By X-ray investigations of tellurium layers in vacuo, Scanlon et al.[31] showed that no structure change of solid tellurium occurred up to fusion. In Fig. 4, the susceptibility-temperature curves for solid tellurium showed no abrupt changes.

Epstein et al.[32] showed that the electrical resistivity, the Hall coefficient and the thermoelectric power of tellurium decreased at the melting point of 445°C. Busch et al.[6] stated that the volume susceptibility of tellurium decreased abruptly together with the decreases in the electrical resistivity, the Hall coefficient and the thermoelectric power. In Fig. 4, the susceptibilities of samples A and B decreased in the ranges from 442° to 462°C and from 448° to 470°C, respectively. On the other hand, as the melting point of tellurium, diversely discordant values from 420° to 455°C have been listed by Machol et al.[33] The results of X-ray investigations[34] on tellurium

18) C. Farr and D. B. Macleod, *Proc. Roy. Soc.*, **A118**, 534 (1928).
19) J. Schenk, *Physica*, **23**, 546 (1957).
20) H. Braune and O. Möller, *Z. Naturforsch.*, **9a**, 210 (1954).
21) A. M. Kellas, *J. Chem. Soc.*, **113**, 903 (1918).
22) G. Gee, *Trans. Faraday Soc.*, **48**, 515 (1952).
23) F. Fairbrother, G. Gee and G. T. Merrall, *J. Polymer Sci.*, **16**, 459 (1955).
24) L. E. Dodd, *J. Am. Chem. Soc.*, **42**, 1579 (1920).
25) E. Berger, *Z. anorg. Chem.*, **85**, 75 (1914).
26) K. Lark-Horovitz and E. P. Miller, *Phys. Rev.*, **51**, 380 (1937).
27) H. Krebs, "Semiconducting Materials", Butterworths, London (1951), p. 246; H. Krebs and F. Schultze-Gebhardt, *Naturwissenschaften*, **41**, 474 (1954); *Acta Cryst.*, **8**, 412 (1955).
28) H. W. Henkel, *Phys. Rev.*, **76**, 1737 (1949); ibid., **77**, 734 (1950); *J. Appl. Phys.*, **21**, 725 (1950); H. W. Henkel and J. Maczuk, ibid., **25**, 1 (1954); P. K. Weimer, *Phys. Rev.*, **79**, 171 (1950); A. I. Blum, N. P. Mokrovskii and A. R. Regel, *Izvest. Akad. Nauk S. S. S. R., Ser. Fiz.*, **16**, 139 (1952); F. Eckart, *Ann. Physik*, **14**, 233 (1954).
29) S. Dobinski and J. Wesolouski, *Bull. intern. acad. polon. sci., Classe sci. math. nat.*, **No. 10A**, 7 (1937).
30) S. Umino, *Kinzoku-no-kenkyu*, **3**, 498 (1926).
31) W. Scanlon and K. Lark-Horovitz, *Phys. Rev.*, **72**, 530 (1947).
32) A. S. Epstein, H. Fritzsche and K. Lark-Horovitz, ibid., **107**, 412 (1957).
33) R. E. Machol and E. F. Westrum, *J. Phys. Chem.*, **62**, 361 (1958).
34) R. Buschert, I. G. Geib and K. Lark-Horovitz, *Phys. Rev.*, **98**, 1157 (1955).

immediately after fusion have shown that the number of nearest neighbors and the distance between the nearest neighbors determined for the crystal persist in the liquid state. This indicates the existence of chain molecules bound by covalent bonds in the liquid. The results of electrical investigations[28,32,35] on tellurium have shown that liquid tellurium shows a semiconducting property in which hole conduction is predominant, and that the semiconductor-metal transition occurs gradually at higher temperatures. From the results of electrical measurements Epstein et al. stated that tellurium atoms bound by covalent bonds into chains of various lengths, tellurium ions, and free electrons will be present in liquid tellurium, and that, as the temperature increases, the chains will be ionized, giving off free electrons which leave behind holes, i. e., missing covalent bonds, which in turn are able to migrate within the chains, until very high temperatures are reached, at which the liquid will be composed of tellurium ions and free electrons. It can, therefore, be considered that the decrease of susceptibility during fusion in Fig. 4 is due to a paramagnetic contribution from unpaired spins produced by incomplete ionization of the valence shell[36]. That the susceptibilities of tellurium after fusion in Fig. 4 are independent of temperature, may be owing to the mixed effects of diamagnetic and paramagnetic contributions associated with the semiconductor-metal transition mentioned above.

Summary

(1) The susceptibility of sulfur showed the first change at about 157°C, showing no changes at the melting point and its neighborhood. The change is attributed to the radical chains owing to the scission of eight-membered sulfur rings.

(2) On fusion the susceptibility-temperature curve for glassy selenium deflected toward sides opposite to that for hexagonal selenium. It is considered that the decrease in susceptibility of glassy selenium can be ascribed to free radicals produced by the scission of selenium rings. On cooling, liquid selenium turned to glassy selenium, showing the increase in susceptibility at about 125°C. It can be considered that this change is related to the reclosing of chains into rings.

(3) The susceptibility of hexagonal tellurium decreased abruptly on fusion. It may be considered that this change is due to a paramagnetic contribution from unpaired spins produced by incomplete ionization of the valence shell.

(4) The susceptibility-temperature curves for sulfur and selenium were deflected toward paramagnetic sides above 353° and 690°C, respectively. The paramagnetism increased reversibly with temperature, while the susceptibility of tellurium was independent of temperature to 1100°C. On sulfur and selenium, the ratios of the weight of the diatomic molecule to the total weight at every temperature were obtained from the weight of the diatomic molecule estimated by comparing the experimental value of paramagnetic susceptibility with the value calculated from Van Vleck's equation.

The author wishes to express his sincere gratitude to Professor Y. Nomura for his helpful suggestions and encouragement in the course of this work. The author is also indebted to Mr. T. Ashida for his valuable assistance in X-ray analysis and to Mr. S. Uchida for his kind assistance.

Department of Chemistry
Defense Academy
Yokosuka

35) N. P. Mokrovskii and A. R. Regel, *Zhur. Tekh. Fiz.*, **25**, 2093 (1955).
36) G. Busch, H. J. Stocker and O. Vogt, *Helv. Phys. Acta*, **31**, 297 (1958).

On the Mechanism of the Extraction of Uranyl Nitrate by Tributyl Phosphate II. Infrared Study

By Kenkichi NUKADA, Keiji NAITO and Utako MAEDA

(Received January 26, 1960)

The uranium extraction by TBP (tri-*n*-butyl phosphate) has been studied by many workers especially from the standpoint of distribution equilibrium. For the extraction of uranyl nitrate by TBP, the following mechanism was presented by Moore[1].

$$UO_2^{2+}(aq.) + 2NO_3^-(aq.) + 2TBP(org.) \rightleftharpoons [UO_2(NO_3)_2](TBP)_2(org.) \quad (1)$$

Naito, one of the present authors, has given an analytical method for studying the extraction mechanism and applied it to a uranyl nitrate extraction system[2]. As a result of this analysis, it was shown that the extraction of nitric acid (Eq. 2) competes with that of uranyl nitrate (Eq. 1), when uranyl nitrate is extracted by TBP from a nitric acid solution,

$$H^+(aq.) + NO_3^-(aq.) + TBP(org.) \rightleftharpoons HNO_3 \cdot TBP(org.) \quad (2)$$

However, the results obtained by the partition study were not enough to demonstrate how the TBP complex was formed from the species involved in the extracted system. In this paper the authors present the results of the infrared study concerning the mechanism of extraction. At first, discussions for the systems TBP-water, TBP-nitric acid and TBP-uranyl nitrate are given individually, and secondly the extraction mechanism of the system TBP-uranyl nitrate-nitric acid is presented.

Experimental

Perkin-Elmer Model 12C and 321 Spectrometers equipped with rock salt prisms were used in the infrared measurement. The liquid cell was constructed from spacers and frames made by polyethylene with silver chloride windows, since the usual cell made from metal spacers and frame with alkaline halide windows is attacked by nitric acid and a considerable loss of nitric acid takes place. The above-mentioned non-metallic cell, designed and constructed by the present authors, was quite useful for this experiment and the detail of the design will be reported elsewhere.

The concentration of nitric acid was determined by titration against standard alkali, and the water content in the TBP phase was determined by the Karl-Fisher titration method. The uranium concentration was determined by the alkaline peroxide method. TBP was purified by refluxing with 0.5% aqueous sodium hydroxide according to the method shown by Alcock et al.[3] In some cases, the purified TBP was further distilled in vacuo in order to remove a trace of water. Analytical-grade uranyl nitrate (after recrystallization), nitric acid and carbon tetrachloride were used.

Results and Discussion

Spectra of Pure TBP.—First of all, tentative assignment of TBP itself will be explained in order to analyze the spectra of the systems

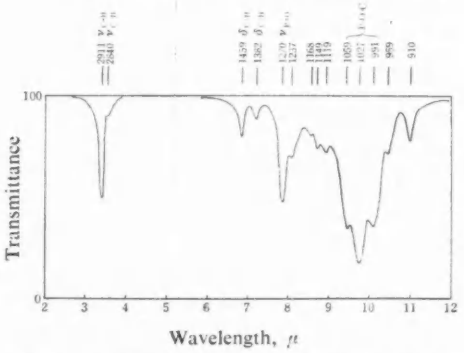

Fig. 1. Infrared spectra of pure TBP capillary.

described below. The spectrum of pure TBP is shown in Fig. 1. Two bands at 2911 and 2840 cm^{-1} are assigned to CH stretching frequencies of *n*-butyl group. Two bands at 1459 and 1382 cm^{-1} are assingned to CH_2 and CH_3 deformation frequencies of *n*-butyl group, respectively. A strong band at 1270 cm^{-1} is assigned to P=O stretching frequency according to Bellamy[4]. A triplet band at 1059, 1027 and 991 cm^{-1} is assigned to the P–O–C group. The assignment of the weak bands at 1237, 1168, 1149, 1119, 959 and 910 cm^{-1} is not clear at present.

TBP-Water System.—The infrared spectra of the system TBP-water, obtained by Cobb, have

1) R. L. Moore, *AECD-3196* (1951).
2) K. Naito, This Bulletin, **33**, 363 (1960).
3) K. Alcock et al., *Trans. Faraday Soc.*, **52**, 39 (1956).
4) L. J. Bellamy, "The Infrared Spectra of Complex Molecules", 2nd Ed., John Wiley and Sons, Inc., New York (1958), p. 258.

been mentioned in the paper by Alcock et al.[3] He has shown that as water is added to pure TBP the band due to the P=O group at 1283 cm^{-1} is shifted to 1267 cm^{-1} and a shift of 16 cm^{-1} suggests the formation of weak hydrogen bonding (with water) at P=O oxygen.

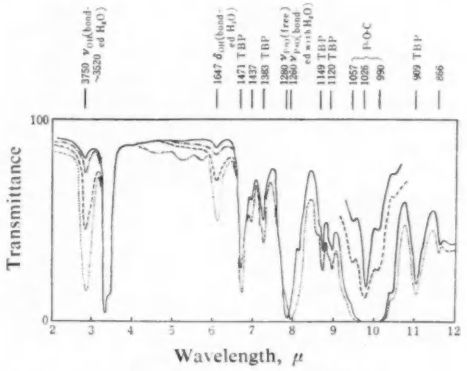

Fig. 2. Infrared spectra of TBP-H_2O system. Thickness: 0.015 mm.
—— No. 1, (0.968 mg. water per ml. of solution)
-·-· No. 2, (5.98 mg. water per ml. of solution)
---- No. 3, (31.9 mg. water per ml. of solution)
····· No. 4, (64.0 mg. water per ml. of solution)

The spectra for this system obtained by the authors are shown in Fig. 2. Samples No. 1, 2, 3 and 4 contain 0.968, 5.93, 31.9 and 64.0 mg. water per ml. of solution, respectively. It is observed from Fig. 2 that as water is added to pure TBP the band due to P=O at 1280 cm^{-1} is shifted to 1260 cm^{-1} in agreement with Cobb's result. At the same time an increase in intensities of bands at 3750~3550 and 1647 cm^{-1}, is observed which are assigned to the stretching and deformation vibrations of the OH group respectively. The positions of these two bands are near to those of stretching and deformation vibrations of free water and this fact also suggests the formation of weak hydrogen bonding between P=O oxygen and water molecules.

Since the positions of the absorption bands due to P-O-C at 1057, 1026 and 990 cm^{-1} have no appreciable change by the addition of water, it is concluded that in this system water does not bond with the P-O-C group.

TBP-Nitric Acid System.—The samples for TBP-nitric acid system were prepared as follows: 5% carbon tetrachloride solution of TBP was shaken with aqueous solution of nitric acid having various concentrations (where the volume ratio of the organic phase to the aqueous is equal to unity). After separating the organic phase from the aqueous phase, the former was used as a sample. A 5% TBP solution was used for the reason that the adequate intensities of bands can be obtained with 0.1 mm. spacer. The results of analysis for nitric acid and water contents in these samples are summarized in Table I.

TABLE 1. RESULT OF ANALYSIS FOR THE SAMPLES OF TBP-NITRIC ACID SYSTEM

Sample No.	Initial conc. (aqueous phase) of HNO_3, M	Equilibrium conc. HNO_3, M	(TBP phase) of H_2O, M
1	0	0	0.0250
2	0.995	0.0095	0.0328
3	3.41	0.099	0.0368
4	5.14	0.151	0.0267
5	7.10	0.173	0.0211
6	9.23	0.188	0.0239
7	10.83	0.192	0.0250

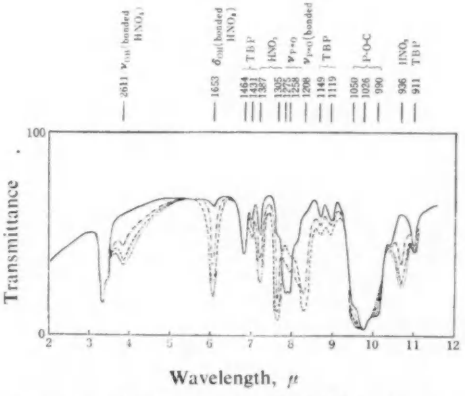

Fig. 3. Infrared spectra of TBP-HNO_3 system. Thickness 0.1 mm.
—— No. 2, (0.995 N HNO_3)
-·-· No. 3, (3.41 N HNO_3)
---- No. 4, (5.14 N HNO_3)
····· No. 5, (7.10 N HNO_3), No. 6, (9.23 N HNO_3) and No. 7, (10.83 N HNO_3)

The infrared spectra obtained for these samples are shown in Fig. 3. As the concentration of nitric acid in the TBP phase increases, the intensities of bands due to P=O at 1275 cm^{-1} and 1258 cm^{-1} decrease and one at 1208 cm^{-1} rises in its place. It is not clear at present whether the branches of the doublet due to P=O are assigned to the free and bonded (with water) P=O respectively or are to be considered as a solvent effect caused by dilution with carbon tetrachloride. A new band at 1208 cm^{-1} is assigned to bonded P=O with

nitric acid. The shift amounts to 50~66 cm^{-1} and this fact suggests a strong bonding between P=O and nitric acid. In the case of samples No. 5—7. the bands at 1275 and 1258 cm^{-1} almost disappear and the same spectra are obtained for all of these samples. Accordingly in the case of samples No. 5—7 all molecules of the TBP are entirety bonded with nitric acid at their P=O bonds. This is in agreement with the analytical data shown in Table I.

The triplet band assigned to the P–O–C group (1050, 1026 and 990 cm^{-1}) shows a change to some extent in samples No. 2—5 in which the increase in nitric acid content brings the increase in the intensity of the band at 1050 cm^{-1} together with the decrease in that at 990 cm^{-1}, whereas the intensity of the band at 1026 cm^{-1} remained unchanged. However, in the case of samples No. 5—7, little change is observed at the P–O–C band. Though it is not easy to interpret the above-mentioned change of spectra due to the P–O–C group, it may be attributed directly to the complex formation at P=O in view of the parallel nature between the spectra of the P–O–C group and that of the P=O group.

The bands at 2611 and 1653 cm^{-1}, the intensities of which are roughly proportional to the content of nitric acid in the TBP phase, are assigned to the stretching and deformation vibrations of the OH group, respectively. The band at 2611 cm^{-1} is shifted obviously from the band due to free OH stretching vibration, so that the formation of strong hydrogen bonding is also confirmed.

The intensities of bands at 1387 and 1305 cm^{-1} are also roughly proportional to the nitric acid content although the former band is overlapped with the band due to the deformation vibration of CH_3 groups of TBP at 1381 cm^{-1}. These two bands are then assigned to the bonds of the bonded nitric acid. It was found by Kamiyama[5] that when an alkaline halide window is used instead of a silver chloride window, a *single band* at 1387 cm^{-1}, which is assigned to the absorption due to the nitrate ion, appeared instead of these two bands*. It was interpreted as the result of the exchange reaction between alkaline halide and nitric acid in the TBP phase, which in turn formed nitrate ion at the surface of the window, so that the use of an alkaline halide window in this case should be strictly avoided. Tuck[6] described briefly the infrared spectra of the TBP-nitric acid system and found bands at 1400 and 810 cm^{-1}, which are assigned to the ionic organic nitrate. The discrepancy between his result and the authors' may have originated from the fact that he used an alkaline halide window.

The intensity of the band at 936 cm^{-1} is also roughly proportional to the content of nitric acid in the TBP phase. Thus the bands at 2611, 1653, 1387, 1305 and 936 cm^{-1} have the same tendency with respect to the content of nitric acid in the TBP phase, and therefore these bands are useful as the indication for bonded nitric acid in TBP phase.

TBP-Uranyl Nitrate System. — The samples used here consist of the following three samples: No. 1; 5% TBP solution (carbon tetrachloride is used as a diluent) saturated with uranyl nitrate monohydrate, No. 2; sample No. 1 was diluted with 5% TBP solution (the volume ratio equals 1 : 1), No. 3; sample No. 1 was diluted with 5% TBP solution (the volume ratio equals 5 : 1).

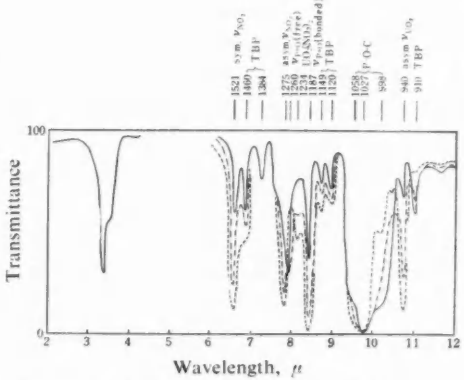

Fig. 4. Infrared spectra of TBP-$UO_2(NO_3)_2$ system. Thickness: 0.1 mm.
---- No. 1 (TBP saturated with $UO_2(NO_3)_2$)
-·-·- No. 2 (1/2 diluted solution of No. 1)
—— No. 3 (1/6 diluted solution of No. 1)

The infrared spectra obtained for these samples are shown in Fig. 4. As the solution is diluted, the intensity of the band at 1187 cm^{-1}, which the authors assign to P=O bonded with uranyl nitrate, decreases and that at 1260 cm^{-1}, due to free or bonded (with water) P=O rises in its place. The shift of frequency between the two bands amounts to 70 cm^{-1} and this fact suggests the strong complex formation between P=O and uranyl nitrate.

The triplet band assigned to P–O–C group at 1058, 1027 and 998 cm^{-1} also shows a similar appreciable change with dilution. As uranyl nitrate content in the TBP phase increases, the intensity of the band at 1058 cm^{-1} increases

5) H. Kamiyama, unpublished.
6) D. G. Tuck, *J. Chem. Soc.*, **1958**, 2783.
* Miller et al. mentioned that the ionic nitrates of alkali metals illustrates the point group D_{3h}, where the strong nitrate asymmetrical stretching frequency is centered in the region of 1380 cm^{-1} and no splitting occurs. F. A. Miller and C. H. Wilkins, *Analyt. Chem.*, **24**, 1253 (1952).

and one at 998 cm^{-1} decreases, whereas one at 1027 cm^{-1} shows little change. As in the case of TBP-nitric acid system, the change of P–O–C band may be directly related to the complex formation at P=O.

The intensities of bands at 1521, 1275, 1234 and 940 cm^{-1} are roughly proportional to the uranyl nitrate content. The band at 940 cm^{-1} is assigned to the uranyl group[7]. According to Ferraro, the former two bands are assigned to NO_2 asymmetric and symmetric stretching of covalent nitrate, respectively[8]. The assignment of the band at 1234 cm^{-1} is not clear at present.

TBP-Uranyl Nitrate-Nitric Acid System.—It is known that when uranyl nitrate is extracted from an aqueous solution of nitric acid by TBP, the extraction peak of uranyl nitrate appears at nitric acid concentration of 5~6 mol./l. in the aqueous phase. As an illustration, the result obtained by McKay is shown in Fig. 5[9]. The existence of such a peak was concluded by Naito as the result of competition to form TBP complex between uranyl nitrate and nitric acid[2]. The mechanism of extraction was described as follows; in low nitric acid concentration the extraction of uranyl nitrate predominates over the extraction of nitric acid which serves merely as a salting-out agent, whereas the increase in nitric acid concentration promotes the extraction of nitric acid into the TBP phase with the progressive replacement of uranyl nitrate by nitric acid. This illustrates the existence of the peak in the extraction curve.

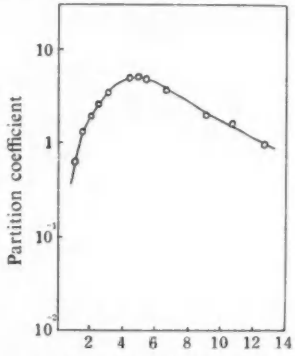

Fig. 5. Extraction of $UO_2(NO_3)_2$ by TBP. Kerosine is used as a diluent. (The original curve by H. A. C. McKay)

The mechanism obtained by the partition study was checked by the infrared spectroscopy as follows:

Replacement of Nitric Acid by Uranyl Nitrate.—Fig. 6 shows the infrared spectra in which the replacement of nitric acid by urany nitrate in TBP phase is demonstrated. The samples were prepared as follows: 5% carbon tetrachloride solution of TBP was shaken with aqueous solution of 5 N nitric acid containing uranyl nitrate of various concentrations (where the volume ratio of organic phase to the aqueous equals unity). After separating the organic phase from the aqueous phase, the former was used as a sample. The initial concentrations of uranyl nitrate in aqueous phase for samples No. 1, 2, 3 and 4 were 0.05, 0.1, 0.3 and 0.5 M, respectively.

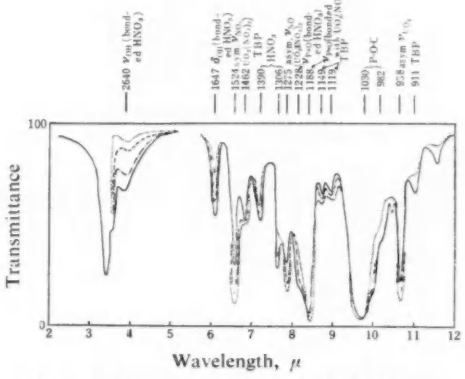

Fig. 6. Infrared spectra of TBP-$UO_2(NO_3)_2$-HNO_3 system. (a) Replacement of nitric acid by uranyl nitrate. Thickness: 0.1 mm.
—— No. 1 (Initial concentration of $UO_2(NO_3)_2$: 0.05 mol./l.)
-·-· No. 2 (Initial concentration of $UO_2(NO_3)_2$: 0.1 mol./l.)
---- No. 3 (Initial concentration of $UO_2(NO_3)_2$: 0.3 mol./l.)
····· No. 4 (Initial concentration of $UO_2(NO_3)_2$: 0.5 mol./l.)

In the spectra of Fig. 6, the bands at 1228 and 1188 cm^{-1} are assigned to the P=O bonded with nitric acid and uranyl nitrate respectively as mentioned above. As going from sample No. 1 to No. 4, the intensity of the band at 1228 cm^{-1} decreases and the one at 1188 cm^{-1} rises in its place. At the same, the intensities of the bands at 1524, 1275 and 940 cm^{-1}, which are assigned to the vibrations of uranyl nitrate, increase and those of the bands at 2640, 1647, 1390 and 1306 cm^{-1}, which are assigned to the vibrations of nitric acid, decrease.

One can obviously observe from these facts that when going from sample No. 1 to No. 4, the concentration of uranyl nitrate in the TBP phase increases, while that of nitric acid decreases, and that all sites at the P=O group initially occupied by nitric acid are progressively replaced by uranyl nitrate.

Replacement of Uranyl Nitrate by Nitric Acid.— Fig. 7 shows the infrared spectra of samples in which nitric acid expels uranyl nitrate. The samples were prepared as follows: 5% carbon tetrachloride solution of TBP was shaken with an aqueous solution of uranyl nitrate (0.05 M) containing nitric acid of various concentrations (where the volume ratio of the organic phase to the aqueous one equals unity). The initial concentrations of nitric acid in aqueous phase of sample No. 1, 2 and 3 are 2, 6 and 12 mol./l., respectively.

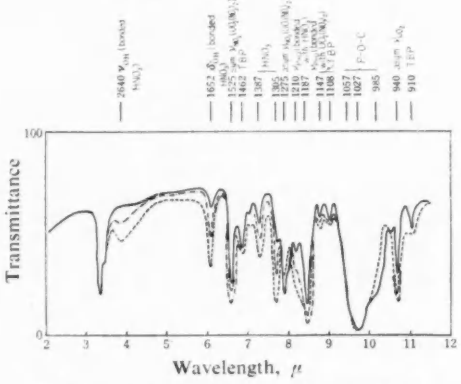

Fig. 7. Infrared spectra of TBP-$UO_2(NO_3)_2$-HNO_3 system. (b) Replacement of uranyl nitrate by nitric acid. Thickness: 0.1 mm.
—— No. 1 (Initial concentration of HNO_3: 2 mol./l.)
·-·- No. 2 (Initial concentration of HNO_3: 6 mol./l.)
---- No. 3 (Initial concentration of HNO_3: 12 mol./l.)

When going from sample No. 1 to No. 3, the intensity of the band at 1210 cm^{-1} due to P=O bonded with nitric acid increases, on the other hand that at 1187 cm^{-1} due to P=O bonded with uranyl nitrate shows a maximum in sample No. 2. At the same time, the intensities of the bands at 2640, 1652, 1387 and 1305 cm^{-1}, which are assigned to the vibrations of nitric acid, increase and those at 1525, 1275 and 940 cm^{-1}, which are assigned to the vibrations of uranyl nitrate, show a maximum at sample No. 2, except for one at 1275 cm^{-1}. The band at 1275 cm^{-1} of sample No. 1 is overlapped with the band due to free or bonded (with water) P=O at 1275~1258 cm^{-1}, therefore this band only looks to be irregular.

Thus it is evidently seen from these facts that when going from sample No. 1 to No. 3 the concentration of nitric acid in the TBP phase increases monotonously, while that of uranyl nitrate shows a maximum in sample No. 2. Therefore the peak of extraction of uranyl nitrate from nitric acid solution appears at 5~6 M of nitric acid concentration in aqueous phase beyond which the sites of P=O occupied by uranyl nitrate are progressively replaced by nitric acid.

In conclusion, the above-mentioned infrared study confirms the competition between uranyl nitrate and nitric acid in TBP phase and is in good agreement with the result obtained by the partition study.

Summary

The complex formation of TBP in the systems TBP-water, TBP-nitric acid, and TBP-uranyl nitrate was confirmed by means of infrared spectroscopy. The infrared spectra of uranyl nitrate in the system TBP-nitric acid-uranyl nitrate lead to the conclusion that the competition extraction of both uranyl nitrate and nitric acid takes place during the extraction process.

The authors would like to express their gratitude to Dr. K. Kimura, Dr. Y. Mashiko, Dr. K. Oshima and Dr. R. Hara for their invaluable assistance and advise in this work. They also wish to thank Mr. T. Suzuki for his help in the laboratory work.

Government Chemical Industrial Research Institute of Tokyo
Shibuya, Tokyo
(Nukada and Maeda)

Japan Atomic Energy Research Institute
Tokai, Ibaragi-ken
(Naito)

7) e. g. see B. M. Gatehouse and A. E. Comyns. *J. Chem. Soc.*, **1958**, 3965.
8) J. R. Ferraro, *J. Inorg. Nucl. Chem.* **10**, 319 (1959).
9) H. A. C. Mckay, Int. Conf. on the Peaceful Uses of Atomic Energy, Geneva, 1955, vol. 7, p. 314.

*Effect of Temperature on the Viscosity and the Optical Rotation of Poly-ε-aminocaproyl-α-alanine**

By Mituo EBATA

(Received November 25, 1959)

An interesting property of the synthetic poly-ε-aminocaproyl-α-alanine, an reversible coagulation by heat in acidic or neutral aqueous solution, has been shown by Noguchi and his coworkers[1,2]. In the previous paper[3] the author reported, that the coagulated form of the polymer is much more susceptible than the dissolved form, to the action of trypsin. This fact has been explained by assuming some probable difference which might be present in the structure of both forms of the polymer, although the mechanism of the reversible heat coagulation was not yet clear. Thus, it is interesting to examine the effect of temperature on some physical property of this material, especially the rotatory dispersion for the estimation of the degree of folding of the polymer chain. The present paper deals with the results obtained from experiments on the viscosity and the optical rotation of the D, L- or L-alanine polymer under several temperatures.

Experimental

The preparation method and some properties of poly-ε-aminocaproyl-D, L-alanine (M. W., 21,800) and poly-ε-aminocaproyl-L-alanine (M. W., 7,000) were described previously[3]. The polymer solution was prepared as follows: To 10 ml. of water 100 mg. of the polymer was added and the mixture was stood for over night. After filtration by a glass filter, polymer concentrations in the solution were determined by the method of Kjeldahl N-analysis. pH value of the solution was adjusted by adding 0.2 volume of M/15 phosphate buffer, if it was necessary, small amounts of N HCl or N NaOH were added.

The viscosity was measured by Ostwald's viscosimeter.

The optical rotation of the polymer was determined with the automatic recording polarimeter[4]. Measurements on the optical dispersion were made at a wavelength of 400, 437, 452, 471, 498, 527, 549 and 589.3 mμ; these were obtained from a tungsten lamp and filters except the last one which was the D line of sodium lamp. As sample tube of the polarimeter the capillary cells of 10 cm. in length were used. Temperature control of the polymer solution was carried out by varying the temperature on the water jacket of the sample tube.

Results

The specific viscosity of the polymer was found in an acidic or alkaline media as shown in Fig. 1. A minimum value of the viscosity of the D, L-alanine polymer was found at 55°C in all cases, and was independent on pH and on the concentration of the polymer. The coagulation of the polymer occured at 40 and 50°C in curves I and II respectively, while no coagulation was found in the curve III owing to its high pH value of the medium. This indicates, therefore, that the result given by curves I and II at high temperatures might be meaningless. However, an analogous curve, curve III, was obtained by an

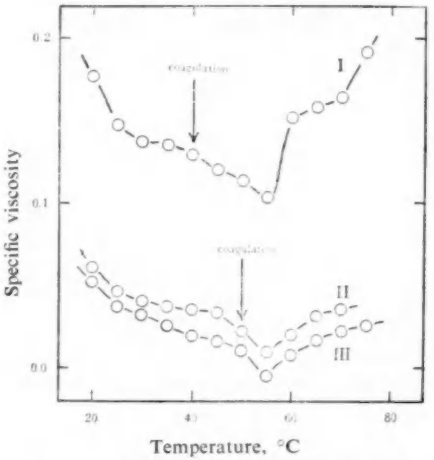

Fig. 1. Effect of temperature on the specific viscosity of the poly-ε-aminocaproyl-DL-alanine.
I: 0.65% polymer, pH 7.1
II: 0.37% polymer, pH 3.7
III: 0.37% polymer, pH 8.7 (no coagulation)
Temperature, ±0.02°C

* This work was presented at the Symposium on Protein Structure, Osaka, October, 1959.

1) J. Noguchi, T. Hayakawa, J. Suzuki and M. Ebata, *J. Chem. Soc. Japan, Pure Chem. Sect.* (*Nippon Kagaku Zasshi*), **76**, 648 (1955).

2) J. Noguchi, T. Hayakawa and M. Ebata, *J. Polymer Sci.*, **23**, 843 (1957).

3) M. Ebata, *J. Biochem.*, **46**, 383 (1959).

4) A. Tsugita, Unpublished (A part appeared in M. Ebata, A. Tsugita and S. Akabori, *Sym. on Enz. Chem. Japan*, 14, (1959), in Japanese).

experiment in the heating process, even under no coagulable conditions. Another experiment in the cooling process agreed with that of the rising one. Curve III shows, that the polymer was transformed to a different type by heating as evidenced by the appearance of a minimum viscosity. The specific viscosity at 55°C in curve III was of a negative value. Thus negative values were often found in the specific viscosity measurement, when the concentrations of the polymer were low although the reason was obscure. Similar curves were also obtained with the viscosity of the L-polymer.

The effect of temperature on the optical rotation of poly-ε-aminocaproyl-L-alanine was studied. The specific rotation of the polymer in aqueous solution was a constant value between 15° to 50°C as shown in Fig. 2. A remarkable increase in *levo*-rotation was found by heating above 53°C. This increase in the rotation was completely reversible with heating and cooling. Addition of a large amount of salts, acids, alkalis and denaturating reagents such as urea did not induce an optical rotation change of the polymer at room temperature, and no coagulation by heat was observed.

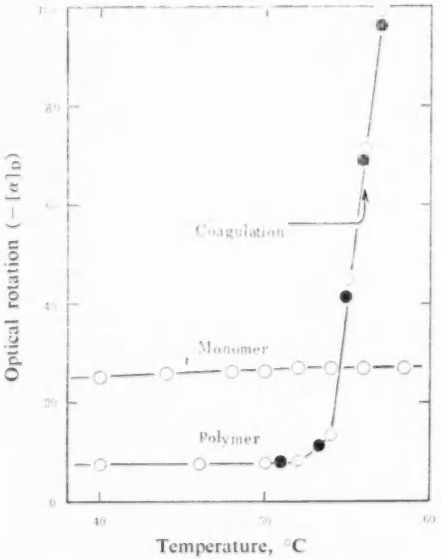

Fig. 2. Optical rotation of poly-ε-aminocaproyl-L-alanine.
Polymer, 0.47% in water (pH 4.0)
Monomer (ε-aminocaproyl-L-alanine), 0.94% in water
○, Points obtained with temperature rising
●, Points obtained with temperature falling
Temperature, ±0.05°C

The rotatory dispersion of the polymer was measured in the aqueous solutions at several different temperatures. When the measurement was made on the solution, its rotatory dispersion was belived to be obeyed Drude's one-term equation, $[\alpha]_\lambda = k_c/(\lambda^2 - \lambda_c^2)$. Where λ stands for the wavelength, $[\alpha]_\lambda$ for the specific rotation at λ, and k_c, λ_c are the rotation constant and the dispersion constant, respectively. In the present experiment the constants were estimated from the data by the usual manner. The λ_c values were 385 mμ (at 30°C), 345 mμ (at 53°C), 315 mμ (at 54°C) and 155 mμ (at 55°C) as can be seen in Fig. 3. No serious coagulation was found at 55°C under the conditions as shown in Fig. 2. Due to the appearance of coagulation, the reasonable value of λ_c could not be estimated from the rotatory dispersion measured at 56°C.

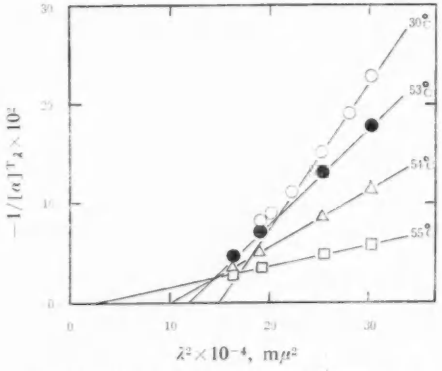

Fig. 3. Rotatory dispersion of poly-ε-aminocaproyl-L-alanine at various temperatures.
Polymer, 0.47% in water (pH 4.0)
Temperature, ±0.05°C

Discussion

The denaturation of protein is known to be accompanied by an increase in specific viscosity and *levo*-rotation and a shift of its λ_c value to shorter wavelength[5,6]. The result on the polymer reported here clearly resembles this information. When the similarity between the protein and the polymer examined here is considered, it is suggested, that a mechanism analogous with protein denaturation might be presented in the nature of the coagulation of the present sample.

According to Doty's results[6,7], a high λ_c value is a measure of the high helix content

5) K. Linderstrøm-Lang and J. A. Schellmann, *Biochim. Biophys. Acta*, **15**, 156 (1954).
6) J. T. Yang and P. Doty, *J. Am. Chem. Soc.*, **79**, 761 (1957).
7) P. Doty and R. D. Lundberg, *Proc. Natl. Acad. Sci.*, **43**, 213 (1957).

of a protein molecule. It is therefore reasonable to assume that the polymer has probably a compact structure in aqueous solution at room temperature and the structure is unfolded by heating. Then, an interesting conclusion described previously[3] that, the coagulated form of the polymer is more susceptible than the dissolved form to the action of trypsin, can be explained by this assumption.

Summary

Viscosity and optical rotation of a synthetic polymer, poly-ε-aminocaproyl-α-alanine, were studied connecting with the reversible heat coagulation. A minimum viscosity of the poly-ε-aminocaproyl-D, L-alanine solution was found at 55°C. Heating of the poly-ε-aminocaproyl-L-alanine solution produces an increase in its *levo*-rotation and a shift of its dispersion constant (λ_c value) to shorter wavelength. The mechanism of the reversible heat coagulation of the polymer was discussed to be based on the obtained result.

The author wishes to express his hearty thanks to Professor S. Akabori of our University and Professor J. Noguchi, Kanazawa University, for their interest and encouragement throughout the course of this work.

Laboratory of Biochemistry
Faculty of Science
Osaka University
Kita-ku, Osaka

Quantitative Spectrochemical Analysis of Minor Elements in Silicates with Double Internal Standards

By Hiroshi HAMAGUCHI, Rokuro KURODA and Ryokichi NEGISHI

(Received December 3, 1959)

The spectrochemical procedures for determining a number of traces of elements in silicate rocks involve some difficult problems. The fact that many of the geochemical studies on the minor elements in the lithosphere have been carried out with a semiquantitative scheme, may be, in part, attributed to the troublesome problems associated with the accurate simultaneous determination of minor elements in silicate rocks. The main difficulty arises from the different rates of volatilization of the elements from the electrode cavity into the arc column.

Ahrens[1] divided the minor elements into two groups, i. e. volatile and involatile group. For the elements of the volatile group which complete their distillation before or at the same time that the alkali metals complete theirs, Ahrens suggested a general arcing procedure with or without an internal standard. In the former case indium has been chosen as the internal standard for its volatility, satisfactory excitation properties and its extremely low concentration in most silicates. For the involatile group that includes all elements which emit their maximum line intensity after the main phase of alkali metal distillation has subsided, one part of the sample was buffered with two parts of carbon powder containing palladium as the internal standard and the mixture was completely distilled with 7 amp. d. c. carbon arc. Shaw[2] employed the total energy method for determining about 19 minor elements in silicate rocks. He also divided the subject elements into two groups according to the volatility difference of the elements, as was done in the case of Ahrens.

These schemes of quantitative spectrochemical analysis are rather tedious and even without the internal standard two arcing procedures are needed. The selection of suitable internal standards, buffer and excitation conditions may eliminate the necessity of separate arcing for volatile and involatile group. An attempt was made to determine the minor elements differing much in the volatilization rates, i. e. lead, gallium, tin, chromium, vanadium, cobalt, nickel and scandium in silicates in a single arcing procedure by using double internal standards. As a result a method was established without serious loss of precision and with reasonably high sensitivities.

1) L. H. Ahrens, "Quantitative Spectrochemical Analysis of Silicates," Pergamon Press, London (1954), p. 74.

2) D. M. Shaw, *Bull. Geol. Soc. Amer.*, **65**, 1151 (1954).

Experimental and Results

Equipment and Procedure.—To establish the procedure the densitometric and the logarithmic sector method were used. Although the logarithmic sector method is rather obsolete, some special advantages are obtained by this method. The intensity ratio of subject to internal standard lines is generally independent of conditions of exposure, slit width, development and plate calibration. The time required for the analysis is shortened by a factor of 2 or 3, compared with the densitometric method. No expensive densitometer is necessary.

Equipment and excitation conditions are listed in Table I for both calibrating methods.

Standard, Internal Standard and Buffer.—As the object for analysis is naturally occurring silicates, the general chemical composition and physical

TABLE I. EQUIPMENT AND EXCITATION CONDITIONS

Subject	Densitometric method	Logarithmic sector method
Spectrograph	Shimadzu-QL170 Littrow type quartz spectrograph	Hilger E_2, medium type quartz spectrograph
Power source	Continuous a. c. arc supplied from the Pfeilsticker type intermittent a. c. arc source unit with radiofrequency spark.	D. c. arc supplied from commercial unit with full wave rectification with radio frequency initiating spark.
Power	8 A	5 A
Working voltage	210 V.	100 V.
Preburn	None	None
Exposure	60 sec.	40 sec.
Arc gap	3 mm.	3 mm.
Electrodes	Upper: 1/4 in. diameter graphite rod (National Carbon Co., "Special Grade") The end is a 30° cone.	Upper (cathode): 5 mm. diameter graphite rod. (Shimadzu Manufacturing Co.) The end is a ca. 60° cone.
	Lower: 1/4 in diameter rod containing an axial crater 1/16 in. diameter, 1/6 in deep. (National Carbon Co. "Special Grade")	Lower (anode): 5 mm. diameter. graphite rod containing an axial crater 3 mm. diameter, 2 mm. deep (Shimadzu Manufacturing Co.)
Spectral region	2650 to 4000 Å	ca 2300 to 4500 Å
Sector	Five step sector: Step ratio 1 : 2	Logarithmic sector
Slit width	30 microns	20 microns
Densitometer	Rigaku Denki Co. Ltd. MD-2 type.	None

TABLE II. INTERNAL STANDARDS AND ANALYSIS LINES

	Element	Wavelength	Excitation potential, eV.	Analysis range, p.p.m.
Volatile group	Sb (internal standard)	2877.915	5.3	
	Ga	2943.637	4.3	10～300 (L) 10～300 (D)
	Pb	2833.069	4.4	30～500 (L) 10～1000 (D)
	Sn	3175.019	4.3	10～3900 (D)
Involatile group	Pd (internal standard)	3242.703 3481.152	4.6 4.8	
	Sc	3613.836	10.1	
	Cr	3593.488	3.4	5～500 (D)
	V	3183.982	3.9	10～400 (L) 10～1000 (D)
	Ni	3414.765	3.6	5～300 (L) 5～500 (D)
	Co	3453.505	4.0	5～300 (D) 5～1000 (L)

L: Logarithmic sector method
D: Densitometric method

properties of the standards should approximate as closely as possible those of the unknown ones. Thus, a potash feldspar was used as a base material of the standards for nickel, chromium, cobalt and scandium. It was also possible to use a serpentinite and two specimens of granite as the base materials for lead, gallium, tin and vanadium. Since traces of gallium were apparent on the granite-base material, the granite was analyzed for gallium fluorometrically (Sandell)[3] and a correction was made for the residual impurity of gallium.

For the simultaneous determination of elements with the arc excitation, it is essential to volatilize all elements in approximately the same rate from the electrode cavity. The addition of carbon causes the elements of widely different volatilities to evaporate simultaneously. Though it would be possible to suppress considerably the selective volatilization with the addition of a large amount of carbon, some loss of sensitivities will result in general. In the present work 1 : 1 ratio of carbon to each of standard and sample was selected to maintain the highest sensitivities for most elements. In the presence of such a small amount of carbon buffer the choice of internal standard is highly critical. Consequently, two internal standards were used to assure the similarity in volatilization rates for the selected pairs of subject and internal standard elements; antimony(III) oxide for the elements of volatile group i. e., lead, tin and gallium, and palladium black for the elements of involatile group i. e., nickel, cobalt, chromium, vanadium (and scandium). The carbon powder as the buffer was previously well mixed with antimony-(III)oxide and palladium black to give the concentrations 0.80 per cent for antimony(III) oxide and 0.04 per cent for palladium Selected internal standard and analysis lines are listed in Table II with their excitation potentials and analysis ranges.

Procedure for Constructing Working Curves.— To one part of the final standard one part of the carbon powder prepared as described in the previous section is added and the mixtures are excited according to the analytical conditions listed in Table I. The spectrograms are recorded on Fuji Process Hard plate. The plate is developed for 3 min. in Fuji FD 31 developer, placed in a 3% acetic acid stop bath for 30 sec., and fixed in Fuji Fixer for 5 min. After washing for 20 min. with running water, the plate is air-dried.

In the case of the densitometric method, the intensity ratios of analysis pairs were obtained by a self-calibrating method. The working curves are

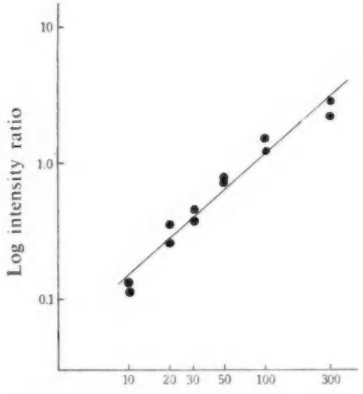

Fig. 1. Working curve for gallium (Densitometric method).
Ga 2943.637
Sb 2877.915

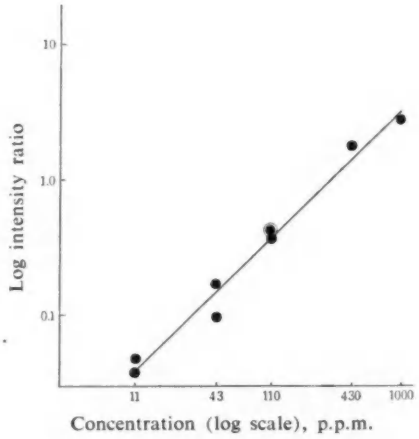

Fig. 2. Working curve for vanadium (Densitometric method).
V 3183.982
Pd 3242.703

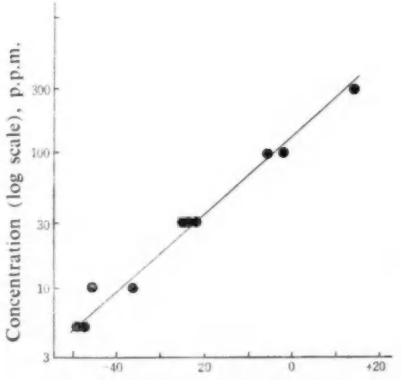

Fig. 3. Working curve for cobalt (Logarithmic method).
Co 3453.505
Pd 3481.152

3) E. B. Sandell, "Colorimetric Determination of Traces of Metals,", 2nd. Ed., Interscience Publishers, Inc., New York (1950), p. 326.

TABLE III. PRECISION DATA

D: Densitometric method, L: Logarithmic sector method

Sample	Subject element	Sx*		Mean p.p.m.		Confidence limit, 68%		Concentration range previously reported p.p.m.	Recommended value by Ahrens (1954) p.p.m.	Analysis line pair	
		D	L	D	L	D	L			D	L
W-1	Ga	0.038	0.124	13.6	18.4	14.8 ~12.5	24 ~13	11~20	14.5	Ga 2943.637 Sb 2877.915	Ga 2943.637 Sb 2877.915
W-1	Co	0.075	0.080	55	53	65 ~46	63 ~44	20~55	36	Co 3453.505 Pd 3481.152	Co 3453.505 Pb 3481.152
Potash-feldspar	Pd	0.040	0.039	177	164	194 ~161	180 ~150	6~7	—	Pb 2833.069 Sb 2877.915	Pb 2833.069 Sb 2877.915
W-1	V	0.047	0.042	236	160	263 ~212	176 ~145	170~340	240	V 3183.982 Pd 3242.703	V 3183.982 Pd 3481.152
Biotite-gneiss	Sn	0.088	0.084	48	—	59 ~39	—	—	—	Sn 3175.019 Sb 2877.915	—
W-1	Cr	0.059	—	139	—	159 ~121	—	100~150	130	Cr 3593.488 Pd 3481.152	Cr 3593.488 Pd 3481.152
W-1	Ni	0.042	0.110	59	84	65 ~54	106 ~65	47~150	90	Ni 3414.765 Pd 3481.152	Ni 3414.765 Pd 3481.152
W-1	Sc	0.119	—	280	—	368 ~213	—	15~51	37	Sc 3613.836 Pd 3242.703	Sc 3613.836 Pd 3481.152

* Sx is the standard deviation of log concentration of a sample for its single analysis.

prepared by plotting the logarithm of the intensity ratios against the logarithm of the concentrations of the elements. Typical results are shown in Figs. 1 and 2.

In the case of the logarithmic sector method, the ratio of intensities between two lines is measured by their difference in lengths. The working curves are obtained in the same manner as by the densitometric method. A typical working curve is shown in Fig. 3.

The procedure for sample analysis is almost the same as that for the standards.

Precision.—The precision of the methods was evaluated from the working curve data and from the standard diabase W-1 (U. S. Geological Survey) analysis, following the treatment of the statistical method described by Shaw and Bankier[4]. The results are listed in Table III. As tin and lead were not detected in the standard diabase W-1, a gneiss and a potash feldspar were analyzed instead of the standard W-1.

Discussion

The procedure presented could be extended to cover further species of minor elements except for extremely involatile elements, e.g., rare earth elements.

To check the accuracy of the methods, the ranges previously reported and the recommended values concerning the contents of minor elements in the standard diabase W-1 are also listed in Table III. Satisfactory agreement is observed with the recommended values by Ahrens except for cobalt, nickel and scandium.

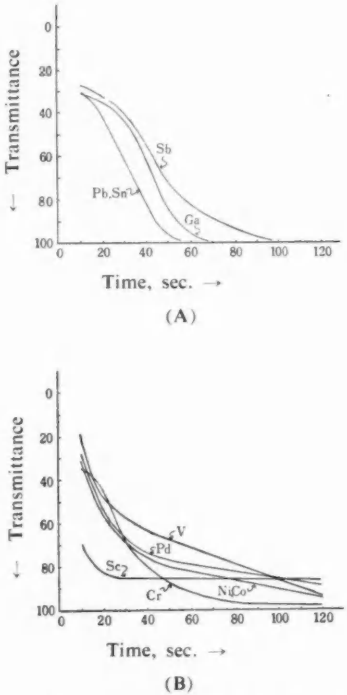

Fig. 4. Volatilization curves for the elements of valatile and involatile groups.
A: Volatile group
B: Involatile group

4) D. M. Shaw and J. D. Bankier, *Geochim. et Cosmochim. Acta*, **5**, 111 (1954).

Smales[5] has found the values 54, 52, 50, 46, 46, 45 p. p. m. Co for the W-1 with the radioactivation method of analysis which may be regarded at present as the most reliable tool for the trace analysis. The present figure for cobalt agrees rather well with the values obtained by Smales. The nickel content of the W-1 was also obtained by Smales, who gave the values of 78, 78, 76, 73, 71, 63, p. p. m. Ni. The recommended value for nickel might be somewhat higher. The present figure for scandium is remarkably high and probably in error. The cause may be attributed to the matrix effect depending on the difference in chemical composition between the potash feldspar used as a base material for the standards and the analyzed diabase W-1. The analysis line Sc II 3613.836 is an ionic line having high excitation potential (10.1 eV.) and its intensity may be largely suppressed in the low temperature arc prevailing in the excitation of the alkali-rich feldspar. The low temperature arc also accelerates the selective volatilization of scandium remarkably, as illustrated in Fig. 4. For other elements the matrix effect may not be remarkable, as judged from the comparison of given data with the recommended value by Ahrens in Table III. The matrix effect on scandium can be completely eliminated by the addition of a large amount of carbon buffer, at least three times the weight of each standard and sample, as pointed out previously by Hamaguchi and coworkers[6]. The requirement for the establishment of highly sensitive methods obliges us to compromise with a 1 : 1 weight ratio of each standard or sample to the carbon buffer. Under this circumstance the volatilization trends of the subject and the selected internal standard elements are illustrated in Fig. 4. Reasonably parallel volatilization trends are found for the pairs of the subject element and its internal standard. However, the volatilization curve for scandium differs significantly from that for palladium, as described previously.

Using the medium type spectrograph, available analysis lines are limited because of the rather complex spectrum of silicate rocks. Especially, highly sensitive analysis of tin is practically impossible owing to the coincidence of its sensitive lines with interfering lines. The entire coverage of concentration range of chromium encountered in silicate rocks is also impossible even with the utilization of several spectral lines. Thus the establishment of procedure for chromium and tin with the medium type spectrograph was not attempted.

5) A. A. Smales, ibid., **8**, 300 (1955).

6) H. Hamaguchi, K. Tomura and R. Kuroda, *J. Chem. Soc. Japan, Pure Chem. Sec.* (*Nippon Kagaku Zasshi*), **79**, 504 (1958).

Summary

Two internal standards have been used in the spectrographic analysis of silicates, antimony(III) oxide for volatile elements and palladium black for the involatile group. The former was used as the standard for the determination of gallium, lead and tin, and the latter for the determination of nickel, cobalt, chromium, vanadium and scandium. A medium spectrograph is not suitable for the determination of chromium or tin, and scandium did not volatilize in a manner parallel to the palladium but it was possible to obtain reasonable results for the other elements.

Department of Chemistry
Faculty of Science
Tokyo University of Education
Koishikawa, Tokyo

*The Transition Polymerization of Acrylamide. I. On the Polymerization Condition and the Property of Polymer**

By Naoya OGATA

(Received November 27, 1959)

Generally, amino acid tends to cause an intermolecular condensation reaction between two molecules to form a ring compound and almost never makes linear polyamide by heating. It was reported by Breslow[1] that acrylamide was polymerized into poly-β-alanine (Nylon 3) of high degree of polymerization in the presence of an alkali catalyst and an inhibitor of the vinyl polymerization. The polymerization proceeds through the transition of an amide hydrogen to a double bond of acrylamide and can be designated as the transition polymerization.

$$n\mathrm{CH_2{=}CHCONH_2} \rightarrow [\mathrm{-CH_2CH_2CONH-}]_n$$

The condition of polymerization and the property of the polymer have been investigated in this study.

Experimental

The Effect of Solvent.—Acrylamide was dissolved in various solvents at the concentration of 10% and the solution was heated at 115°C for 2 hr. in the presence of 1/32 mol./mol. of sodium-*tert*-butyrate and 0.02% of phenyl-β-naphthylamine. Polymer precipitated gradually from the solution after the addition of catalyst and adhered massively to the wall of a reaction vessel or a stirrer. Polymer was extracted with water for an hour and the weight of water-soluble and water-insoluble polymer was determined. The relative viscosity of the polymer was determined for 1% solution in 98% sulfuric acid. Polymer was hydrolyzed by sulfuric acid and the qualitative and quantitative analyses of β-alanine were carried out by paperchromatography, using a mixed solvent of *n*-butanol/ammonia =80/20 as a developer. These results are shown in Table I.

The yields of polymer are larger in the solvents of lower dielectric constant and in aromatic solvents than in aliphatic solvents. The polymerization hardly ever occurs in the solvents with active hydrogen, such as alcohol, amine or amide.

In the case of a *N*-substituted amide such as dimethylformamide or dimethylacetamide, the polymer was obtained in the form of suspension in spherical particles of about 100 μ diameters.

The Concentration of Monomer and Inhibitor.—Acrylamide was dissolved in pyridine at various concentrations and the solution was heated in the presence of sodium-*tert*-butyrate. The yield and the relative viscosity of polymer was largest at 10% monomer concentrations, as shown in Table II.

The quantity of an inhibitor of the vinyl polymerization, such as hydroquinone or phenyl-β-naphthylamine, does not necessarily affect the yield of the polymer, and poly-β-alanine is obtained without such inhibitors. These results are shown in Table III.

Contamination of water in the solvents decreases the yield of polymer and the vinyl polymerization occurs in the presence of more than 1% of water in the solvents, as shown in Table IV.

The Effect of Catalyst.—The catalytic effect of several alkali compounds was investigated in chlorobenzene at 10% monomer concentrations, which is shown in Table V. The yield of polymer is largest for tertiary alkoxide and the catalytic effect of alkali metals is in the order of K>Na>Li.

The yield of the polymer is approximately in proportion to the square root of the concentration of the catalyst, while the relative viscosity of the polymer does not change markedly, as shown in Table VI and Fig. 1.

The Rate of Polymerization.—The rates of polymerization of acrylamide were determined in various solvents at 10% monomer concentrations in the presence of 1/32 mol./mol. of sodium-*tert*-butyrate and 0.02% of phenyl-β-naphthylamine. These

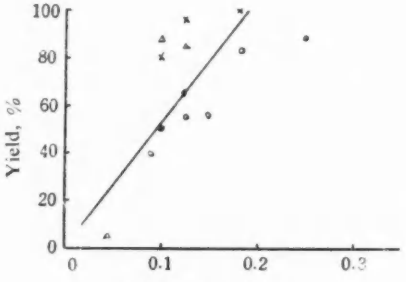

Fig. 1. The relation between the yield of the polymer and the concentration of catalyst.
○ Pyridine
× Monochlorobenzene
△ *N*,*N*-Dimethylaniline
● *N*,*N*-Dimethylformamide

* Presented at the Symposium of High Polymer, held at Tokyo on November 20, 1959, under the auspices of the Chemical Society of Japan.

1) D. S. Breslow, G. E. Hulse and A. S. Matlack, *J. Am. Chem. Soc.*, 79, 3760 (1957).

Table I. The transition polymerization of acrylamide in various solvents
(○ : colored deeply by ninhydrin)

Solvent	Dielectric constant of solvent	Water-insoluble polymer %	Water-soluble polymer %	Total polymer %	η_{rel} of water-insoluble polymer	Confirmation of β-alanine
Toluene	2.38(25°C)	22	62	84	—	○
Dowtherm-A	—	74	22	96	—	○
Tetraline	2.66(20°C)	12	81	93	1.406	○
Diphenyl	2.53(73°C)	84	16	100	1.813	○
Tricresol	5.0 (24°C)	0	0	0	—	—
Aniline	7.2 (20°C)	18	25	43	1.483	○
Monomethylaniline	5.97(22°C)	37	30	67	1.719	○
Dimethylaniline	4.91(20°C)	60	23	83	1.835	○
Chlorobenzene	5.62(25°C)	80	20	100	1.903	○
o-Dichlorobenzene	7.47(25°C)	86	12	98	1.736	○
p-Dichlorobenzene	2.86(53°C)	74	26	100	1.837	○
Nitrobenzene	35.8 (20°C)	2	98	100	—	○
Acetophenone	18.3 (20°C)	0	5	5	—	○
Pyridine	12.3 (25°C)	43	40	83	1.923	○
Quinoline	9.0 (25°C)	36	40	76	1.555	○
Dioxiane	2.21(25°C)	0	69	69	—	○
Methylcellosolve	16 (30°C)	0	0	0	—	—
Methanol	—	0	0	0	—	—
tert-Butanol	—	0	40	40	—	○
Formamide	84 (20°C)	0	0	0	—	—
Dimethylformamide	26.6 (25°C)	46	42	88	1.714	○
Dimethylacetamide	—	84	16	100	1.670	○
Adiponitrile	—	0	16	16	—	—
Mareic Anhydride	—	0	0	0	—	—

Table II. The effect of monomer concentration
(Polymerized in the presence of 1/32 mol./mol. of sodium-*tert*-butyrate and 0.02% of phenyl-β-naphthylamine at 115°C for 2 hr.)

Monomer concentration %	Water-insoluble polymer %	Water-soluble polymer %	Total polymer %	η_{rel} of water-insoluble polymer
3.5	32	24	56	1.938
5.0	42	30	72	2.043
6.6	39	28	67	2.037
10.0	43	40	83	2.010
13.4	41	37	78	1.962
20.0	43	32	75	1.975
40.0	44	32	76	1.882

Table III. The effect of an inhibitor of the vinyl polymerization
(Polymerized in pyridine at 10% monomer concentrations at 115°C for 2 hr. in the presence 1/32 mol./mol. of sodium-*tert*-butyrate.)

Kind of inhibitor	Inhibitor %/monomer	Water-insoluble polymer %	Water-soluble polymer %	Total polymer %	η_{rel} of water-insoluble polymer
Phenyl-β-naphthylamine	0	32	34	66	2.048
	0.05	34	27	61	2.062
	0.1	37	24	61	1.941
	0.2	43	40	83	2.010
	0.5	34	26	60	1.980
	1.0	37	31	68	1.955
Hydroquinone	0.1	40	—	—	—
Diphenylamine	0.2	40	—	—	—

TABLE IV. THE EFFECT OF WATER

(Monomer concentration = 10%)
(Phenyl-β-naphthylamine = 0.02%/monomer)
(Sodium-*tert*-butyrate = 1/32 mol.)
(Temperature = 115°C)

Solvent	Water content %	Time hr.	Water-insoluble polymer %	Water-soluble polymer %	Total polymer %	η_{rel} of water-insoluble polymer	η_{rel} of water-soluble polymer	Confirmation of β-alanine
Dimethyl-formamide	0.13	1	82	16	98	1.624	1.067	○
	0.61	1	70	18	88	1.544	1.087	○
	0.85	1	65	20	85	1.569	1.087	○
Monochloro-benzene	0.02	2	84	16	100	2.063	1.488	○
	1.0	3	9	89	98	—	—	×
	10.0	1	—	90	90	—	—	×

TABLE V. THE CATALYTIC EFFCT OF ALKALI COMPOUNDS
(Polymerized at the catalyst concentration of 1/32 mol./mol., with 0.02% phenyl-β-naphthylamine, at 115°C for 3 hr.)

Catalyst	Water-insoluble polymer %	Water-soluble polymer %	Total polymer %	η_{rel} of water-insoluble polymer	η_{rel} of water-soluble polymer
CH_3ONa	25	63	88	1.447	1.286
n-BuONa	66	20	86	1.780	1.147
tert-BuOLi	67	32	99	1.841	1.308
tert-BuONa	84	16	100	2.085	1.244
tert-BuOK	86	14	100	2.118	1.170
Na	9	89	98	—	1.357
NaOH	3	89	92	—	1.283
Na_2CO_3	0	0	0	—	—

TABLE VI. THE CONCENTRATION OF CATALYST

(Polymerized at 10% monomer concentration in the presence of 0.02% phenyl-β-naphthylamine for 2 hr.)

Solvent	Temp. °C	Concentration of catalyst (mol./mol.)	Water-insoluble polymer %	Water-soluble polymer %	Total polymer %	η_{rel} of water-insoluble polymer	η_{rel} of water-soluble polymer
Pyridine	115	0	0	0	0	—	—
		1/30	20	20	40	2.118	—
		1/65	32	23	55	2.033	—
		1/43	33	23	56	2.075	—
		1/32	43	40	83	2.010	—
		1/15	59	27	86	1.967	—
Monochloro-benzene	115	1/200	0	0	0	—	—
		1/100	13	67	80	1.820	1.601
		1/64	71	25	96	1.920	1.339
		1/32	84	16	100	2.082	1.287
N,*N*-dimethyl-aniline	130	1/200	0	5	5	—	—
		1/100	45	43	88	1.734	1.351
		1/64	62	23	85	1.833	1.305
N,*N*-dimethyl-formamide	130	1/200	0	0	0	—	—
		1/100	15	35	50	1.296	1.171
		1/64	35	31	66	1.462	1.173
		1/32	89	11	100	1.614	1.063

Table VII. The rate of polymerization in pyridine at 115°C

Time hr.	Water-insoluble polymer %	Water-soluble polymer %	Total polymer %	η_{rel} of water-insoluble polymer
0.5	17	42	59	1.820
1	36	34	70	1.912
2	43	40	83	2.010
3	43	40	83	1.923
5	46	22	68	1.946
7.5	54	27	81	1.826

Table VIII. The rate of polymerization in chlorobenzene

Temp. °C	Time hr.	Water-insoluble polymer %	Water-soluble polymer %	Total polymer %	η_{rel} of water-insoluble polymer	η_{rel} of water-soluble polymer
80	1	0	86	86	—	1.256
	1.5	0	95	95	—	1.251
	2	0	97	97	—	1.306
	4	0	95	95	—	1.314
	7	0	100	100	—	1.314
100	0.5	0	96	96	—	1.337
	1	0	97	97	—	1.451
	1.5	0	97	97	—	1.472
	2	4	85	89	—	1.500
	4	48	44	92	1.929	1.373
	7	74	24	98	2.035	1.318
115	0.5	15	76	91	1.905	1.488
	1	75	21	96	2.063	1.336
	1.5	82	18	100	2.095	1.283
	2	84	16	100	2.085	1.244
	4	91	9	100	2.123	1.244
	7	92	8	100	2.133	1.243

Table IX. The rate of polymerization in *o*-dichlorobenzene

Temp. °C	Time hr.	Water-insoluble polymer %	Water-soluble polymer %	Total polymer %	η_{rel} of water-insoluble polymer	η_{rel} of water-soluble polymer
100	0.25	0	86	86	—	1.343
	0.5	0	82	82	—	1.390
	0.75	0	86	86	—	1.435
	1	0	86	86	—	1.435
	1.5	0	92	92	—	1.493
	2	3	87	90	—	1.543
	4	43	42	85	2.014	1.493
	7	71	29	100	2.061	1.340
115	0.25	0	91	91	—	1.543
	0.5	9	89	98	—	1.555
	0.75	59	30	89	1.998	1.377
	1	69	23	92	2.082	1.417
	1.5	76	24	100	2.072	1.324
	2	86	12	98	2.205	1.298
	4	93	17	100	2.035	1.309

TABLE X. THE RATE OF POLYMERIZATION IN *p*-DICHLOROBENZENE

Temp. °C	Time hr.	Water-insoluble polymer %	Water-soluble polymer %	Total polymer %	η_{rel} of water-insoluble polymer	η_{rel} of water-soluble polymer
100	0.25	0.4	85	85	—	1.326
	0.50	—	94	94	—	1.390
	0.75	0.5	93	93	—	1.397
	1	0.7	93	94	—	1.433
	1.5	0.8	81	82	—	1.454
	2	17	78	95	1.946	1.452
	4	41	57	98	2.021	1.403
	7	59	41	100	2.071	1.343
115	0.25	2	96	98	—	1.428
	0.50	14	80	94	2.003	1.444
	0.75	43	49	92	1.976	1.404
	1	70	27	97	2.072	1.336
	1.5	82	18	100	2.120	1.316
	2	80	20	100	2.086	1.310
	4	91	9	100	2.163	1.315

TABLE XI. THE RATE OF POLYMERIZATION IN *N,N*-DIMETHYLFORMAMIDE

Temp. °C	Time min.	Water-insoluble polymer %	Water-soluble polymer %	Total polymer %	η_{rel} of water-insoluble polymer	η_{rel} of water-soluble polymer
115	30	0	37	37	—	1.223
	60	0	52	52	—	1.250
	90	41	37	78	1.525	1.200
	120	37	40	77	1.475	1.221
	240	59	21	80	1.500	1.100
	420	45	34	79	1.505	1.176
130	5	7	61	68	—	1.226
	10	75	17	92	1.485	1.087
	20	79	16	95	1.521	1.067
	30	83	14	97	1.605	1.061
	60	82	16	98	1.624	1.061
	120	82	18	100	1.614	1.063
144	5	55	22	77	1.386	1.084
	10	80	14	94	1.600	1.059
	20	81	16	97	1.616	1.058
	30	82	14	96	1.589	1.058
	60	81	16	97	1.569	1.057
	120	82	14	96	1.575	1.046

results are shown in Tables VII—XII.

The Property of Polymer. — *i) Melting Point.*— The melting point of water-soluble and water-insoluble polymer was determined in the nitrogen atomosphere in an electric heater, which was 330°~335°C.

ii) Infrared Spectrum.—The infrared spectrum of water-soluble and water-insoluble polymer was determined with KBr disc. by Hitachi spectrophotometer IR II. The characteristic absorption band (Amide II band) of a monosubstituted amide appears at 6.5 μ and no absorptions due to ethylenic double bond appear in comparison with the spectrum of polyacrylamide, which is shown in Figs. 2—5.

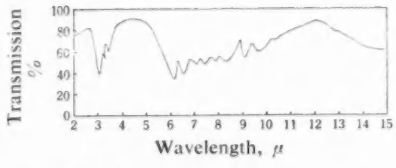

Fig. 2. The infrared spectrum of water-insoluble poly-β-alanine, which is obtained in chlorobenzene at 115°C for 30 min. (KBr disc).

TABLE XII. THE RATE OF POLYMERIZATION IN ANILINE AND ITS DERIVATIVES

Solvent	Temp. °C	Time hr.	Water-insoluble polymer %	Water-soluble polymer %	Total polymer %	η_{rel} of water-insoluble polymer	η_{rel} of water-soluble polymer
Aniline	115	0.5	16	21	37	1.541	1.229
		1	17	11	28	1.508	1.224
		1.5	22	15	37	1.497	1.234
		2	23	15	38	1.410	1.206
		4	26	15	41	1.435	1.176
		7	23	19	42	1.405	1.185
Monomethylaniline	115	0.5	8	50	58	—	1.388
		1	40	34	74	1.670	1.243
		1.5	38	37	75	1.709	1.248
		2	37	30	67	1.719	1.239
		4	40	34	74	1.670	1.243
		7	48	32	80	1.625	1.227
Dimethylaniline	115	0.5	3	80	83	—	1.354
		1	40	52	92	1.802	1.322
		1.5	61	37	98	1.810	1.296
		2	60	23	83	1.835	1.256
		4	64	32	96	1.805	1.254
		7	67	18	85	1.705	1.220

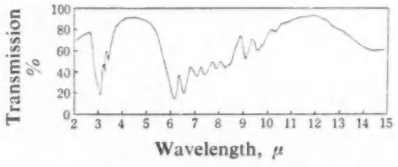

Fig. 3. The infrared spectrum of water-soluble poly-β-alanine, which is obtained in chlorobenzene at 115°C for 30 min. (KBr disc).

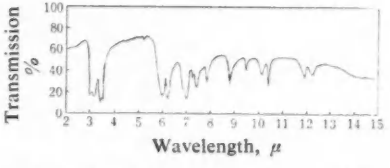

Fig. 4. The infrared spectrum of acrylamide. (KBr disc).

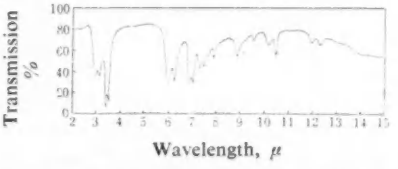

Fig. 5. The infrared spectrum of polyacrylamide. (Film).

TABLE XIII. SOLUBILITY OF POLY-β-ALANINE

Solvent	Concentration of polymer %	Solubility
1,1-Dichloroethanol-1	10	Insoluble
1,1-Dichloroethanol-2	10	〃
1,1-Dichloropropanol-2	10	〃
Trichloroethanol	10	〃
α-Dichlorohydrin	10	〃
1,1,1-Trichloroisopropanol	10	〃
m-Cresol	10	〃
Resorcinol	30	〃
52% Aqueous $SnCl_2$ solution	30	〃
50% Aqueous $CaCl_2$ solution	30	〃
Alkaline cupro-glycerol solution	30	〃
Cupro-ethylenediamine solution	30	〃
Cupro-ammonium solution	30	〃
Phosphoric acid	30	〃
ε-Caprolactam	10	〃
α-Pyrrolidone	10	〃
α-Pyperidone	10	〃
Acetamide	10	〃
Dimethylformamide	10	〃
Urea	10	Swelling
70% Aqueous $CaCl_2$ solution	30	〃
Anhydrous formic acid	30	〃
Phenol	30	〃
98% Sulfuric acid	10	Soluble
Aqua regia	30	〃
60% Nitric acid	30	〃
Anhydrous formic acid (containing 5% $CaCl_2$)	30	〃
Methanol saturated with $ZnBr_2$	10	〃
Methanol saturated with $CaCl_2$	10	〃

iii) Moisture Absorption. — The moisture content of the polymer ($\eta_{rel}=1.9-2.1$) at various relative humidities is shown in Fig. 6.

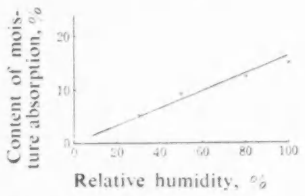

Fig. 6. The moisture content of poly-β-alanine.

iv) Solubility of polymer.—The solubility of the polymer in various solvents at 25°C is shown in Table XIII. Anhydrous formic acid containing 5% of calcium chloride is a good solvent for poly-β-alanine.

Discussion

The conversion curve of acrylamide to water-soluble poly-β-alanine shows a maximum, while the yield of water-insoluble polymer increases with time after a short induction period. The total yield of water-soluble and insoluble polymer is not affected so much with time. The final yield of water-insoluble polymer increases as the reaction temperature becomes higher. Therefore, it is expected that the transition reaction of acrylamide to poly-β-alanine occurs very rapidly as soon as a catalyst is added and then the growth of polymer follows slowly.

It is assumed that the transition of an amide hydrogen may be hindered in the solvents with active hydrogen, as the yield of polymer decreases with the amount of active hydrogen of the solvents. The alkoxide ion may decompose in the solvents with active hydrogen, as follows:

$$RO\text{-}Na + H\text{-}X \rightleftarrows ROH + Na\text{-}X$$

It is expected that the transition polymerization may proceed at first through the addition of alkoxide ion to acrylamide, because no absorptions due to double bond appear in the infrared spectrum of water-soluble polymer which is obtainded at the initial stage of the reaction.

The reaction mechanism will be proposed in a later paper, and the further investigation on the property of polymer and the application to fiber or plastics is now being carried out.

Summary

The polymerization condition for the transition polymerization of acrylamide to poly-β-alanine has been investigated in the presence of alkali catalyst. The catalytic effect of alkali catalysts is largest for tertiary alkoxide and that of alkali metals is in the order as K > Na > Li. The yield of polymer is larger in the solvents of lower dielectric constant and in aromatic solvents than in aliphatic solvents. The polymerization seldom occurs in the solvents with active hydrogen. The property of the polymer has also been investigated.

The author wishes to express his gratitude to Dr. K. Hoshino and Dr. H. Kobayashi for their instructions and permissions to publish this study, and he also thanks Mr. K. Sugii for his assistance in experiments.

Nylon Laboratory, Research Department
Toyo Rayon Co. Ltd.
Minato-ku, Nagoya

Absorption Spectra of Dyes. VI.[1] *Steric Effects in Conjugated Systems of Benzidine Disazo Dyes and their Copper Derivatives*

By Teruaki KOBAYASHI, Yoshié TANIZAKI and Noboru ANDO

(Received December 25, 1959)

The first absorption bands of dyes are considered to be due to the longest conjugated systems connected with auxochromes, and as is well known, their intensities are the highest when these systems are coplanar. For examples, ε_{max} of the first absorption band of Benzopurpurine 4B in methanol is 55,000, compared with 42,000 for that of meta-Benzopurpurine[2]. The case is the same with Congo Red. The corresponding value of it in ethanol is 54,000, while there can always be seen remarkable reductions in those of its dimethyl, dichloro and dibromo derivatives, which are prepared with the substituents introduced into the 2- and the 2'-positions of the diphenyl nucleus[3]. Such a decrease in intensity should apparently be caused by steric effects of the substituents. The same phenomena are also found for other dyes: Chlorazol Sky Blue FF has ε_{max} of 100,000, compared with 74,000 for Direct Sky Blue 5B which is different from the former only in positions of sulfonic groups. Further, their copper derivatives have weaker intensities. Such difference in intensity also seems to be caused by steric effects.

In previous works of this series, absorption spectra of dyes under various conditions have been studied mainly with respect to their first absorption bands, in order to see how they vary with aggregation or formation of complexes. In this paper, absorption spectra in aqueous solutions of both benzidine disazo dyes such as Chlorazol Sky Blue FF and their copper derivatives have been studied in connection with their stereochemical forms and steric hindrances.

Experimental

Preparation of Samples.—The following dyes were used in the present work. They will be called the abbreviations shown in the parentheses.

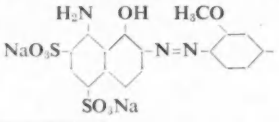

(Dye I)

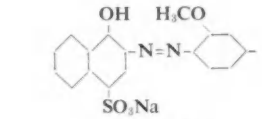

(Dye II)

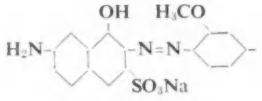

(Dye III)

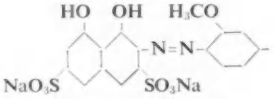

(Dye IV)

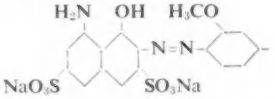

(Dye V)

Where the halves of their structures are shown. Their copper derivatives will be called Dye I', Dye II', etc., corresponding to each of them. These copper derivatives are known to have the following structures[4]; e. g., Dye I' is

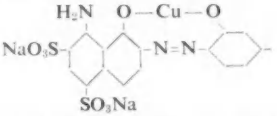

(Dye I')

Dye I—Dye V were purified by Robinson and Mills' method[5]. The copper derivatives were prepared from these dyes by a method reported elsewhere.[4],*1 The purification of them followed the above method. Found values of copper contents of Dye III' and Dye V' were 90% and 86%, respectively*2. The concentrations of dye solutions were $(1\sim130)\times10^{-6}$ mol./l., which were determined by weight.

Absorption Spectra.—All the absorption spectra were measured in 0.2 to 10 cm. cells by a Shimadzu QR-50 spectrophotometer at room temperature (ca. 20°C).

Results

The absorption spectra of Dye I and Dye I' and of Dye V and Dye V' are illustrated as

1) Part V of this series, This Bulletin, **33**, 661 (1960).
2) H. A. Standing aud M. Stein, *J. Text. Inst.*, **44**, T224 (1953).
3) F. H. Holmes, *Trans. Faraday Soc.*, **54**, 1166 (1958).
4) U. S. Pat., 2,036,159 (1935).
5) C. Robinson and H. A. T. Mills, *Proc. Roy. Soc. (London)*, **A131**, 576 (1931).
* Some of the dyes were presented by Mr. Yoshiji Ishii of the Faculty of Technology, the Gumma University.
*2 For the other dyes see the reference, Y. Ishii, *J. Soc. Tex. Cell. Ind. Japan*, **14**, 718 (1958).

TABLE I. COMPARISON OF THE FIRST ABSORPTION BANDS OF THE DYES

Dyes	Concn. mol./l×10⁵	Temp. °C	λ_{max} mμ	$\varepsilon_{max}\times10^{-4}$			Oscillator strength		
				ε	ε_c	$\frac{\varepsilon-\varepsilon_c}{\varepsilon}\times100$	f	f_c	$\frac{f-f_c}{f}\times100$
I	0.946	18~19	620	10.1			1.44		
I′	1.000	〃	596		5.1	50		1.01	30
II	1.008	〃	568	6.7			1.14		
II′	1.006	〃	555		4.1	39		0.75	34
III	15.62	15~16	562	6.2			1.22		
III′*	19.65	〃	548		4.6	26		0.96	21
IV	1.003	18~19	612	7.6			1.20		
IV′	0.997	〃	588		6.0	21		1.04	13
V	1.509	〃	612	7.4			1.21		
V′	1.275	〃	611		6.5	12		1.09	10

* See foot note 3.

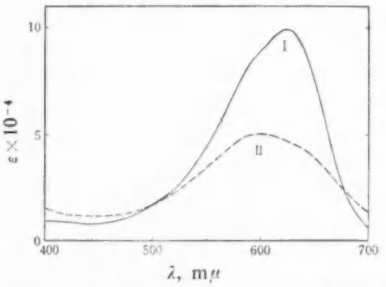

Fig. 1. Absorption spectra of Chlorazol Sky Blue FF (Dye I) and its copper derivative (Dye I′) in aqueous solution at room temperature.
I: Dye I, 1.03×10^{-5} mol./l.; II: Dye I′, 1.01×10^{-5} mol./l.

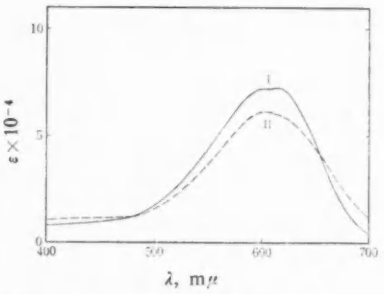

Fig. 2. Absorption spectra of Direct Sky Blue 5B (Dye V) and its copper derivative (Dye V′) in aqueous solution at room temperature.
I: Dye V, 1.13×10^{-5} mol./l.; II: Dye V′, 0.946×10^{-5} mol./l.

examples in Figs. 1 and 2 respectively, in which the full lines mean the results of Dye I and Dye V and the dotted lines those of Dye I′ and Dye V′. Inspection of them shows that the absorption intensity of Dye I is high compared with that of Dye V, and the copper derivatives have remarkably decreased intensities. The same phenomena are observed for the other dyes. In order to investigate these changes in spectra in more detail, λ_{max}, ε_{max} and oscillator strengths of the first absorption bands of the dyes are shown in Table I. Variation of the concentrations of these dyes over a wide range revealed that λ_{max}, ε_{max} and the shapes of their first bands all vary with concentrations: e.g., results of Dye IV′ are shown in Fig. 3. Therefore, the values in Table I correspond only with the respective concentrations shown in the same table and

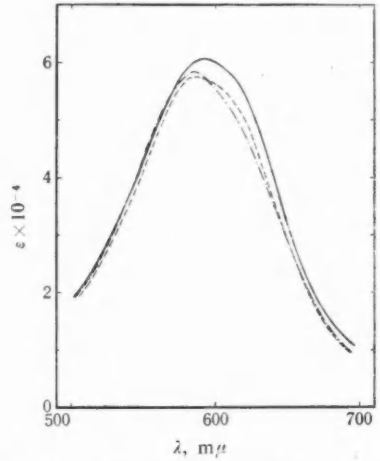

Fig. 3. Absorption spectra of Dye IV′ in aqueous solution at room temperature.
—— 1.01×10^{-6} mol./l.
---- 1.01×10^{-5} 〃
-·-· 0.87×10^{-4} 〃

will somewhat vary with concentrations*3. Oscillator strengths f were calculated by[6]

$$f = 4.31 \times 10^{-9} \int \varepsilon_\nu d\nu$$

As the calculation was carried out for the absorptions longer than 460 mμ because their train in short wavelengths were obscure, the values are not true ones. However, they will at least satisfy the purpose of mere mutual comparisons. The molecular extinction coefficients and the oscillator strengths of the copper derivatives were distinguished by the suffix c as ε_c and f_c from those of the non-copper dyes. The table shows that

1. The absorption intensity of Dye I is the highest of all.
2. All the intensities of the dyes are decreased by the introduction of copper into them. The relative order of the percentage decrease in intensity is

Dye I ≈ Dye II > Dye III > Dye IV > Dye V

The copper derivatives have nearly equal intensities to one another, except Dye II'

3. λ_{max} of each dye shifts somewhat to shorter wavelengths by the introduction of copper*4.

Discussion

As shown in the previous section, the intensities of the first absorption bands of Dye I—Dye V all decrease by the introduction of copper. Comparison of the intensities of Dye I, Dye IV and Dye V which have similar structures to one another shows that while Dye IV and Dye V have nearly equal values, Dye I has a very large one relative to them. If the first absorption bands of these dyes are due to the conjugated double bond chains connecting their auxochromes, they should be the same with one another, because they have the same conjugated chains and auxochromes. The difference in the structures of the dyes is found in positions of sulfonic groups. It should reasonably be considered that the difference in intensity was caused not by the difference in auxochromic effects of the sulfonic groups due to their positions on the naphthalene rings, but rather by their steric effects. On the other hand, the strain in a conjugated system generally causes a decrease in absorption intensity*5. Some of the present results seem to be the case: the intensity of Dye IV or Dye V, which has sulfonic groups in the positions adjacent to the azo groups is remarkably weak compared with that of Dye I which has sulfonic groups in the positions far from the azo groups. Consequently, it would be proper to discuss the experimental results with respect to the positions of sulfonic groups from the stand point of steric effects.

If the dyes are of coplanar structures, scale drawings give conformations as in Fig. 4, in which the halves of the structures of Dye I, Dye II and Dye V are shown. The figure clearly shows that a repulsion between the sulfonic group and the unshared electrons of N may be anticipated in Dye V, but not in

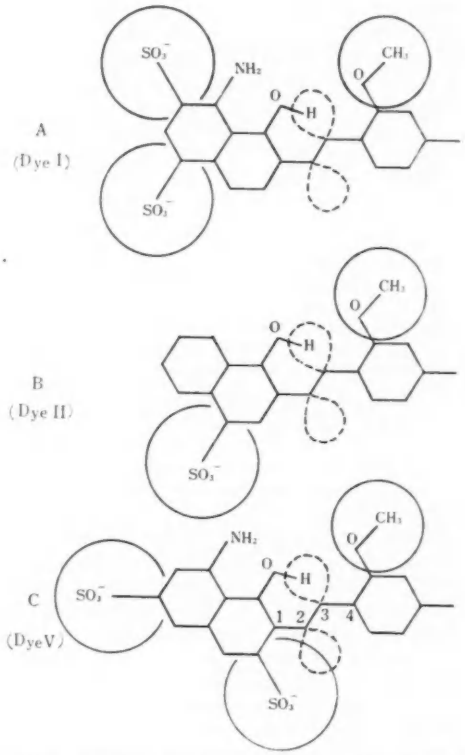

Fig. 4. Models of Dye I, Dye II and Dye V.

*3 The first absorption band of Dye III' varied remarkably with changes in outside conditions and time from preparation of its solutions till measurements. Hence, its values in Table I are less valid.

6) W. West, "Technique of Organic Chemistry", Interscience Publisher, New York (1956), Vol. IX, p. 66.

*4 The first absorption bands of these dyes are considered to be composed of two bands [Y. Tanizaki, T. Kobayashi and N. Ando, This Bulletin, 32, 119 (1959)]. In fact, their behaviors are complicated, apart from variations owing to changes in concentrations. This leads us to difficulty in our exact investigation of their behaviors.

*5 It is not always easy to predict whether absorption bands are shifted to red or blue by steric hindrances. Recently Dewar has discussed the relationship between noncoplanarity of cyanine dyes and shifts of wavelengths of their absorption (M. J. S. Dewar, "Steric Effects in Conjugated Systems", Proceedings of a Symposium held at the University, Hull, 1958, by the Chemical Society (Butterworths, London, 1958), p. 46).

Dye I and Dye II[*6]. Hence, Dye V (also Dye III and Dye IV) seems to be less planar relative to Dye I (or Dye II) because of the repulsion owing to the sulfonic group. Propriety of this expectation is proved by the fact that ε_{max} of Dye I is 100,000, compared with 74,000 for that of Dye V which has the same structure as Dye I except the positions of the sulfonic groups.

Now, let us suppose simply that in such a dye as Dye V the repulsion by the sulfonic group only results in twist of the 1–2 bond (see Fig. 4C). Then, owing to the bond twist, the repulsion between the sulfonic group and the unshared electrons of N in position 2 (N(2)) will decrease, whereas the one by the unshared electrons of N(3) will increase. The exchange integral of the 1–2 bond also changes. Hydrogen of the auxochrome OH is generally considered to form a hydrogen bond with N(3), hence the energy of the bond will also change with the twist. On the basis of such consideration, an approximate calculation of the change in energy of the molecule with the twist will be performed.

The change of the exchange integral of a bond with twist has already been studied[7]. According to this procedure, the exchange integral of the 1–2 bond is expressed by

$$V_1(\theta) = \beta S(R)\cos\theta / S(1.39) \qquad (1)$$

$$\frac{S(R) - S(1.47)}{S(1.40) - S(1.47)} = \cos\theta \qquad (2)$$

where $S(1.39)$, $S(1.47)$, $S(1.40)$ and $S(R)$ are the π–π overlap integrals of the C–C bond of benzene, the normal C–N single bond, the conjugated C–N bond of azobenzene and the 1–2 bond when its length is R corresponding to the angle of twist θ, respectively. These values can be obtained from Mulliken's Table[8].

The repulsion between the charges on the sulfonic group and of the unshared electrons may roughly be estimated, if the center of the charge on the sulfonic group is approximately taken at the point where the extension of the C–S bond crosses the plane decided by the three oxygen atoms, and the distance between this point and the center of the unshared electrons (1.2 Å from the nitrogen nucleus) is taken as that between the two charges, though the effective charges spread widely. Let us put $a_S e$ and $a_N e$ (where a_S and a_N are numerical constants) as the effective charges, with $a_S a_N = a$, and the repulsive energy is expressed by

$$V_2(\theta) = ae^2\{1/r_2(\theta) + 1/r_3(\theta)\} \qquad (3)$$

where $r_2(\theta)$ and $r_3(\theta)$ are the distances between the sulfonic group and the unshared electrons of N(2) and N(3) respectively.

As mentioned above, the auxochrome OH is considered to form a hydrogen bond with N(3). If the energy of the hydrogen bond O–H···N is approximately estimated to be -5 kcal. and is assumed to be electrostatic, it becomes

$$V_3(\theta) = -2.45/r(\theta) \qquad (4)$$

where $r(\theta)$ means the distance between hydrogen and the unshared electrons.

On putting $V(\theta) = V_1(\theta) + V_2(\theta) + V_3(\theta)$ (5)

the change in energy of the molecule becomes

$$\Delta V(\theta) = V(\theta) - V(0)$$

Fig. 5 illustrates $\Delta V(\theta)$-θ curves, which were drawn by use of various values of a appeared in Eq. 3. As a relates mainly to the effective charges of the sulfonic group and the unshared electrons, it would not exceed two. Although the above calculation is quite simple, the appearance of minima in the curves in a certain range of a suggests that the molecule becomes stable when the 1–2 bond was twisted by 50° to 60° on account of the repulsion. This coincides with the result that the absorption intensity of the dyes in which a sulfonic group is adjacent to the C–N bond is remarkably weak compared with that of the dye which has no such sulfonic group.

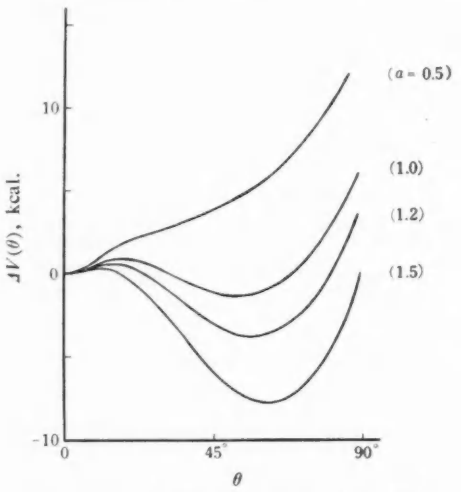

Fig. 5. The change in energy of the sterically hindered dyes with the angle of twist.

*6 The steric effect of unshared electrons of N has been discussed concerning phenyl-azo-azulene, and a reasonable result has been obtained [F. Gerson, T. Gäumann und E. Heilbronner, *Helv. Chim. Acta*, **41**, 1481 (1958)].

7) H. Suzuki, This Bulletin, **25**, 145 (1952); **27**, 597 (1954).

8) R. S. Mulliken, C. A. Lieke, D. Orloff and H. Orloff, *J. Chem. Phys.*, **17**, 1248 (1949).

Copper derivatives of *o*, *o'*-dihydroxy-azo-compounds or of similar compounds have been studied by many workers[9-11], but little is known about their stereochemical forms. In general, coplanar structures seem to be adopted[9], whereas a structure in which a copper atom is centralized on the –N=N– double bond is also considered[11]. Consequently, the stereochemical forms of the dyes studied in the present work are not yet clear.

Absorption spectra of copper derivatives of this kind have also been measured. Inspection of them reveals that intensities of their first bands are generally weak or equal as compared with those of the non-copper substances, without showing any tendency to increase. All of the present copper derivatives have decreased intensities, as mentioned in the previous section, and further a certain tendency was observed in the decrease in intensity: the decrease in intensity of the copper derivative of Dye V (or Dye IV or Dye III) which seems to have a strained conformation was slight, compared with the very remarkable one of the copper derivative of Dye I (or Dye II) which is considered to have a relatively planar conformation. Further the absorption intensities of the copper derivatives are nearly equal to one another. These results prove a great possibility that copper derivatives may have strained conformations.

9) H. D. K. Drew and J. K. Landquist, *J. Chem. Soc.*, **1938**, 292.
10) M. Elkins and L. Hunter, ibid., **1935**, 1598; F. A. Snavely and W. C. Fernelius, *Science*, **117**, 15 (1953); H. B. Jonassen, M. M. Cook and J. S. Wilson, *J. Am. Chem. Soc.*, **73**, 4683 (1951); H. B. Jonassen and J. S. Wilson, ibid., **75**, 4201 (1953).
11) L. G. Van Uitert and W. C. Fernelius, *J. Am. Chem. Soc.*, **76**, 379 (1954).

Summary

1. Absorption spectra of benzidine disazo dyes and their copper derivatives in aqueous solution were measured at room temperature, and they are compared with one another.
2. It was shown by a simple calculation that the dyes, each of which has sulfonic groups adjacent to the azo groups, have strained conformations caused by the repulsion between the sulfonic groups and the unshared electrons of nitrogen. It was also shown that the relationship between the relative positions of sulfonic groups to the azo groups and the relative absorption intensities could well be explained.
3. The absorption intensities of the copper derivatives were nearly equal, having no relation to the positions of the sulfonic groups, and in addition they were near to those of the non-copper dyes which have the sulfonic groups adjacent to the azo groups. Hence, it was pointed out that the introduction of copper caused the same extent of strain in conjugated systems as sulfonic groups did.

The authors wish to express their thanks to Mr. Yoshiji Ishii of the Gumma University for his kind present of some of the dyes.

Department of Physical Chemistry
Tokyo Institute of Technology
Meguro-ku, Tokyo

π-Electronic Structure of Diphenoquinone

By Akira KUBOYAMA

(Received January 11, 1960)

In previous papers the π-electronic structures of *p*-quinones[1] (*p*-benzoquinone, α-naphthoquinone and anthraquinone) and *o*-quinones[2] (*o*-benzoquinone, β-naphthoquinone and phenanthrenequinone) were studied by the aid of the simple LCAO MO method, with good agreement between the calculated and experimental results concerning the near UV absorption bands of these quinones. In the present paper, it is undertaken to carry out a similar study on the π-electronic structure of diphenoquinone*, the spectroscopic feature of which has never been theoretically studied.

1) A. Kuboyama, This Bulletin, **31**, 752 (1958).
2) A. Kuboyama, ibid., **32**, 1226 (1959).

Method of Calculation

As the molecular dimension of diphenoquinone(DQ) has never been known, it is

* C. A. Coulson has studied the bond orders of diphenoquinone [*Trans. Faraday Soc.*, **42**, 106 (1946)].

impossible to calculate the overlap integrals necessary for the evaluation of exchange integrals (β_{ij}). Therefore, the values of exchange integrals as well as of Coulomb integrals (α_i) were determined by referring to the corresponding values for *p*-benzoquinone(BQ)[1]. The values of these integrals eventually used for the present calculation are shown in Chart I. As it was expected that owing to the steric hindrance between hydrogen atoms at the 2, 6-positions and at the 2′, 6′-positions, two six-membered rings of DQ are somewhat twisted together around the C_1–$C_{1'}$ bond, the adopted value for $\beta_{11'}$ was a little smaller than that for β_{23}.

Chart I. Values of exchange and Coulomb integrals

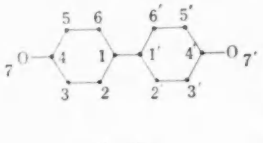

$\alpha_7=\alpha+1.3\beta$,
$\alpha_4=\alpha+0.2\beta$,
$\alpha_1=\alpha_2=\alpha_3=\alpha$,
$\beta_{47}=\beta_{23}=\beta$,
$\beta_{11'}=0.9\beta$,
$\beta_{12}=\beta_{34}=0.8\beta$

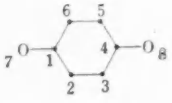

$\alpha_7=\alpha+1.3\beta$,
$\alpha_1=\alpha+0.2\beta$,
$\alpha_2=\alpha$,
$\beta_{17}=\beta$,
$\beta_{12}=0.8\beta$,
$\beta_{23}=1.1\beta$

Results

The molecular diagrams are given in Charts II and III, together with those of BQ.

Chart II. Charge densities and bond orders

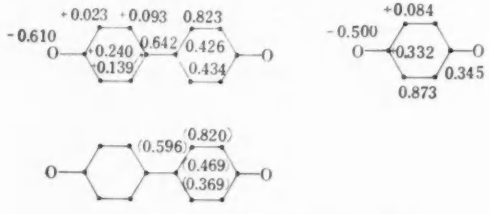

Chart III. Free valences and unpaired electron densities

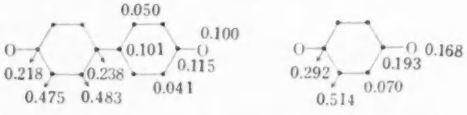

In these diagrams, the unpaired electron densities are the squares of the coefficients of atomic orbitals in the lowest unfilled orbital. The bond order values of DQ in parentheses are those obtained by Coulson**. The orbital

** In the calculation*, the adopted integral values are as follows. α_7 and β_{17} are respectively $\alpha+2\beta$, 2β and the other Coulomb and exchange integrals are all α and β, respectively.

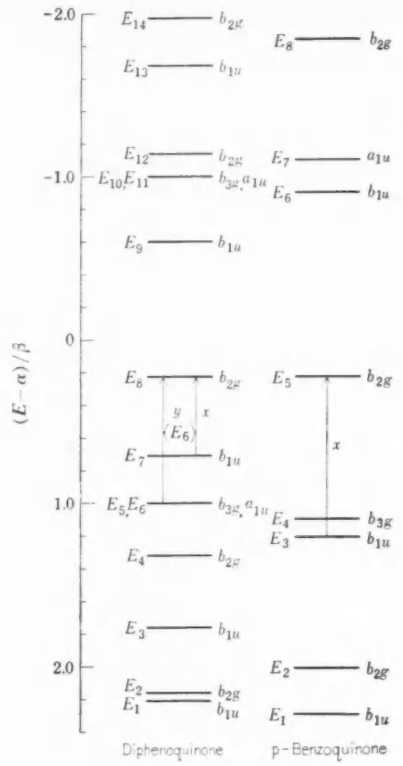

Fig. 1.

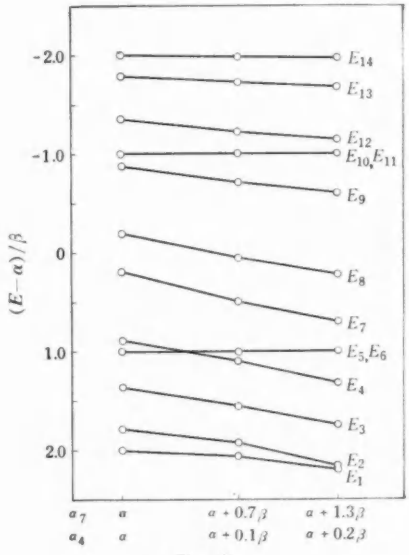

Fig. 2.

energies of DQ are given in Fig. 1, together with those of BQ. The dependence of the orbital energies upon the Coulomb integral of the oxygen atoms of DQ is shown in Fig. 2. the molecular orbitals are classified according to their symmetry properties in the symmetry group (D_{2h}), the O–O direction being taken as the x-axis and the molecular plane as the xy plane. The E_5 and E_6 orbitals as well as the E_{10} and E_{11} orbitals are accidentally degenerate. The letter "x" or "y" attached to the arrow showing a transition denotes the direction of polarization in an allowed transition. The filled and the lowest unfilled molecular orbitals of DQ are given below with their energy values. χ_i denotes the $2p\pi$ atomic orbital of the ith atom.

$$E_1\ 0.2100(\chi_1+\chi_{1'})+0.1721(\chi_2+\chi_6+\chi_{2'}+\chi_{6'})+0.2127(\chi_3+\chi_5+\chi_{3'}+\chi_{5'})+0.3726(\chi_4+\chi_{4'})+0.4091(\chi_7+\chi_{7'})$$

$$E_2\ 0.0611(\chi_1-\chi_{1'})+0.1169(\chi_2+\chi_6-\chi_{2'}-\chi_{6'})+0.2041(\chi_3+\chi_5-\chi_{3'}-\chi_{5'})+0.4058(\chi_4-\chi_{4'})+0.4701(\chi_7-\chi_{7'})$$

$$E_3\ 0.4604(\chi_1+\chi_{1'})+0.2465(\chi_2+\chi_6+\chi_{2'}+\chi_{6'})+0.0650(\chi_3+\chi_5+\chi_{3'}+\chi_{5'})-0.1654(\chi_4+\chi_{4'})-0.3616(\chi_7+\chi_{7'})$$

$$E_4\ 0.2255(\chi_1-\chi_{1'})+0.3128(\chi_2+\chi_6-\chi_{2'}-\chi_{6'})+0.2325(\chi_3+\chi_5-\chi_{3'}-\chi_{5'})-0.0075(\chi_4-\chi_{4'})-0.3804(\chi_7-\chi_{7'})$$

$$E_5\ 0.3535(\chi_2+\chi_3-\chi_5-\chi_6+\chi_{2'}+\chi_{3'}-\chi_{5'}-\chi_{6'})$$

$$E_6\ 0.3535(\chi_2+\chi_3-\chi_5-\chi_6-\chi_{2'}-\chi_{3'}+\chi_{5'}+\chi_{6'})$$

$$E_7\ 0.3459(\chi_1+\chi_{1'})-0.0406(\chi_2+\chi_6+\chi_{2'}+\chi_{6'})-0.3056(\chi_3+\chi_5+\chi_{3'}+\chi_{5'})-0.2211(\chi_4+\chi_{4'})+0.3759(\chi_7+\chi_{7'})$$

$$E_8\ 0.3185(\chi_1-\chi_{1'})+0.2246(\chi_2+\chi_6-\chi_{2'}-\chi_{6'})-0.2015(\chi_3+\chi_5-\chi_{3'}-\chi_{5'})-0.3388(\chi_4-\chi_{4'})+0.3161(\chi_7-\chi_{7'})$$

$E_1(b_{1u})$	$\alpha+2.21098\beta$	$E_8(b_{2g})$	$\alpha+0.22822\beta$
$E_2(b_{2g})$	$\alpha+2.16326\beta$	$E_9(b_{1u})$	$\alpha-0.60266\beta$
$E_3(b_{1u})$	$\alpha+1.75738\beta$	$E_{10}(b_{3g})$	$\alpha-\beta$
$E_4(b_{2g})$	$\alpha+1.31977\beta$	$E_{11}(a_{1u})$	$\alpha-\beta$
$E_5(b_{3g})$	$\alpha+\beta$	$E_{12}(b_{2g})$	$\alpha-1.13941\beta$
$E_6(a_{1u})$	$\alpha+\beta$	$E_{13}(b_{1u})$	$\alpha-1.67736\beta$
$E_7(b_{1u})$	$\alpha+0.71165\beta$	$E_{14}(b_{2g})$	$\alpha-1.97184\beta$

Discussion

Molecular Diagram.—As for charge distribution, the negative charge of the oxygen atom of DQ is a little larger than that of BQ and of anthraquinone (0.567 e). As for bond orders, the general feature of DQ is in qualitative agreement with the one obtained by Coulson. The bond order of the C_2–C_3 bond of DQ is nearly as large as that of the C_2–C_3 bond of BQ, and the bond orders of the C_1–C_2 and C_3–C_4 bonds of DQ are nearly equal. The bond order obtained by Coulson is considerably smaller in the C_3–C_4 bond than in the C_1–C_2 bond. The free valences of DQ are in general nearly equal to those of BQ. In DQ the free valency value of the C_1 atom is almost the same as that of the C_4 atom. As for the unpaired electron densities, in o- and p-quinones previously studied, the part larger than sixty percent of the total unpaired electron density exists at the two carbonyl groups, while in DQ the part smaller than fifty percent of the total unpaired electron density exists at the two carbonyl groups. The relatively large unpaired electron density value for the C_1 atom of DQ is noticeable. Unfortunately, in DQ the hfs of the electron paramagnetic resonance absorption of the semiquinone ion has never been measured due to the unstability of the ion, but for 3, 5, 3′, 5′-tetramethyl-DQ Matsunaga*** obtained the splitting constant (0.78 gauss) of the hfs due to ring protons. This value is considerably smaller than the one (1.39 gauss) calculated from the combination of the obtained unpaired electron density with McConnell's formula[3].

Energy Levels.—Concerning the energy levels given above, two points should be mentioned. First, the lowest unfilled orbital (E_8) is far lower than the other unfilled orbitals, as was previously obtained with o- and p-quinones, and is near the orbital (E_5) of BQ. Second, the highest filled orbital (E_7) is considerably higher than the ones of the p-quinones. The electronic spectrum of DQ in dioxane obtained by Hartmann and Lorenz[4] is given in Fig. 3. As is seen in Fig. 3, DQ has three adsorption bands at about 500, 390 and 260 mμ. Now these absorption bands are reasonably attributed to the transitions from the rather higher filled

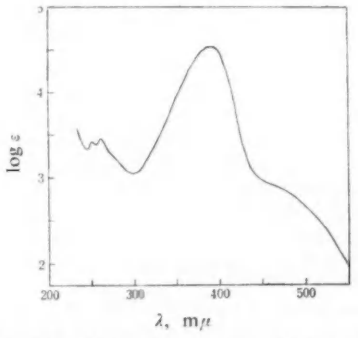

Fig. 3[4]. Electronic spectrum of diphenoquinone, solvent dioxane.

*** Unpublished data.

3) H. M. McConnell, *J. Chem. Phys.*, **24**, 632 (1956).

4) H. Hartmann and E. Lorenz, *Z. Naturforsch.*, **7a**, 360 (1952).

orbitals to the lowest unfilled orbital(E_8) of DQ. The transitions $E_1 \rightarrow E_8$, $E_5 \rightarrow E_8$ are forbidden. The dipole strengths, calculated with Mulliken's approximation[5], are 0.0014 (Å^2) and 5.97 (Å^2) for the transitions $E_6 \rightarrow E_8$ and $E_7 \rightarrow E_8$, respectively. Thus, the strong band near 390 mμ is unambiguously assigned to the transition $E_7 \rightarrow E_8 (A_{1g} \rightarrow B_{3u})$. This transition corresponds to the transition $E_3 \rightarrow E_5 (A_{1g} \rightarrow B_{3u})$ of BQ. For the $A_{1g} \rightarrow B_{3u}$ transition bands, the calculated transition energies (0.979β for BQ, 0.483β for DQ) are reasonable in comparison with the observed ones (ca. 5.0 e. V. for BQ, ca. 3.2 e. V. for DQ). The weak band near 500 mμ may be assigned to the transition $E_6 \rightarrow E_8 (A_{1g} \rightarrow B_{2u})$ or $E_5 \rightarrow E_8 (A_{1g} \rightarrow B_{1g})$, but the transition energy (0.772β) seems too great for this assignment. This band may tentatively be due to the n-π^* transition. The intensity of this band seems considerably great compared with the n-π^* transition band of other quinones but is nearly equal to that of the n-π^* transition band of *trans*-azobenzene[6]. The band near 260 mμ is tentatively assigned to the transition $E_1 \rightarrow E_g (A_{1g} \rightarrow A_{1g})$.

Summary

The electronic structure of diphenoquinone was studied with the simple MO method using the similar integral values as adopted in our previous work on *p*-quinones. The obtained result was discussed in comparison with the previously obtained one for *p*-benzoquinone. As for energy levels, the lowest unfilled orbital (b_{2g}) of diphenoquinone is far lower than the other unfilled orbitals as was obtained with the *p*-quinones The highest filled orbital (b_{1u}) of diphenoquinone is considerably higher than the ones of the *p*-quinones. From the calculated result the intense absorption band near 390 mμ was unambiguously assigned to the $A_{1g} \rightarrow B_{3u}$ transition.

The author wishes to express his sincere thanks to Professor S. Nagakura of the University of Tokyo for his kind guidance and to Dr. Y. Mashiko of this Institute for his kind offices. The author's thanks are also due to Dr. Y. Matsunaga of the University of Tokyo for his kindness in giving valuable information on the EPR data of semiquinone ions prior to publication.

Government Chemical Industrial Research Institute, Tokyo
Shibuya-ku, Tokyo

5) R. S. Mulliken, *J. Chem. Phys.*, 7, 20 (1939).
6) P. P. Birnbaum, J. H. Linford and D. W. G. Style, *Trans. Faraday Soc.*, **49**, 735 (1953).

Harmonic Oscillator Model for the Analysis of NMR Spectra of Di-substituted Benzenes

By Hiroshi SHIMIZU* and Shizuo FUJIWARA*

(Received December 28, 1959)

Since the experiments of the high-resolution spectrum of the proton magnetic resonance in organic compounds showed very fruitful results, many efforts have been made to continue the measurements and to analyze the spectra of many compounds[1]. During these measurements, one encountered spectra so complicated that they can not be analyzed by the simple inspection of the chemical formula of the samples. These complicated spectra arise in the systems where the differences of the chemical shift values, $\Delta\sigma_{ij}$, and the spin-spin coupling constants, J_{ij}, are comparable to each other, where i and j refer to the resonating nuclei, and they can be analyzed by quantum-mechanical procedures. Two methods have so far been proposed for the analysis of these complicated spectra; one was shown by Banerjee, Das, and Saha[2] in the treatments of the two- and three-proton systems and the other, which is more general than the former, was shown by McConnell, McLean and Reilley[3].

This paper concerns the analyses of such

* Present address: Department of Chemistry, Faculty of Science, The University of Tokyo, Hongo, Tokyo.

1) See, for example, Pople, Schneider and Bernstein, "High Resolution Nuclear Magnetic Resonance," McGraw Hill Book Co. Inc., New York (1959).

2) N. K. Banerjee, T. P. Das and A. K. Saha, *Proc. Roy. Soc. (London)*, **A, 226**, 490 (1954).

3) H. M. McConnell, A. D. McLean and C. A. Reilley, *J. Chem. Phys.*, **23**, 1152 (1955).

complicated spectra, using di-substituted benzenes of the type X- -Y as an example. The method to be shown here is based on the classical treatment of the nuclear magnetic resonance (NMR) phenomena, and is assumed to be helpful for chemists who are not familiar with the quantum-mechanical procedures to obtain the necessary understanding of the analysis of the NMR spectrum.

Analysis of NMR Spectrum by a Harmonic Oscillator Model

First, the nuclear magnetic resonance of a molecule which has only one hydrogen atom is considered. As there is no interest in the time-dependent phenomena, the equation of the classical or macroscopic vector $\vec{M}$ placed in a static magnetic field $\vec{H}_0$ may be written as

$$d\vec{M}/dt = \gamma\vec{M}\times\vec{H}_0 \qquad (1)$$

where, γ is the gyromagnetic ratio of proton. Eq. 1 is the formula given by Bloch[4]. The intensity of the signal due to the nuclear magnetic resonance can be measured by the x-component $\vec{M}(z//H_0)$ when $\vec{M}$ is forced to flip down onto the x-y plane by the interaction of the nucleus with the oscillating magnetic field $\vec{H}_1(t)$ which rotates in the x-y plane with the angular frequency ω_0. Thus, the resonance angular frequency is defined as that of $\vec{H}_1$ which flips $\vec{M}$ most effectively, called as the angular frequency of the Larmor precessional motion of $\vec{M}$ in the field of $\vec{H}_0$. Hence, we can calculate the resonant frequency and the relative intensity of the spectrum, even if we omit the effect of $\vec{H}_1$, and the contribution of $\vec{H}_1$ is taken into account in the considerations of the amplitude of the precession.

From (1), it is easily seen that M_x behaves as a simple harmonic oscillator which obeys Eq. 2 at resonance:

$$d^2M_x/dt^2+\omega_0^2M_x=0 \qquad (2)$$

On the other hand, the equation of the motion of a simple harmonic oscillator may be written as

$$m(d^2X/dt^2)+fX=0 \qquad (3)$$

where m and f are the mass and the force constant of the oscillator. Eq. 3 will become equal to Fig. 2 by making the following interpretation:

$$X=M_x,$$
$$f=\gamma H_0=\omega_0 \text{ and} \qquad (4)$$
$$m=1/\omega \ (=1/\omega_0 \text{ at resonance})$$

4) F. Bloch, *Phys. Rev.*, **70**, 460 (1946).

These relations can be extended to any many-spin system by slight modification of the definition of the force constants. For example, the straightforward extension to a two-spin system composed of two protons, A and B, may be made by additional replacement of the force constant, f, by the spin-spin coupling constant J as

$$f_{AB}=\pm J_{AB}/2 \qquad (4a)$$

A positive sign is used when $\vec{M}_A$ and $\vec{M}_B$ are parallel, and the negative sign antiparallel. The situation of this model of the interacting oscillators is illustrated in Fig. 1. The interaction energies of these oscillators refer the off-diagonal terms of secular equations, where the sign of eac term his taken to be positive as well as that of J. Justification of this choice of the sign will be given later.

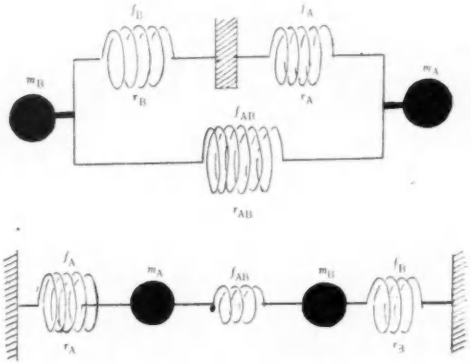

Fig. 1. Explanation of the oscillator model.
(a) $f_{AB}=J_{AB}/2$
(b) $f_{AB}=J_{AB}/2$

The potential energy of the system may be written as Eq. 5,

$$V=1/2\cdot[f_A(\Delta r_A)^2+f_{AB}(\Delta r_{AB})^2+f_B(\Delta r_B)^2] \qquad (5)$$

where r_A, r_B and r_{AB} are the elongations of the springs, A, B and C, whose force constants are f_A, f_B, and f_{AB}, respectively. The expression (5) may be rewritten by the Cartesian coordinate x as

$$\begin{aligned} V&=1/2\cdot[(f_A+f_{AB})x^2_A+2f_{AB}x_Ax_B \\ &\quad+(f_B+f_{AB})x^2_B] \\ &=1/2\cdot[(\omega_A+J_{AB}/2)M^2_{Ax}+J_{AB}M_{Ax}M_{Bx} \\ &\quad+(\omega_B+J_{AB}/2)M^2_{Bx}] \end{aligned} \qquad (6)$$

In Eq. 6 we used the relations, $\Delta r_A=x_A$, $\Delta r_B=-x_B$ and $\Delta r_{AB}=x_A+x_B$.

The kinetic energy of the system, T, is as shown by

$$T=m[\dot{x}^2_A+\dot{x}^2_B]/2 \tag{7}$$

$$=[\dot{M}^2_{Ax}+\dot{M}^2_{Bx}]/2\omega \tag{7a}$$

As the x-y components of the magnetic vectors, $\vec{M}_{Axy}$ and $\vec{M}_{Bxy}$ rotate about the z-axis, the x-components of these vectors may be written as

$$\left.\begin{aligned} M_{Ax}&=M_{Axy}\cos\omega t \\ M_{Bx}&=M_{Bxy}\cos\omega t \end{aligned}\right\} \tag{8}$$

Substituting Eq. 8 into Eqs. 6a and 7a, the motion of M_{Ax} and M_{Bx} are given by the classical equation of motion,

$$\frac{d}{dt}\left(\frac{\partial T}{\partial \dot{M}_{ix}}\right)+\frac{\partial V}{\partial M_{ix}}=0 \quad (i=A,\ B)$$

which leads a set of two homogeneous equations,

$$(\omega_A+J_{AB}/2-\omega)M_{Ax}+J_{AB}M_{Bx}/2=0 \tag{10}$$

$$J_{AB}M_{Ax}/2+(\omega_B+J_{AB}/2-\omega)M_{Bx}=0 \tag{10a}$$

These equations have a non-vanishing solution only when the determinant of the coefficients of M_{Ax} and M_{Bx} is zero, i.e.,

$$\begin{vmatrix} \omega_A+J_{AB}/2-\omega, & J_{AB}/2 \\ J_{AB}/2, & \omega_B+J_{AB}/2-\omega \end{vmatrix}=0 \tag{11}$$

and from the secular equation (11), we obtain the relation,

$$\omega_0=1/2\cdot[(\omega_A+\omega_B)+J_{AB}\pm(\sigma^2{}_{AB}+J^2{}_{AB})^{1/2}] \tag{12}$$

where $\sigma_{AB}=\delta_A-\delta_B$ is the chemical shift between the protons of A and B. Similar treatment of model 2b gives the resonant frequency,

$$\omega_0=1/2\cdot[(\omega_A+\omega_B)-J_{AB}\pm(\sigma^2{}_{AB}+J^2{}_{AB})^{1/2}] \tag{12a}$$

It is reasonable to assume that the energy absorbed by the system at resonance is proportional to the magnitude of the mean kinetic energy of the oscillator, i.e., to the square of the vector $\vec{M}_{xy}=\vec{M}_{Axy}+\vec{M}_{Bxy}$. Hence, the relative intensity of the spectrum at the frequency ω_0, $I(\omega_0)$, is calculated from Eq. 10 or 10a with the normalization condition of the magnetic vector, (13),

$$M_{Axy}(\omega_0)^2+M_{Bxy}(\omega_0)^2=1 \tag{13}$$

as

$$I(\omega_0)=[M_{Axy}(\omega_0)+M_{Bxy}(\omega_0)]^2 \tag{14}$$

$$=1-2\frac{(\omega_A-\omega_0)(\omega_B-\omega_0)}{(\omega_A-\omega_0)^2+(\omega_B-\omega_0)^2} \tag{15}$$

The calculated spectrum is shown in Fig. 2.

Although the present method of analysis is based on the classical treatment of an oscillator model, it is shown that the results of this analysis are in accordance with those to be obtained quantum-mechanically.

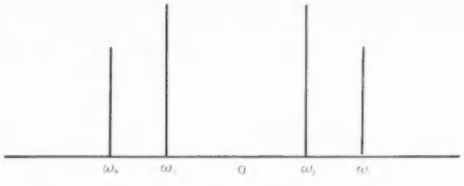

$$\omega_1=\frac{1}{2}\left[J_{AB}+\sqrt{\sigma^2+J^2_{AB}}\right],\quad I(\omega_1)=\left|-\frac{J_{AB}}{\sqrt{\sigma^2+J^2_{AB}}}\right|$$

$$\omega_2=\frac{1}{2}\left[-J+\sqrt{\sigma^2+J^2}\right],\quad I(\omega_2)=\left|+\frac{J}{\sqrt{\sigma^2+J^2}}\right|$$

$$\omega_3=\frac{1}{2}\left[J-\sqrt{\sigma^2+J^2}\right],\quad I(\omega_3)=\left|+\frac{J}{\sqrt{\sigma^2+J^2}}\right|$$

$$\omega_4=\frac{1}{2}\left[-J-\sqrt{\sigma^2+J^2}\right],\quad I(\omega_4)=\left|-\frac{J}{\sqrt{\sigma^2+J^2}}\right|$$

Fig. 2. Calculated spectrum.

The quantum-mechanical Hamiltonian of a two-spin system in a laboratory coordinate system may be expressed as

$$\mathcal{H}=-\gamma_A\vec{I}_A\cdot\vec{H}_A-\gamma_B\vec{I}_B\cdot\vec{H}_B+J_{AB}\vec{I}_A\cdot\vec{I}_B \tag{16}$$

The time-dependent Schroedinger equation is given by Eq. 17 in a rotating coordinate system which rotates with angular velocity, $\vec{\omega}$, as

$$i\hbar\dot{\Psi}_r=[-\gamma_A\vec{I}_A(\vec{H}_A+\omega/\gamma_A)-\gamma_B\vec{I}_B(\vec{H}_B+\omega/\gamma_B)+J\vec{I}_A\vec{I}_B]\Psi_r \tag{17}$$

The fields at I_A and I_B are effectively reduced to zero, provided that the angular velocities of the coordinates are given by

$$\vec{\omega}_A=-\gamma_A(\vec{H}_A-J_{AB}\vec{I}_B/\gamma_A) \tag{18}$$

and

$$\vec{\omega}_B=-\gamma_B(\vec{H}_B-J_{AB}\vec{I}_A/\gamma_B) \tag{18a}$$

If we return to the laboratory coordinate system, the effective fields at $\vec{I}_A$ and $\vec{I}_B$ are written as

$$\vec{H}_A-J_{AB}\vec{M}_B/2\gamma_A \tag{19}$$

and

$$\vec{H}_B-J_{AB}\vec{M}_A/2\gamma_B \tag{19a}$$

respectively.

By assuming the macroscopic equations which have the same form as Eq. 1, we obtain the equations,

$$d\vec{M}_A/dt=\gamma_A\vec{M}_A\times(\vec{H}_A-J_{AB}\vec{M}_B/2\gamma_A) \tag{20}$$

and

$$d\vec{M}_B/dt=\gamma_B\vec{M}_B\times(\vec{H}_B-J_{AB}\vec{M}_A/2\gamma_B) \tag{20a}$$

By taking the time-independence of the components of M_{Az} and M_{Bz} into consideration,

Eqs. 22 and 22a are substituted into Eqs. 21 and 21a, respectively.

The equations for the x-components of Eqs. 20 and 20a are

$$dM_{Ax}/dt=(\gamma_A-J_{AB}M_{Bz}/2)M_{Ay}+J_{AB}M_{By}M_{Az}/2 \quad (21)$$

and

$$dM_{Bx}/dt=(\gamma_B-J_{AB}M_{Az}/2)M_{By}+J_{AB}M_{Ay}M_{Bz}/2 \quad (21a)$$

where

$$\left.\begin{aligned}M_{Ax}&=M_{Axy}\cos\omega t\\M_{Ay}&=-M_{Axy}\sin\omega t\end{aligned}\right\} \quad (22)$$

and

$$\left.\begin{aligned}M_{Bx}&=M_{Bxy}\cos\omega t\\M_{By}&=-M_{Bxy}\sin\omega t\end{aligned}\right\} \quad (22a)$$

Experimental

Calculations and measurements of the NMR spectra were performed for the di-substituted benzenes of the type of X- -Y: *p*-aminobenzoic acid was dissolved in a concentrated aqueous solution of potassium hydroxide, and *p*-toluidine, *p*-nitrophenol, and *p*-nitrobenzaldehyde were dissolved in carbon tetrachloride, methanol and acetone, respectively. These solutions were saturated at 28°C and sealed in the glass tubes with the diameter of 3.5~3.8 mm.

The apparatus of the NMR measurements is the one constructed in this laboratory having the same structure as the one reported by Gutowsky et al. before[5], and operated at the frequency of 27.030 Mc. The samples were spinned during the measurements. The separations of each component of the spectra were measured on the recorded charts using the records of ethanol as the standard reference: the J value of the coupling between the methyl and methylene groups in ethanol was taken as 6.90 cps.[5]

Discussion

In Fig. 3, the spectrum for the anisaldehyde is shown as an example of NMR measurements. The values of the chemical shift and the spin-spin couplings were calculated from Eqs. 12 and 12a as listed in Table I. The maximum error in the results of Table I is about 10%, which is assumed to be mainly due to the fluctuations in the chart speed of the recorder. Rigorously speaking, the compounds used here are not the two-spin system, but belong to four-spin system, and the values listed in Table I contain some error due to this approximation. But, this error is assumed to be quite small.

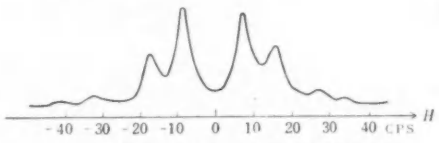

Fig. 3. The spectrum of anisaldehyde. Resonance frequency=27 Mc.

Table I. J and σ values of the ring protons of X- -Y type molecules

Res. freq. = 27 Mc.

X	Y	J cps.	σ cps.
-CHO	CH_3O-	8.62	24.2
-COOH	NH_2-	8.21	30.1
$-CH_3$	NH_2-	8.70	13.54
$-NO_2$	HO-	9.06	31.1
$-NO_2$	OHC-	9.24	6.6

It is seen in Table I that the σ's are dependent on the species of the substituents of X and Y, whereas J's are not dependent with a constant value of about 8.7($\pm$0.5) cps. If we can assume that an additive law holds with the chemical shifts of the ring protons, δ, of monosubstituted benzenes, the magnitudes of σ's could be related by the relation,

$$|\sigma|=|(\delta_X{}^o-\delta_Y{}^m)-(\delta_Y{}^o+\delta_X{}^m)| \quad (23)$$

where, for example, $\delta_X{}^o$ and $\delta_Y{}^m$ refer to the chemical shifs of *ortho*-proton of X and the meta-proton of Y, respectively.

We calculated the magnitudes of σ by using the values of δ's for the monosubstituted benzenes reported by Corio and Dailey[7], and compared the calculated results with those obtained experimentally. Agreements are not good between the σ's of calculation and of observation whereas the observed values of σ's showed good proportionality to $|\delta_x{}^o-\delta_y{}^o|$. This seems to suggest that the additivity does not hold with the δ's for the ring protons of di-substituted benzenes.

The authors are indebted to Professor Shōji Shibata and Professor Tyūnoshin Ukita and to Miss Motoko Nakahara of the University of Tokyo for their help in the preparation of the samples. Thanks are also due to Mr. Ichiro Yamaguchi of the Japan Atomic Energy Research Institute, who kindly sent us the preprint of his work on the substituted benzenes.

University of Electro-Communications
Chofu, Tokyo

5) H. S. Gutowsky, L. Meyer and R. E. McClure, *Rev. Sci. Inst.*, **24**, 644 (1953).
6) J. T. Arnold, *Phys. Rev.*, **102**, 136 (1956).
7) P. L. Corio and B. P. Dailey, *J. Am. Chem. Soc.*, **78**, 3043 (1956).

*Polyethers. III. Polymerizations and Polymers of Some Substituted Ethylene Oxides**

By Shin'ichi ISHIDA**

(Received December 18, 1959)

A variety of polyethers has been prepared by ring-opening polymerization of cyclic ethers, for example from ethylene oxide[1], propylene oxide[2], fluorine-containing olefine oxides[3], oxacyclobutanes[4] and from tetrahydrofuran[5].

A systematic survey in this field will offer an interesting new field for studies both on stereospecific polymerization and on structure of crystalline polyethers.

In the light of this consideration, polymerizations of some substituted ethylene oxides were tried with attempts to obtain crystalline polymers by a stereospecific polymerization for some oxides of the types.

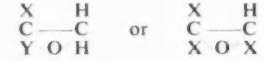

The present paper is in the nature of a survey and a tentative report on some oxides involved.

Experimental

Materials.—*1-Chloro-2-methyl-2-propanol.*— It was prepared by Burgin's method[6]. After the treatment of 90 g. of methallyl chloride with molar proportion of 80% sulfuric acid at 5~10°C for 2.5 hr. with vigorous stirring, the reaction mixture was hydrated on cracked ice. The chlorohydrin was distilled as a constant boiling mixture which, after being salted out, redistilled, b. p. 126~129°C. The yield was about 40~50% (63~66% reported).

1,1-Dimethyl Ethylene Oxide.— The preceding chlorohydrin (50 g.) was slowly added to powdered potassium hydroxide (120 g.) with stirring at such a rate that the temperature of the distillate did not exceed 55°C. When the reaction ceased the remaining volatile matter was distilled off under water pump vacuum at room temperature to a trap cooled at −70°C. The total condensate was dried with potassium hydroxide and fractionated to yield the desired oxide; 25 g., 63% of theory, b. p. 50.2~50.5°C. n_D^{20} 1.3730 (reported b. p. 53°C, n_D^{20} 1.3730)[7].

2-Methyl-3-chloro-2-butanol.—It was prepared from 3-chlorobutanone-2 (b. p. 114°C) obtained by chlorination of methylethylketone in the presence of marbel and methyl magnesium bromide by Fourneau's method[8]. 20% yield of light yellow liquid boiled at 140°C (reported b. p. 141~142°C). This chlorohydrin was also prepared by the action of hypochlorous acid on trimethyl ethylene in some runs but the yield and the purity were rather poor.

1,1,2-Trimethyl Ethylene Oxide.—It was prepared by dehydrochlorination of trimethyl ethylene chlorohydrin. Dehydrochlorination was carried out in all cases by adding the chlorohydrin slowly on to solid potassium hydroxide with stirring. The yield was about 30% based on the chlorohydrin.

Tetramethyl Ethylene Oxide.— Anhydrous pinacol (115 g.) obtained from acetone was treated with molar proportion of anhydrous hydrogen chloride (41 g.) at 35~45°C and the resulting chlorohydrin was recrystallized (melted at 63°C) and treated as above with solid potassium hydroxide to produce the epoxide (35 g.), b. p. 90~93°C, n_D^{20} 1.3985 (lit. b. p. as reported[9], n_D^{20} 1.3986). The yield was 13% based on anhydrous pinacol.

1-Methyl-1-phenyl-2-chloro Ethanol.—It was prepared by King's procedure[10] from monochloroacetone and phenylmagnesium bromide.

The reaction mixture was stirred at −10°C during the addition of Grignard reagent under the protection of dry nitrogen and then allowed to warm slowly to room temperature after being kept standing overnight. To the cold reaction mixture was then added dropwise with stirring a solution of ammonium chloride (100 g.) in water (400 ml.). The ether layer was separated and the aqueous layer was extracted with ether. The combined ether extracts were washed once with 250 ml. of water and dried over anhydrous sodium sulfate. Removal of the ether by distillation gave a crude residue (50 g.) which was fractionated under reduced pressure. Eighty grams (72.7%) of the product distilled at 109~112°C/12 mmHg were obtained (lit. b. p. 129~132°C/21 mmHg).

1-Methyl-1-phenyl Ethylene Oxide.—The chlorohydrin was decomposed with sodium ethoxide to give methylphenyl ethylene oxide. A colorless liquid

* Presented at the 8th Annual Meeting of the Society of the Polymer Science of Japan, Tokyo, May, 1959. Part I and II: This Bulletin, 33, 727, 731 (1960).

** Present address; The Textile Research Laboratory, Asahi Chemical Industry, Co. Ltd., 118 Ama, Takatsuki, Osaka.

1) H. Staudinger, "Hochmolekularen Organischen Verbindungen", Springer (1932), p. 287.

2) For example; C. C. Price et al., *J. Am. Chem. Soc.*, **78**, 690, 4787 (1956).

3) D. D. Smith et al., *Ind. Eng. Chem.*, **49**, 1241 (1957).

4) A. C. Farthing et al., *J. Chem. Soc.*, **1955**, 3648.

5) K. Hamnan, *Angew. Chem.*, **63**, 231 (1951).

6) J. Burgin and G. Hearne, *Ind. Eng. Chem.*, **33**, 385 (1941).

7) W. T. Somerville, *J. Am. Chem. Soc.*, **72**, 737, 2185 (1950).

8) M. M. Fourneau and M. Tiffeneau, *Compt. rend.*, **145**, 437 (1907).

9) F. H. Norton, *J. Am. Chem. Soc.*, **58**, 2147 (1936).

10) L. F. King, ibid., **61**, 2383 (1959); W. J. Hickinbottom et al., *J. Chem. Soc.*, **1954**, 4200.

b. p. 75～76°C/12 mmHg (lit.[10] b. p. 72～75°C/11 mmHg).

1,1-Diphenyl-2-chloroethanol.—To a stirred solution of ethyl chloroacetate (84 g.) in dry ether (300 ml.) was added dropwise over a period of 4.5 hr. a solution of phenylmagnesium bromide previously prepared from magnesium (36.5 g.) and bromobenzene (252 g.) in dry ether (650 ml.). The reaction mixture was maintained at 0 to −5°C and then treated according to the procedure similar to the synthesis of 1-methyl-1-phenyl-2-chloroethanol. The product was isolated by distillation under reduced pressure and purified by recrystallization from ligroin. A yield 46 g. (26%), m. p. 53～56°C (lit. m. p. 52～57°C).

1,1-Diphenyl Ethylene Oxide.—A yield of an almost quantitative amount of crude oxide (m. p. 42～45°C) was obtained by action of the chlorohydrin on the aqueous solution of sodium hydroxide by Zaugg's method[11]. Twice recrystallization from absolute ethanol gave a pure oxide, m. p. 55～56°C (reported m. p. 56～57°C).

1,1-Diethyl-2-chloroethanol.—It was prepared by the same procedure used in the synthesis of 1,1-diphenyl-2-chloroethanol. To a stirred solution of ethylchloroacetate (65 g.) in dry ether (300 ml.) was added a solution of ethylmagnesium bromide previously prepared from magnesium (24 g.) and ethyl bromide (109 g.) in dry ether (200 ml.). Resulting chlorohydrin was obtained in a yield of 44%, b. p. 66～67°C/16～18 mmHg (lit.[12] b. p. 70°C/20 mmHg).

1,1-Diethyl Ethylene Oxide.—It was prepared by the conversion of the chlorohydrin by the same procedure as in the synthesis of 1,1-dimethyl ethylene oxide mentioned above. Thirty grams of the chlorohydrin gave 15 g. of the raw epoxide, which gave by the fractional distillation a distillate boiling at 105～106°C (lit. b. p. 107°C).

General Procedure of Polymerization.—A catalyst was added to a monomer or a monomer solution in a glass tube which was flashed by nitrogen previously and then cooled in dry ice-acetone.

The tube was sealed and placed in a constant temperature bath. At the end of the reaction time, the tube was recooled and opened. To the reaction mixture, a small quantity of methanol or some appropriate agents for stopping the reaction were added and the resulting polymer was washed thoroughly with methanol so as to remove the catalyst residue. In the case when the reaction product was an oil it was dissolved in acetone and precipitated with a large volume of methanol.

Results and Discussion

1, 1-Dimethyl Ethylene Oxide (D. M. E. O.).—1,1-Dimethyl ethylene oxide was attempted to polymerize by different catalysts and some details were given in Table I. The polymer was found to consist of two fractions; fraction I was insoluble in acetone, benzene, methanol and ether and soluble in hot tetrahydrofuran, dioxane and dimethylformamide, except in some cases, where a small quantity of the insoluble part in these solvents was contained. Fraction II was soluble in acetone but insoluble in methanol.

Fraction I, a white and nontacky powder, was shown by X-ray examination to be crystalline. The melting points of these materials obtained from the different catalysts varied from 127 to 155°C. Fraction II was usually a white solid, melting at about 90～100°C, but in the case, where diethyl zinc and $FeCl_3$-PO was used as catalyst, it was a tacky semi-solid or a pasty mass.

As may be seen in Table I, the polymerization with the catalysts borontrifluoride etherate (BF_3-Et_2O) and triethyl aluminum ($AlEt_3$) and diethyl zinc ($ZnEt_2$) respectively proceeded very rapidly at low temperatures;

Table I. Polymerization of 1,1-dimethyl ethylene oxide with different catalysts

Catalyst	wt. %	Reaction temp. °C	Time hr.	Yield, %	Fraction, %		m. p. of I, °C
					I	II	
$FeCl_3$-PO	5	70	64	15.0	42	58	—
$FeCl_3$[a]	5	80	20	15.6	major	minor	—
BF_3Et_2O	5	r. t.	24	considerable	major	minor	159～160
$TiCl_4$	3.5	−78-r. t.	48	28.5	68.0	32.0	—
$TiCl_4$	3.0	r. t.	3 days	25.9	83.0	17.0	127
AIP[b]	2	80	20 days	nil	—	—	—
AIP-$ZnCl_2$[c]	2	80	6 days	nil	—	—	—
$AlEt_3$[d]	3.5	−78-r. t.	6 days	57.2	91.4	8.6	155
$AlEt_3$	5	r. t.	5	—	27.2	—	152
$ZnEt_2$[e]	5	r. t.	4 days	46.8	83.4	16.6	151～152
$ZnEt_2$-Al_2O_3[f]	2	r. t.	20 days	nil	—	—	—

a) anhydrous ferric chloride, b) aluminum isopropoxide, c) aluminum isopropoxide-zinc chloride, d) trimethyl aluminum in *n*-hexane, e) diethyl zinc in diethyl ether, f) diethyl zinc on alumina.

11) H. E. Zaugg et al., *J. Am. Chem. Soc.*, **80**, 2770 (1958).

12) R. Dalebroux and H. Wuyps, *Chem. Zentr.*, **1906 II**, 1179.

TABLE II. COPOLYMERIZATION OF 1,1-DIMETHYL ETHYLENE OXIDE (M_1) WITH EPICHLOROHYDRIN (M_2) USING $AlEt_3$ AS CATALYST IN *n*-HEXANE AT LOW TEMPERATURE

M_1 in comonomer		Total conversion	Fraction, %		Chlorine content	m. p. of I	X-ray pattern
wt. %	mol. %	%	I	II	in I, %	°C	of I
100	100	57.2	91.0	9.0	—	155	DMEO
68.0	74.0	22.6	36.6	63.4	8.66	125	DMEO
41.3	47.0	34.3	8.5	91.5	37.37	117	EpCl
19.0	23.0	39.1	84.9	15.1	—	—	EpCl
0	0	72.7	73.7	26.3	—	117	EpCl

Fraction I: methanol-insoluble part, Fraction II: methanol-soluble part

TABLE III. COPOLYMERIZATION OF 1,1-DIMETHYL ETHYLENE OXIDE (M_1) WITH EPICHLOROHYDRIN (M_2) BY 4% OF $AlEt_3$ IN *n*-HEXANE AT 80±0.5°C

M_1 in comonomer		Total conversion	Fraction			Chlorine content	m. p. of I	X-ray pattern
wt. %	mol. %	%	I	II	III	in I, %	°C	of I
86.4	89.8	80.8	16.7	83.3		2.44	140	DMEO
68.0	74.0	47.0	13.4	54.3	32.3	2.22	140	DMEO
41.3	47.0	76.6	4.3	3.2	92.5	36.45	117	EpCl
19.0	23.0	83.8	9.5	11.5	79.0	32.07	117	EpCl

the reaction mixture was solidified as soon as the catalyst was added. Aluminum isopropoxide (AIP) and the one in conjunction with zinc chloride (AIP-$ZnCl_2$)[13] as well as diethyl zinc-alumina system[14] were completely inactive for this monomer in contrast to the fact of their being active for propylene oxide.

Copolymerizations of 1,1-dimethyl ethylene oxide with epichlorohydrin (EpCl) were also studied. Epichlorohydrin was chosen for the convenience of its analysis and $AlEt_3$ was used as catalyst because of the feasibility of its purification from resulting polymer compared with those from $FeCl_3$-PO catalyst. Some runs of polymerization were carried out at a low temperature. (The catalyst was added to the monomer solution in a glass tube cooled in dry ice-acetone, the reaction started and the reaction mixture was solidified immediately, and then the glass ampoule was placed in a water bath and kept at room temperature for further promotion of polymerization.) The other runs were done in an oil bath at 80°C from the beginning. The resulting products were in both cases fractionated by the precipitation method. In the case at low temperature, the products were divided into two fractions; methanol-insoluble fraction (I) and methanol-soluble fraction (II). In the latter case at the higher temperature, the product was separated into three fractions; acetone-soluble fraction (I'), acetone-soluble but methanol-insoluble fraction (II') and methanol-soluble fraction (III). These results were shown in Tables II and III.

In both the cases, there existed a minimum of conversion versus monomer composition fed in the range of monomer composition of about 70% of 1,1-dimethyl ethylene oxide (M_1) in comonomer, and this corresponded also with a minimum yield of fractions I, I' and II' at about 40% of M_1. Of these fractions, fractions I and I' were white powders and these two were examined in some details. Melting points, chlorine contents and X-ray patterns of these fractions showed that these fractions were either homopolymer of D. M. E. O. or that of EpCl depending upon the preference of one monomer in the monomer composition.

The critical monomer composition coincided with the composition corresponding to a minimum percent of fraction I and I'.

From the results mentioned above, it may be seen, in this comonomer system, that a crystalline copolymer had not been obtained and fractions I and I' are both of the pure homopolymers.

1,1,2-Trimethyl Ethylene Oxide (tri-M.E.O.). —This oxide was polymerized neither with $FeCl_3$-PO nor with AIP-$ZnCl_2$ as catalyst but with BF_3Et_2O it was rapidly polymerized at low temperature to a viscous liquid (Table IV). A tacky solid or an elastic mass could be obtained only with $AlEt_3$ at room temperature. The polymer was soluble in ether and acetone but insoluble in methanol.

1,1,2,2-Tetramethyl Ethylene Oxide (tetra-M. E. O.). —Both the catalysts $AlEt_3$ and AIP-$ZnCl_2$ were inactive for the polymerization

13) M. Osgan and C. Price, *J. Polymer Sci.*, **34**, 153 (1959).
14) J. Furukawa et al., ibid., **36**, 541 (1959).

TABLE IV. POLYMERIZATION OF 1,1,2-TRIMETHYL ETHYLENE OXIDE

Catalyst	%	Temp., °C	Time, hr.	Conversion, %	Remarks
BF_3Et_2O	0.5	−68-r. t.	24	ca. 98	viscous liquid
$FeCl_3$-PO	ca. 2	80	20 days	none	
AIP-$ZnCl_2$	2	80	1 month	none	
$AlEt_3$	2	r. t.	68	57.0	tacky solid

TABLE V. POLYMERIZATION OF TETRAMETHYL ETHYLENE OXIDE

Catalyst	wt. %	Solvent	Temp., °C	Time, hr.	Conversion, %
BF_3Et_2O	2	CH_2Cl_2	r. t.	72	51.3
AIP-$ZnCl_2$	2	benzene	80	5 days	none
$AlEt_3$	5	benzene	r. t.	〃	trace
〃	5	none	r. t.	〃	trace

of this monomer but BF_3Et_2O gave a crystalline polymer (Table V). The polymer neither melted and nor decomposed even at 300°C. No usual organic solvents could be found for this polymer but the polymer was swollen by decalin or tetralin at 80~90°C. An attempt to copolymerize this monomer with 1,1-dimethyl ethylene oxide by BF_3Et_2O was failed and gave only polymer of tetra-M. E. O. which was proved by X-ray examination, melting point and solubility (Table VI).

TABLE VI. ATTEMPTED COPOLYMERIZATION OF TETRAMETHYL ETHYLENE OXIDE (M_1) with 1,1-dimethyl ethylene oxide
catalyst: BF_3-Et_2O 2% wt.,
solvent: methylene chloride,
temp.: r. t., reaction time: 4 days

M_1 in comonomer mol. %	Total conversion wt %	Remarks
100	51.3	Poly-tetra-M. E. O.
90	20.6	〃
75	5.9	〃
50	3.9	〃
25	trace	〃
10	1.8	〃
0	36.7	Poly-D.M.E.O.

1-Methyl-1-phenyl Ethylene Oxide (M.P.E.O.)—BF_3Et_2O, $AlEt_3$ and $ZnEt_2$ were active to polymerize this epoxide which was converted into viscous liquid polymers which were insoluble in methanol. BF_3Et_2O gave a reddish brown oily polymer, while the others gave colorless polymers.

No polymer could be obtained with AIP-$ZnCl_2$ system even after prolonged heating at 80°C for two days. $FeCl_3$-PO catalyst gave a colored oily product accompanied by a small quantity of needle crystals whose structure has not yet been determined in this work.

1.1-Diphenyl Ethylene Oxide (D.P.E.O.).—$AlEt_3$ and AIP-$ZnCl_2$ were inactive for this monomer while both BF_3Et_2O and $TiCl_4$ were active catalysts. To a cooled solution of the oxide in methylene dichloride, the catalyst, for instance BF_3Et_2O 3% by weight was added slowly and the reaction mixture was sealed and placed in a dry ice-acetone bath for two days. The glass ampoule was then opened and an ammoniacal methanol was poured into the ampule and the product was washed thoroughly with methanol.

The product (38.5% yield) was needle crystals and did not melt at 300°C but was found to sublime slightly. This material was believed to be a ring dimer of the epoxide

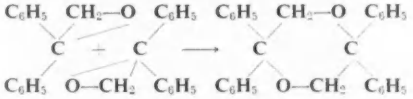

and was shown from the elemental analysis and the molecular weight determination, both of which were demonstrated in good accordance with a calculated value for the ring dimer (Table VII).

TABLE VII. SOME ANALYSIS OF THE REACTION PRODUCT

	C	H	O	Mol. wt*
Obs.	87.75	6.24	8.01	383
Calc. for ring dimer	85.68	6.16	8.15	392.3

* by cryoscopic method using camphor

Infrared spectra of the product showed the absence of the characteristic absorption band of hydroxyl group at near 3500 cm^{-1} and disappearance of bands of epoxy ring observed in the monomer at 825 and 925 cm^{-1}. Bands associated with an epoxy ring of monomer epoxide were estimated to be at 825 and 925 cm^{-1} by comparative method of spectra of 1, 1-diphenyl ethylene, its polymer[15] and 1.4-

15) K. Kuwata et al., *J. Chem. Soc. Japan, Pure Chem. Section* (*Nippon Kagaku Zasshi*), **80**, 25 (1959).

TABLE VIII. INFRARED SPECTRA OF THE POLYMERS FROM FOUR METHYL-SUBSTITUTED ETHYLENE OXIDES

Propylene oxide (cryst.)		D.M.E.O.		Tri-M.E.O.		Tetra-M.E.O.	
cm^{-1}	Relative intensity	cm^{-1}	Relative intensity	cm^{-1}	Relative intensity	cm^{-1}	Relative intensity
2980	7	2970	6	2975	8	2990	6
2910	sh 8	2920	5	2940	7	2960	sh 6
2880	sh 8	2880	4.5	2885	sh 5	2880	sh 2
1480	8 cr	1465	3.5	1465	4.5	1477	3.5
1453	9						
1375	10	1386	4	1370	6.5	1377	6
1342	8	1354	6	1360	6.5	1361	6
1330	8 cr						
1293	9	1266	2				
1240	8 cr	1245	b 2	1235	b 1		
1140	8 cr	1163	8.5	1160	7.5	1163	9
1105	9	1115	8	1105	9	1120	10
				1090	9		
1038	8.5 cr			1044			
1010	8	1013	3.5	1020	b 4		
				993	4	985	b 5
				970	b 2	975	4.5
932	9 cr			930	b 2	944	b 2
917	8.5	890	5.5			905	b 2
905	sh 6						
866	4.5					714	1
831	6						

sh: shoulder absorption band, b: broad band, cr: crystalline sensitive band*.

TABLE IX. SOME PHYSICAL PROPERTIES OF POLYMERS OF SUBSTITUTED ETHYLENE OXIDES

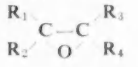

	R_1	R_2	R_3	R_4	m. p., °C	Remarks
PO	CH_3	H	H	H	72	crystalline
D.M.E.O.	CH_3	CH_3	H	H	155	crystalline
Tri-M.E.O.	CH_3	CH_3	CH_3	H	—	amorphous, pasty
Tetra-M.E.O.	CH_3	CH_3	CH_3	CH_3	<300	crystalline
M.P.E.O.	CH_3	C_6H_5	H	H	—	amorphous, liquid
D.P.E.O.	C_6H_5	C_6H_5	H	H	—	ring dimer

TABLE X. X-RAY DIFFRACTION SPECTRA OF CRYSTALLINE POLYMER

Propylene oxide		D.M.E.O.		tetra-M.E.O.	
Spacing, Å	Relative intensity	Spacing, Å	Relative intensity	Spacing, Å	Relative intensity
5.17	s	5.20	vs	6.04	vs
		4.58	w	4.61	w
4.23	s	4.12	s		
4.05	w	3.53	m	3.43	s
3.63	w	3.03	s	2.96	vw
3.46	w	2.79	m	2.68	w
3.10	w	2.54	m	2.31	m
2.78	w	2.23	w		
2.61	w	2.12	m		
		1.96	w		

* Part I. This Bulletin, 33, 727 (1960).

dioxane and these bands were in agreement with 877 (11.40 μ), 812 (12.3 μ) cm^{-1} of styrene oxide and 863 (11.85 μ), 786 (12.72 μ) cm^{-1} of α-methyl styrene oxide oberved by Patterson[16] (Fig. 1).

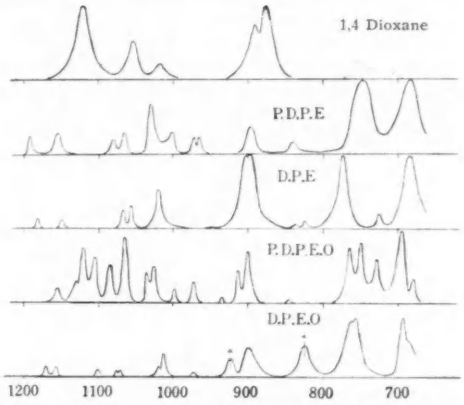

Fig. 1. Infrared spectra of diphenyl ethylene oxide and related compounds; D.P.E.O.; diphenyl ethylene oxide P.D.P.E.O.; polymer of D.P.E.O., D.P.E.: diphenyl ethylene, P.D.P.E.: polymer of D.P.E. Epoxy bands were marked by triangle.

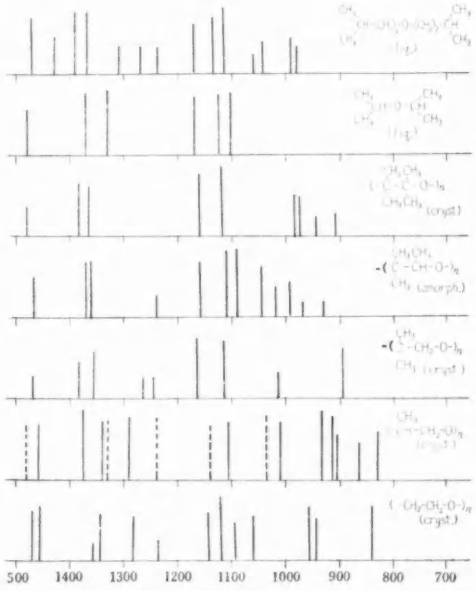

Fig. 2. Infrared spectra of polymers of methyl-substituted ethylene oxides and some related ethers (dotted line: crystalline sensitive bands).

Since absorption bands characteristic of 6-membered carbon oxygen ring had been noted to occur at near 11 μ and in the range 1124~1030 cm^{-1} by Shreve[17], bands at near 1100 cm^{-1} and 912 cm^{-1} which appeared in the spectra of the dimer, would be bands characteristic of ring ether.

1,1-Diethyl Ethylene Oxide.—Using both BF_3Et_2O and $TiCl_4$ as catalyst, no polymer-like substance could be obtained while a resin-like material was produced by $AlEt_3$ as catalyst. But no further experiments could proceed because of paucity of the material.

Infrared spectra of polymers from four methyl-substituted ethylene oxides together with some related ethers for comparison were shown in Fig. 2 and their characteristic bands were tabulated for comparison in Table VIII.

Some properties of polymers were summarized in Table IX and X-ray spectra of crystalline polymers were shown in Table X and Figs. 3 and 4.

The action of $AlEt_3$ as polymerization catalyst for epoxides used in this experiment might well be compared with those of cationic

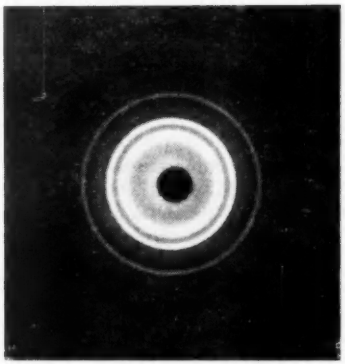

Fig. 3. X-ray pattern of the polymer of 1,1-dimethyl ethylene oxide.

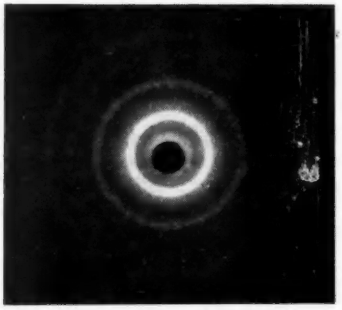

Fig. 4. X-ray pattern of the polymer of tetramethyl ethylene oxide.

16) W. A. Patterson, *Anal. Chem.*, **26**, 823 (1954).

17) O. D. Shreve et al., *Anal. Chem.*, **23**, 382 (1951).

catalysts. These epoxides were polymerized by $AlEt_3$ as well as BF_3Et_2O and $TiCl_4$ at low temperature. The similar feature was illustrated in the case of four and five membered cyclic oxides[18], that is, ring ethers such as oxacyclobutanes, tetrahydrofuran were polymerized by $AlEt_3$ as well as BF_3Et_2O. While catalyst $ZnEt_2$ seemed to act in a manner unlike that of $AlEt_3$.

"Coordinated complex catalyst" such as $FeCl_3$-PO and AlP-$ZnCl_2$ could be applied to polymerization of limited kinds of epoxides and the polymerization by these catalysts proceeded much slower in the rate than that both by some cationic catalysts and some organometallic compounds such as $AlEt_3$ and $EnEt_2$.

The author offers sincere thanks to Professor Dr. S. Murahashi for his kind guidance and encouragement throughout this work and he is indebted to Dr. H. Tani, Dr. T. Takizawa and Dr. S. Nozakura for their valuable discussions and helpful suggestions in the experiments and to Mr. K. Katayama (Textile Res. Lab., Asahi Chem. Ind. Co. Ltd.) for X-ray examinations.

Department of Polymer Science
Faculty of Science
Osaka University
Nakanoshima, Osaka

18) S. Kambara et al., *J. Polymer Sci.*, **27**, 586 (1958).

Spectrochemical Study of Microscopic Crystals. XXI[1]. *The Structure and Absorption Spectra of the Red and the Black Form of Nitrosopentammine-cobalt Salts*[2]

By Shoichiro YAMADA, Hiroaki NISHIKAWA and Ryutaro TSUCHIDA

(Received December 16, 1959)

Two series of compounds with the same composition of $[Co(NH_3)_5NO]X_2$, have been known for a long time[3], one of them being colored black and the other red. The marked difference in the color and other properties between the two series of compounds has attracted a number of investigators[4-10], but rather conflicting conclusion have so far been drawn about the configuration and the electronic structure of the two compounds. It seems, therefore, to be of significance to examine the compounds using some new sorts of materials which have neither been much discussed nor obtained before. This paper presents ultraviolet absorption spectra of the black and the red salt in the crystalline state, and discusses their structure on the basis of the present measurement.

Experimental

Materials. — Red nitrosopentammine-cobalt(III) nitrate, $[Co(NH_3)_5NO](NO_3)_2$, was prepared in rectangular, thin plates by the method of Asmussen and others[9]. The compound is comparatively stable, and may be recrystallized from water.

Black nitrosopentammine-cobalt chloride, $[Co(NH_3)_5NO]Cl_2$ was prepared according to the direction of Asmussen and others[9]. The compound is unstable, undergoing decomposition by water, acid or alkali. On exposure to the air, the compound gradually changes into a red material. The decomposition, however, seemed to be so slow that no change of the crystal surface was observed under the microscope after the dichroism measurement. The compound is often contaminated with the $[Co(NH_3)_6]^{2+}$, which is very sensitive with respect to magnetic susceptibility, but not to ultraviolet spectra of the salt.

Measurements. — Visible and ultraviolet spectra of both the red and the black compound in the crystalline state have been quantitatively determined

1) Part XX of this series, S. Yamada and R. Tsuchida, This Bulletin, **33**, 98 (1960).
2) Presented before the 12th Annual Meeting of Japan Chemical Society, Kyoto, April, 1959.
3) J. Sand and O. Gennsler, *Ann.*, **123**, 43 (1862); ibid., **329**, 194 (1903); *Ber.*, **36**, 2083 (1903).
4) A. Werner and P. Karrer, *Helv. Chim. Acta*, **1**, 54 (1918).
5) D. P. Mellor and D. P. Craig, *J. Proc. Roy. Soc. N. S. Wales*, **78**, 25 (1944); L. N. Short, *Rev. Pure Appl. Chem.*, **4**, 41 (1954).
6) S. P. Ghosh and P. Rây, *J. Indian Chem. Soc.*, **20**, 409 (1943).
7) J. L. Milward, W. Wardlaw and W. J. R. Way, *J. Chem. Soc.*, **1938**, 233; N.V. Sidgwick and R. Bailey, *Proc. Roy. Soc. (London)*, **A144**, 521 (1934).
8) W. P. Griffith, J. Lewis and G. Wilkinson, *J. Inorg. Nuclear Chem.*, **7**, 38 (1958).
9) R. W. Asmussen, O. Bostrup and J. P. Jensen, *Acta Chem. Scand.*, **12**, 24 (1958).
10) E. P. Bertin, S. Mizushima, T. J. Lane and J. V. Quagliano, *J. Am. Chem. Soc.*, **81**, 3821 (1959).

at room temperature on well-developed planes by Tsuchida and Kobayashi's microscopic method[11] using linearly polarized light. The A- and the B-absorption refer to the direction shown in the figures.

Visible and ultraviolet absorption spectrum of the red salt in an aqueous solution was measured by a Beckman DU spectrophotometer.

The symbols used in the present paper are the same as those in the former reports of this series.

In the analysis of the absorption curve in Fig. 4, it is assumed that the second absorption band has a molar extinction coefficient almost equal to that of the first band, the distance between the maxima of the first and the second bands being almost equal for complexes of cobalt(III).

Results and Discussion

Structure of Black Nitrosopentammine-cobalt Salt. — Uninuclear and binuclear structures have been given to the black nitrosopentammine-cobalt salt. Contrary to the result by former investigators that the "black salts" were paramagnetic, Asmussen and others[9] found that the "black salts", when carefully purified, actually showed diamagnetism. The structures, as suggested formerly on the erroneous magnetic data, need not be given serious consideration. The black series of the salts were regarded by Asmussen and others as a co-ordination compound of cobalt(III), the lowest energy level being very close to the level of the bivalent cobalt.

Bertin and others[10] concluded on the basis of the infrared spectra of these compounds that the isomerism of the black and the red series is dependent upon the nature of the linkages of the co-ordinated NO-group and not upon difference in the oxidation state of the central metal. However, they did not discuss the structure of the salts in detail. Griffith and others[8] discussed the same problem on the basis of the chemical reactions, and finally favored the binuclear structure for the "black salt". Most of their discussion, however, seems to be rather speculative, and reexamination from materials of different kinds might be desirable.

Dichroism in the visible and ultraviolet region of the "black salt" is shown in Fig. 1. It seems fortunate that the impurity, $[Co(NH_3)_6]^{2+}$, often appearing in the "black salt" is not important in the UV-absorption spectra of the compound, in contrast to magnetic susceptibility which is affected seriously by a small amount of the impurity. The absorption spectra, as shown in Fig. 1, seem to be so complicated that they would not be understandable on the assumption of the uninuclear

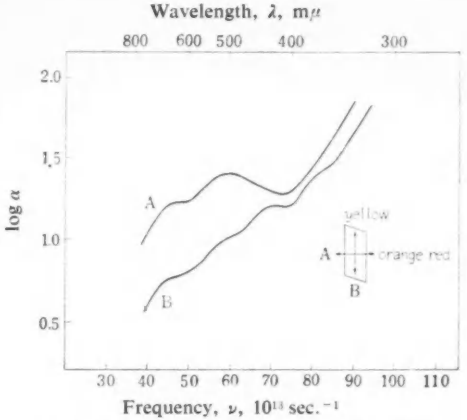

Fig. 1. Absorption spectra of black nitrosopentammine-cobalt chloride, $[Co(NH_3)_5NO]Cl_2$, in the crystalline state.

model of the "black salt". Thus the "black salt" exhibits an absorption band at about $46\times10^{13}\,sec^{-1}$, the wavelength region which is much longer than would be expected for the uninuclear nitrosopentammine-cobalt(III) complex. There might be a possibility that the band at about $46\times10^{13}\,sec^{-1}$ would originate from a nitroso-group. In fact, a number of nitroso-derivatives, such as nitroso-benzene and its derivatives, are known to show a rather special type of an absorption band characteristic of a nitroso-group in the long wavelength region. It may be difficult, however, to assume that the NO-group in the "black salt" should be isolated electronically from the cobalt ion to such an extent that the band of this sort may appear in this wavelength region. The band at about $46\times10^{13}\,sec^{-1}$ of the "black salt", therefore, may not be regarded as due to a nitroso-group which is rather isolated in the cobalt-complex. Moreover, the absorption curve of the "black salt" appears to be too complicated for a uninuclear complex of cobalt(III).

On the contrary, the absorption curve of the "black salt" may be understood much more readily as that of a binuclear complex than as that of a uninuclear complex. Possible structures for a binuclear form are shown in Fig. 2, the π-bonding between the metal and the NO^- ion being neglected for the present. It is to be noted that the dichroism of the "black salt" is markedly similar to that of μ-peroxo-dicobalt complexes with an O^{2-} group which connects two cobalt ions together[12]. Moreover, just as the peroxo-dicobalt compound

11) R. Tsuchida and M. Kobayashi, "The Color and the Structure of Metallic Compounds", Zoshindo, Osaka (1944), p. 180 (in Japanese), This Bulletin, 13, 619 (1938).

12) S. Yamada, Y. Shimura and R. Tsuchida, This Bulletin, 26, 72 (1953).

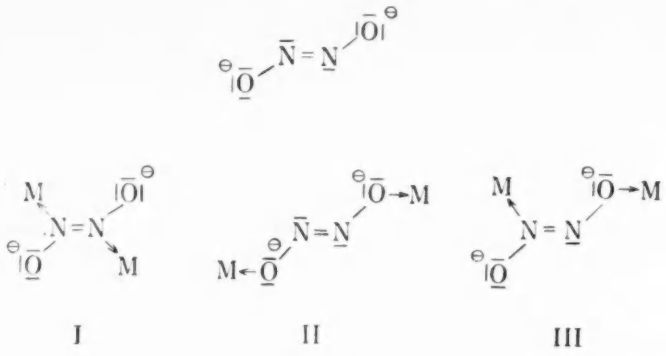

Fig. 2.

has an absorption band in the very long wavelength region, so the "black salt" shows an absorption band at about $46\times10^{13}\,sec^{-1}$. The band of the peroxo-dicobalt compound in the longer wavelength region, with maximum at about $46\times10^{13}\,sec^{-1}$, was ascribed to a group of Co–O_2–Co with a special electronic structure which gives rise to a special absorption band due to the interaction between the two cobalt ions through the peroxide group[12]. The band in question of the "black salt", therefore, may be a special type of the interaction band due to a group of atoms having an electronic structure of Co–X–Co somewhat similar to that of Co–O_2–Co, originating from the interaction between the two cobalt ions through N_2 group. A-absorption in Fig. 1 may be regarded as representing the main features of the component absorption which is richer with the interaction absorption due to the Co–N_2–Co group than is the other component absorption.

Since it is difficult to expect the interaction band with structure II and structure III, structure I having a group of Co–N–N–Co may be favored best as a model of the "black salt" by the ultraviolet absorption spectra with the interaction band. The conclusion obtained here by the present authors about the structure of the "black salt" is found to be in agreement with the view of Griffith and others[8], who regarded it as most likely that the "black salt" has a binuclear structure with a hyponitrite-group as a bridge, on the ground that the "black salt" undergoes decomposition by acid or carbon dioxide to give nitrous oxide and that the salt can be prepared, though in a low yield, from sodium hyponitrite and a cobalt salt.

It may also be noteworthy that an infrared absorption band at 1620 to 1640 cm^{-1} due to the NO part of the "black salt"[10] is very close to the frequency of the –N=N– group in ordinary azo-compounds. This to beseems consistent with structure I, having a kind of interaction between the two cobalt ions through the N_2 group, as has been concluded to be most probable in the present work. The order of the N–N bond may be almost equal to the bond order in ordinary azo-groups of organic azo-compounds.

In summary, it may be concluded that *the "black salt" has structure I with the Co–N=N–Co group, displaying the special band due to the interaction between the two cobalt ions through the –N=N– group.*

Polarized Absorption Spectra of Red Nitrosopentammine-cobalt(III) Nitrate. — Ultraviolet absorption spectra of the "red salt" in the crystalline state are shown in Fig. 3 and Table I. The crystal structure analysis has not been

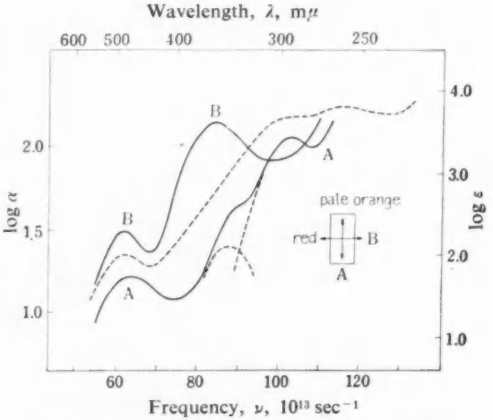

Fig. 3. Absorption spectra of red nitrosopentammine-cobalt nitrate, $[Co(NH_3)_5ON](NO_3)_2$, in the crystalline state (——) and in aqueous solution (----).

TABLE I. UV ABSORPTION SPECTRA OF RED NITROSOPENTAMMINE-COBALT(III) NITRATE $[Co(NH_3)_5NO](NO_3)_2$ IN THE CRYSTALLINE STATE AND IN SOLUTION

Absorption band	Spin-forbidden	I	NO-spec.	II	III	IV
		ν, log α	ν, log α	ν, log α	ν, log α	
In crystalline state						
B-abs.		62, 1.5	84, 2.3	(covered)	— —	
A-abs.		1.15	1.2	87, 1.5	102, 2.1	
Stronger component[a)]		Z	Z	(X, Y)	X, Y	
In aqueous solution						
	ν, log ε	ν, log ε	ν, log ε		ν, log ε	ν, log ε
	38.5, 1.85	62.1, 1.98	83.5, 2.6	(covered)	100, 3.6	114.5, 3.83

ν: $10^{13}\,sec^{-1}$

a) Z refers to the direction combining the cobalt ion with the ON-group in the complex-ion.

reported with the compound as yet. However, the dichroism, as has been determined in the present work, may be regarded to represent the main characteristics of the component absorptions of the complex-ion itself under slight perturbation from the surrounding ions.

A striking dichroism is observed with the first absorption band. It may be assumed that A-absorption in Fig. 3, having the stronger absorption band at about $62\times10^{13}\,sec^{-1}$ represents characteristics of the component absorption of the complex-ion with electric vector along the direction connecting the cobalt(III) ion and the nitroso-group.

The specific band due to the NO-group in co-ordination is observed as a distinct maximum at about $84\times10^{13}\,sec^{-1}$ in Fig. 3, whereas the band is obscured by neighboring stronger absorption in the absorption curve of the compound in solution. The present measurement shows that the specific band is greatly polarized along the Co–ON direction. This is readily understandable if it is assumed that the band is due to electron transfer, possibly from the ON-group to the central metal-ion.

The band at about $102\times10^{13}\,sec^{-1}$ is seen to be polarized in the direction perpendicular to the Co–ON direction. The absorption band due to nitrate ions is expected to appear at about $100\times10^{13}\,sec^{-1}$, but the band of the nitrate ion is so low that the band at about $102\times10^{13}\,sec^{-1}$, as observed with the "red salt" in the present work, may be due to another origin. This band may be a sort of charge transfer band, but its origin is not quite clear for the present.

The second ligand field band is covered under greater specific band in A-absorption, but appears as inflation at about $87\times10^{13}\,sec^{-1}$ in B-absorption. This may be consistent with the frequency difference of about $25\times10^{13}\,sec^{-1}$ between the first and the second band, which was reported with numerous cobalt(III)-complexes.

Structure of Red Nitrosopentammine-cobalt Salts.—Both the uni- and the bi-nuclear structure have been proposed for the "red salt". Very recently Asmussen et al.[9] regarded, mostly from magnetic measurements, that the "red salt" may be either a uninuclear or a binuclear complex of cobalt(III). Griffith et al.[8] concluded from examination of its chemical property that the "red salt" may be uninuclear. Bertin et al.[10] concluded, from its infrared spectrum, the oxidation state of the cobalt to be tervalent, but presented no detailed discussion about the structure of the "red salt". Thus the "red salt" may be a uninuclear or a binuclear complex of cobalt(III). In the following, we shall discuss about the structure of the "red salt" on the basis of the present measurements with consideration to the former results.

Possible structures of the binuclear ions for the "red salt" are shown in Fig. 2. Structure I is assigned to the "black salt", as discussed above. Structure II and structure III may be rejected on the ground of the chemical reactions of the "red salt", since the compound with structure II or structure III would be expected to give nitrous oxide in acidic solution, just like the hyponitrite ion. In fact, the "red salt" is stable in water, whereas the "black salt" is readily decomposed to give nitrous oxide. Moreover, the fact that the "red salt" in solution or in the crystalline state shows a definite maximum for the first absorption band seems to be inconsistent with structure III, which would show two "first ligand field absorption bands" originating from the two kinds of cobalt ions. Therefore, the "red salt" can not be assigned to a binuclear form. Thus the present authors are inclined to assume that the "red salt" be uninuclear.

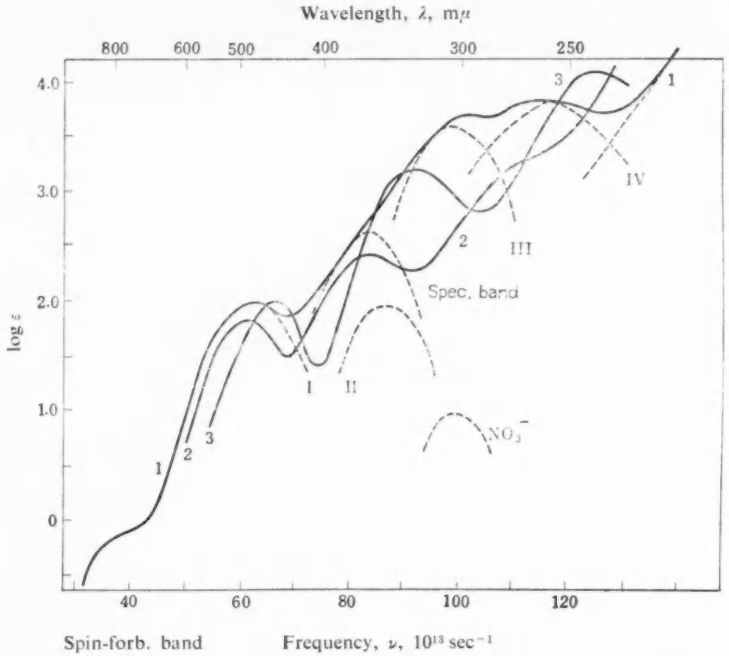

Fig. 4. Absorption spectra of $[Co(NH_3)_5X]^{2+}$ in aqueous solution: 1, $X=NO^-$; 2, $X=ONO^-$ (nitrito); 3, $X=NO_2^-$ (nitro-). Dotted curves represent absorption bands obtained by analysis of the absorption curve 1. The curves 1 and 2 are taken from Ref. 13 in the text.

In addition, the absorption spectra of the "red salt" may be consistent with the assumption of the uninuclear model of the "red salt", as shown in the succeeding paragraph of the present discussion.

Ultraviolet absorption spectra of the "red salt" in solution and in the crystalline state have been determined in the present work, and are shown in Figs. 3 and 4 and Table I. The absorption curve of the compound in solution, as determined in the present work, shows absorption maxima which generally agree with those reported by the former investigators with the compound in solution[9]. Asmussen and others[9] pointed out vague similarity of its absorption spectrum to spectra of most cobaltic compounds, but gave no further discussion about the spectrum. After all, they seemed to conclude that the "red salt" may be either uninuclear or binuclear. It is seen in Fig. 3 and Table I that the "red salt" shows a well-defined maximum for the first band at about 61 to $62\times10^{13}\,sec^{-1}$. The second band, which is characteristic of most complexes of cobalt(III), is covered under strong neighboring absorption bands in the curve of the salt in aqueous solution. Analysis of the absorption curve reveals that there appears a band at about $84\times10^{13}\,sec^{-1}$ which may be regarded as a specific band due mainly to an NO-group in combination with the cobalt(III)-ion. The intensity of the specific band is found to be much smaller than the intensity of the specific band due to a nitro-, an isothiocyanato- or an azide group in the pentammine-cobalt(III) complex. As is evident from inspection of the data in Table II, it is difficult to assume that the band at about $100\times10^{13}\,sec^{-1}$ in the curve of the "red salt"

TABLE II. ABSORPTION MAXIMA OF COMPLEXES OF A TYPE, $[Co(NH_3)_5X]^{2+}$, IN SOLUTION

X	1st band		Specific band		Ref.
	ν	log ε	ν	log ε	
NO_2^-	65.8	2.00	92.4	3.22	a
NH_3	63.2	1.78	—	—	b
ONO^-	61.2	1.86	82.9	2.44	a
ON^-	62.1	1.98	84	2.5	c

ν: $10^{13}\,sec^{-1}$.

a) M. Linhard, H. Siebert and M. Weigel, *Z. anorg. allgem. Chem.*, **278**, 287 (1955).

b) M. Linhard, *Z. Elektrochem.*, **50**, 224 (1944).

c) Present measurement.

may correspond to the specific band due to the NO-group in the complex-ion. On the contrary, it is noteworthy that the band at about 84×10^{13} sec^{-1} of the "red salt" is almost as intense as the specific band of a nitrite-group in the pentammine-cobalt(III) in which a nitrite group is co-ordinated to the cobalt-(III) ion through its oxygen atom.

It also is to be noted that the absorption curve of the "red salt", $[Co(NH_3)_5ON](NO_3)_2$ in solution bears a resemblance to the curve[13] of the $[Co(NH_3)_5ONO]^{2+}$ ion in which a nitrite ion is co-ordinated to the cobalt(III) ion through its oxygen atom. This seems to indicate that the NO-group in the "red salt" is co-ordinated to the cobalt(III) ion through its oxygen atom, as will be described in more detail in the later part of the present discussion.

It is known from existing data that substitution of a nitro-group for ammonia in the hexammine-cobalt(III) ion gives rise to a hypsochromic shift of the first absorption band, whereas the substitution of a nitrite group for ammonia yields a bathochromic shift of the first band. In the case of a nitrate-group, an even greater bathochromic shift is observed. It is found in Fig. 4 and Table II that the first absorption band of the "red salt" lies at a longer wavelength than the first band of the hexammine-cobalt(III) ion. Therefore, it may be concluded, from comparison of the wavelength of the first absorption band of the "red salt" with those of the relevant complexes, that *the NO-group in the "red salt" is co-ordinated to the cobalt(III) ion throuh its oxygen atom, and not through the nitrogen atom*, as is customarily assumed for this compound.

Inspection of existing data, summarized in Table II and Fig. 4, also reveals that the specific band due to a nitrite-group lies at about 83 to 84×10^{13} sec^{-1} and the band due to a nitro-group lies at about 92×10^{13} sec^{-1} in the pentammine-cobalt(III) complex. It is seen that the nitrite-group with its oxygen co-ordinated to the cobalt(III) ion shows its specific absorption band at a longer wavelength than does the nitro-group with its nitrogen co-ordinated to the cobalt(III) ion. The present measurement shows that the "red salt" has its specific band at about 84×10^{13} sec^{-1} with log ε of about 2.6. Thus it is concluded also from examination of the specific band that the NO-group in the "red salt" is co-ordinated to the cobalt(III) ion through its oxygen atom.

The intensity of the specific band due to the nitroso-group in the "red nitroso-pentammine complex" is found to be smaller than the intensity of the specific band due to a nitro-group in the metallic complex, but is almost equal to the intensity of the specific band due to the nitrite group in the pentammine-cobalt(III) complex. This fact also may be consistent with the conclusion that the nitroso-group is co-ordinated to the cobalt(III) ion through the oxygen atom in the "red salt".

In this connection, the close similarity of the absorption curve of the "red salt" to the curve of the nitritopentammine-cobalt(III) complex is noteworthy. In the case of the "red salt", band III and band IV are seen to be displaced to a little longer wavelength than the corresponding bands of the nitritopentammine-cobalt(III) complex, as is seen in Fig. 4, but the correspondence of the absorption bands between the "red salt" and the nitritopentammine-cobalt(III) complex may be evident. This fact also may be taken as indicating that the absorption spectrum of the "red salt" is understood on the assumption of the mononuclear model with the cobalt-to-oxygen bond.

It is interesting to find that a very weak absorption system appears at about 39×10^{13} sec^{-1} in the absorption curve of the "red salt" in solution, as shown in Fig. 4. This absorption band is regarded as being due to electronic transitions between levels with different multiplicities. This spin-forbidden band of the "red salt" is found to lie in the longer wavelength region than $[Co(NH_3)_6]Cl_3$ which shows the band at about 40×10^{13} sec^{-1}. This fact is also compatible with the conclusion in the present article that the NO-group is bound to the cobalt ion through its oxygen atom, since the band of this kind would appear in the shorter wavelength region if the NO-group were bound to the cobalt(III) ion through its nitrogen atom.

Summarizing the above discussion, mainly on the basis of the absorption spectra, it is concluded that *the "red salt" is uninuclear, with the nitroso-group co-ordinated to the cobalt-(III) ion through the oxygen atom.*

Summary

In order to examine the structure of the red and the black nitrosopentammine-cobalt salts, their dichroism in the visible and near-ultraviolet region has been quantitatively determined at room temperature by the microscopic method.

The absorption spectrum of the "black salt" is found to be understandable best on the assumption that the "black salt" has binuclear complexes of cobalt(III), showing a special kind of absorption band due to the interaction between the two cobalt(III) ions through the N_2 group.

13) M. Weigel, H. Siebert and M. Linhard, *Z. anorg. allgem. Chem.*, 278, 287 (1955).

The absorption spectrum of the "red salt" is concluded to be consistent with the model of the uninuclear complex of cobalt(III) with the NO-group co-ordinated to the cobalt(III) ion through its oxygen atom.

Department of Chemistry
Faculty of Science
Osaka University
Nakanoshima, Osaka

Chemisorption of Hydrogen on Zinc Oxide. III. The Effect of Additions of Foreign Ions to Zinc Oxide

By Yutaka KUBOKAWA

(Received January 20, 1960)

Since the electron barrier theory was suggested for the chemisorption on semiconductors by Hauffe, Weisz, and others[1], the importance of the electronic structure of oxides in catalysis has been emphasized by various workers. As an approach along this line, the following method has often been adopted. The electronic structure of a given oxide is modified by the addition of small amounts of foreign ions, and the resulting changes in catalytic activity are then studied. As regards the hydrogen-deuterium exchange reaction on zinc oxide, Parravano et al.[2] found that the addition of Al^{3+} or Ga^{3+}, which should increase its electrical conductivity, increased the activity and lowered the activation energy, while the addition of Li^{+} showed a reverse effect. On the basis of these results, Hauffe[3] suggested that the rate-determining step in this case was the electron transfer from zinc oxide to adsorbed hydrogen ions to allow it to desorb, closely correlating the catalytic activity of zinc oxide with its properties as a semiconductor.

Whatever mechanism may be operative in the hydrogen-deuterium exchange reaction, it is obvious that the hydrogen chemisorption on zinc oxide samples containing these foreign ions must be studied before any conclusive explanation of the activity changes caused by such additions can be given. Apart from the exchange reaction, such a study may be of considerable interest concerning the relation between the electronic structure of oxide and its hydrogen chemisorption. At present the only work along this line seems to be that of Cimino et al.[4] In this work, as described in previous papers,[5,6] hydrogen chemisorption has been investigated by measuring the rates of adsorption and desorption, and the adsorption equilibrium, with zinc oxide modified by the addition of foreign ions such as Li^{+}, Al^{3+} and Ga^{3+}.

Experimental

Materials.—Zinc oxide without foreign ions was prepared by sintering at 800°C for 5 hr. of non-sintered zinc oxide, which was obtained from zinc oxalate as described previously.[5] ZnO+1 mole % Al_2O_3, ZnO+1 mole% Ga_2O_3, and ZnO+0.5 mole% Li_2O: Non-sintered zinc oxide was impregnated with a solution containing a desired amount of aluminum, gallium, or lithium nitrate, dried at 110°C, and sintered at 800°C for 5 hr. Hydrogen and other gases used were prepared and purified as described in the previous work[5,7].

The weight of adsorbent and the surface area determined by the B. E. T. method using nitrogen adsorption are shown in Table I.

TABLE I.

Adsorbent	Weight, g.	Surface area, $m^2/g.$
ZnO	19.6	1.0
ZnO+1 mole% Al_2O_3	20.6	1.7
ZnO+1 mole% Ga_2O_3	22.7	3.6
ZnO+0.5 mole% Li_2O	27.5	0.40

Apparatus and Procedure.—Details of the apparatus and procedure were already described in the previous paper[5]. Prior to a series of experiments, all the adsorbents used in the present work

1) K. Hauffe and H. J. Engell, *Z. Elektrochem.*, **56**, 366 (1952); **57**, 763, 773 (1953); P. Aigrain and C. Dugas, ibid., **56**, 363 (1952); P. B. Weisz, *J. Chem. Phys.*, **21**, 1531 (1953).
2) E. Molinari and G. Parravano, *J. Am. Chem. Soc.*, **75**, 5233 (1953).
3) K. Hauffe, *Angew. Chem.*, **67**, 189 (1955).
4) A. Cimino, E. Cipollini and E. Molinari, *Naturwissenschaften*, **43**, 58 (1956).
5) Y. Kubokawa, This Bulletin, **33**, 546(1960).
6) Y. Kubokawa, ibid., **33**, 550 (1960).
7) Y. Kubokawa, ibid., **33**, 555 (1960).

were subjected to repeated pretreatments with hydrogen at 450°C followed by evacuation at the same temperature.

Results

The Variation in the Adsorbed Amount on Raising Temperature During Adsorption. — Hydrogen was allowed to be chemisorbed by the adsorbent at room temperature and the temperature of the whole system was raised up to a higher temperature in stages, at each of which, in most cases, a rapid desorption followed by a slow uptake was observed. The activation energy of adsorption was determined by comparison of the rates at different temperatures corresponding to equal amount of the slow chemisorption as described in the previous paper[6]. As an example, a run between 215 and 266°C on ZnO+1 mole% Ga_2O_3 is shown in Fig. 1. The activation energies thus obtained in various temperature ranges with ZnO, ZnO+1 mole% Ga_2O_3, and ZnO+0.5 mole% Li_2O are shown in Table II. Here, the activation energies in similar temperature ranges are almost of the same order of magnitude throughout all the adsorbents, suggesting that the activation energy of adsorption is not affected seriously by the addition of foreign ions. However, the proportion of the amount rapidly desorbed on an abrupt temperature rise to the total amount adsorbed is clearly affected by the addition of foreign ions. The amount of such rapid desorption at each stage is shown in Figs. 2—4, together with the amount adsorbed in a certain constant time period at each temperature. Comparison between Figs. 2 and 3 shows that for ZnO+1 mole% Ga_2O_3 the rapid desorption occurs to a much less extent than for ZnO.

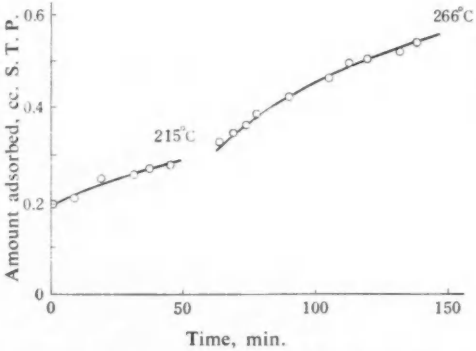

Fig. 1. Rate of hydrogen chemisorption on ZnO+1 mole% Ga_2O_3 in case of temp. change during adsorption ; Pressure, 50~60 mmHg.

TABLE II. ACTIVATION ENERGY OF ADSORPTION*

Adsorbent	Temp. range, °C	Activation energy of adsorption, kcal./mole
ZnO	72~143	—
	143~203	12
	203~254	15
ZnO+0.5 mole% Li_2O	98~146	7.5
	146~196	11
	196~244	14.5
ZnO+1 mole% Ga_2O_3	124~171	8.5
	171~215	11.5
	215~266	16

* The upper limit of the experimental error was ±10%.

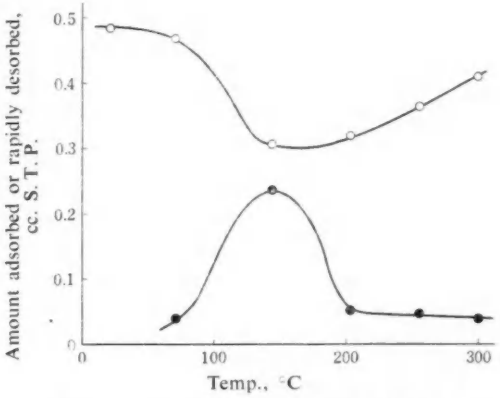

Fig. 2. Variation in the amount adsorbed on ZnO on raising temp. ; Hydrogen pressure, 80~90 mmHg ; -○-, the amount adsorbed after 3 hr. ; -●-, the amount rapidly desorbed.

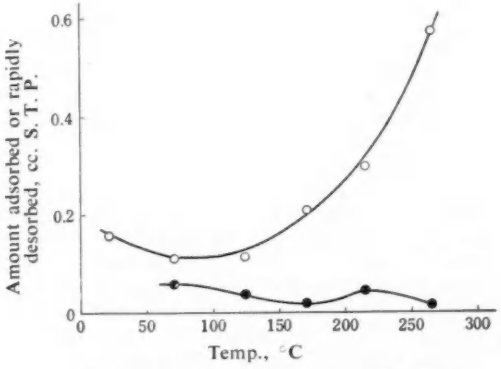

Fig. 3. Variation in the amount adsorbed on ZnO+1 mole% Ga_2O_3 on raising temp. ; Hydrogen pressure, 50~60 mmHg ; -○-, the amount adsorbed after 1.5 hr. -●-, the amount rapidly desorbed.

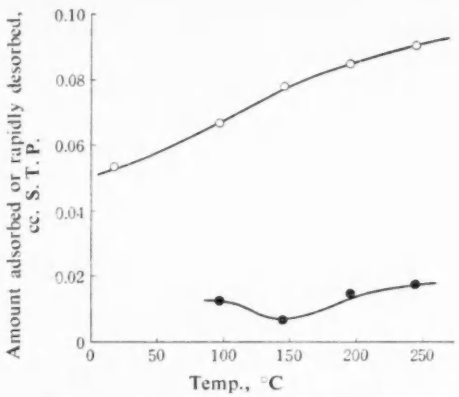

Fig. 4. Variation in the amount adsorbed on ZnO+0.5 mole% Li_2O; on raising temp.; Hydrogen pressure, 0.2~0.3 mmHg; -○-, the amount adsorbed after 1 hr.; -●-, the amount rapidly desorbed.

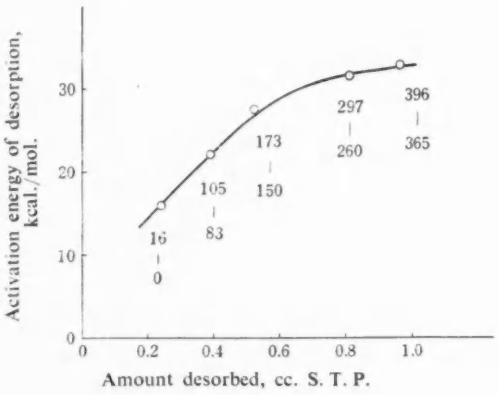

Fig. 5. Activation energies of desorption of hydrogen chemisorbed on ZnO. The amount adsorbed and equilibrium pressure at room temp. before desorption were 1.10 cc. and 42.2 mmHg, respectively. Numerical values in Figs. 5, 6, and 7 refer to the temp. interval where the activation energies were determined.

The results with ZnO+0.5 mole% Li_2O can not be compared directly with the others owing to different pressure conditions.

The Activation Energies of Desorption at Various Coverages.—After hydrogen was allowed to be adsorbed at about 400°C, the temperature of the specimen was raised from 0 to 400°C in stages, at each of which the activation energy of desorption was determined from comparison between the rates of desorption at different temperatures corresponding to equal amounts left adsorbed as stated

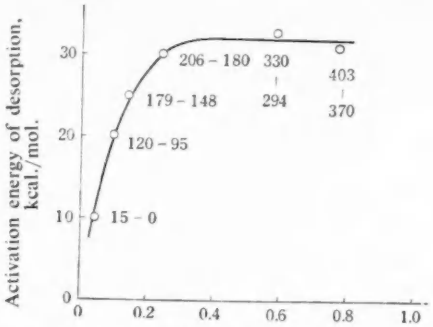

Fig. 6. Activation energies of desorption of hydrogen chemisorbed on ZnO+1 mole% Ga_2O_3. The amount adsorbed and equilibrium pressure at room temp. before desorption were 0.98 cc. and 52.3 mmHg, respectively.

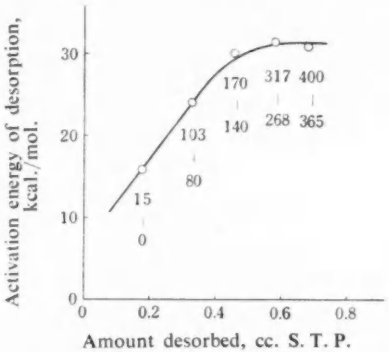

Fig. 7. Activation energies of desorption of hydrogen chemisorbed on ZnO+0.5 mole% Li_2O. The amount adsorbed and equilibrium pressure at room temp. before desorption were 0.78 cc. and 41.0 mmHg, respectively.

in the previous paper[5]. The results obtained with ZnO, ZnO+1 mole% Ga_2O_3 and ZnO+0.5 mole% Li_2O are shown in Figs. 5—7. Here, it was confirmed, in the same manner as described previously, that the rate of adsorption was negligible during the desorption experiment for all the adsorbents studied. From these figures the following picture would be obtained. For all the adsorbents with and without foreign ions, the activation energy increases with decreasing amount adsorbed up to almost the same value of 30~33 kcal./mol., although the proportions of the amounts desorbed with a lower activation energy (<20 kcal./mol.) to the total amount desorbed are different from one another, the smallest value being found with ZnO+1 mole% Ga_2O_3 in accordance with the results of adsorption experiment above mentioned.

Adsorption Isotherms. — Adsorption equilibrium measurements were carried out only with ZnO and ZnO+1 mole% Al_2O_3 in the same manner as described previously[5]: After hydrogen was allowed to be adsorbed at about 350°C, the isotherms were determined by successive withdrawals of the gas. The isotherms thus obtained were found to be reproduced on increasing or decreasing pressure subsequently. For both systems the Langmuir plot was applicable in the pressure range

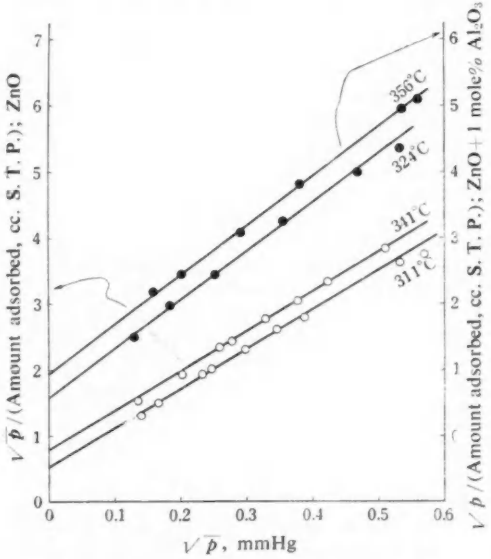

Fig. 8. Langmuir plots for ZnO and ZnO +1 mole% Al_2O_3; -○-, ZnO; -●-, ZnO+1 mole% Al_2O_3.

studied as seen in Fig. 8. It follows from this figure that the heat of adsorption is unaffected by the addition and is equal to 18 kcal./mol. Although such applicability of the Langmuir plot probably results from a limited range of coverage, the slopes of the lines in Fig. 8 may be utilized to estimate the magnitude of the surface available for the chemisorption under the given experimental conditions; (Reciprocal of the slope per unit area) is 0.0039 cc. for ZnO+1 mole% Al_2O_3 and 0.0085 cc. for ZnO.

The Effect of Additions of Foreign Ions on Carbon Monoxide Chemisorption. — According to the previous work[7] on carbon monoxide chemisorption on zinc oxide, there are two types of chemisorption, one predominating at low and the other at high temperatures. The effect of foreign ions was studied only for the adsorption of the former type. Because of a small amount adsorbed on ZnO+0.5 mole% Li_2O, the adsorption isotherms were determined only with ZnO and ZnO+1 mole% Al_2O_3 in similar way to that given previously. The heats of adsorption thus obtained for the two adsorbents proved to be almost the same, i.e., 10~12 kcal./mol.

Discussion

In view of the low temperature used in preparing the samples, it seems unlikely that the added foreign ions are distributed uniformly throughout. As seen in Table I, however, surface area of the adsorbents is increased by the addition of Ga_2O_3 or Al_2O_3 and decreased by that of Li_2O. According to Hauffe[8] and Parravano[3], such variation in surface area suggests a decrease in the concentration of interstitial zinc ions, i.e., an increase in the concentration of free electrons in the former case, and the reverse change in the latter case. It may therefore be supposed that at least in a qualitative sense the electronic structure of the adsorbents in this work has been modified by such addition in the manner predicted by the theory of Hauffe and others.

As for the interpretation of the effect of the addition of foreign ions in the present work, it should be taken into consideration that such addition will change the heterogeneity of the surface as well as the electronic state of zinc oxide, both affecting the features of its hydrogen chemisorption. Although it is difficult to separate these two effects, the results obtained in this work, however, may be interpreted as follows: The identical heat of adsorption of 18 kcal./mol. for ZnO and ZnO +1 mole% Al_2O_3 is in agreement with the maximum heat of adsorption for non-sintered zinc oxide given in the previous work[7], suggesting that the maximum heat of adsorption is probably unaffected by the additions of foreign ions. This result together with the identical maximum activation energy of desorption throughout all the adsorbents with and without foreign ions would be unexpected, if the electronic state of zinc oxide played a large part in determining the features of hydrogen chemisorption. In addition, the activation energies of adsorption in similar temperature ranges are almost the same throughout all the adsorbents. Moreover, as described in the previous paper[9], the oxygen pretreatment at a high temperature which should change the electronic state of zinc oxide, gives little effect on its hydrogen chemisorption. Thus, taking account of the existence of surface heterogeneity in this system, the following tentative conclusion may be drawn:

8) K. Hauffe and A. L. Vierk, *Z. physik. Chem.*, **196**, 160 (1950).
9) Y. Kubokawa, This Bulletin, **33**, 743 (1950).

The heat of adsorption and the activation energy of adsorption associated with each set of sites may not be affected seriously by the addition of foreign ions; the variation in the features of the hydrogen chemisorption caused by such addition can probably be attributed to the change in the distribution function of sites rather than to that in the electronic structure of the adsorbents.

According to Cimino et al.[9], the adsorption isobars obtained with ZnO and ZnO + 0.5 mole% Li_2O show one or two maxima, while on ZnO + 0.3 mole% Ga_2O_3 the amount adsorbed increases steadily with temperature, in qualitative agreement with the results mentioned above; the addition of Ga_2O_3 reduces the amount adsorbed over the whole range of temperature in an analogous way to that of Al_2O_3 (Fig. 8). This is reflected in the change of the amount adsorbed before desorption experiments (Figs. 5—7); the amount adsorbed on unit surface area is 0.056 cc. for ZnO, 0.012 cc. for ZnO + 1 mol% Ga_2O_3, and 0.071 cc. for ZnO + 0.5 mole% Li_2O. Although the true nature of such change in the amount adsorbed is not yet clear, there seems to be little or no doubt that such behavior can not be explained in terms of the change in the electronic structure of zinc oxide alone.

As regards the change in activity towards the hydrogen-deuterium exchange reaction caused by the addition of foreign ions, the considerations given above seem to indicate that it is doubtful that such an effect is attributed to the change in the electronic structure of zinc oxide. In fact, according to Heckelsberg et al.[10], although the activity is higher on ZnO + 1 mole% Al_2O_3 than on ZnO, the activation energy is essentially the same for the two adsorbents, in contradiction with the results of Parravano. Such an identical activation energy is, however, what would rather be expected from the results in the present work. Further study of the hydrogen chemisorption and the exchange reaction with one and the same specimen of zinc oxide will probably lead us to a more consistent picture of all the related phenomena.

10) L. F. Heckelsberg, A. Clark and G. C. Bailey, *J. Phys. Chem.*, **60**, 559 (1956).

Summary

The hydrogen chemisorption on zinc oxide samples modified by the addition of foreign ions such as Li^+, Al^{3+}, and Ga^{3+} was investigated by measuring the rates of adsorption and desorption, and the adsorption equilibrium. The addition of foreign ions gave little or no effect on the maximum values of the activation energy for desorption and of the heat of adsorption, and the activation energies of adsorption in similar temperature ranges. On the basis of these results combined with the effect of oxygen treatment on this chemisorption on zinc oxide described previously, it was tentatively concluded that the variation in the features of hydrogen chemisorption caused by the addition of foreign ions is probably attributable to the change in a heterogeneity of the surface rather than that in the electronic state of zinc oxide. Finally, it was mentioned that the heat of adsorption of carbon monoxide at room temperature was also unaffected by such additions.

The author wishes to express his sincere thanks to Professor O. Toyama for his guidance and encouragement throughout the course of this study.

Department of Applied Chemistry
College of Engineering
University of Osaka Prefecture
Sakai-shi, Osaka

Zur Darstellung von 3-Methylpolymethoxyphthaliden

Von Eturô MAEKAWA und Yukiko SUMIMOTO

(Eingegangen am 23. Januar, 1960)

3-Methylpolymethoxyphthalide erweckten unser Interesse, weil sie durch Grignardreaktion mit Alkylmagnesiumbromiden und durch anschließende Oxydation mit Kaliumpermanganat Polymethoxy-*o*-acyl-acetophenon ergeben, die dann durch Oxydation mit Selendioxyd in Polymethoxynaphthochinone übergehen[1]. Aus *o*-Phthalaldehydsäure wurde 3-Methylphthalid durch Grignardreaktion mit Methylmagnesiumjodid in guter Ausbeute[2] dargestellt. Auf diese Weise wurden auch 3-Methyl-6. 7-dimethoxy-[2,3], 3-Methyl-4. 5. 6-trimethoxy-[4] und 3-Methyl-4. 5. 6. 7-tetramethoxyphthalid[1] aus den entsprechenden polymethoxylierten *o*-Phthalaldehydsäuren gewonnen. Bei den polymethoxylierten Derivaten, besonders bei Opiansäure nimmt die Ausbeute der Grignardreaktion jedoch stark ab, offenbar weil die Löslichkeit der Polymethoxyphthalaldehydsäuren in Äther viel geringer ist. Obwohl die Ausbeute dadurch einigermaßen verbessert werden konnte[5], daß man die Dosis des Äthers als Lösungsmittels bei der Grignardreaktion erhöhte, oder, daß man einer ätherischen Suspension der Polymethoxyphthalaldehydsäuren des vorher hergestellten Grignardreagens zutropft, und obwohl es uns weiter gelingt, drei in der Literatur noch nicht beschriebene Produkte, nämlich 3-Methyl-5. 6-dimethoxy-, 3-Methyl-5. 6. 7-trimethoxy- und 3. 7-Dimethyl-4. 5. 6-trimethoxyphthalid, auf diese Weise darzustellen, erscheint diese Methode der Darstellung nicht sehr praktisch.

Andererseits stellten Gabriel und Michael aus *o*-Acetylbenzoesäure, die aus Phthalsäureanhydrid und Malonsäure in Pyridin leicht zugänglich ist[6], durch Reduktion mit Natriumamalgam 3-Methylphthalid in einer fast quantitativen Ausbeute dar[7]. Es wurde von uns fesgestellt[4], daß sich aus Polymethoxyphthaliden durch Behandeln mit doppeltermolekularer Menge *N*-Bromsuccinimid (abgekürzt NBS) unter Bestrahlung und durch anschließende Hydrolyse des bromierten Produktes neben den Polymethoxyphthalaldehydsäuren die entsprechenden Polymethoxy-*o*-phthalsäuren bilden. Um eine praktische Darstellungsmethode der Polymethoxyphthalsäure zu finden, wurde nun die Reaktion des NBS auf Polymethoxyphthalaldehydsäuren, die aus den entsprechenden Phthaliden durch Versetzen mit NBS leicht hergestellt werden können[1,4,5], ausführlich untersucht. Yamaguchi stellte fest, daß Piperonal beim Versetzen mit NBS 3. 4-Methylendioxybenzoesäure und daneben noch Protocatechualdehyd sowie 6-Brom-3. 4-methylendioxybenzoesäure ergab[9], während Vanilin keine Carbonsäuren sondern 5-Bromvanilin und daneben wenig Dehydrodivanilin lieferte[10], und nahm an, daß die Aldehydgruppe über Bromcarbonyl- in die Carboxylgruppe übergeht[11].

Erhitzt man *o*-Phthalaldehydsäure oder deren

TABELLE I. DARSTELLUNG VON POLYMETHOXYPHTHALSÄUREANHYDRIDEN AUS POLYMETHOXYPHTHALALDEHYDSÄUREN MIT NBS

Phthalaldehydsäure	Phthalsäureanhydrid[a] (°C, aus Benzol umkristallisiert)
I	VII, Fp. 127~128[b] (96,4%)[c]
II	VIII, Fp. 172~174[d] (90,0%)
III	IX, Fp. 166~167[e] (96,3%)
IV	X, Fp. 143~144[f] (95,0%)
V	X, Fp. 143~144 (96,7%)
VI	XI, Fp. 137~138[g] (93,7%)

a) Die Produkte wurden sowohl durch Mikroanalysen als auch durch Mischschmelzpunkt der freien Phthalsäuren mit den durch in der Literatur beschriebenen Methoden hergestellten Produkten identifiziert;
b) Lit. 12, Fp. 130, 8°C;
c) in Klammern Ausbeute;
d) R. G. Fargher u. a., *J. Chem. Soc.*, **119**, 1724 (1921), Fp. 179°C;
e) W. H. Perkin u. a., ebenda, **1925**, 127, Fp. 167°C;
f) G. Bergellini u. a., *Atti Acad. Lincei*, **21** II, 146 (1912), Fp. 143°C;
g) Lit. 4, Ep. 137, 5~138°C.

1) F. Weygand, H. Weber und E. Maekawa, *Chem. Ber.*, **90**, 1879 (1957).
2) H. Simonis, E. Marben und E. Mermod, *Ber.* **38**, 3981 (1905).
3) E. Mermod und H. Simonis, ebenda, **41**, 982 (1907).
4) E. Maekawa und S. Nan'ya, dieses Bulletin, **32**, 1311 (1959).
5) E. Maekawa, Dissertation, Berlin-Charlottenburg (1956).
6) S. Gabriel und A. Michael, *Ber.* **10**, 2205 (1877).
7) H. L. Yale, *J. Am. Chem. Soc.*, **69**, 1547 (1947).
8) J. J. Brown und G. T. Newbold, *J. Chem. Soc.*, **1952**, 4397.
9) M. Yamaguchi, *J. Chem. Soc. Japan, Pure Chem. Sect.* (*Nippon Kagaku Zasshi*), **77**, 515 (1956).
10) M. Yamaguchi, ebenda, **77**, 593 (1956).
11) M. Yamaguchi, ebenda, **77**, 591 (1956).

polymethoxylierte Derivate in Tetrachlorkohlenstoff in Gegenwart von Dibenzoylperoxyd (abgekürzt BPO), so entwickelt sich Bromwasserstoff und aus dem Reaktionsgemisch können die entsprechenden Phthalsäureanhydride in guter Ausbeute leicht isoliert werden. Da die Reaktion unter Bromwasserstoffentwicklung zu Phthalsäureanhydriden führt, scheint sie gemäß folgendem Schema zu verlaufen:

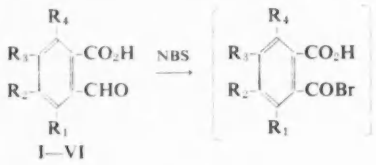

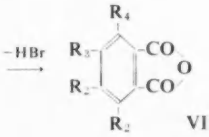

I: $R_1=R_2=R_3=R_4=H$
II: $R_1=R_4=H$, $R_2=R_3=OCH_3$
III: $R_1=R_2=H$, $R_3=R=OCH_3$
IV: $R_1=R_2=R_3=OCH_3$, $R_4=H$
V: $R_1=H$, $R_2=R_3=R_4=OCH_3$
VI: $R_1=R_2=R_3=R_4=OCH_3$
VII: $R_1=R_2=R_3=R_4=H$
VIII: $R_1=R_4=H$, $R_2=R_3=OCH_3$
IX: $R_1=R_2=H$, $R_3=R_4=OCH_3$
X: $R_1=R_2=R_3=OCH_3$, $R_4=H$
XI: $R_1=R_2=R_3=R_4=OCH_3$

Die Ergebnisse sind zusammenfassend in der Tabelle I angegeben. Weder kernbromierte noch dimerisierte Produkte wurden in den Reaktionsgemischen gefunden; Bildung von Substanzen, die mit Eisenchlorid eine violette Farbreaktion zeigen, wurde auch nicht festgestellt.

Da die Ausbeute an den Phthalsäuren bei der Reaktion der Polymethoxyphthalide mit doppelter molekularer Menge NBS von der Feuchtigkeit der Reaktionssysteme abhängig ist, scheinen die Phthalsäuren zum Teil über die freien *o*-Phthalaldehydsäuren, die sich durch die Wirkung der Feuchtigkeit auf die 3-Bromphthalide bilden, durch deren Reaktion mit NBS über die Phthalsäuremonobromide zu entsehen. Die Entstehung von Phthalsäuren muß jedoch aus Polymethoxyphthaliden auch anders, als über die freien *o*-Phthalaldehydsäuren möglich sein, da sich Phthalsäuren auch unter Feuchtigkeitsausschluß ohne Entwicklung von Bromwasserstoff bilden, man kann sie erst nach der Hydrolyse des Produktes isolieren.

Die gebildeten Polymethoxyphthalsäuren werden durch Erhitzen zu ihren Anhydriden geführt, welche dann mit Malonsäure in Pyridin erwärmt werden. Da es im allgemeinen schwierig war, aus den Reaktionsgemischen die erwarteten Polymethoxy-*o*-acetylbenzoesäuren rein zu isolieren, werden sie in rohem Zustand mit Natriumamalgam oder Zink und Essigsäure versetzt und 3-Methylpolymethoxyphthalide aus den schwach angesäuerten Reaktionsgemischen ausgeäthert (Tabelle II). Hemipinsäure- bzw. 3. 4. 5-Trimethoxyphthalsäureanhydrid ergibt 3-Methylmekonin bzw. 3-Methyl-5. 6. 7-trimethoxyphthalid, wobei 3-Methyl-4. 5-dimethoxy- bzw. 3-Methyl-4. 5. 6-trimethoxyphthalid im Reaktionsgemisch nicht gefunden wurden, was vermutlich auf die sterische Behinderung durch die *o*-stehende Methoxygruppe zurückzuführen ist. Bei der Reduktion des rohen Reaktionsproduktes aus 4. 5-Dimethoxyphthalsäureanhydrid und Malonsäure, das noch die entsprechende freie Phthalsäure zu erheblicher Menge enthält, bildete sich auch daneben durch deren Reduktion 5. 6-Dimethoxyphthalid. Die Kondensation der Polymethoxyphthalsäureanhydride, die in Pyridin als Phthalsäureanhydrid viel weniger löslich sind, verlief mit Malonsäure nur in sehr schlechten Ausbeuten, und ihre präparative Bedeutung blieb noch zweifelhaft, obgleich wir noch nicht versucht haben, optimale Bedingungen zu suchen.

TABELLE II. 3-METHYLPOLYMETHOXYPHTHALIDE AUS POLYMETHOXYPHTHALSÄUREANHYDRIDEN

Phthalsäureanhydrid	Produkt (°C)
VIII	3-Methyl-5. 6-dimethoxyphthalid, Fp. 109~110 (35%)[a] u. daneben 5. 6-Dimethoxyphthalid, Fp. 154~155[b] (1%)
IX	3-Methyl-6. 7-dimethoxyphthalid, Fp. 100~101[c] (17%)
X	3-Methyl-5. 6. 7-trimethoxyphthalid, Fp. 103,5~104,5 (12%)
XI	kein Phthalid erhalten

a) In Klammern die auf das umgesetzte Anhydrid bezogene Ausbeute;
b) J. A. McRae u. a., *Can. J. Chem.*, **29**, 482 (1951), Fp. 155°C;
c) Lit. 2, Fp. 101°C.

Beschreibung der Versuche

1. *o*-Phthalaldehydsäuren.—Wurden aus den entsprechenden Phthaliden durch Versetzen mit NBS und durch anschließende Hydrolyse der bromierten Produkte hergestellt[1].

2. Phthalsäureanhydrid.—5 g (1/30 mol) *o*-Phthalaldehydsäure wurden in 200 ccm Benzol gelöst, ca. 20 ccm des Benzols abdestilliert, um die Feuchtigkeit des Systems azeotropisch zu beseitigen, dann mit 200 ccm Tetrachlorkohlenstoff und 5,9 g (1/30 mol) NBS in Gegenwart von wenig BPO und unter Bestrahlung mit einer 500 W-Wolframlampe

1 Std. am Rückfluß erhitzt. Das beim Erkalten ausgeschiedene Succinimid (ca. 3,3 g) wurde abgesaugt, das Filtrat eingeengt, der Rückstand vorsichtig mit wenig kaltem Wasser zum Beseitigen des Succinimids gewaschen und aus Benzol umkristallisiert, 4,66 g (94,5%) farblose Nadeln, Fp. 127~128°C* (Lit.[12] 130, 8°C).

3. Polymethoxyphthalsäureanhydride.—Die entsprechenden Polymethoxyphthalaldehydsäuren wurden wie vorstehend mit NBS versetzt: die besten Ergebnisse sind in der Tabelle I zusammenfassend angegeben.

4. 3-Methyl-5. 6-dimethoxyphthalid (*α*-Methyl-*m*-mekonin).—(a) Einer gut umgerührten Suspension von 3,7 g 4. 5-Dimethoxyphthalaldehydsäure (*m*-Opiansäure) in 500 ccm Äther wurde ein Grignardreagens aus 9,5 g Methyljodid und 1,7 g Magnesiumspänen unter Eiskühlung langsam zugetropft. Das Gemisch wurde 1 Std. unter Eiskühlung und noch 1 Std unter Erwärmen am Rückfluß umgerührt, dann mit 2 N Schwefelsäure angesäuert und mit Äther ausgezogen, wobei aus der wässerigen Schicht 3.1 g nicht umgesetzte *m*-Opiansäure zurückgewonnen wurden. Die ätherische Lösung wurde mit Sodalösung und anschließend mit Wasser gewaschen, mit Natriumsulfat getrocknet und eingeengt. Der Rückstand wurde aus ca. 250 ccm Wasser kristallisieren gelassen, 160 mg farblose Prismen oder Nadeln, Fp. 108~110°C.

Gef.**: C 63,20; H 5,62. Ber. für $C_{11}H_{11}O_4$ (208,2): C 63,50; H 5,81.

Es fiel unter Umständen aus den Wasser in durchsichtigen Nadeln aus, die bei 118,5~120°C schmelzen; sie scheinen kristallwasserhaltig zu sein, reichten jedoch zu einer Elementaranalyse nicht.

(b) 4 g 4. 5-Dimethoxyphthalsäureanhydrid wurden 3 Std mit 2,3 g Malonsäure und 3 ccm Pyridin in 10 ccm Xylol auf dem Wasserbad unter Feuchtigkeitsausschluß erwärmt. Beim Erkalten des Reaktionsgemisches fielen 3,3 g des Anhydrids aus. Das Gemisch wurde abfiltriert, das Filtrat mit 80 ccm Wasser gemischt, mit Salzsäure angesäuert und mit Äther ausgezogen. Der ätherische Auszng wurde mit Wasser gewaschen und einge engt, der Rückstand mit Wasser zum Sieden erhitzt, um das Xylol azeotropisch zu entfernen, und die wässerige Lösung eingeengt. Der Rückstand (0,45 g) wurde 2 Std. mit 1 g Zinkstaub in einem Gemisch aus 1 ccm Wasser und 4 ccm Essigsäure am Rückfluß erhitzt, das Gemisch im Vakuum eingeengt, der Rückstand in Äther gelöst und die ätherische Lösung mit Sodalösung gewaschen und eingeengt. Aus Wasser umkristallisiert ergab der Rückstand wenig *m*-Mekonin (Fp. 154~155°C) und daneben 185 mg 3-Methyl-5. 6-dimethoxyphthalid (Fp. 109~110°C), der beim Mischschmelzpunkt mit dem obenerwähnten Produkt keine Depression zeigte.

5. 2. 7-Dimethyl-4. 5. 6-trimethoxyphthalid.—Einem Geignardreagens aus 0,8 g Magnesiumspänen und 5,5 g Methyljodid wurde eine Lösung von 2 g 3. 4. 5-Trimethoxy-6-methylphthalaldehydsäure (Fp. 109~113°C) in 320 ccm Äther unter kräftigem Umrühren und Eiskühlung langsam zugetropft und das Gemisch wie üblich aufgearbeitet. Aus der ätherischen Lösung wurden durch Waschen mit Sodalösung 0,2 g Ausgangsprodukt und durch anschließendes Einengen ein fettartiger Rückstand gewonnen, der aus alkoholhaltigem Wasser in farblosen Nadeln ausfiel, 0,76 g, Fp. 80~81,5°C.

Gef.: C 62,16; H 6,33. Ber. für $C_{13}H_{16}O$ (252,2): C 61,89; H 6,39.

6. 3-Methyl-5. 6. 7-trimethoxyphthalid. — (a) Einem Grignardreagens aus 0,5 g Magnesiumspänen und 3,0 g Methyljodid wurde eine Suspension von 1,5 g 4. 5. 6-Trimethoxyphthalaldehydsäure in 500 ccm Äther unter Eiskühlung zugetropft. Es wurde wie üblich aufgearbeitet und das Produkt aus Wasser umkristallisiert, 0,80 g farblose Nadeln, Fp. 103, 5~104,5°C.

Gef. C 60,53; H 6,00. Ber. für $C_{12}H_{14}O_5$ (238,2): C 60,50; H 5,92.

(b) 3,5 g 3. 4. 5-Trimethoxyphthalsäureanhydrid wurden 3 Std in 4,5 ccm Pyridin mit 1,8 g Malonsäure auf dem Wasserbad unter Feuchtigkeitsausschluß erwärmt. Das Reaktionsgemisch wurde in 25 ccm Wasser gelöst, die Lösung mit Salzsäure angesäuert und mit Äther ausgezogen. Die ätherische Lösung wurde nach dem Waschen mit Wasser eingeengt, der Rückstand in wenig Wasser gelöst und die wässerige Lösung bei Zimmertemperatur eindunsten gelassen, wobei 2,3 g 3. 4. 5-Trimethoxyphthalsäure zurückgewonnen wurden. Die Mutterlauge wurde eingeengt und der Rückstand (1 g) in einer Natronlauge aus 2 g Natriumhydroxyd und 150 ccm Wasser gelöst, mit einem Natriumamalgam aus 0,65 g Natrium und 30 g Quecksilber 24 Std. bei Raumtemperatur stehengelassen und anschließend 8 Std. unter Zusatz von 50 ccm Wasser auf dem Wasserbad erwärmt. Die wässerige Schicht wurde mit Salzsäure angesäuert, auf 50 ccm eingeengt und ausgeäthert. Die ätherische Lösung wurde mit Wasser, mit Natriumhydrogencarbonatlösung und mit Wasser gewaschen und eingeengt. Der Rückstand wurde aus Wasser mit Aktivkohle kristallisieren gelassen, 150 mg farblose Nadeln, Fp. 103,5~104,5°C, die beim Mischschmelzpunkt mit dem oberen Produkt keine Depression zeigte.

7. 3-Methyl-6. 7-dimethoxyphthalid (*α*-Methyl-mekonin).—4 g 3. 4-Dimethoxyphthalsäureanhydrid (Hemipinsäureanhydrid) wurden 3 Std mit 5 ccm Pyridin und 2,3 g Malonsäure auf dem Wasserbad in Abwesenheit von Feuchtigkeit erwärmt. Das Reaktionsgemisch wurde wie bei Darstellung der von 3-Methyl-5. 6. 7-trimethoxyphthalid nach der Methode (b) aufgearbeite, wobei 2,67 g 3. 4-Dimethoxyphthalsäure zurückgewonnen und 230 mg des Produktes erhalten wurden. Das Produkt zeigte aus Wasser umkristallisiert einen Fp. von 100~101°C (Lit.[2] 101°C).

Zusammenfassung

Polymethoxy-*o*-phthalaldehydsäuren wurden mit *N*-Bromsuccinimid zu den entsprechenden Phthalsäureanhydriden unter Bromwasserstoffentwicklung in guter Ausbeute oxydiert, wobei kernbromierte bzw. dimerisierte Produkte oder

* Schmelzpunkte wurden mikroskopisch bestimmt, aber nicht korrigiert.

12) K. P. Monroe, *Ind. Eng. Chem.*, **11**, 1116 (1919).

** Für Mikroanalyse der Verbindungen sind wir der Zentralen Mikroanalysenstelle Univ. Kyoto sehr dankbar.

phenolische Verbindungen nicht nachgewiesen wurden. Aus den Polymethoxyphthalsäureanhydriden wurden durch Versetzen mit Malonsäure in Pyridin die *o*-Acetylpolymethoxybenzoesäuren hergestellt, die zu den 3-Methylpolymethoxyphthaliden reduziert wurden, obwohl die erste Stufe der Reaktion, nämlich die Kondensation mit Malonsäure, nur in sehr schlechter Ausbeute verlief. Bei dieser Kondensation wurde eine sterische Behinderung durch die *o*-ständige Methoxygruppe beobachtet, wie sich aus 3. 4. 5-Trimethoxyphthalsäureanhydrid nur 3-Methyl-5. 6. 7-trimethoxyphthalid bildet. 3-Methyl-5. 6-dimethoxy-, 3-Methyl-5. 6. 7-trimethoxy- und 3. 7-Dimethyl-4. 5. 6-trimethoxyphthalid wurden aus den entsprechenden *o*-Phthalaldehydsäuren durch die Grignardreaktion unter Verwendung von großer Dosis des Äthers, oder durch eine umgekehrte Grignardreaktion dargestellt.

Herrn Prof. Dr. F. Weygand, München, sind wir für seine Anregung und Anleitung zu vorstehender Arbeit zum aufrichtigsten Dank verpflichtet. Auch Doktor der Technology, Frau Seiko Nan'ya danken wir für ihre intensive Mitwirkung bestens.

Organisch-Chemisches Laboratorium
der Technischen Hochschule Nagoya
Syówa-ku, Nagoya

The Ultraviolet Absorption Spectra of Stilbene and Some Related Compounds in the Solid State Measured by the Pressed KCl Disk Technique

By Hiroshi SUZUKI

(Received December 15, 1959)

Molecular structures are, needless to say, not rigid. Even the equilibrium or most probable conformation of a compound can vary, depending on, above all, the aggregation state and the temperature. Thus, the equilibrium conformation of a compound determined by the X-ray crystal analysis, for example, is not necessarily maintained in a state other than the crystalline state. A typical example is biphenyl. This compound is planar in the crystalline state, non-planar in the gaseous state, and probably slightly non-planar in solution[1-1].

If the most probable conformation of a compound is appreciably different in various states, the electronic absorption spectra of the compound in the various states must be correspondingly different from each other. The author has shown in a series of papers[1] that the most probable conformations of many conjugated componds in various states, especially in solution, can be inferred with almost complete satisfaction from the electronic absorption spectra. The principle of the inference consists in comparison of the spectrum of a given compound under a given condition with that of a suitable reference compound under a suitable condition, whose conformation is already known, or else, can be presumed reasonably. Since the conformation of the reference compound is determined by the X-ray crystal analysis in most cases, it is frequently necessary to compare the concerned spectrum with the spectrum of the reference compound in the crystalline state.

The spectra of compounds in the crystalline state have been measured so far by various methods and for various purposes. Thus, they have been measured often with single crystals and with polarized light[2]. This method is useful particularly for the assignment of absorption bands. Alternatively, they have been measured also with solid films prepared on quartz, silica, or glass plates by sublimation of crystals, by evaporation of thin layers of solutions, or by solidification of melted substances[3]. These methods have been used sometimes for the purpose of studying the crystal spectra themselves, and sometimes simply for the reason that the spectra can not be measured in solutions because of the low solubilities of the substances.

In the crystal spectra measured by these

1) H. Suzuki This Bulletin, (I) **32**, 1340, (II) 1350, (III) 1357 (1959), (IV) **33**, 109, (V) 379, (VI) 389, (VII) 396, (VIII) 406, (IX) 410, (X) 613, (XI) 619 (1960).

2) See, for example, A. C. Albrecht and W. T. Simpson, *J. Chem. Phys.*, **23**, 1480 (1955).

3) See, for example; J. W. Weigl, ibid., **24**, 364 (1956).

methods the effect of the orientation of molecules in crystals reveals itself markedly[4]. This marked orientation effect is, of course, essential to the purpose of assignment of bands. However, this effect makes the spectra measured by these methods unsuitable for direct comparison with the spectra of solutions where molecules are oriented at random.

For this reason, in the foregoing series of papers the spectra measured by the "pressed KCl disk technique" were used as the crystal spectra of the reference compounds. The pressed KCl disk technique is quite analogous to the well-known pressed KBr disk technique developed for infrared spectroscopy, and was applied to electronic absorption spectroscopy first by Dale[4] in 1957. It may be somewhat doubtful whether or not the state of molecules in pressed KCl disks is quite the same as that in the crystals. Thus, there may be a possibility that the state is near to that of solid solutions. It seems, however, to be more probable that micro-crystals are oriented at random in disks. If it is so, it seems reasonable to consider that the spectra measured by this method are most suitable, as the spectra of the compounds in the crystalline state, to be directly compared with the solution spectra.

An additional advantage of this method over the others is that the influence of reflection at the disk surface can approximately be eliminated by using a pressed disk of pure potassium chloride as the reference in measurement of the spectra. In contrast, in spectra measured by the other methods the influence of reflection at the crystal surface, at the surface of the plate, or at the crystal-plate interface is frequently sufficiently great to cause serious distortion of the absorption spectra[5], and consequently it is necessary to correct for this influence of reflection. In addition, the pressed KCl disk technique will be very useful to measure the spectra of compounds of low solubility in usual solvents, and particularly of crystalline molecular complexes, whose spectra are difficult in general to measure by other methods.

It is to be noted here that the difference between the spectrum of a compound in the crystalline state and that in solution may be due partly at least to the effect of intermolecular interactions in crystals, besides the possible difference of the most probable conformation in both the states. In general, molecules in crystals can not be treated simply by a so-called oriented gas model. Forces between molecules in aromatic crystals are small compared with intramolecular forces, but they frequently exert appreciable effects on the electronic states of molecules and consequently affect the electronic absorption spectra. In a spectrum measured with a single crystal and with polarized light, the most important effect of a crystal field appears to reveal itself as a so-called Davydov splitting[6]. It seems to be of interest to notice how the effect of a crystal field manifests itself in the spectrum measured by the pressed KCl disk technique, if the spectrum is the one of micro-crystals oriented at random.

At any rate, in view of the possible usefulness of the pressed KCl disk technique in electronic absorption spectroscopy, it seems to be not only interesting but also desirable to study general characteristic features, if any, of the spectra measured by this technique as compared with the corresponding solution spectra.

The author has measured the spectra of stilbene and its related compounds by this technique, of which the spectra of *trans*-stilbene and tolan were already reported in previous papers (Refs. I–V and VI), and he has found that some generalizations can be drawn from comparison of the spectra with the corresponding spectra of solutions in *n*-heptane, although their theoretical interpretation has not yet been attained. In the present paper, the results of the measurement are summarized and discussed mainly from a phenomenological standpoint.

Experimental

Materials.—The compounds used in this study were prepared as reported previously[I-V-IX]. Potassium chloride was precipitated from water solution with hydrochloric acid to obtain small particle size and dried at 400~450°C for about 6 hr., according to the procedure described by Hales and Kynaston[7].

Measurements of the Solid State Spectra.—The general procedure of measurements of the solid state spectra by the pressed KCl disk technique is quite analogous to the procedure for *trans*-stilbene and tolan described in the previous papers. Thus, 1 to 10 mg. of the pure organic compound was thoroughly ground in an agate mortar (for about 15~20 min.) with about 200 mg. of the pure potassium chloride. About 10 mg. of the mixture was then ground with about 350 mg. of new potassium chloride. The concentration of the substance in the final mixture, from which a disk was prepared, was adjusted in order that the disk might show suitable absorbances (about 0.8~1.9 at the most intense absorption maximum). For example, in

4) J. Dale, *Acta Chem. Scand.*, **11**, 650 (1957).
5) J. W. Weigl, *J. Chem. Phys.*, **24**, 577 (1956).
6) See, for example, D. P. Craig and P. C. Hobbins, *J. Chem. Soc.*, **1955**, 539; D. P. Craig, ibid., **1955**, 2302; D. P. Craig and P. C. Hobbins, ibid., **1955**, 2309.
7) J. L. Hales and W. Kynaston, *Analyst*, **79**, 702 (1954).

the case of *trans-p*-phenylstilbene, the mixing was carried out as follows; 2.35 mg. of the substance was ground with about 200 mg. of KCl, and about 10 mg. of the first mixture was ground with about 350 mg. of KCl to get the final mixture. In the case of triphenylethylene, 8.35 mg. of the compound was ground with 200 mg. of KCl, 10 mg. of the first mixture was ground with 350 mg. of KCl, and finally 80 mg. of the second mixture was ground with 177 mg. of KCl. As will be described later, the apparent molecular extinction coefficients in the spectra measured by this technique were generally lower than the corresponding values in the solution spectra, and furthermore, were not reproducible. Therefore, the adjustment of the concentrations in the final mixtures was not straightforward and frequently had to be carried out by the method of trial and error.

In most cases except for the cases of *trans*-stilbene and tolan, about 150 mg. (146~148 mg.) of each final mixture was pressed under vacuum in the usual manner into a transparent disk (pressure: about 12 tons per sq. cm.). The ultraviolet absorption spectrum of the disk was measured with a Cary recording spectrophotometer Model 14 by using a disk prepared of about 150 mg. (146 and 148 mg.) of pure potassium chloride as the reference. The transmission spectrum of one of the reference disks used (weight: 146.25 mg.) is shown in Fig. 1. It is characteristic that the spectrum exhibits a feeble absorption band at near 270.5 mμ. This band was observed similarly in all the spectra of the reference disks used.

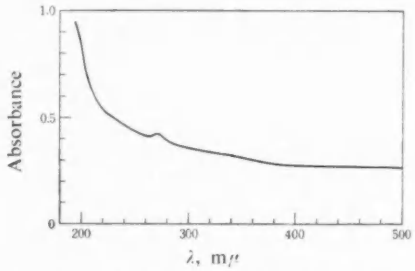

Fig. 1. The transmission spectrum of a reference KCl disk (weight: 146.25 mg.).

Calculations of Thicknesses of Disks, Concentrations, and Molecular Extinction Coefficients.— The radius of a disk is 0.65 cm. Since the weights of the disks used are 146~148 mg. in most cases, the thicknesses of the disks are calculated to be 0.055~0.056 cm, when it is assumed that the density of the disks is 1.988. These values of the thicknesses are in fairly good agreement with the rough values obtained by direct measurement. The concentrations of the organic substances in the disks can be calculated easily, on the basis of an assumption that micro-crystals or molecules are evenly dispersed in each mixture. Then, the molecular extinction coefficients (ε) are evaluated in the usual manner as the values of absorbance divided by the thickness of the disk and the molar concentration of the substance in the disk.

Discussion

In the ensuing discussion, the spectra measured by the pressed KCl disk technique are referred to as the solid state spectra. The solution spectra refer to the spectra of solutions in *n*-heptane, except where indicated otherwise.

The newly measured solid state spectra are shown in Figs. 2—6, together with the corresponding solution spectra reported in previous

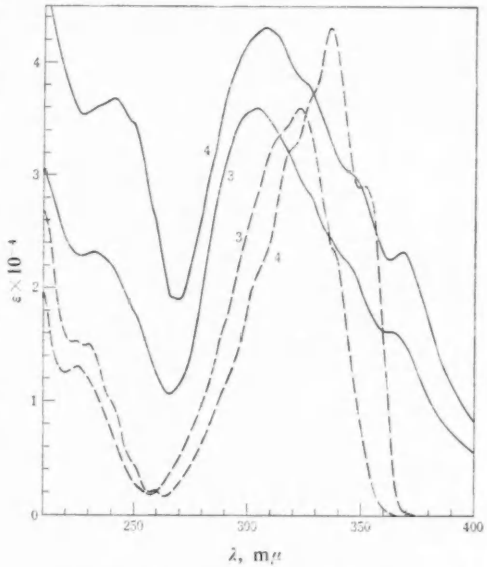

Fig. 2. Ultraviolet absorption spectra: 3, *trans-p*-phenylstilbene; 4, *trans*-1-phenyl-2-(2-fluorenyl)-ethylene.

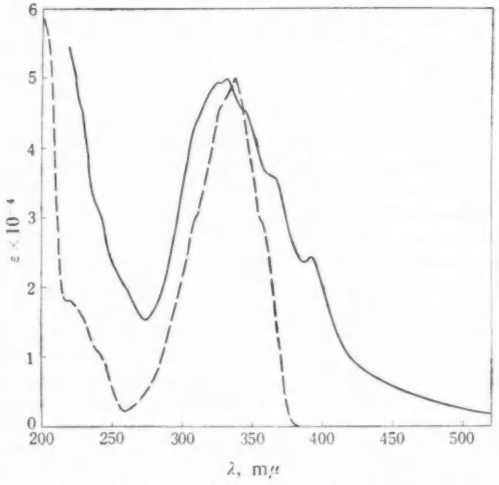

Fig. 3. Ultraviolet absorption spectra: *trans-p, p'*-diphenylstilbene.

papers (Refs. 1-VI—IX). The solid lines represent the solid state spectra and the broken lines the solution spectra. In these figures, the extinction of the most intense maximum of the conjugation band in each solid state spectrum has been arbitrarily set equal to the extinction of the most intense maximum of the conjugation band in the corresponding solution spectrum, because reliable solute extinction values for the solid state spectra could not be obtained. In addition, in Fig. 3 the extinction of the maximum of the conjugation band in the spectrum of *n*-heptane solution has been

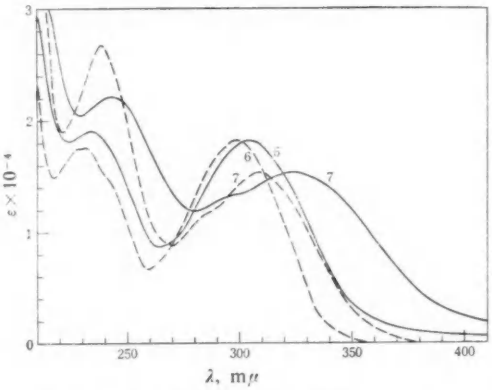

Fig. 4. Ultraviolet absorption spectra: 6, triphenylethylene; 7, tetraphenylethylene.

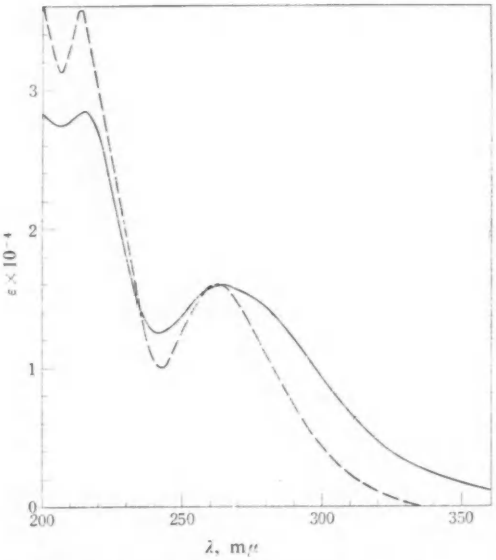

Fig. 5. Ultraviolet absorption spectra: *trans*-1, 2-dimesitylethylene.

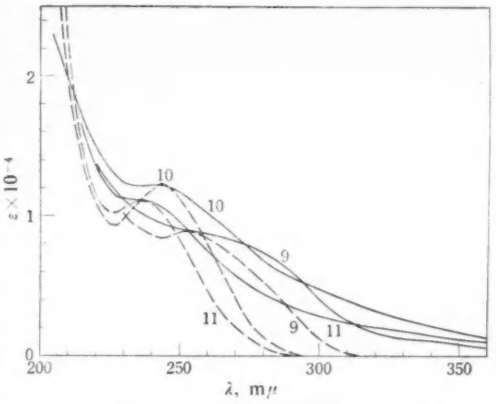

Fig. 6. Ultraviolet absorption spectra: 9, *cis*-α, α'-dimethylstilbene; 10, *trans*-α, α'-dimethylstilbene; 11, *trans*-α, α'-diethylstilbene.

arbitrarily set equal to that in the spectrum of benzene solution (cf. Ref. 1-IX). It is seen that the solid state spectra resemble considerably the corresponding solution spectra on the whole.

The data of the maxima and the inflections in these spectra as well as in the spectra of *trans*-stilbene and tolan are summarized in Table I. In this table, A refers to the A-band, i.e. the conjugation band due to transitions from the highest occupied orbital to the lowest vacant orbital, and B refers to the B-band, i.e. the band probably due to transitions from the highest occupied orbital to the vacant orbitals localized in the benzene nuclei or from the occupied orbitals localized in the benzene nuclei to the lowest vacant orbital (cf. Ref. 1-V). The symbol △ denotes the most intense maximum of fine structure of the conjugation band in each spectrum. Wavelengths (in mμ) in parentheses denotes inflections, and those in double parentheses denote very indistinct inflections. $\Delta\lambda$ represents the wavelength difference (in mμ) between the band in the solid state spectrum and the probably corresponding band in the solution spectrum. Values of $\Delta\lambda$ in parentheses are values for the cases in which either or both of the bands to be compared are inflections. $\varepsilon_K/\varepsilon_H$ represents the ratio of the apparent value of the molecular extinction coefficient of the band in the solid state spectrum to the value of the corresponding band in the solution spectrum.

Absorption Intensities.—The molecular extinction coefficients in the solid state spectra, calculated by the above mentioned procedure, were not reproducible. Not withstanding, it may be said that they are generally considerably

TABLE I. THE SOLID STATE SPECTRA (BY THE PRESSED KCl DISK TECHNIQUE) AND THE SOLUTION SPECTRA (IN *n*-HEPTANE) OF STILBENE AND RELATED COMPOUNDS

Entry No.	Compound		Solid state spectrum		Solution spectrum		$\Delta\lambda$, mμ	$\varepsilon_K/\varepsilon_H$
			λ_{max}, mμ	$\varepsilon(\varepsilon_K)$	λ_{max}, mμ	$\varepsilon(\varepsilon_H)$		
1	Tolan							
		A	301.6	1920	297.2	27500	4.4	0.070
			292.4	1680	288.5	20800	3.9	0.081
			△ 283.3	2380	△ 279.9	30800	3.4	0.077
			(275.8)	1960	272.7	22400	(3.1)	0.088
			268.0	1760	265.3	20600	2.7	0.085
		B	(239.0)	680	237.2	6930	(1.8)	0.098
					232.2	6520		
			(223.5)	1540	222.0	16500	(1.5)	0.093
			(218.5)	1790	217.2	19000	(1.3)	0.094
2	*trans*-Stilbene							
		A	(327.5)	960	(320.5)	16000	(7.0)	0.060
			(312.5)	1500	306.9	26500	(5.6)	0.057
			(298.5)	1750	△ 294.1	27950	(4.4)	0.063
			△ 287.0	1790	(283)	24500	(4.0)	0.073
			(276)	1610				
		B	(241.5)	1420	(236)	10400	(5.5)	0.137
			233.0	1670	228.5	16200	4.5	0.103
			(225.5)	1640	(222)	15500	(3.5)	0.106
3	*trans-p*-Phenylstilbene							
		A	(364.4)	6850				
			((343))	9540	((338))	23200	(5.0)	0.411
			((328))	11880	△ 322.5	36000	(5.5)	0.330
					(311.5)	33200		
			△ 303.6	15240				
		B	232.3	9810	225.5	13100	6.8	0.749
4	*trans*-1-Phenyl-2-(2-fluorenyl)-ethylene							
		A	368.0	5370				
					351.2	29100		
			(345)	6980	△ 335.8	43100	(9.2)	0.162
			(325)	8820	(318.5)	32450	(6.5)	0.272
			(313)	9750				
			△ 307.0	9920	((303.5))	21000	(3.5)	0.472
			((299))	9580				
		B	(249.5)	7970	((237.5))	10900	(12.0)	0.731
			241.0	8470	230.0	15230	11.0	0.556
			(233.5)	8290	223.7	15420	(9.8)	0.538
5	*trans-p, p'*-Diphenylstilbene							
		A	391.8	12260				
			(366.0)	17980	((357))	29400*	(9.0)	0.612
			(345.2)	22970	△ 337.4	49900*	(7.8)	0.460
			△ 331.6	25130	(327.5)	46200*	(4.1)	0.544
			(324)	24820				
		B	((229))	18640	(220.5)	18200*	(8.5)	1.024
6	Triphenylethylene							
		A	((308))	8090				
			303.8	8180	298.5	18220	5.3	0.449
					(242.5)	14570		
		B	233.9	8550	232.0	17580	1.9	0.486
			((230))	8500	(228)	17540	(2.0)	0.485

TABLE I (continued)

7	Tetraphenylethylene						
	A	322.9	10970	308.7	15300	14.2	0.717
		(296)	9480	(285.8)	11700	(10.2)	0.810
	B	243.3	15940	238.5	26800	4.8	0.595
8	*trans*-1,2-Dimesitylethylene						
	A	264.4	9170	262.7	16000	1.7	0.573
	B	215.0	16340	214.0	35700	1.0	0.458
9	*cis*-α, α'-Dimethylstilbene						
	A	252.4	570	252.0	8880	0.4	0.064
10	*trans*-α, α'-Dimethylstilbene						
	A	(240.6)	2250	243.3	12270	(−2.7)	0.183
11	*trans*-α, α'-Diethylstilbene						
	A	(236.9)	2220	236.6	11090	(0.3)	0.200

* Values estimated by taking the value for the maximum of the conjugation band in the spectrum of the *n*-heptane solution to be equal to the value in the spectrum of the benzene solution.

smaller than the values in the corresponding solution spectra. Thus, as is seen in Table I, the values of $\varepsilon_K/\varepsilon_H$ are about 1/3~2/3 for the compounds of the numbers 3—8, and are only about 1/20~1/5 for the compounds of the entry numbers 1, 2, 9, 10 and 11.

These depressions of intensities seem to be partly at least intrinsic ones. As is seen in Figs. 2—6, the bands, especially the A-bands, are markedly more broad in the solid state spectra than in the solution spectra. Therefore, it is believed that the intensities of especially the A-bands are actually considerably smaller in the former spectra than in the latter. This presumption is supported also by the fact that in the figures the intensities of the B-bands are apparently much larger in the solid state spectra than in the solution spectra in most cases. If it is assumed that the actual intensities of the B-bands are not markedly different in both spectra, this fact is, of course, considered to indicate the actual depressions of intensities of the A-bands in the solid state spectra.

In addition to the actual or intrinsic depressions, the intensities may be apparently depressed by contribution of other factors. As the factor contributing to the apparent depressions, the following possibilities may be considered. (1) A part of the organic substance weighed in may be lost during grinding and evacuation of the press, as pointed out already by Dale[4]. (2) Mixing may be imperfect in each process of grinding. That is, the substance may be unevenly dispersed in each mixture, and consequently, the actual concentration in the final mixture may be more or less different from the culculated value. (3) The absorption intensities in the solid state spectra may essentially depend on the condition of dispersion of the micro-crystals or the sizes of the micro-crystals, as suggested by the somewhat similar phenomenon observed by Weigl[5] in his study on the absorption spectra of some crystalline cationic dyes. Especially in the cases where the values of $\varepsilon_K/\varepsilon_H$ are extraordinarily small, the contribution of factor 1 may be predominant.

Shapes of Absorption Curves and Wavelengths of Bands.—Although the shape of the absorption curve of the solid state spectrum of a compound varies slightly from disk to disk in some cases, the reproducibility of the wavelength positions of the absorption maxima and the inflections was almost always fairly good.

Comparison of the solid state spectra with the solution spectra seems to suggest that it is convenient to divide the compounds into the following four groups with respect to the shapes of the absorption curves as well as the magnitudes of the wavelength displacements $\Delta\lambda$: (I) entry 1 in Table I, (II) entries 2—5, (III) entries 6 and 7, and (IV) entries 8—11.

Group I.—Tolan. The solid state spectrum it not significantly different from the solution spectrum, except for the bathochromic displacement of the normal magnitude (see below) of each band (cf. Fig. 2 in Ref. 1–VI). *trans*-Azobenzene also belongs to this group, whose spectra will be reported and discussed in a

later publication.

Group II.—Redistribution of Intensity among the Vibrational Sub-bands.—*trans*-Stilbene, *trans*-*p*-phenylstilbene, *trans*-1-phenyl-2-(2-fluorenyl)-ethylene, and *trans*-*p*,*p*'-diphenylstilbene. All these compounds are *trans*-stilbene-type compounds which have no substituent at sterically hindering positions and consequently are probably planar. It is a common distinctive feature of the spectra of these compounds that the bands, especially the conjugation bands, exhibit more or less well-resolved fine structures. With these compounds, a marked redistribution of intensity among the vibrational fine structure bands of the conjugation band occurs, that is, the relative intensities of the vibrational bands change markedly, when the state is changed from solution to solid. Thus, the band which appears as the most intense maximum in the solution spectrum, appears as the inflection at a longer wavelength than the most intense maximum in the solid state spectrum. On the other and the band which appears as the inflection at a shorter wavelength than the most intense maximum in the solution spectrum, appears as the most intense maximum in the solid state spectrum.

A typical example is *trans*-stilbene. As described in Ref. I–V, when the vibrational sub-bands of the conjugation band of this compound are called α, β, γ, δ, ... in the order from longer-wavelength-side, the most intense maximum is the γ-band in the solution spectrum, and is the δ-band in the solid state spectrum. In this connection, it has been known that the temperature affects markedly the relative intensities of the vibrational sub-bands. Thus, in the spectrum of *trans*-stilbene in mixed alcohols at -130°C measured by Beale and Roe[8], the fine structure is much more sharply resolved, the intensities of the α- and the β-bands are much greater, and the intensity of the γ-band is much smaller than in the solution spectrum measured at room temperature. In this low temperature spectrum, the most intense maximum is the β-band. To illustrate the situation, the three spectra of *trans*-stilbene are shown in Fig. 7.

In the present case, both the solution spectra and the solid state spectra are the ones measured at room temperature. Therefore, the fact that the marked redistribution of intensity among the vibrational sub-bands occurs between them may be said to be rather surprising. Further investigation seems to be necessary to interpret satisfactorily this interesting phenomenon.

8) R. N. Beale and E. M. F. Roe, *J. Chem. Soc.*, 1953, 2755.

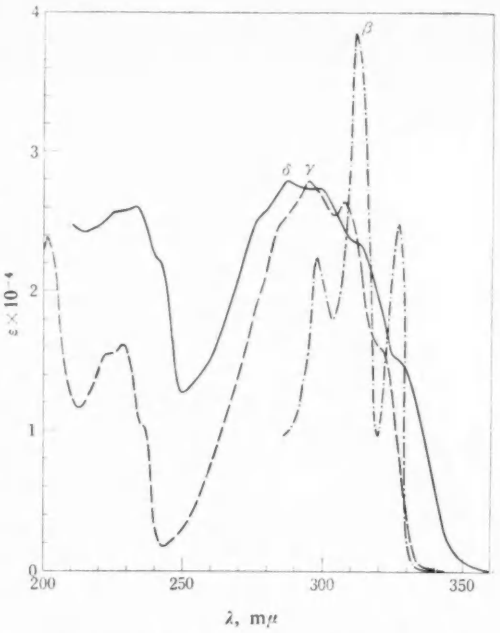

Fig. 7. Ultraviolet absorption spectra of *trans*-stilbene: ——, the solid state spectrum; – – –, the solution spectrum; –·–·–, the low temperature spectrum (in mixed alcohols at -130°C, redrawn from Beale and Roe's paper[8]).

Wavelength Shifts of Bands.—In Fig. 8, the values of $\Delta\lambda$ for the compounds belonging to Groups I and II are plotted against the wavelengths λ of the corresponding maxima or inflections in the solution spectra. As mentioned already, $\Delta\lambda$ represents the magnitude of the wavelength shift of the band associated with the change of the state from *n*-heptane solution to solid.

A positive value of $\Delta\lambda$ indicates that the shift is bathochromic. As is seen in Table I, all the shifts, except for that in the case of *trans*-α,α'-dimethylstilbene, are bathochromic. Of course, the individual numerical values of $\Delta\lambda$ may not be decisive because of inevitable uncertainty in determination of the wavelength positions of the absorption maxima and especially of the inflections. Notwithstanding, it may be said that a rough correlation exists between λ and $\Delta\lambda$. Thus, in Fig. 8, almost all the points for the A-bands of all the compounds as well as the B-band of tolan are nearly on a correlation line, which has been drawn as the solid line in the figure. This means that $\Delta\lambda$ for these increases fairly regularly with λ from about 1.5 mμ at 220 mμ to about 5 mμ at 300 mμ, and to about 9.5 mμ

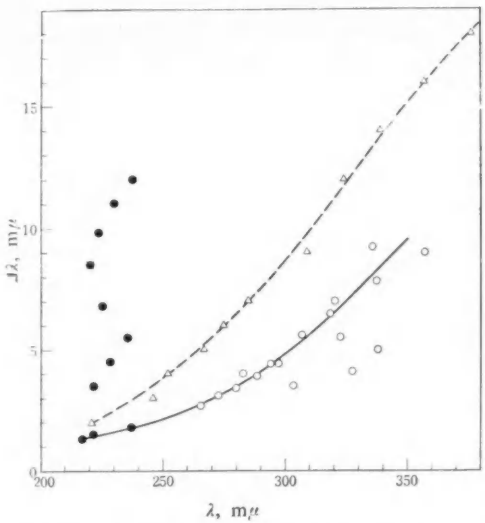

Fig. 8. Correlations between the magnitudes of wavelength shifts of bands (from solution to the solid state) and the wavelengths of the bands in the solution spectra.
○, for the A-bands of tolan and the stilbenes.
●, for the B-bands of tolan and the stilbenes.
△, for the bands of naphthalene and anthracene (according to Dale's data[4]).

at 350 mμ. On the other hand, most of the points for the B-bands, the bands which appear in the region about 220~250 mμ, are markedly deviating from the correlation line. There appears to be a very rough relation that the longer the conjugated system is, or in other words, the longer the wavelength of the A-band is, the value of $\Delta\lambda$ for the corresponding B-band is the larger.

What is the cause of such bathochromic shifts of bands? This problem is unsettled. If the solid state spectra can be considered to be the spectra of micro-crystals oriented at random directions, the shifts are probably due to the intermolecular interactions in the crystals. Alternatively, if the solid state spectra are to be considered as the spectra of solid solutions, the shifts are probably due to a sort of solvent effect. Furthermore, the shifts may be due to other unknown causes. At any rate, whatever the mechanism of the shifts may be, the fact that there is a regular relation between the magnitudes of the shifts and the wavelengths of the bands is very interesting.

A similar regular relation has been found already by Dale[4] for the spectra of naphthalene and anthracene. According to him, the magnitude of the wavelength shift of a band of these "rigid" molecules due to the change of the state from hexane solution to solid, viz. the "normal red-shift", increases regularly with the wavelength of the band, from about 2 mμ at 220 mμ to about 8 mμ at 300 mμ, and to about 19 mμ at 400 mμ. As discussed in a previous paper (Ref. 1-I), this regular relation appears to hold good regardless of kinds of compounds, of characters of bands, and of intensities of bands. In Fig. 8, the values of the "normal red-shifts" are also plotted against the wavelengths of the bands in the spectra of hexane solutions according to Dale's data. A correlation line for these points is shown as the broken line.

It may be noteworthy that the correlation line obtained in the present work for stilbenes, which is subsequently referred to as the present correlation line, is located considerably lower than Dale's correlation line. That is, it may be said that the *trans*-stilbene-type compounds show the red-shifts of the normal magnitudes in themselves, which are smaller than the magnitudes of the normal red-shifts of naphthalene and anthracene. The latter compounds are, to use Dale's words, the "rigid" compounds which obviously can not assume other conformations in solution thanin the crystal lattice. Therefore, the above mentioned fact may be considered as an evidence indicating that the most probable conformationsof these stilbenes in solution are not significantly different from those in the solid, probably crystalline state, and accordingly, are probably planar.

While the probably planar compounds show the red-shifts of normal magnitudes, some compounds, which are discussed in the succeeding paragraphs as belonging to Groups III and IV, show the shifts of more or less abnormal magnitudes. It may be significant that the latter compounds are evidently non-planar. The conjugation bands of these compounds have no distinct fine structure, in contrast with the foregoing sterically unhindered compounds, and as a matter of fact, the shapes of the solid state spectra of these compounds are apparently not markedly different from those of the solution spectra.

Group III.—Triphenylethylene and tetraphenylethylene. The values of $\Delta\lambda$ for triphenylethylene are very slightly greater, and the values for tetraphenylethylene are much greater than those anticipated from the present correlation line in Fig. 8. The extraordinarily large shifts especially in the case of tetraphenylethylene may be considered to indicate that the most

probable conformation of this compound in the solid state is considerably different from that in solution. That is, it may be inferred that the interplanar angles between the phenyl groups and the ethylenic bond are appreciably smaller in the most probable conformation in the solid, probably crystalline state, than in that in solution (cf. Ref. I–VI).

Group IV.—*trans*-2, 4, 6, 2', 4', 6'-Hexamethylstilbene (*trans*-1, 2-dimesitylethylene), *cis*- and *trans*-α, α'-dimethylstilbenes, and *trans*-α, α'-diethylstilbene. The values of $\Delta\lambda$ for these compounds are smaller than anticipated from the present correlation line. Thus, the value for dimesitylethylene is slightly smaller, and the values for α, α'-dialkylstilbenes are much smaller than anticipated from the correlation line. The value for *trans*-α, α'-dimethylstilbene is apparently even negative.

The most probable conformations of these compounds are undoubtedly non-planar, owing to the steric effects of the alkyl substituents (cf. Refs. I–VII and VIII). Therefore, it seems quite reasonable to correlate the smallness of the shifts with the non-planarity of the molecular structures. It may be presumed that with these non-planar compounds the intermolecular interactions in the crystals (or the interactions of the molecules with potassium chloride) are smaller than in the case of the foregoing planar compounds.

The author desires to thank Mr. Akira Kuboyama of Government Chemical Industrial Research Institute, Tokyo, for the use of the spectrophotometer.

Department of Chemistry
College of General Education
The University of Tokyo
Meguro-ku, Tokyo

Paramagnetic Resonance of Radicals of Some Aromatic Vinyl Compounds. I

By Kazuo MORIGAGI, Keiji KUWATA and Kozo HIROTA

(Received January 20, 1960)

Free radicals produced by the reaction of aromatic hydrocarbons with alkali metals have been investigated by the paramagnetic resonance method for several years by Weissman[1] and others. Usually the paramagnetic resonance spectra of these radicals consist of many lines which are coming from the hyperfine interaction of the unpaired electron with protons in these radicals. We have observed the paramagnetic resonance of radicals. We have obtained from the following aromatic vinyl compounds: styrene, α-methyl styrene, *p*-methyl styrene, 1, 1-diphenylethylene, stilbene and 1, 4-diphenylbutadiene. A part of the experimental results has been already reported briefly[2]. The paramagnetic resonance of the above radicals, except that of stilbene, shows many absorption lines, which are attributed to the hyperfine structure arising from the hyperfine interaction of the unpaired electron with protons in the radicals.

1) S. I. Weissman, T. R. Tuttle, Jr. and E. De Boer, *J. Phys. Chem.*, **61**, 28 (1957); T. R. Tuttle, Jr., R. L. Ward and S. I. Weissman, *J. Chem. Phys.*, **25**, 189 (1956).
2) K. Hirota, K. Kuwata and K. Morigaki, This Bulletin, **31**, 538 (1958); **32**, 100 (1959).

The results obtained by the analysis of these spectra contribute not only to the determination of the unpaired electron density in the radicals, but also give some information about the mechanism of polymerization of these aromatic hydrocarbons, because some of the above compounds polymerize easily by the reaction with monomer, turning into so called "living polymers".

The experimental results and discussion in the case of styrene, α-methyl styrene and *p*-methyl styrene will de described in the present paper, and the forthcoming paper will describe the results in the case of 1, 1-diphenyl-ethylene, stilbene and 1, 4-diphenylbutadiene.

Experimental

1) Paramagnetic Resonance Spectrometer and Experimental arrangement.—The measurements of paramagnetic resonance of the above radicals were performed at room temperature, except that of styrene radicals which were measured at about -100°C and -40°C besides room temperature. The spectrometer used for the paramagnetic resonance measurements was a transmission type operating at 9300 Mc. The rectangular cavity, which has a

hole at the half-point of the narrow side, was excited at the mode of TE_{012}. The sample, being enclosed in a glass tube, was put into the cavity through the hole. By modulating the applied magnetic field at the frequency of 315 c/s, the resonance signal was detected with a phase sensitive detector, and was recorded on a milliampere recorder. The cavity system and the Dewar arrangement for measurement at low temperatures were designed as shown in Fig. 1. The sample enclosed in a

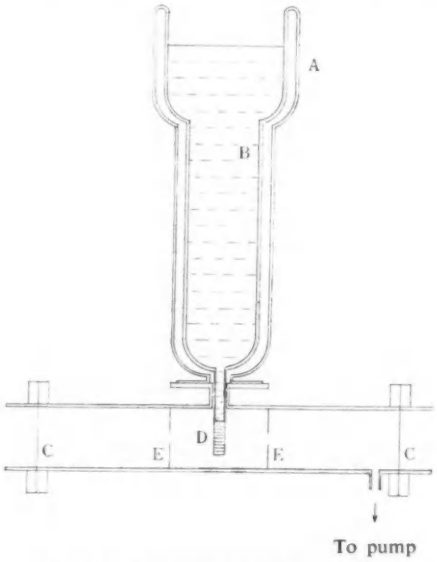

Fig. 1. Cryostat and cavity assembly

(A) Glass Dewar (D) Sample
(B) Liquid nitrogen (E) Iris
(C) Mica

small glass-tube was attached with some cement to the end-plane of the inner glass tube of the Dewar inserted into the cavity. The temperature at the position of the sample was measured by a copper-constantan thermocouple, which indicated a temperature of -100°C or -40°C when liquid nitrogen or methanol mixed with dry-ice was filled in the Dewar, respectively. As the outer part of the Dewar was jointed on a copper-head standing out of the cavity on its narrow side, removal of the entire assembly from the cavity for cleaning or using the cavity for measurements at room temperature was done easily. The space between the inner and outer parts of the Dewar and the inside part of the cavity were pumped out to get vacuum by closing the waveguide with thin mica foils in front of and behind the cavity.

2) Preparation of Samples.—The samples used in our experiment were prepared by two ways. One of them may be called the method I, while the other the method II. The latter will be described in details. As shown in Fig. 2, the apparatus for preparing the samples consists of several reaction vessels, all of which can be kept at high vacuum.

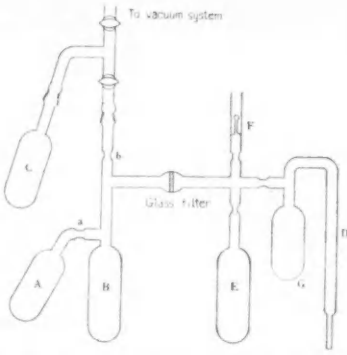

Fig. 2. Apparatus for preparation of sample.

The samples were prepared using this apparatus as follows. Connecting the entire vessel to the vacuum system, water and oxygen adsorbed on the wall of the glass vessels were excluded by heating and discharging the tube with a tesla coil. The sodium metal contained inside the glass vessel A was distilled into the reaction vessel B under reduced pressure, and the vessel A was sealed off from the system at the part "a". Then the aromatice hydrocarbons and toluene contained in the vessel were distilled into the vessel B under reduced pressure, and the vessels B, D, E and G were taken off from the vacuum system at the part of "b". The reaction vessel B was kept at about 100°C for a long time, in order to change the high-polymerized adduct of the aromatic hydrocarbon, formed inside the reaction vessel B before the heat-treatment, to a low-polymerized one. After the precipitate* inside the reaction vessel B was separated from the solvent, was transfered into the vessel E and was distilled under reduced pressure through the breakable joint, the precipitate was dissolved into the tetrahydrofuran or dioxane which was stored in the vessel G through the breakable joint F. Tetrahydrofuran and dioxane were used here as the solvent in which paramagnetic free radicals were contained as a diluted state. For the measurement of paramagnetic resonance the sample thus prepared was used in the glass tube D, the end part of which was inserted into the cavity. The method II described above was applied to the production of radicals of styrene, α-methyl styrene, *p*-methyl styrene and 1, 1-diphenylethylene.

In the method I the aromatic hydrocarbon whose radical was to be produced was reacted directly with sodium metal in tetrahydrofuran or dioxane in a way similar to that of the method II without using toluene. The radicals of styrene, α-methylstyrene, *p*-methylstyrene, 1, 1-diphenylethylene, stilbene, 1, 4-diphenylbutadiene and isoprene** could be produced by this method.

Determining the concentration of sodium ion in

* A strong paramagnetic resonance line was observed in the precipitate of the sodium adducts of styrene. The line width and g-factor were about 2 gauss and 2.002 respectively, and the line shape was Lorentzian.

** Reported briefly: K. Kuwata, K. Morigaki and K. Hirota, This Bulletin, 32, 895 (1959).

sample of styrene by flame spectroscopy, the ratio of radical part to an ionic part was estimated. It was of the order of one tenth. All measurements were carried out in the concentration range of about 10^{-3} to 10^{-4} spin per liter.

In the preparation of radicals described above precautions are taken against contamination of the reaction vessel used, because a trace of water and oxygen, if left in the vessel, may react easily with the adduct of the aromatic hydrocarbon and make the concentration of radicals decrease. Purification of aromatic hydrocarbons, sodium metal and solvents was performed in the following way. The aromatic hydrocarbons purified by the usual method were put in contact with sodium metal so as to remove the remaining water and were purified by vaccum distillation. The solvent purified in the usual way was reacted with stilbene anions or naphthalene anions by utilizing the reactive properties of these anions with the water and oxygen, and then the stilbene or the naphthalene was removed from the solvent by distillation. Naphthalene was used only in the preparation of the first samples of styrene radical. In the other samples, stilbene was used in most cases including the preparation of the styrene radical, because the stilbene anion gave no more than a broad resonance line without any structure even if it remained in the solvent.

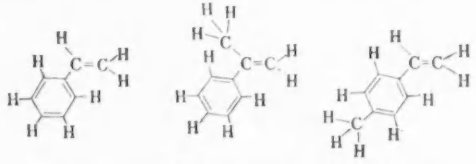

Styrene α-Methyl styrene p-Methyl styrene

Fig. 3

Results and Discussion

Styrene.—We have observed three kinds of paramagnetic resonance spectra in the styrene radical*. They were i) four lines, ii) nine lines and iii) many complex lines respectively.

i) Four lines.—The four-lines spectrum has been observed in many samples of dilute solution of the styrene adduct with sodium metal, when the solvent is tetrahydrofuran or dioxane. Even if either solvent is used and potassium metal is used in place of sodium metal, almost identical spectra of four lines were given. The above samples were prepared by the methods I and II described in the section 2. The spectrum consists of almost equally spaced four lines of which the intensities of each components are 1 : 3.2 : 3.3 : 1.2 in ratio in order of the strength of the magnetic field corresponding to the resonance lines. From the above results the hyperfine splitting is considered to arise from the hyperfine interaction between the unpaired electron and three equivalent protons. The hyperfine splitting is 4.3 ± 0.5 gauss and the g-factor is 2.0031 ± 0.0006.

The line-shape of each components is almost Gaussian with the half-width of about 3.9 gauss as shown in Fig. 5 (B).

The spectra observed at low temperatures, $-40°C$ and $-100°C$, were almost identical with those observed at room temperature. From these results the width of each component is attributed to the unresolved hyperfine interaction with protons.

Three equivalent protons contributing to the

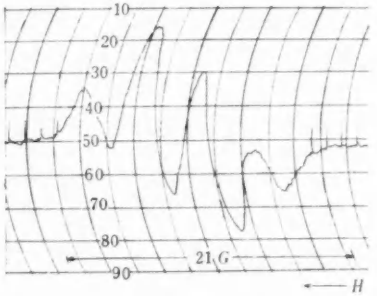

Fig. 4. Paramagnetic resonance spectrum of styrene radical.

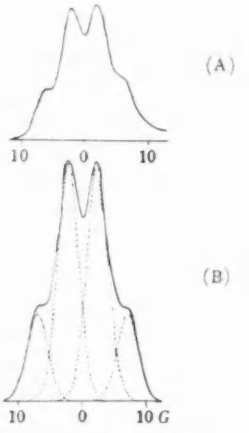

Fig. 5. Paramagnetic resonance spectra of styrene radical.

(A) The observed spectrum obtained by numerical integration.

(B) The calculated spectrum constructed from four Gaussian shaped lines with relative intensities of 1 : 3 : 3 : 1.

* Besides the three kinds of spectra, the other spectrum similar to that of the naphthalene anion was observed in the styrene radical in the tetrahydrofuran solution prepared by the methods I and II with sodium metal at the first stage of our experiment, which has been already reported briefly[21]. As it has not been reproducible, it will not be described here.

hyperfine splitting and some protons constructing the line-width of each components have not been able to be given a definite correspondence to the protons of the styrene anion.

ii) Nine lines.—The spectrum consisting of equally spaced nine lines has been observed in the styrene radical in the tetrahydrofuran solution prepared by the method I with sodium metal. The spacing between each components was 2.2±0.2 gauss.

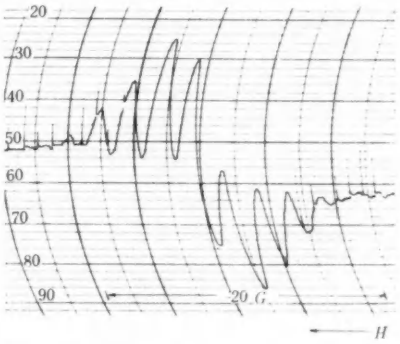

Fig. 6. Paramagnetic resonance spectrum of styrene radical

iii) Many complex lines.—The complex spectrum has been observed in the styrene radical in the tetrahydrofuran solution prepared by the method I with sodium metal. The spectrum extends to the length of 24±3 gauss on the scale of the magnetic field. The *g*-factor is 2.0028±0.0005.

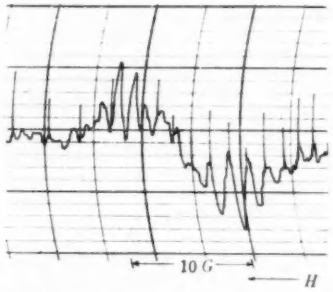

Fig. 7. Paramagnetic resonance spectrum of styrene radical.

The relation among the above three spectra on the point of the preparation of the styrene radical and the magnetic centers corresponding to the spectra have not been found in the present stage, so further experiments will be required to obtain some information about this problem.

On the other hand, we tried to observe the paramagnetic resonance of the styrene radical formed on the film of the vaporized sodium metal, but it gave a negative result*.

α-Methylstyrene.—We have observed the paramagnetic resonance spectrum, as shown in Fig. 8, of the α-methylstyrene radical in the tetrahydrofuran solution prepared by the method I with sodium metal. This spectrum extends to the length of about 32 gauss on the scale of the magnetic field. It may be explained by assuming that the hyperfine splitting is mainly attributed to the hyperfine interaction with three equivalent protons and another two equivalent protons with the coupling constant of 4.2 gauss and 2.5 gauss respectively and some protons contribute to construct the line shape of each components. If the magnetic center corresponding to the above spectrum is assumed to be the unpaired electron being localized on the α-methylstyrene anion, the following assignment might be reasonable on the basis of the unpaired electron density calculated by using the simple LCAO-MO theory: the three equivalent protons and two equivalent protons in the above analysis correspond to the *ortho*, *para*-protons and β-protons respectively, and the *meta*-protons

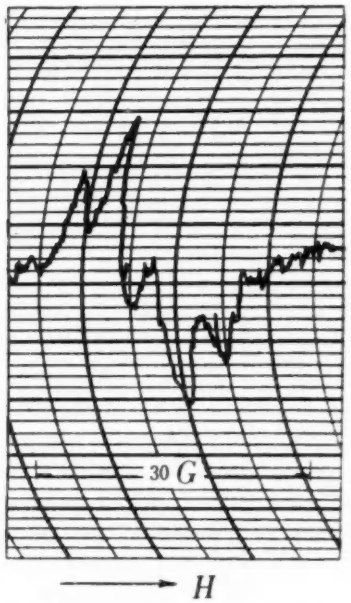

Fig. 8. Paramagnetic resonance spectrum of α-methylstyrene radical.

* It might be necessary to refer to the Weissman's answer in discussion [*J. Phys. Chem.*, **57**, 507 (1953)], that "the paramagnetic resonance absorption in styrene as it is undergoing polymerization initiated by metallic sodium is not reproducible".

and the protons belonging to the methyl-group construct the line width of each components. The simple LCAO-MO calculation gives the following unpaired electron densities on the carbon atom of *ortho*, *meta*, *para*, H_3 and β positions respectively.

$$\rho_o = 0.091, \quad \rho_m = 0.016, \quad \rho_p = 0.149,$$
$$\rho_{H_3} = 0.026, \quad \rho_\beta = 0.355.$$

p-Methylstyrene.—The observed spectrum of the *p*-methylstyrene radical is shown in Fig. 9. This sample consists of *p*-methylstyrene and *ortho*-methylstyrene with concentration of 60% and 40% respectively. This situation complicates the spectrum. Besides, the proton of the methyl group seems to contribute to the observed spectrum much more than in the case of the α-methylstyrene radical. We have not been able to analyze the observed spectrum.

A few months later than the time of preparation of the samples during which the sample was kept at room temperature, the spectrum became simpler and weaker than that observed immediately after the preparation of the samples. This changes of the spectrum is shown in Fig. 10. No change of the color and viscosity accompained with that of the spectrum were observed. The hyperfine structure of the spectrum exists in the region of the length of about 25 ($\pm$5) gauss on the scale of the magnetic field. After this change, the samples always showed the same patterns of the spectrum as the above one, but the intensity of the resonance lines has decreased gradually with time.

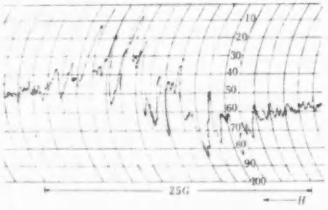

Fig. 9. Paramagnetic resonance spectrum of *p*-methylstyrene radical.

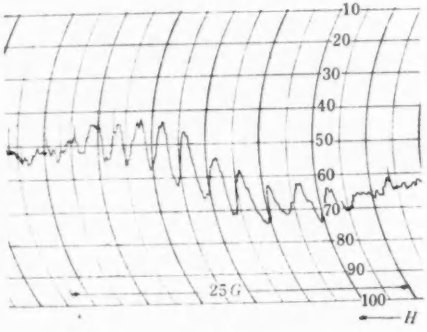

Fig. 10. Paramagnetic resonance spectrum of *p*-methylstyrene radical

Reaction of the Aromatic Hydrocarbons with Alkali Metals

As described briefly in the section 1, the aromatic vinyl compounds, especially styrene, are initiated to polymerize with alkali metal. This property of styrene adducts with sodium metal as chain initiators was found independently by Szwarc et al.[3] and by Meshitsuka et al.[4] When the monomers of styrene exist in some suitable solvents (toluene, tetrahydrofuran, dioxane etc.), polymerization of them proceeds under existence of the adducts which produce the living polymer. The styrene adducts similar to that in the above case are produced by Scott's method in which naphthalene anions are used as a substitute of alkali metal. In this case, according to Szwarc, the living polymers consist of the dimerized styrene anions with both ends "living",

$$[:\mathrm{CH}(\phi)-\mathrm{CH_2}-\mathrm{CH_2}-\ddot{\mathrm{C}}\mathrm{H}(\phi)]^{2-} \quad (\phi = \mathrm{C_6H_5})$$

which is formed by dimerization of univalent monomer anions

$$[:\mathrm{CH}(\phi)-\dot{\mathrm{C}}\mathrm{H_2}] \quad \text{or} \quad [\dot{\mathrm{C}}\mathrm{H}(\phi)-\ddot{\mathrm{C}}\mathrm{H_2}]^-$$

being produced through the following process of electron transfer,

$$\text{naphthalene}^- + \text{styrene} \rightarrow \text{naphtharene} + \text{stylene}^-$$

The above situation in the case of polymerization of styrene initiated by the styrene adduct formed through electron transfer which takes place between naphthalene anions and the monomers of styrene will be applied to our cases in which the styrene adducts with sodium metal form the living polymers. Then, the existence of the radical anions will not be detected because dimerization of univalent monomer anions is performed in a very short time in the above process.

On the other hand, two of the present authors found that if the styrene adduct with a high degree of polymerization formed at the first stage of the reaction of styrene with sodium metal reacts with sodium metal still

3) M. Szwarc, M. Levy and R. Milkovich, *J. Am. Chem. Soc.*, 78, 2656 (1958); M. Szwarc, *Nature*, 178, 1168 (1956).
4) G. Meshitsuka and Y. Okada, *Chem. High Polymers (Tokyo)*, (*Kobunshi Kagaku*) 14, 33, 37, 123 (1957).

more, the dark red precipitates are formed in the solution of toluene as a result of dissociation of the styrene polymer. These precipitates showed a strong paramagnetic resonance line, of which the line width and *g*-factor were about 2 gauss and 2.002 and the line shape was Lorentzian, and when they were diluted into the tetrahydrofuran, the hyperfine splitting in the paramagnetic resonance spectra was observed as described in the former sections. These spectra were attributed to be coming from monomer anions of styrene or polymer radicals with the low degree of polymerization.

The observations of the paramagnetic resonance of radicals of the aromatic vinyl compounds may be considered to become possible for the following reasons. Under non-existence of the monomer of aromatic vinyl compounds radical anions will exist stably in the polar solvents*, as tetrahydrofuran and dioxane, because they are electrically repulsed by each other in the polar solvent to be obstructed to dimerize.

In the case of the radicals with a high degree of polymerization, it will be difficult to observe their paramagnetic resonance owing to the following two reasons; one of the reasons is that the concentration of radicals in the solution becomes small, and the other is that the motion of such radicals becomes slower than that of monomer radicals or radicals with a low degree of polymerization to extend the linewidth of each components of the hyperfine structure by contribution of the anisotropic hyperfine interaction of the unpaired electron with the protons. Indeed, no paramagnetic resonance of the radicals of a highly polymerized styrene diluted in the tetrahydrofuran was observed and the intensity of the resonance lines which were observed in most of the other samples of the aromatic vinyl compounds, described in the present paper, decreased gradually with time in accordance with the progress of polymerization. In some cases the change of patterns of the paramagnetic resonance spectrum was accompanied by decrease of intensity. As an example of such a change of spectrum we can see clearly the tendency in the case of *p*-methylstyrene as described in the section 3.

In the forthcoming paper, which will describe the results of the paramagnetic resonance of radicals of 1, 1-diphenylethylene, stilbene and 1, 4-diphenylbutadiene, a formulation which describes the process of polymerization will be presented.

* We could not observe paramagnetic resonance of the styrene radicals diluted in the solution of toluene which was a non-polar solvent.

Summary

Paramagnetic resonance of radicals of the aromatic vinyl compounds in the tetrahydrofuran and dioxane solutions was observed: styrene, *α*-methyl styrene and *p*-methyl styrene. By analyzing the observed spectra the structure of the radicals is discussed. From these results it may be concluded that the reaction of the aromtic vinyl compounds with alkali metal proceeds through two steps; formation of their radical anions, and successive addition of the monomers to this radical anion turning into "living polymers".

The authors wish to express their sincere thanks to Professor Junkichi Itoh of Osaka University for his continuous encouragement and his helpful discussions throughout this work.

Physics Department (K. M.)
Chemistry Department
(K. K. and K. H.)
Osaka University
Nakanoshima, Osaka

Paramagnetic Resonance of Radicals of Some Aromatic Vinyl Compounds. II

By Kazuo MORIGAKI, Keiji KUWATA and Kozo HIROTA

(Received January 20, 1960)

In the preceding paper[1] the results of the paramagnetic resonance of radicals of styrene, α-methylstyrene and *p*-methylstyrene were described. Here the results of the paramagnetic resonance of radicals of 1, 1-diphenylethylene, stilbene and 1, 4-diphenylbutadiene will be described and will be discussed in connection with the problem of the process of the polymerization of these compounds.

Experimental

The measurements of paramagnetic resonance of the above radicals were performed at room temperature by using the same apparatus as that being described in the preceding paper and the samples were also prepared by the same method as that described in the preceding paper.

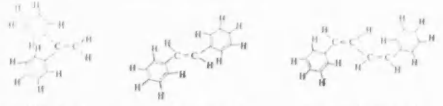

1-1 Diphenylethylene — Stilbene — 1-4 Diphenylbutadiene

Fig. 1.

Results and Discussion

1,1-Diphenylethylene (DPE). — Two spectra have been observed in the 1, 1-diphenylethylene (DPE) radical in the tetrahydrofuran solution with its concentration of $10^{-3}\sim10^{-4}$ M under different conditions of the sample. In the DPE radical produced by method I described in section 2 of the preceding paper, many lines were observed as shown in Fig. 2.

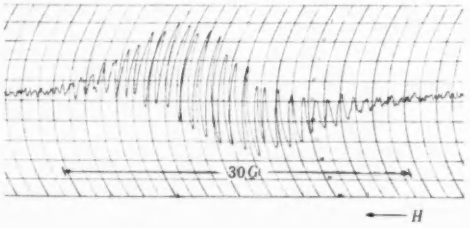

Fig. 2. Paramagnetic resonance spectrum of 1-1 diphenylethylene radical.

We tried to explain the observed spectrum through the following spin Hamiltonian,

$$\mathcal{H}=g\beta\boldsymbol{H}\boldsymbol{S}+\sum_{i=1}^{4}A_o\boldsymbol{I}_{o_i}\boldsymbol{S}+\sum_{i=1}^{4}A_m\boldsymbol{I}_{m_i}\boldsymbol{S}$$
$$+\sum_{i=1}^{2}A_p\boldsymbol{I}_{p_i}\boldsymbol{S}+\sum_{i=1}^{2}A_\beta\boldsymbol{I}_{\beta_i}\boldsymbol{S} \qquad (1)$$

where the first term describes the Zeeman energy and $\boldsymbol{I}_o$, $\boldsymbol{I}_m$, $\boldsymbol{I}_p$ and $\boldsymbol{I}_\beta$ describe the spin of the proton in the *ortho-*, *meta-*, *para-* and β position respectively, and the suffix i given under the spins of the proton $\boldsymbol{I}$ shows a different position in the same site with respect to the symmetry of the molecule. Although the observed spectrum is so complicated that we can not analyze it definitely, the following values of the parameters, g, A_o, A_m, A_p and A_β, in the above spin Hamiltonian seem to fit best with the observed spectrum: $g=2.002$ $A_p=A_p\sim6$ gauss, $A_m\sim1$ gauss, $A_\beta\sim3$ gauss. However, some ambiguities are left in these values except in the case of g. The calculated spectrum is shown in Fig. 3, where several lines at both sides apart from the center are assumed not to be observed owing to their weak intensities. The above analysis indicates that the magnetic center corresponding to the observed spectrum is the unpaired electron in the DPE monomer anion.

Fig. 3. The calculated spectrum of 1-1 diphenylethylene anion.

According to McConnell[2] the hyperfine splitting constant is proportional to the unpaired electron density on the carbon atom adjacent to the proton in the aromatic hydrocarbon. From the above hyperfine splitting

1) K. Morigaki, K. Kuwata and K. Hirota, This Bulletin, **33**, 952 (1960).

2) H. M. McConnell, *J. Chem. Phys.*, **24**, 764 (1956); H. M. McConnell and D. B. Chesnut, ibid., **28**, 107 (1958).

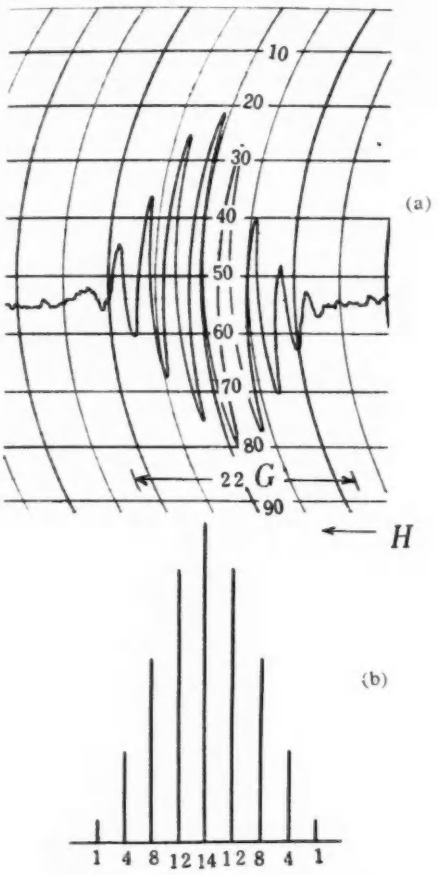

Fig. 4. (a) Paramagnetic resonance spectrum of 1-1 diphenylethylene radical.
(b) The calculated spectrum of 1-1 diphenylethylene radical.

constant in Eq. (1) the unpaired electron densities of the DPE monomer anion at each carbon atom in the aromatic ring can be derived, i.e., they are given in ratio as follows:

$$\rho_o : \rho_p : \rho_m = 6 : 6 : 1$$

where ρ_o, ρ_p and ρ_m give the unpaired electron densities on the carbon atom adjacent to the *ortho*-, *para*- and *meta*-hydrogen atom respectively.

On the other hand, the simple LCAO-MO calculation gives the normalized unpaired electron densities the following values,

$$\rho_o = 0.05521, \quad \rho_p = 0.07813, \quad \rho_m = 0.00622$$

or

$$\rho_o : \rho_p : \rho_m = 8.9 : 12 : 1$$

The observed spin densities on the *ortho*- and *para*-carbon atoms are smaller than those expected from the simple LCAO-MO calculation. The normalized unpaired electron density on the β-carbon atom given by the simple LCAO-MO calculation is given by $\rho_\beta = 0.3856$. In spite of the large value of the electron density on the β carbon atom, the observed hyperfine splitting is half as much as that corresponding to the unpaired electron densities on the *para*- and *ortho*- carbon atoms. This means that there is a marked difference between the cases of the β-proton and the ring proton in the proportionality constants connecting the unpaired electron density to the hyperfine splitting. However, the origin of the small proportionality constant for the hyperfine splitting at the β-proton has not been found.

Another spectrum, as shown in Fig. 4 (a), was observed in the sample of DPE which has been kept at 110°C for two days after the observation of the first spectrum shown in Fig. 2. The change of the spectrum coming from the heat-treatment of the sample is drastic and is accompanied with that of its color from dark yellow to green. This indicates that the DPE radical was changed into another kind of radical through the heat-treatment. From the following analysis of the observed spectrum the magnetic center corresponding to the second spectrum seems to be identified with the unpaired electron being localized around the end of the anion of the DPE polymer as shown in Fig. 5.

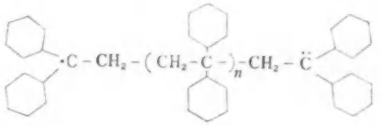

Fig. 5. Structural formula for 1-1 diphenyl polymer anion.

The observed spectrum can be explained by the following spin Hamiltonian,

$$\mathcal{H} = g\beta \boldsymbol{H}\boldsymbol{S} + \sum_{i=1}^{4} \boldsymbol{A}_o \boldsymbol{I}_{oi} \boldsymbol{S} + \sum_{i=1}^{4} \boldsymbol{A}_m \boldsymbol{I}_{mi} \boldsymbol{S} + \sum_{i=1}^{2} \boldsymbol{A}_p \boldsymbol{I}_{pi} \boldsymbol{S} \qquad (2)$$

with $g = 2.0026 \pm 0.0005$, $A_p = 5.4 \pm 0.5$ gauss, $A_o = 2.7 \pm 0.3$ gauss and $A_m \sim 0$ gauss. Although two kinds of hyperfine interaction with four equivalent protons are indistinguishable from each other in the resonance experiment, it is assumed in the above assignment from the theoretical point of view that the hyperfine interaction with the *ortho*-protons will be stronger than that with the *meta*-protons. A pattern of the spectrum is constructed from the above spin Hamiltonian with the parameters given above

as shown in Fig. 4 (b). This spectrum consists of nine lines with relative intensities of 1 : 4 : 8 : 12 : 14 : 12 : 8 : 4 : 1. The relative intensities of each component in the calculated spectrum are in good agreement with the observed ones of 1 : 4 : 8 : 12.5 : 14 : 12.5 : 7.5 : 3.8 : 1. If the line widths of each component are attributed to the unresolved hyperfine interaction due to the four *meta*-protons, the coupling constant A_m is given by the value of about 0.7 gauss.

The above model of the magnetic center is similar to the diphenylmethyl radical concerned with the part on which the unpaired electron is localized. The calculation of the spin densities of the π-electrons on the carbon atoms in the diphenylmethyl radical performed by using the Pauling-Wheland valence-bond theory shows that the spin densities of the π-electrons on the *para*-, *ortho*- and *meta*-carbon atoms are given as follows (See Appendix):

$$\rho_p = 0.2790, \quad \rho_o = 0.2732, \quad \rho_m = -0.1483.$$

The spectrum constructed on the basis of the above spin densities, as shown in the appendix, is slightly different from the observed spectrum. The relative spin densities obtained from the above analysis of the observed spectrum are not in agreement with the calculated ones. The actual situation of distribution of the π-electrons in the DPE polymer radical will not be so simple as the case of diphenylmethyl. Indeed the DPE polymer forms a bending chain, so the two benzene rings in which the unpaired electron is to be localized may not be on the co-plane. However, it has not been clear at the present stage whether the above difference between the observed spectrum and the calculated one shows that the magnetic center corresponding to the observed paramagnetic resonance may not be the unpaired electron in the DPE polymer radical.

Stilbene.—A resonance line without any structures was observed in the stilbene radical in tetrahydrofuran solution with its concentration of $10^{-3} \sim 10^{-4}$ M (Fig. 6). It has the maximum separation of thirteen gauss in the derivatives of the absorption line and the *g*-factor of 2.002. This result indicates that the hyperfine structure can not be resolved because many protons contribute to the hyperfine splitting. This situation is consistent with the simple LCAO-MO calculation of the unpaired electron density in the stilbene anion. The stilbene radical in tetrahydrofuran with its concentration of 10^{-1} M showed a Lorentzian-shaped line with the line width of 1.8 gauss.

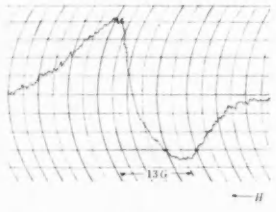

Fig. 6. Paramagnetic resonance spectrum of stylbene radical.

1,4-Diphenylbutadiene.—In a sample including the radical of 1,4-diphenylbutadiene prepared by method I, a resonance spectrum with unresolved h. f. s., which extends in the region of the magnetic field of about thirty-four gauss with $g = 2.00$, has been observed as shown in Fig. 7. But it has not been investigated in detail.

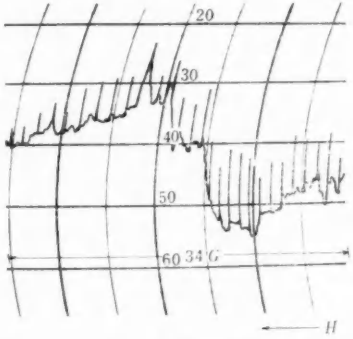

Fig. 7. Paramagnetic resonance spectrum of 1,4-diphenylbutadiene radical.

Discussions on the Process of Polymerization

As described in the preceding paper, the pattern of the paramagnetic resonance spectra of radicals of styrene and *p*-methylstyrene depends sensitively on the degree of polymerization. In the latter substance changes of pattern and intensity of the paramagnetic resonance with time have been clearly observed. In the former samples three kinds of spectra have been observed, according to the conditions of preparation of the radicals. In the preceding paper the situations under which the polymerization of styrene and its derivatives proceeds were discussed by considering the above results.

In the case of DPE radicals, when a renewed reaction of DPE adducts, which had shown many resonance lines, with the sodium metal was performed by keeping the sample at 100°C for two days, another new spectrum was observed, which was considered to be coming from the hyperfine interaction of the unpaired electron being localized around the end molecule of DPE polymer, probably with a

low degree of polymerization, with its protons.

From these results it may be considered that polymerization is initiated through the process in which the monomer of the aromatic vinyl compound forms a bond between itself and the α- or β-carbon atoms of the radical anion to grow into the polymer. This situation can be described in the following formula.

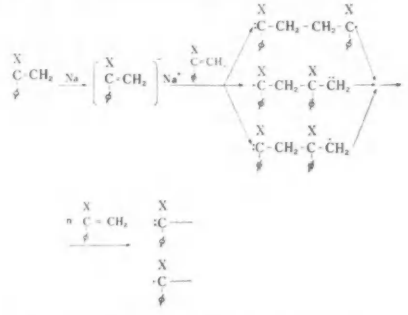

where X means H, CH_3 or $\phi(=C_6H_5)$.

The process of polymerization of the aromatic vinyl compounds has been studied through the optical absorption spectroscopy[3]. In order to confirm the above model of the process of polymerization, further experiments will be necessary.

Summary

Paramagnetic resonance absorption of the radicals of 1, 1-diphenylethylene, stilbene and 1, 4-diphenylbutadiene in tetrahydrofuran solution was investigated at room temperature. In diphenylethylene (DPE) radicals two kinds of spectra were observed corresponding to two states of the radicals; one is the DPE monomer anion and the other the DPE polymer anion. In connection with the experimental results in the case of styrene, α-methylstyrene and *p*-methylstyrene described in the preceding paper, the process of polymerization of some aromatic vinyl compounds was discussed.

The authors wish to express their sincere thanks to Professor Junkichi Itoh of Osaka University for his continuous encouragement and his helpful discussions throughout this work.

Physics Department (K. M.)
Chemistry Department
(K. K. and K. H.)
Osaka University
Nakanoshima, Osaka

3) K. Hirota, K. Kuwata, H. Togawa and S. Ishida, *J. Chem. Soc. Japan, Pure Chem. Sec.* (*Nippon Kagaku Zasshi*), **79**, 602 (1958); K. Kuwata, to be published in This Bulletin.

Appendix

Spin Densities in the Diphenylmethyl Radical

Spin densities of π-electrons on carbon atoms in the diphenylmethyl radical are calculated by using valence-bond theory. Valence-bond theory has been so far applied also to calculations of spin densities on carbon atoms in the triphenylmethyl radical by Brovetto and Ferroni[4] and in the perinaphthenyl radical by McConnell and Dearman[5] in good agreements with the experimental results. Therefore, valencebond theory is adequate to calculate the spin densities of π-electrons in these odd-alternant hydrocarbon radicals.

Valence-bond structures for calculation of the spin densities of π-electrons on carbon atoms in the diphenylmethyl radical can be divided into three groups shown in Fig. 8. To these three groups belong the 4, 4, 8 independent wave functions for the unpaired electron on the methylic carbon atom, and the *para*- and the *ortho*-carbon atoms of the benzene ring respectively. All functions related to Dewar structures will be neglected.

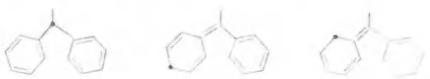

φ_1 φ_2 φ_3

Fig. 8.

With a linear combination for the φ_{ik} the wave function Ψ in the ground state can be constructed in such a way as to minimize the total energy of electrons. Then, Ψ is given by the following equation,

$$\Psi = \sum_i C_i \sum_k \varphi_{ik} \tag{A1}$$

The total Hamiltonian fo the π-electrons under the existence of the external magnetic field is:

$$\mathcal{H} = \mathcal{H}_0 + \mathcal{H}_1 + \mathcal{H}_2 \tag{A2}$$

$$\mathcal{H}_1 = g_i \beta \boldsymbol{H} \boldsymbol{S}$$

$$\mathcal{H}_2 = -(8\pi/3) g_i \beta g_N \beta_N \sum_k \boldsymbol{I}_k \boldsymbol{S} \delta(\boldsymbol{r}_i - \boldsymbol{r}_k)$$

where $\mathcal{H}_0$ means the kinetic energy and the Coulomb potential energy of the electrons; $\mathcal{H}_1$ is Zeeman energy in which the external magnetic field and the electronic spin are described by $\boldsymbol{H}$ and $\boldsymbol{S}$ respectively, $\mathcal{H}_2$ is the hyperfine interaction energy coming from the Fermi type contact hyperfine interaction between the electron and the *k*th-proton with

4) P. Brovetto and S. Ferroni, *Nuovo Cimento*, **5**, 142 (1957).

5) H. M. McConnell and H. H. Dearman, *J. Chem. Phys.*, **28**, 51 (1958).

the nuclear spin I_k, β and β_N are the electronic and nuclear Bohr magnetrons respectively, and g and g_N are the electronic and nuclear g-factors and $\delta(\boldsymbol{r}_e-\boldsymbol{r}_k)$ means the Dirac delta function for the distance between the electron and the kth-proton. In the above Hamiltonian the dipolar interaction between the electron and the proton is neglected, because it is averaged out not to contribute to the paramagnetic resonance spectrum by a tumbling motion of the molecule in the solution.

After some computations the minimum energy W of the Hamiltonian $\mathcal{H}_0$ is given in the following equation,

$$W=Q+4.7046\alpha \qquad \text{(A3)}$$

where Q means the Coulomb integral and α the single exchange integral.

Corresponding to the state with the minimum energy, the wave function in the ground state is given as follows:

$$\Psi=0.1572\varphi_1+0.1341\varphi_2+0.1312\varphi_3 \qquad \text{(A4)}$$

The matrix element of the hyperfine interaction $\mathcal{H}_2$ is calculated by using the Brovetto-Ferroni method as applied to triphenylmethyl. By using Eq. (A1) the matrix element $\langle\Psi|\mathcal{H}_2|\Psi\rangle$ is given in the following equation,

$$\langle\Psi|\mathcal{H}_2|\Psi\rangle=\sum_{ij}c_ic_j\sum_{kl}\langle\varphi_{ik}|\mathcal{H}_2|\varphi_{jl}\rangle \qquad \text{(A5)}$$

The matrix elements $\langle\varphi_{ik}|\mathcal{H}_2|\varphi_{jl}\rangle$ can be calculated in a similar way to the case of triphenylmethyl.

$$\langle\Psi|\mathcal{H}_2|\Psi\rangle=-(8\pi/3)g_i\beta g_N\beta_N A \times[0.2790I_{ip}-0.1483I_{im}+0.2732I_{io}]\cdot S_z \qquad \text{(A6)}$$

where I_{ip}, I_{im} and I_{io} mean the component along the external magnetic field of the total spin of the protons in the *para*, *ortho* and *meta* position of the benzene ring respectively, and A is the factor which depends on the strength of the $\sigma-\pi$ interaction.

The magnetic field H corresponding to the transition $\Delta S_z=\pm1$, $\Delta I_z=0$ in the experiment using the microwave with the frequency ν is given by the following equation

$$H=h\nu/g_i\beta+(8\pi/3)g_N\beta_N A \times[0.2790I_{ip}-0.1483I_{im}+0.2732I_{io}] \qquad \text{(A7)}$$

Then, the paramagnetic resonance spectrum can be constructed by Eq. (A7) as shown in Fig. 9, where only the upper part of the spectrum corresponding to the value of H larger than $h\nu/g_i\beta$ is given, because the spectrum is symmetrical with respect to the value of the magnetic field $H=h\nu/g\beta$.

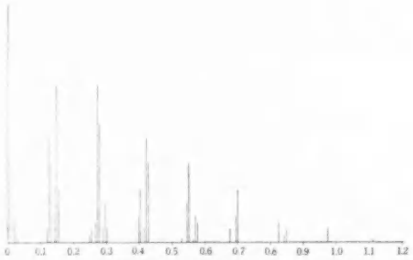

Fig. 9. The calculated spectrum of diphenylmethyl radical.

A comparison of the above calculated spectrum with the observed one in the DPE radical shows some differences as shown in Fig. 9. Though the observed spectrum consists of nine lines, more lines should be expected from the results of the calculation. Especially, the fifth line from the central one, which has about half the intensity in comparison with the fourth line in the calculated spectrum, should be observed from the experimental condition of our spectrometer. The origin of the above differences between the theoretical spectrum and experimental one is discussed in the text.

A Further Study of Simple LCAO MO Perturbation Treatment of Conjugated Molecules

By Kenichi FUKUI, Keiji MOROKUMA, Teijiro YONEZAWA and Chikayoshi NAGATA

(Received December 19, 1959)

The perturbation theory in the simple LCAO MO method has been studied by many authors, for instance, by Coulson and Longuet-Higgins[1] and by Dewar[2]. Recently, by the present authors[3], a new mathematical method of perturbation theory, named the method of perturbed secular determinant, has been developed and several useful equations have been derived which give the orbital energy, the electron density and the bond order of the perturbed system.

The only system involved in these works, however, was the one which suffered only one perturbation, that is, a small change of a Coulomb integral or of a resonance integral, or a weak bonding to another system. There could be seen no systematic perturbation treatment of the system which was affected by two or more perturbations, for instance, changes of two Coulomb integrals, changes of a Coulomb integral and of a resonance integral, and a weak bonding with a change of a Coulomb integral. To deal with such a system would be of practical interest in discussing the chemical reactivity, absorption spectrum, dipole moment and other electronic properties of large conjugated molecules.

In the present paper are derived several equations or relations which give the molecular orbital, its orbital energy, the electron density and the bond order of systems affected by two perturbations, and lastly they are extended to a more general case of many perturbations.

Non-degenerate System

1. Summary of Results for Single Perturbation.—In order to simplify the expression of various equations appearing in the treatment of multiple-perturbed systems, it would be convenient to summarize the results for single perturbation. The following formulae, obtained by the method of perturbed secular determinant and also by the existing method of perturbation, were given in the previous paper, though some of them not explicitly.

In this section it is assumed that the system to be treated is not degenerate in itself, nor has it any degenerate level between another system to conjugate with.

First, if the Coulomb integral, α_r, of the rth atom in a conjugated system, $\Delta(\varepsilon)$,* is increased by α_r' (Case A of Ref. 3), then, as its consequence, the jth orbital energy, ε_j, will increase by $(\delta\varepsilon_j)_r$, the separate bond order, p_{uv}^j, by $(\delta p_{uv}^j)_r$, the separate electron density, p_{uu}^j, by $(\delta p_{uu}^j)_r$, the total π electronic energy, ε, by $(\delta\varepsilon)_r$, the bond order, p_{uv}, by $(\delta p_{uv})_r$, the electron density, p_{uu}, by $(\delta p_{uu})_r$ and the jth molecular orbital, Ψ_j, by $(\delta\Psi_j)_r$, in such a way that**

$$(\delta\varepsilon_j)_r = (c_r^j)^2\alpha_r' + \sum_{k(\neq j)}^{\text{all}} \frac{(c_r^j c_r^k)^2}{\varepsilon_j - \varepsilon_k}(\alpha_r')^2 + \cdots\cdots \tag{1}$$

$$(\delta p_{uv}^j)_r = \sum_{k(\neq j)}^{\text{all}} \frac{c_r^j c_r^k (c_u^j c_v^k + c_v^j c_u^k)}{\varepsilon_j - \varepsilon_k}\alpha_r' + \sum_{k(\neq j)}^{\text{all}} \frac{c_r^j c_r^k}{\varepsilon_j - \varepsilon_k}\left[\sum_{m(\neq j)}^{\text{all}} \frac{c_r^m\{c_r^j c_u^k c_v^m + c_r^m(c_u^j c_v^k + c_v^j c_u^k)\}}{\varepsilon_j - \varepsilon_m}\right.$$
$$\left. - \frac{c_r^j\{c_r^k c_u^j c_v^j + c_r^j(c_u^j c_v^k + c_v^j c_u^k)\}}{\varepsilon_j - \varepsilon_k}\right](\alpha_r')^2 + \cdots\cdots \qquad (u = v \text{ or } u \neq v) \tag{2}$$

1) C. A. Coulson and H. C. Longuet-Higgins, *Proc. Roy. Soc. (London)*, **A191**, 39 (1947); **A192**, 16 (1947); **A193**, 447, 456 (1948); **A195**, 188 (1948).
2) M. J. S. Dewar, *J. Am. Chem. Soc.*, **74**, 3341 (1952).
3) K. Fukui, C. Nagata, T. Yonezawa, H. Kato and K. Morokuma, *J. Chem. Phys.*, **31**, 287 (1959).

* $\Delta(\varepsilon)$ is the secular determinant of the system and will be used also to characterize a conjugated system.

** As for the nomenclature, see Ref. 3. Electron density will be looked upon as a special case ($u = v$) of bond order in the further discussion.

$$(\delta\varepsilon)_r = p_{rr}\alpha_r' + 2\sum_j^{\text{occ}}\sum_k^{\text{unocc}} \frac{(c_r^j c_r^k)^2}{\varepsilon_j - \varepsilon_k}(\alpha_r')^2 + \cdots\cdots \tag{3}$$

$$(\delta p_{uv})_r = 2\sum_j^{\text{occ}}\sum_k^{\text{unocc}} \frac{c_r^j c^{\,k}(c_u^j c_v^k + c_v^j c_u^k)}{\varepsilon_j - \varepsilon_k}\alpha_r' + 2\sum_j^{\text{occ}}\{\text{the second order term in}(\delta p_{uv}^j)_r\} + \cdots\cdots \quad (u=v \text{ or } u\neq v) \tag{4}$$

$$(\delta\Psi_j)_r = \sum_{k(\neq j)}^{\text{all}} \frac{c_r^j c_r^k}{\varepsilon_j - \varepsilon_k}\alpha_r'\Psi_k - \frac{1}{2}\left\{\sum_{k(\neq j)}^{\text{all}} \frac{(c_r^j c_r^k)^2}{(\varepsilon_j - \varepsilon_k)^2}\right\}(\alpha_r')^2\Psi_j + \sum_{k(\neq j)}^{\text{all}} \frac{c_r^j c_r^k}{\varepsilon_j - \varepsilon_m}\left\{\sum_{m(\neq j)}^{\text{all}} \frac{(c_r^m)^2}{\varepsilon_j - \varepsilon_m} - \frac{(c_r^j)^2}{\varepsilon_j - \varepsilon_k}\right\}(\alpha_r')^2\Psi_k + \cdots\cdots \tag{5}$$

Secondly, when the resonance integral, β_{st}, of the bond (st) in the system $\Delta(\varepsilon)$ is increased by β_{st}' (Case B of Ref. 3), increases of those quantities are written as follows:

$$(\delta\varepsilon_j)_{st} = 2c_s^j c_t^j \beta_{st}' + \sum_{k(\neq j)}^{\text{all}} \frac{(c_s^j c_t^k + c_t^j c_s^k)^2}{\varepsilon_j - \varepsilon_k}(\beta_{st}')^2 + \cdots\cdots \tag{6}$$

$$(\delta p_{uv}^j)_{st} = \sum_{k(\neq j)}^{\text{all}} \frac{(c_s^j c_t^k + c_t^j c_s^k)(c_u^j c_v^k + c_v^j c_u^k)}{\varepsilon_j - \varepsilon_k}\beta_{st}' + \sum_{k(\neq j)}^{\text{all}} \frac{(c_s^j c_t^k + c_t^j c_s^k)}{\varepsilon_j - \varepsilon_k}\left\{\sum_{m(\neq j)}^{\text{all}} \frac{(c_s^j c_t^m + c_t^j c_s^m)c_u^k c_v^m + (c_s^k c_t^m + c_t^k c_s^m)(c_u^j c_v^m + c_v^j c_u^m)}{\varepsilon_j - \varepsilon_m} - \frac{(c_s^j c_t^k + c_t^j c_s^k)c_u^j c_v^j + 2c_s^j c_t^j (c_u^j c_v^k + c_v^j c_u^k)}{\varepsilon_j - \varepsilon_k}\right\}(\beta_{st}')^2 + \cdots\cdots \quad (u=v \text{ or } u\neq v) \tag{7}$$

$$(\delta\varepsilon)_{st} = 2p_{st}\beta_{st}' + 2\sum_j^{\text{occ}}\sum_k^{\text{unocc}} \frac{(c_s^j c_t^k + c_t^j c_s^k)^2}{\varepsilon_j - \varepsilon_k}(\beta_{st}')^2 + \cdots\cdots \tag{8}$$

$$(\delta p_{uv})_{st} = 2\sum_j^{\text{occ}}\sum_k^{\text{unocc}} \frac{(c_s^j c_t^k + c_t^j c_s^k)(c_u^j c_v^k + c_v^j c_u^k)}{\varepsilon_j - \varepsilon_k}\beta_{st}' + 2\sum_j^{\text{occ}}\{\text{the second order term in}(\delta p_{uv}^j)_{st}\} + \cdots\cdots \quad (u=v \text{ or } u\neq v) \tag{9}$$

$$(\delta\Psi_j)_{st} = \sum_{k(\neq j)}^{\text{all}} \frac{(c_s^j c_t^k + c_t^j c_s^k)}{\varepsilon_j - \varepsilon_k}\beta_{st}'\Psi_k - \frac{1}{2}\sum_{k(\neq j)}^{\text{all}} \frac{(c_s^j c_t^k + c_t^j c_s^k)^2}{(\varepsilon_j - \varepsilon_k)^2}(\beta_{st}')^2\Psi_j + \sum_{k(\neq j)}^{\text{all}} \frac{c_s^j c_t^k + c_t^j c_s^k}{\varepsilon_j - \varepsilon_k}\left\{\sum_{m(\neq j)}^{\text{all}} \frac{c_s^k c_t^m + c_t^k c_s^m}{\varepsilon_j - \varepsilon_m} - \frac{2c_s^j c_t^j}{\varepsilon_j - \varepsilon_k}\right\}(\beta_{st}')^2\Psi_k + \cdots\cdots \tag{10}$$

Thirdly, when a conjugated system, $\Delta(\varepsilon)$, conjugates at the rth atom through a weak bonding, whose resonance integral is γ_r, with another conjugated system, whose secular determinant is $\Delta_1(\varepsilon)$, (Case C of Ref. 3), then the increases of molecular quantities by this perturbation are given by the following formulae. The orbital energy of the kth orbital ψ_{1k} of the system $\Delta_1(\varepsilon)$ is η_{1k} and the coefficient of the ξth atomic orbital in that molecular orbital is written as d_ξ^{1k}.

$$(\delta\varepsilon_j)_{r\xi} = \sum_k^{\text{all}} \frac{(c_r^j d_\xi^{1k})^2}{\varepsilon_j - \eta_{1k}}(\gamma_r)^2 + \left\{\sum_k^{\text{all}} \frac{(c_r^j d_\xi^{1k})^2}{\varepsilon_j - \eta_{1k}}\left[\sum_k^{\text{all}} \frac{(d_\xi^{1k})^2}{\varepsilon_j - \eta_{1k}}\left\{\sum_{m(\neq j)}^{\text{all}} \frac{(c_r^m)^2}{\varepsilon_j - \varepsilon_m} - \frac{(c_r^j)^2}{\varepsilon_j - \eta_{1k}}\right\}\right]\right\}(\gamma_r)^4 + \cdots\cdots \tag{11}$$

$$(\delta p_{uv}^j)_{r\xi} = \sum_k^{\text{all}} \frac{c_r^j d_\xi^{1k}}{\varepsilon_j - \eta_{1k}}\left\{\sum_{m(\neq j)}^{\text{all}} \frac{c_r^m d_\xi^{1k}(c_u^j c_v^m + c_v^j c_u^m)}{\varepsilon_j - \varepsilon_m} - \frac{c_r^j d_\xi^{1k} c_u^j c_v^j}{\varepsilon_j - \eta_{1k}}\right\}(\gamma_r)^2 + \cdots\cdots \quad (u=v \text{ or } u\neq v) \tag{12}$$

$$(\delta p_{r\xi}^j)_{r\xi} = \sum_k^{\text{all}} \frac{(c_r^j d_\xi^{1k})^2}{\varepsilon_j - \eta_{1k}}\gamma_r + 2\sum_k^{\text{all}}\sum_n^{\text{all}} \frac{(c_r^j d_\xi^{1k} d_\xi^{1n})^2}{(\varepsilon_j - \eta_{1k})(\varepsilon_j - \eta_{1n})}\left\{\sum_{m(\neq j)}^{\text{all}} \frac{(c_r^m)^2}{\varepsilon_j - \varepsilon_m} - \frac{(c_r^j)^2}{\varepsilon_j - \eta_{1k}}\right\}(\gamma_r)^3 + \cdots \tag{12'}$$

$$(\delta p_{uv}^{1k})_{r\xi} = \sum_j^{\text{all}}\sum_m^{\text{all}} \frac{c_r^j c_r^m (d_\xi^{1k})^2 c_u^j c_v^m}{(\eta_{1k} - \varepsilon_j)(\eta_{1k} - \varepsilon_m)}(\gamma_r)^2 + \cdots\cdots \quad (u=v \text{ or } u\neq v) \tag{13}$$

$$(\delta\Psi_j)_{r\xi}=\sum_k^{all}\frac{c_r{}^j d_\xi{}^{1k}}{\varepsilon_j-\eta_{1k}}\gamma_r\psi_k-\frac{1}{2}\sum_k^{all}\frac{(c_r{}^j d_\xi{}^{1k})^2}{(\varepsilon_j-\eta_{1k})^2}(\gamma_r)^2\Psi_j+\sum_{m(\neq j)}^{all}\frac{c_r{}^j c_r{}^m}{\varepsilon_j-\varepsilon_m}\sum_k^{all}\frac{(d_\xi{}^{1k})^2}{\varepsilon_j-\eta_{1k}}(\gamma_r)^2\Psi_m+\cdots\cdots \quad (14)$$

where the atom u and the bond (uv) are in the system $\Delta(\varepsilon)$, and ξ is the position of weak conjugation in the system $\Delta_1(\varepsilon)$. Similar formulae would be obtained for the system $\Delta_1(\varepsilon)$. Thus the change of bond order and that of electron density and total π electronic energy change of the combined system are obtained as follows:

$$\begin{aligned}(\delta\varepsilon)_{r\xi}&=2\sum_j^{occ}(\delta\varepsilon_j)_{r\xi}+2\sum_k^{occ}(\delta\eta_{1k})_{r\xi}\\&=2\Big(\sum_j^{occ}\sum_k^{unocc}-\sum_j^{unocc}\sum_k^{occ}\Big)\frac{(c_r{}^j d_\xi{}^{1k})^2}{\varepsilon_j-\eta_{1k}}(\gamma_r)^2+2\sum_j^{occ}\{\text{the fourth order term in}(\delta\varepsilon_j)_{r\xi}\}\\&\quad+2\sum_k^{occ}\{\text{the fourth order term in}(\delta\eta_{1k})_{r\xi}\}+\cdots\cdots\end{aligned} \quad (15)$$

$$\begin{aligned}(\delta p_{uv})_{r\xi}&=2\sum_j^{occ}(\delta p_{uv}{}^j)_{r\xi}+2\sum_k^{occ}(\delta p_{uv}{}^{1k})_{r\xi}\\&=2\Big(\sum_k^{occ}\sum_j^{unocc}-\sum_k^{unocc}\sum_j^{occ}\Big)\Big[\frac{(d_\xi{}^{1k})^2}{\varepsilon_j-\eta_{1k}}\Big\{\frac{(c_r{}^j)^2 c_u{}^j c_v{}^j}{\varepsilon_j-\eta_{1k}}\\&\quad-\sum_{m(\neq j)}^{all}\frac{c_r{}^j c_r{}^m(c_u{}^j c_v{}^m+c_v{}^j c_u{}^m)}{\varepsilon_j-\varepsilon_m}\Big\}\Big](\gamma_r)^2+\cdots\cdots\end{aligned} \quad (u=v \text{ or } u\neq v) \quad (16)$$

$$(\delta p_{r\xi})_{r\xi}=2\Big(\sum_j^{occ}\sum_k^{unocc}-\sum_k^{unocc}\sum_j^{occ}\Big)\frac{(c_r{}^j d_\xi{}^{1k})^2}{\varepsilon_j-\eta_{1k}}\gamma_r+2\sum_j^{occ}\{\text{the third order term in}(\delta p_{r\xi}{}^j)_{r\xi}\}$$

$$+2\sum_k^{occ}\{\text{the third order term in}(\delta p_{r\xi}{}^{1k})_{r\xi}\}+\cdots\cdots \quad (16')$$

Here it was assumed that the highest occupied orbitals of the systems $\Delta(\varepsilon)$ and $\Delta_1(\varepsilon)$ are lower than the lowest unoccupied orbitals of the systems $\Delta_1(\varepsilon)$ and $\Delta(\varepsilon)$, respectively. The total charge transfer, δQ, from the system $\Delta_1(\varepsilon)$ to the system $\Delta(\varepsilon)$ is defined by

$$\delta Q=\sum_{u=1}^{n}\delta p_{uu} \quad (17)$$

where n is the number of atomic orbitals in the system $\Delta(\varepsilon)$.

For this case δQ is given by the following equation.

$$(\delta Q)_{r\xi}=2\Big(\sum_k^{occ}\sum_j^{unocc}-\sum_k^{unocc}\sum_j^{occ}\Big)\frac{(c_r{}^j d_\xi{}^{1k})^2}{(\varepsilon_j-\eta_{1k})^2}(\gamma_r)^2+\cdots\cdots \quad (18)$$

As a special case involved in the Case C, when the system $\Delta_1(\varepsilon)$ is an atom or a mesomeric group, X, Eqs. 11 to 16 and 18 become

$$(\delta\varepsilon_j)_{rX}=\frac{(c_r{}^j)^2}{\varepsilon_j-\alpha_X}(\gamma_r)^2+\frac{(c_r{}^j)^2}{\varepsilon_j-\alpha_X}\Big\{-\frac{(c_r{}^j)^2}{(\varepsilon_j-\alpha_X)^2}+\sum_{m(\neq j)}^{all}\frac{(c_r{}^m)^2}{(\varepsilon_j-\alpha_X)(\varepsilon_j-\varepsilon_m)}\Big\}(\gamma_r)^4+\cdots\cdots \quad (11\text{-a})$$

$$(\delta\alpha_X)_{rX}=\sum_j^{all}\frac{(c_r{}^j)^2}{\alpha_X-\varepsilon_j}(\gamma_r)^2+\Big\{\sum_j^{all}\frac{(c_r{}^j)^2}{\alpha_X-\varepsilon_j}\Big\}\Big\{-\sum_j^{all}\frac{(c_r{}^j)^2}{(\alpha_X-\varepsilon_j)^2}\Big\}(\gamma_r)^4+\cdots\cdots \quad (11\text{-b})$$

$$(\delta p_{uv}{}^j)_{rX}=\Big\{\sum_{m(\neq j)}^{all}\frac{c_r{}^j c_r{}^m(c_u{}^j c_v{}^m+c_v{}^j c_u{}^m)}{(\varepsilon_j-\varepsilon_m)(\varepsilon_j-\alpha_X)}-\frac{(c_r{}^j)^2 c_u{}^j c_v{}^j}{(\varepsilon_j-\alpha_X)^2}\Big\}(\gamma_r)^2+\cdots\cdots \quad (12\text{-a})$$

$$(\delta p_{rX}{}^j)_{rX}=\frac{(c_r{}^j)^2}{\varepsilon_j-\alpha_X}\gamma_r+\frac{2(c_r{}^j)^2}{(\varepsilon_j-\alpha_X)^2}\Big\{\sum_{m(\neq j)}^{all}\frac{(c_r{}^m)^2}{\varepsilon_j-\varepsilon_m}-\frac{(c_r{}^j)^2}{\varepsilon_j-\alpha_X}\Big\}(\gamma_r)^3+\cdots\cdots \quad (12'\text{-a})$$

$$(\delta p_{uv}{}^X)_{rX}=\Big\{\sum_j^{all}\sum_m^{all}\frac{c_r{}^j c_r{}^m c_u{}^j c_v{}^m}{(\varepsilon_j-\alpha_X)(\varepsilon_m-\alpha_X)}\Big\}(\gamma_r)^2+\cdots \quad (13\text{-a})$$

$$(\delta p_{rX}{}^X)_{rX}=\sum_j^{all}\frac{(c_r{}^j)^2}{\alpha_X-\varepsilon_j}\gamma_r-2\Big\{\sum_j^{all}\sum_m^{all}\frac{(c_r{}^j c_r{}^m)^2}{(\alpha_X-\varepsilon_j)^2(\alpha_X-\varepsilon_m)}\Big\}(\gamma_r)^3+\cdots\cdots \quad (13'\text{-a})$$

$$(\delta p_{rX}{}^{j})_{rX}=\frac{(c_r{}^{j})^2}{(\varepsilon_j-\alpha_X)^2}(\gamma_r)^2+\cdots\cdots \tag{12-b}$$

$$(\delta p_{XX}{}^{j})_{rX}=-\sum_{j}^{\text{all}}\frac{(c_r{}^{j})^2}{(\alpha_X-\varepsilon_j)^2}(\gamma_r)^2+\cdots\cdots \tag{13-b}$$

$$(\delta p_{uv})_{rX}=(\nu\sum_{j}^{\text{all}}-2\sum_{j}^{\text{occ}})\left\{\frac{(c_r{}^{j})^2c_u{}^{j}c_v{}^{j}}{(\varepsilon_j-\alpha_X)^2}+\sum_{m(\neq j)}^{\text{all}}\frac{c_r{}^{j}c_r{}^{m}(c_u{}^{j}c_v{}^{m}+c_v{}^{j}c_u{}^{m})}{(\alpha_X-\varepsilon_j)(\varepsilon_j-\varepsilon_m)}\right\}(\gamma_r)^2+\cdots\cdots \tag{16-a}$$

$$(\delta p_{YX})_{rX}=(2\sum_{j}^{\text{occ}}-\nu\sum_{j}^{\text{all}})\frac{(c_r{}^{j})^2}{(\alpha_X-\varepsilon_j)^2}(\gamma_r)^2+\cdots\cdots \tag{16-b}$$

$$(\delta p_{rX})_{rX}=(2\sum_{j}^{\text{occ}}-\nu\sum_{j}^{\text{all}})\frac{(c_r{}^{j})^2}{\varepsilon_j-\alpha_X}\gamma_r+2\sum_{j}^{\text{occ}}\{\text{the third order term in}(\delta p_{rX}{}^{j})_{rX}\}$$
$$+\nu\{\text{the third order term in}(\delta p_{rX}{}^{X})_{rX}\}+\cdots\cdots \tag{16'-a}$$

$$(\delta Q)_{rX}=(\nu\sum_{j}^{\text{all}}-2\sum_{j}^{\text{occ}})\frac{(c_r{}^{j})^2}{(\alpha_X-\varepsilon_j)^2}(\gamma_r)^2+\cdots\cdots \tag{18-a}$$

where ν is the number of electrons in the atom X. The equations corresponding to Eqs. 14 and 15 are omitted for simplicity.

In the following paragraphs some important cases of doubly perturbed systems will be treated.

2. Case I. Changes of Two Coulomb Integrals.—If two atoms, say the rth and the sth atoms, in a conjugated molecule, $\Delta(\varepsilon)$, are replaced by two heteroatoms, the Coulomb integrals of these atoms will become $\alpha_r+\alpha_r'$ and $\alpha_s+\alpha_s'$, respectively. Then the perturbed secular determinant of the system will be written

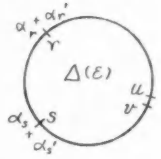

$$D(\varepsilon)=\Delta(\varepsilon)+\alpha_r'\Delta_{rr}(\varepsilon)+\alpha_s'\Delta_{ss}(\varepsilon)+\alpha_r'\alpha_s'\Delta_{rrss}(\varepsilon) \tag{19}$$

where $\Delta_{rr}(\varepsilon)$ and $\Delta_{rrss}(\varepsilon)$ are the (rr) minor and the (rr, ss) minor of $\Delta(\varepsilon)$, respectively. Regarding these changes, α_r' and α_s', as perturbations, one can easily obtain the perturbed orbital energy, of the jth molecular orbital, the perturbed bond order and the perturbed electron density by the use of the method of perturbed secular determinant, as will be briefly explained in the following.

First if one intermediately considers a system where α_s' is zero, the intermediate perturbed secular determinant is given as:

$$\square(\varepsilon)=\Delta(\varepsilon)+\alpha_r'\Delta_{rr}(\varepsilon) \tag{20}$$

According to the procedure utilized in the previous paper, the intermediate perturbed orbital energy, $\tilde{\varepsilon}_j$, and the intermediate perturbed separate bond order, $\tilde{p}_{uv}{}^{j}$, are expanded in powers of α_r':

$$\left.\begin{aligned}\tilde{\varepsilon}_j&=\sum_{m=0}^{\infty}a_r{}^{j(m)}(\alpha_r')^m\\ \tilde{p}_{uv}{}^{j}&=\sum_{m=0}^{\infty}a_{r,uv}{}^{j(m)}(\alpha_r')^m\end{aligned}\right\} \tag{21}$$

and the coefficients, $a_r{}^{j(m)}$ and $a_{r,uv}{}^{j(m)}$, are given by the following formulae.

$$\left.\begin{aligned}a_r{}^{j(m)}&=\frac{(-1)^m}{m!}\left[\frac{\mathrm{d}^m}{\mathrm{d}z^m}\frac{z\{\Delta_{rr}(z)\}^{m-1}\{\Delta'(z)\Delta_{rr}(z)-\Delta(z)\Delta_{rr}'(z)\}}{\{\Delta(z)/(z-\varepsilon_j)\}^{m+1}}\right]_{z=\varepsilon_j}\\ &\qquad(m=0,1,2,\cdots\cdots)\\ a_{r,uv}{}^{j(m)}&=\frac{(-1)^{m+1}}{m!}\left[\frac{\mathrm{d}^m}{\mathrm{d}z^m}\frac{\{\Delta_{rr}(z)\}^m\Delta_{ur}(z)\Delta_{rv}(z)}{\{\Delta(z)/(z-\varepsilon_j)\}^{m+1}}\right]_{z=\varepsilon_j}\\ &\qquad(m=0,1,2,\cdots\cdots)\end{aligned}\right\} \tag{22}$$

Directly from these formulae the following expressions are obtained

$$\left.\begin{aligned}\tilde{\varepsilon}_j &= \varepsilon_j + (\delta\varepsilon_j)_r \\ \tilde{p}_{uv}{}^j &= p_{uv}{}^j + (\delta p_{uv}{}^j)_r\end{aligned}\right\} \tag{23}$$

where $(\delta\varepsilon_j)_r$ and $(\delta p_{uv}{}^j)_r$ are given by Eqs. 1 and 2.

Then the second perturbation, α_s', is to be taken into account. The perturbed secular determinant of the system in question is expressed with the aid of the secular determinant of the intermediate system,

$$D(\varepsilon) = \square(\varepsilon) + \alpha_s' \square_{ss}(\varepsilon) \tag{24}$$

A similar procedure leads to the expansion formulae

$$\left.\begin{aligned}\varepsilon_j' &= \sum_{m=0}^{\infty} b_s{}^{j(m)} (\alpha_s')^m \\ P_{uv}{}^j &= \sum_{m=0}^{\infty} b_{s,uv}{}^{j(m)} (\alpha_s')^m\end{aligned}\right\} \tag{25}$$

where the coefficients, $b_s{}^{j(m)}$ and $b_{s,uv}{}^{j(m)}$, are the functions of α_r' and are given by

$$\left.\begin{aligned} b_s{}^{j(m)} &= \frac{(-1)^m}{m!}\left[\frac{\mathrm{d}^m}{\mathrm{d}z^m}\frac{z\{\square_{ss}(z)\}^{m-1}\{\square'(z)\square_{ss}(z) - \square(z)\square_{ss}'(z)\}}{\{\square(z)/(z-\tilde{\varepsilon}_j)\}^{m+1}}\right]_{z=\tilde{\varepsilon}_j} \\ &\qquad (m = 0, 1, 2, \cdots\cdots) \\ b_{s,uv}{}^{j(m)} &= \frac{(-1)^{m+1}}{m!}\left[\frac{\mathrm{d}^m}{\mathrm{d}z^m}\frac{\{\square_{ss}(z)\}^m \square_{us}(z)\square_{sv}(z)}{\{\square(z)/(z-\tilde{\varepsilon}_j)\}^{m+1}}\right]_{z=\tilde{\varepsilon}_j} \\ &\qquad (m = 0, 1, 2, \cdots\cdots)\end{aligned}\right\} \tag{26}$$

Thus we finally reach the following results for this perturbed system.

$$\varepsilon_j' = \varepsilon_j + (\delta\varepsilon_j)_r + (\delta\varepsilon_j)_s + 2\sum_{k(\neq j)}^{\text{all}} \frac{c_r{}^j c_r{}^k c_s{}^j c_s{}^k}{\varepsilon_j - \varepsilon_k}\alpha_r'\alpha_s' + \cdots\cdots \tag{27}$$

$$\begin{aligned} P_{uv}{}^j = {} & p_{uv}{}^j + (\delta p_{uv}{}^j)_r + (\delta p_{uv}{}^j)_s \\ & + \left[\sum_{k(\neq j)}^{\text{all}}\sum_{m(\neq j)}^{\text{all}} \frac{c_r{}^j c_s{}^j (c_r{}^k c_s{}^m + c_s{}^k c_r{}^m) c_u{}^k c_v{}^m + c_r{}^m c_s{}^m (c_r{}^j c_s{}^k + c_s{}^j c_r{}^k)(c_u{}^j c_v{}^k + c_v{}^j c_u{}^k)}{(\varepsilon_j - \varepsilon_k)(\varepsilon_j - \varepsilon_m)}\right. \\ & \left. - \sum_{k(\neq j)}^{\text{all}} \frac{c_r{}^j c_s{}^j \{(c_r{}^j c_s{}^k + c_s{}^j c_r{}^k)(c_u{}^j c_v{}^k + c_v{}^j c_u{}^k) + 2c_r{}^k c_s{}^k c_u{}^j c_v{}^j\}}{(\varepsilon_j - \varepsilon_k)^2}\right]\alpha_r'\alpha_s' + \cdots\cdots \end{aligned} \tag{28}$$

where $(\delta\varepsilon_j)_r$ and $(\delta p_{uv}{}^j)_r$ are the change of the orbital energy and the separate bond order (or the separate electron density) respectively, of the jth molecular orbital caused by the perturbation α_r', as were given in Eqs, 1 and 2.

On inspection of Eqs. 27 and 28 it is clearly seen that, as concerns the first order terms, two perturbations have no effect upon each other and, therefore, the so-called "additivity rule" comes into being. That is to say, the change of the orbital energy, the bond order or the electron density caused by two perturbations is expressed by the mathematical sum of its changes caused by each perturbation. In the second order a cross term appears, which may become comparable in magnitude with the non-cross term and cannot be neglected. Also as for the total π electronic energy, the bond order and the electron density, which are expressed by the sum of corresponding separate quantity, the circumstances are the same, as follows:

$$\varepsilon' = \varepsilon + (\delta\varepsilon)_r + (\delta\varepsilon)_s + 2\sum_{j}^{\text{occ}}\sum_{k}^{\text{unocc}} \frac{c_r{}^j c_r{}^k c_s{}^j c_s{}^k}{\varepsilon_j - \varepsilon_k}\alpha_r'\alpha_s' + \cdots\cdots \tag{29}$$

$$P_{uv} = p_{uv} + (\delta p_{uv})_r + (\delta p_{uv})_s + \sum_{j}^{\text{occ}} \{\text{cross term of the order } \alpha_r'\alpha_s' \text{ in } P_{uv}{}^j\} + \cdots\cdots \tag{30}$$

where $(\delta\varepsilon)_r$ and $(\delta p_{uv})_r$, given by Eqs. 3 and 4, are the changes of total π electronic energy and the bond order (or the electron density) respectively, caused by the perturbation α_r'. Eqs. 27 to 30 can also be derived by the existing method of perturbation.

The explicit expression of perturbed molecular orbital would be useful for some purposes. It is

$$\Psi_j' = \Psi_j + (\delta\Psi_j)_r + (\delta\Psi_j)_s - \sum_{k(\neq j)}^{\text{all}} \frac{c_r^j c_r^k c_s^j c_s^k}{(\varepsilon_j - \varepsilon_k)^2} \alpha_r' \alpha_s' \Psi_j$$
$$+ \sum_{k(\neq j)}^{\text{all}} \frac{(c_r^j c_s^k + c_s^j c_r^k)}{\varepsilon_j - \varepsilon_k} \left\{ \sum_{m(\neq j)}^{\text{all}} \frac{c_r^m c_s^m}{\varepsilon_j - \varepsilon_m} - \frac{c_r^j c_s^j}{\varepsilon_j - \varepsilon_k} \right\} \alpha_r' \alpha_s' \Psi_k + \cdots\cdots \quad (31)$$

where $(\delta\Psi_j)_r$ is given by Eq. 5.

3. Case II. Changes of a Coulomb Integral and a Resonance Integral.—When at the same time the Coulomb integral of the rth atom is increased by α_r' and the resonance integral of the bond (st), β_{st}, by β_{st}', then the perturbed secular determinant of the system is expressed* by

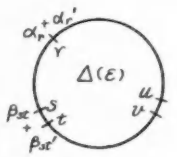

$$D(\varepsilon) = \Delta(\varepsilon) + \alpha_r' \Delta_{rr}(\varepsilon) + (-1)^{s+t} 2\beta_{st}' \Delta_{st}(\varepsilon) - (\beta_{st}')^2 \Delta_{sstt}(\varepsilon)$$
$$+ (-1)^{s+t} \alpha_r' \beta_{st}' \Delta_{rrst}(\varepsilon) - \alpha_r' (\beta_{st}')^2 \Delta_{rrsstt}(\varepsilon) \quad (32)$$

As well as in Case I, the following expressions of the orbital energy, the separate bond order and the separate electron density are obtained.

$$\varepsilon_j' = \varepsilon_j + (\delta\varepsilon_j)_r + (\delta\varepsilon_j)_{st} + 2 \sum_{k(\neq j)}^{\text{all}} \frac{c_r^j c_r^k (c_s^j c_t^k + c_t^j c_s^k)}{\varepsilon_j - \varepsilon_k} \alpha_r' \beta_{st}' + \cdots\cdots \quad (33)$$

$$P_{uv}^j = p_{uv}^j + (\delta p_{uv}^j)_r + (\delta p_{uv}^j)_{st}$$
$$+ \sum_{k(\neq j)}^{\text{all}} \sum_{m(\neq j)}^{\text{all}} \frac{c_r^j c_r^k (c_s^j c_t^m + c_t^j c_s^m)(c_u^k c_v^m + c_v^k c_u^m)}{(\varepsilon_j - \varepsilon_k)}$$
$$\times \frac{\{c_r^k c_r^m (c_s^j c_t^m + c_t^j c_s^m) + c_r^m c_r^j (c_s^k c_t^m + c_t^k c_s^m)\}(c_u^j c_v^k + c_v^j c_u^k)}{(\varepsilon_j - \varepsilon_m)}$$
$$- \sum_{k(\neq j)}^{\text{all}} \frac{2\{2c_r^j c_r^k c_s^j c_t^j + (c_r^j)^2 (c_s^j c_t^k + c_t^j c_s^k)\}(c_u^j c_v^k + c_v^j c_u^k) c_r^j c_r^k (c_s^j c_t^k + c_t^j c_s^k) c_u^j c_v^j}{(\varepsilon_j - \varepsilon_k)^2} \Bigg] \alpha_r' \beta_{st}'$$
$$+ \cdots\cdots \quad (34)$$

where $(\delta\varepsilon_j)_r$, $(\delta\varepsilon_j)_{st}$, $(\delta p_{uv}^j)_r$ and $(\delta p_{uv}^j)_{st}$ are given by Eqs. 1, 6, 2 and 7, respectively. Also in this case a cross term between the two perturbations, both in the orbital energy and in the bond order (and the density), first arises in the second order, and therefore the additivity rule is correct in the first order. The circumtances are the same for the total energy, the bond order and the electron density.

$$\left.\begin{aligned} \varepsilon' &= \varepsilon + (\delta\varepsilon)_r + (\delta\varepsilon)_{st} + 2\sum_j^{\text{occ}} \{\text{cross term of the order } \alpha_r'\beta_{st}' \text{ in } \varepsilon_j'\} + \cdots\cdots \\ P_{uv} &= p_{uv} + (\delta p_{uv})_r + (\delta p_{uv})_{st} + 2\sum_j^{\text{occ}} \{\text{cross term of the order } \alpha_r'\beta_{st}' \text{ in } P_{uv}^j\} \\ &\quad + \cdots\cdots \end{aligned}\right\} \quad (35)$$

where $(\delta\varepsilon)_{st}$ and $(\delta p_{uv})_{st}$ are given by Eqs. 8 and 9. The perturbed molecular orbital is obtained as follows:

$$\Psi_j' = \Psi_j + (\delta\Psi_j)_r + (\delta\Psi_j)_{st} + \sum_{k(\neq j)}^{\text{all}} \left\{ \sum_{m(\neq j)}^{\text{all}} \frac{c_r^k c_r^m (c_s^j c_t^m + c_t^j c_s^m) + c_r^j c_r^m (c_s^k c_t^m + c_t^k c_s^m)}{(\varepsilon_j - \varepsilon_k)(\varepsilon_j - \varepsilon_m)} \right.$$
$$\left. - \frac{2c_r^j c_r^k c_s^j c_t^j + (c_r^j)^2 (c_s^j c_t^k + c_t^j c_s^k)}{(\varepsilon_j - \varepsilon_k)^2} \right\} \alpha_r' \beta_{st}' \Psi_k$$
$$- \sum_{m(\neq j)}^{\text{all}} \frac{c_r^j c_r^k (c_s^j c_t^k + c_t^j c_s^k)}{(\varepsilon_j - \varepsilon_k)^2} \alpha_r' \beta_{sr}' \Psi_k + \cdots\cdots \quad (36)$$

where $(\delta\Psi_j)_{st}$ is given by Eq. 10.

4. Case III. A Weak Bonding with a Change of a Coulomb Integral.—When a conjugated system, $\Delta(\varepsilon)$, conjugates at the sth atom through a weak bonding, whose

* When $r = t$, though the perturbed secular determinant becomes $D(\varepsilon) = \Delta(\varepsilon) + \alpha_r' \Delta_{rr}(\varepsilon) + (-1)^{s+r} 2\beta_{sr}' \Delta_{sr}(\varepsilon) - (\beta_{sr}')^2 \Delta_{ssrr}(\varepsilon)$, Eqs. 33 to 36 are valid.

resonance integral is γ_s, with another conjugated system $\Delta_1(\varepsilon)$, and at the same time the Coulomb integral of the rth atom is increased by α_r', as illustrated in the figure, then the following formulae are obtained.

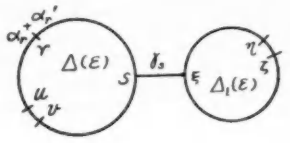

$$D(\varepsilon)=\Delta(\varepsilon)\Delta_1(\varepsilon)+\alpha_r'\Delta_{rr}(\varepsilon)\Delta_1(\varepsilon)-(\gamma_s)^2\Delta_{ss}(\varepsilon)\Delta_{1\xi\xi}(\varepsilon)-\alpha_r'(\gamma_s)^2\Delta_{rrss}(\varepsilon)\Delta_{1\xi\xi}(\varepsilon) \tag{37}$$

$$\varepsilon_j'=\varepsilon_j+(\delta\varepsilon_j)_r+(\delta\varepsilon_j)_{s\xi}+\sum_k^{\text{all}}\frac{c_r^j c_s^j (d_\xi^{1k})^2}{\varepsilon_j-\eta_{1k}}\left\{2\sum_{m(\neq j)}^{\text{all}}\frac{c_r^m c_s^m}{\varepsilon_j-\varepsilon_m}-\frac{c_r^j c_s^j}{\varepsilon_j-\eta_{1k}}\right\}\alpha_r'(\gamma_s)^2+\cdots\cdots \tag{38}$$

$$\eta_{1k}'=\eta_{1k}+(\delta\eta_{1k})_{s\xi}+\sum_j^{\text{all}}\frac{c_r^j c_s^j (d_\xi^{1k})^2}{\eta_{1k}-\varepsilon_j}\left\{2\sum_{m(\neq j)}^{\text{all}}\frac{c_r^m c_s^m}{\varepsilon_j-\varepsilon_m}-\frac{c_r^j c_s^j}{\varepsilon_j-\eta_{1k}}\right\}\alpha_r'(\gamma_s)^2+\cdots\cdots \tag{39}$$

$$P_{uv}^{\,j}=p_{uv}^{\,j}+(\delta p_{uv}^{\,j})_r+(\delta p_{uv}^{\,j})_{s\xi}+\{\text{cross term of the order } \alpha_r'(\gamma_s)^2\}+\cdots\cdots \tag{40}$$

$$P_{s\xi}^{\,j}=(\delta p_{s\xi}^{\,j})_{s\xi}+\sum_k^{\text{all}}\frac{c_r^j c_s^j (d_\xi^{1k})^2}{\varepsilon_j-\eta_{1k}}\left\{2\sum_{m(\neq j)}^{\text{all}}\frac{c_r^m c_s^m}{\varepsilon_j-\varepsilon_m}-\frac{c_r^j c_s^j}{\varepsilon_j-\eta_{1k}}\right\}\alpha_r'\gamma_s+\cdots\cdots \tag{40'}$$

$$P_{uv}^{\,1k}=(\delta p_{uv}^{\,1k})_{s\xi}+\{\text{cross term of the order } \alpha_r'(\gamma_s)^2\}+\cdots \tag{41}$$

$$P_{\eta\zeta}^{\,1k}=p_{\eta\zeta}^{\,1k}+(\delta p_{\eta\zeta}^{\,1k})_{s\xi}+\{\text{cross term of the order } \alpha_r'(\gamma_s)^2\}+\cdots \tag{42}$$

$$P_{s\xi}^{\,1k}=(\delta p_{s\xi}^{\,1k})_{s\xi}+\sum_j^{\text{all}}\frac{c_r^j c_s^j (d_\xi^{1k})^2}{\eta_{1k}-\varepsilon_j}\left\{2\sum_{m(\neq j)}^{\text{all}}\frac{c_r^m c_s^m}{\varepsilon_j-\varepsilon_m}-\frac{c_r^j c_s^j}{\varepsilon_j-\eta_{1k}}\right\}\alpha_r'\gamma_s+\cdots\cdots \tag{42'}$$

$$P_{\eta\zeta}^{\,j}=(\delta p_{\eta\zeta}^{\,j})_{s\xi}+\{\text{cross term of the order } \alpha_r'(\gamma_s)^2\}+\cdots \tag{43}$$

where ξ is the position of weak conjugation in the system $\Delta_1(\varepsilon)$, the bond $(\eta\zeta)$ is in the system $\Delta_1(\varepsilon)$; and $(\delta\varepsilon_j)_{s\xi}$, $(\delta p_{uv}^{\,j})_{s\xi}$, $(\delta p_{s\xi}^{\,j})_{s\xi}$ and $(\delta p_{uv}^{\,1k})_{s\xi}$ are given by Eqs. 11, 12, 12′ and 13, from which $(\delta\eta_{1k})_{s\xi}$, $(\delta p_{\eta\zeta}^{\,j})_{s\xi}$, $(\delta p_{\eta\zeta}^{\,1k})_{s\xi}$ and $(\delta p_{s\xi}^{\,1k})_{s\xi}$ will easily be formulated. Therefore the total π electronic energy of the combined system is

$$\varepsilon'=\varepsilon+(\delta\varepsilon)_r+(\delta\varepsilon)_{s\xi}+2\Big(\sum_j^{\text{occ}}\sum_k^{\text{unocc}}-\sum_j^{\text{unocc}}\sum_k^{\text{occ}}\Big)\times\left[\frac{c_r^j c_s^j (d_\xi^{1k})^2}{\varepsilon_j-\eta_{1k}}\left\{2\sum_{m(\neq j)}^{\text{all}}\frac{c_r^m c_s^m}{\varepsilon_j-\varepsilon_m}-\frac{c_r^j c_s^j}{\varepsilon_j-\eta_{1k}}\right\}\right]\alpha_r'(\gamma_s)^2+\cdots\cdots \tag{44}$$

And

$$P_{uv}=p_{uv}+(\delta p_{uv})_r+(\delta p_{uv})_{s\xi}+\{\text{cross term of the order } \alpha_r'(\gamma_s)^2\}+\cdots \tag{45}$$

$$P_{s\xi}=(\delta p_{s\xi})_{s\xi}+2\Big(\sum_j^{\text{occ}}\sum_k^{\text{unocc}}-\sum_j^{\text{unocc}}\sum_k^{\text{occ}}\Big)\left[\frac{c_r^j c_s^j (d_\xi^{1k})^2}{\varepsilon_j-\eta_{1k}}\left\{2\sum_{m(\neq j)}^{\text{all}}\frac{c_r^m c_s^m}{\varepsilon_j-\varepsilon_m}-\frac{c_r^j c_s^j}{\varepsilon_j-\eta_{1k}}\right\}\right]\alpha_r'\gamma_s+\cdots\cdots \tag{45'}$$

$$P_{\eta\zeta}=p_{\eta\zeta}+(\delta p_{\eta\zeta})_{s\xi}+\{\text{cross term of the order } \alpha_r'(\gamma_s)^2\}+\cdots \tag{46}$$

$$\delta Q=(\delta Q)_{s\xi}+\{\text{cross term of the order } \alpha_r'(\gamma_s)^2\}+\cdots \tag{47}$$

where $(\delta\varepsilon)_{s\xi}$, $(\delta p_{uv})_{s\xi}$, $(\delta p_{s\xi})_{s\xi}$ and $(\delta Q)_{s\xi}$ are given by Eqs. 15, 16, 16′ and 18. $(\delta p_{\eta\zeta})_{s\xi}$ is easily written on inspection of Eq. 16. As is seen in Eqs. 45 to 47, a cross term first appears in the third order, that is, the order of $\alpha_r'(\gamma_s)^2$, and the additivity rule is valid up to the second order perturbation.

The wave functions of this perturbed system are represented by

$$\Psi_j'=\Psi_j+(\delta\Psi_j)_r+(\delta\Psi_j)_{s\xi}+\sum_k^{\text{all}}\frac{c_r^j d_\xi^{1k}}{\varepsilon_j-\eta_{1k}}\left\{\sum_{m(\neq j)}^{\text{all}}\frac{c_r^m c_s^m}{\varepsilon_j-\varepsilon_m}-\frac{c_r^j c_s^j}{\varepsilon_j-\eta_{1k}}\right\}\alpha_r'\gamma_s\psi_{1k}+\cdots\cdots \tag{48}$$

$$\psi_{1k}'=\psi_{1k}+(\delta\psi_{1k})_{s\xi}+\sum_j^{\text{all}}\frac{c_r^j d_\xi^{1k}}{\eta_{1k}-\varepsilon_j}\sum_{m(\neq j)}^{\text{all}}\frac{c_r^m c_s^m}{\eta_{1k}-\varepsilon_m}\alpha_r'\gamma_s\Psi_j+\cdots \tag{49}$$

where $(\delta\Psi_j)_{s\xi}$ is given by Eq. 14, from which also $(\delta\psi_{1k})_{s\xi}$ may easily be written.

5. Case IV. Weak Bondings to Two Conjugated Systems.—Here we consider a case in which a conjugated system, $\Delta(\varepsilon)$, conjugates at the rth and the sth atoms with two other

conjugated systems, $\Delta_1(\varepsilon)$ and $\Delta_2(\varepsilon)$, respectively, making weak bondings whose resonance integrals are γ_r and γ_s, respectively. The molecular orbital, its orbital energy and the coefficient of atomic orbital in the non-perturbed $\Delta_1(\varepsilon)$ system are designated by ψ_{1k}, η_{1k} and d_μ^{1k}, respectively, and in the system $\Delta_2(\varepsilon)$ by ψ_{2k}, η_{2k} and d_ν^{2k}. Then the following expressions are easily obtained for the perturbed combined system.

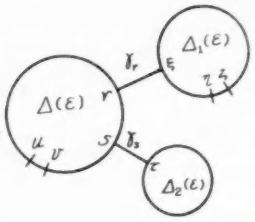

$$D(\varepsilon)=\Delta(\varepsilon)\Delta_1(\varepsilon)\Delta_2(\varepsilon)-(\gamma_r)^2\Delta_{rr}(\varepsilon)\Delta_{1\xi\xi}(\varepsilon)\Delta_2(\varepsilon)$$
$$-(\gamma_s)^2\Delta_{ss}(\varepsilon)\Delta_1(\varepsilon)\Delta_{2\tau\tau}(\varepsilon)+(\gamma_r\gamma_s)^2\Delta_{rrss}(\varepsilon)\Delta_{1\xi\xi}(\varepsilon)\Delta_{2\tau\tau}(\varepsilon) \tag{50}$$

$$\varepsilon_j'=\varepsilon_j+(\delta\varepsilon_j)_{r\xi}+(\delta\varepsilon_j)_{s\tau}+\sum_k^{\text{all}}\frac{c_r^j(d_\xi^{1k})^2}{\varepsilon_j-\eta_{1k}}U_{jk}(\gamma_r\gamma_s)^2+\cdots\cdots \tag{51}$$

$$U_{jk}=\sum_l^{\text{all}}\frac{c_s^j(d_\tau^{2l})^2}{\varepsilon_j-\eta_{2l}}\left\{2\sum_{m(\approx j)}^{\text{all}}\frac{c_r^m c_s^m}{\varepsilon_j-\varepsilon_m}-\frac{c_r^j c_s^j}{\varepsilon_j-\eta_{1k}}-\frac{c_r^j c_s^j}{\varepsilon_j-\eta_{2l}}\right\} \tag{51-a}$$

$$\eta_{1k}'=\eta_{1k}+(\delta\eta_{1k})_{r\xi}+\sum_j^{\text{all}}\frac{c_r^j(d_\xi^{1k})^2}{\eta_{1k}-\varepsilon_j}U_{jk}(\gamma_r\gamma_s)^2+\cdots\cdots \tag{52}$$

$$P_{uv}^{\,j}=p_{uv}^{\,j}+(\delta p_{uv}^{\,j})_{r\xi}+(\delta p_{uv}^{\,j})_{s\tau}+\{\text{cross term of the order }(\gamma_r\gamma_s)^2\}+\cdots\cdots \tag{53}$$

$$P_{r\xi}^{\,j}=(\delta p_{r\xi}^{\,j})_{r\xi}+\sum_k^{\text{all}}\frac{c_r^j(d_\xi^{1k})^2}{\varepsilon_j-\eta_{1k}}U_{jk}\gamma_r(\gamma_s)^2+\cdots\cdots \tag{53'}$$

$$P_{uv}^{\,1k}=(\delta p_{uv}^{\,1k})_{r\xi}+\{\text{cross term of the order }(\gamma_r\gamma_s)^2\}+\cdots\cdots \tag{54}$$

$$P_{r\xi}^{\,1k}=(\delta p_{r\xi}^{\,1k})_{r\xi}+\sum_j^{\text{all}}\frac{c_r^j(d_\xi^{1k})^2}{\eta_{1k}-\varepsilon_j}U_{jk}\gamma_r(\gamma_s)^2+\cdots\cdots \tag{54'}$$

$$P_{uv}^{\,2l}=(\delta p_{uv}^{\,2l})_{s\tau}+\{\text{cross term of the order }(\gamma_r\gamma_s)^2\}+\cdots\cdots \tag{55}$$

$$P_{r\xi}^{\,2k}=\sum_k^{\text{all}}\frac{(d_\xi^{1k})^2}{\eta_{2l}-\eta_{1k}}\sum_j^{\text{all}}\sum_m^{\text{all}}\frac{c_r^j c_r^m c_s^j c_s^m(d_\tau^{2l})^2}{(\eta_{2l}-\varepsilon_j)(\eta_{2l}-\varepsilon_m)}\gamma_r(\gamma_s)^2+\cdots\cdots \tag{55'}$$

$$P_{\eta\zeta}^{\,1k}=p_{\eta\zeta}^{\,1k}+(\delta p_{\eta\zeta}^{\,1k})_{r\xi}+\{\text{cross term of the order }(\gamma_r\gamma_s)^2\}+\cdots\cdots \tag{56}$$

$$P_{\eta\zeta}^{\,j}=(\delta p_{\eta\zeta}^{\,j})_{r\xi}+\{\text{cross term of the order}(\gamma_r\gamma_s)^2\}+\cdots\cdots \tag{57}$$

$$P_{\eta\zeta}^{\,2l}=\{\text{cross term of the order}(\gamma_r\gamma_s)^2\}+\cdots\cdots \tag{58}$$

where ξ and τ are the positions of the weak conjugation in the systems $\Delta_1(\varepsilon)$ and $\Delta_2(\varepsilon)$, respectively, and the bond (uv) or the atom u is assumed to be in the system $\Delta(\varepsilon)$, and the bond $(\eta\zeta)$ or the atom η in the system $\Delta_1(\varepsilon)$. Similar expressions as above may be written for the system $\Delta_2(\varepsilon)$. Thus the total π electronic energy and the bond order of this perturbed system are given as follows:

$$\varepsilon'=2\sum_j^{\text{occ}}\varepsilon_j'+2\sum_k^{\text{occ}}\eta_{1k}'+2\sum_l^{\text{occ}}\eta_{2l}'$$
$$=\varepsilon+(\delta\varepsilon)_{r\xi}+(\delta\varepsilon)_{st}$$
$$+\left\{\sum_j^{\text{occ}}\left(\sum_k^{\text{unocc}}\sum_l^{\text{unocc}}-\sum_k^{\text{occ}}\sum_l^{\text{occ}}\right)-\sum_j^{\text{unocc}}\left(\sum_k^{\text{occ}}\sum_l^{\text{all}}+\sum_k^{\text{all}}\sum_l^{\text{occ}}\right)\right\}\frac{c_r^j c_s^j(d_\xi^{1k})^2(d_\tau^{2l})^2}{(\varepsilon_j-\eta_{1k})(\varepsilon_j-\eta_{2l})}$$
$$\times\left(2\sum_{m(\approx j)}^{\text{all}}\frac{c_r^m c_s^m}{\varepsilon_j-\varepsilon_m}-\frac{c_r^j c_s^j}{\varepsilon_j-\eta_{1k}}-\frac{c_r^j c_s^j}{\varepsilon_j-\eta_{2l}}\right)(\gamma_r\gamma_s)^2+\cdots\cdots \tag{59}$$

$$P_{uv}=p_{uv}+(\delta p_{uv})_{r\xi}+(\delta p_{uv})_{s\tau}+\{\text{cross term of the order }(\gamma_r\gamma_s)^2\}+\cdots\cdots \tag{60}$$

$$P_{r\xi}=(\delta p_{r\xi})_{r\xi}+\left[2\left(\sum_j^{\text{occ}}\sum_k^{\text{unocc}}-\sum_j^{\text{unocc}}\sum_k^{\text{occ}}\right)\frac{c_r^j(d_\xi^{1k})^2}{\varepsilon_j-\eta_{1k}}U_{jk}\right.$$
$$\left.+2\sum_l^{\text{occ}}\sum_k^{\text{all}}\frac{(d_\xi^{1k})^2}{\eta_{2l}-\eta_{1k}}\sum_j^{\text{all}}\sum_m^{\text{all}}\frac{c_r^j c_r^m c_s^j c_s^m(d_\tau^{2l})^2}{(\eta_{2l}-\varepsilon_j)(\eta_{2l}-\varepsilon_m)}\right]\gamma_r(\gamma_s)^2+\cdots \tag{60'}$$

$$P_{\eta\zeta} = p_{\eta\zeta} + (\delta p_{\eta\zeta})_{r\xi} + \{\text{cross term of the order } (\gamma_r\gamma_s)^2\} + \cdots\cdots \tag{61}$$

The changes of total charge involved in the systems $\Delta(\varepsilon)$ and $\Delta_1(\varepsilon)$ are designated as δQ and δQ_1, respectively, which are written as follows:

$$\delta Q = (\delta Q)_{r\xi} + (\delta Q)_{s\tau} + \{\text{cross term of the order } (\gamma_r\gamma_s)^2\} + \cdots\cdots \tag{62}$$

$$\delta Q_1 = (\delta Q)_{r\xi} + \{\text{cross term of the order } (\gamma_r\gamma_s)^2\} + \cdots\cdots \tag{63}$$

A similar equation may be written also for the system $\Delta_2(\varepsilon)$.

The molecular orbitals of this perturbed system are

$$\Psi_j' = \Psi_j + (\delta\Psi_j)_{r\xi} + (\delta\Psi_j)_{s\tau} + \{\text{cross term of the orders } \gamma_r(\gamma_s)^2 \text{ and } (\gamma_r)^2\gamma_s\} + \cdots\cdots \tag{64}$$

$$\psi_{1k}' = \psi_{1k} + (\delta\Psi_{1k})_{r\xi} + \sum_{j}^{\text{all}}\sum_{l}^{\text{all}} \frac{c_r{}^j c_s{}^j d_\xi{}^{1k} d_\eta{}^{2l}}{(\eta_{1k}-\eta_{2l})(\eta_{1k}-\varepsilon_j)} \gamma_r\gamma_s\psi_{2k} + \cdots\cdots \tag{65}$$

As to special cases in which either or both of the systems $\Delta_1(\varepsilon)$ and $\Delta_2(\varepsilon)$ are single atoms, one may simplify the results of Cases III and IV by using Eqs. 11-a to 18-a instead of Eqs. 11 to 18 for non-cross terms and by abridging cross terms.

6. More General Case of Many Perturbations. — Perturbation treatment of systems affected by two perturbations stated above may be extended to a more general case of many perturbations. As illustrated in the figure, we consider a conjugated system, $\Delta(\varepsilon)$, and increase the Coulomb integrals of the rth atoms in it ($r = 1', 2', \cdots\cdots, f'$) by α_r' and the resonance integrals of the bonds (st) ($st = 1'', 2'', \cdots\cdots, g''$) by β_{st}', and make weak bondings, whose resonance integral is γ_q, between the qth atoms ($q = 1, 2, \cdots\cdots, h$) in the system and the ξ_qth atoms in other conjugated systems $\Delta_q(\varepsilon)$. Here some of the r's, s's and q's may be the identical atoms.

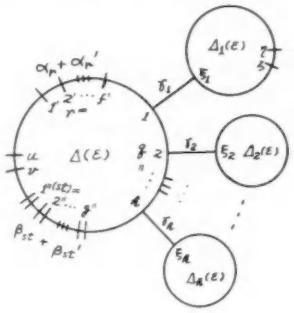

Then the perturbed jth orbital energy of the system $\Delta(\varepsilon)$ is

$$\begin{aligned}\varepsilon_j' = \varepsilon_j &+ \sum_{r=1'}^{f'} (\delta\varepsilon_j)_r + \sum_{(st)=1''}^{g''} (\delta\varepsilon_j)_{st} + \sum_{q=1}^{h} (\delta\varepsilon_j)_{q\xi} \\ &+ C(\alpha^2, \alpha\beta, \beta^2) + C(\alpha^3, \alpha^2\beta, \alpha\beta^2, \beta^3, \alpha\gamma^2, \beta\gamma^2) \\ &+ C(\alpha^4, \alpha^3\beta, \alpha^2\beta^2, \alpha\beta^3, \beta^4, \alpha^2\gamma^2, \alpha\beta\gamma^2, \beta^2\gamma^2, \gamma^4) + \cdots\cdots\end{aligned} \tag{66}$$

where $(\delta\varepsilon_j)_r$, $(\delta\varepsilon_j)_{st}$ and $(\delta\varepsilon_j)_{q\xi}$ are energy changes caused by perturbations α_r', β_{st}' and γ_q, respectively, and are given by Eqs. 1, 6 and 11. and C means the cross term among perturbations. For instance $C(\alpha^2, \alpha\beta, \beta^2)$ consists of cross terms of orders $\alpha_1'\alpha_2'$, $\alpha_1'\alpha_3'$, $\cdots\cdots$, $\alpha_2'\alpha_3'$, $\cdots\cdots$, $\alpha_1'\beta_1'$, $\alpha_1'\beta_2'$, $\cdots\cdots$, $\alpha_2'\beta_1'$, $\cdots\cdots$, $\beta_1'\beta_2'$, $\beta_1'\beta_3'$, $\cdots\cdots$, $\beta_2'\beta_3'$, $\cdots\cdots$; and $C(\alpha^3, \alpha^2\beta, \alpha\beta^2, \beta^3, \alpha\gamma^2, \beta\gamma^2)$ of orders $(\alpha_1')^2\alpha_2'$, $\cdots\cdots$, $\alpha_1'\alpha_2'\alpha_3'$, $\cdots\cdots$, $(\alpha_1')^2\beta_1'$, $\cdots\cdots$, $\alpha_1'\alpha_2'\beta_1'$, $\cdots\cdots$, $\alpha_1'(\beta_1')^2$, $\cdots\cdots$, $\alpha_1'\beta_1'\beta_2'$, $\cdots\cdots$, $(\beta_1')^2\beta_2'$, $\cdots\cdots$, $\beta_1'\beta_2'\beta_3'$, $\cdots\cdots$, $\alpha_1'(\gamma_1)^2$, $\cdots\cdots$, $\beta_1'(\gamma_1)^2$, $\cdots\cdots$. The perturbed separate bond order by this orbital of the bond (uv) in the system $\Delta(\varepsilon)$ is

$$\begin{aligned}P_{uv}{}^j = p_{uv}{}^j &+ \sum_{r=1'}^{f'} (\delta p_{uv}{}^j)_r + \sum_{(st)=1''}^{g''} (\delta p_{uv}{}^j)_{st} + \sum_{q=1}^{h} (\delta p_{uv}{}^j)_{q\xi} \\ &+ C(\alpha^2, \alpha\beta, \beta^2) + C(\alpha^3, \alpha^2\beta, \alpha\beta^2, \beta^3, \alpha\gamma^2, \beta\gamma^2) \\ &+ C(\alpha^4, \alpha^3\beta, \alpha^2\beta^2, \alpha\beta^3, \beta^4, \alpha^2\gamma^2, \alpha\beta\gamma^2, \beta^2\gamma^2, \gamma^4) + \cdots\cdots\end{aligned} \tag{67}$$

where $(\delta p_{uv}{}^j)_r$, $(\delta p_{uv}{}^j)_{st}$ and $(\delta p_{uv}{}^j)_{q\xi}$ are the changes caused by α_r', β_{st}' and γ_q, respectively, and are given by Eqs. 2, 7 and 12. The perturbed separate bond order by this orbital of the bond $(\eta\zeta)$ in another system, say, the system $\Delta_1(\varepsilon)$, is

$$\begin{aligned}P_{\eta\zeta}{}^j = (\delta p_{\eta\zeta}{}^j)_{1\xi} &+ C\{\alpha(\gamma_1)^2, \beta(\gamma_1)^2\} \\ &+ C\{\alpha^2(\gamma_1)^2, \alpha\beta(\gamma_1)^2, \beta^2(\gamma_1)^2, \gamma^2(\gamma_1)^2\} + \cdots\cdots\end{aligned} \tag{68}$$

The perturbed kth orbital energy of a system, say, the system $\Delta_1(\varepsilon)$, is

$$\eta_{1k}' = \eta_{1k} + (\delta\eta_{1k})_{1\xi} + C\{\alpha(\gamma_1)^2, \beta(\gamma)_1)^2\} + C\{\alpha^2(\gamma_1)^2, \alpha\beta(\gamma_1)^2, \beta^2(\gamma_1)^2, \gamma^2(\gamma_1)^2\} + \cdots\cdots \quad (69)$$

The perturbed separate bond orders by this orbital of bonds $(\eta\zeta)$ and $(\mu\nu)$ are

$$P_{\eta\zeta}{}^{1k} = p_{\eta\zeta}{}^{1k} + (\delta p_{\eta\zeta}{}^{1k})_{1\xi} + C\{\alpha(\gamma_1)^2, \beta(\gamma_1)^2\} + C\{\alpha^2(\gamma_1)^2, \alpha\beta(\gamma_1)^2, \beta^2(\gamma_1)^2, \gamma^2(\gamma_1)^2\} + \cdots\cdots \quad (70)$$

$$P_{\mu\nu}{}^{1k} = (\delta p_{\mu\nu}{}^{1k})_{1\xi} + C\{\alpha(\gamma_1)^2, \beta(\gamma_1)^2\} + C\{\alpha^2(\gamma_1)^2, \alpha\beta(\gamma_1)^2, \beta^2(\gamma_1)^2, \gamma^2(\gamma_1)^2\} + \cdots\cdots \quad (71)$$

Also this bond order by this orbital of the bond $(\mu\nu)$, which is located in another system, say, the system $\Delta_k(\varepsilon)$, is given by

$$P_{\mu\nu}{}^{1k} = C\{(\gamma_1)^2(\gamma_k)^2\} + \cdots\cdots \quad (72)$$

The perturbed separate bond order of the bond which is made anew by perturbation between conjugated systems, say, the bond $(1\xi_1)$ between the systems $\Delta(\varepsilon)$ and $\Delta_1(\varepsilon)$, may be written as

$$P_{1\xi}{}^{j} = (\delta p_{1\xi}{}^{j})_{1\xi} + C\{\alpha\gamma_1, \beta\gamma_1\} + C\{\alpha^2\gamma_1, \alpha\beta\gamma_1, \beta^2\gamma_1, \gamma^2\gamma_1\} + C\{\alpha^3\gamma_1, \alpha^2\beta\gamma_1, \alpha\beta^2\gamma_1, \beta^3\gamma_1, \alpha\gamma^2\gamma_1, \beta\gamma^2\gamma_1, \alpha(\gamma_1)^3, \beta(\gamma_1)^3\} + \cdots\cdots \quad (73)$$

$$P_{1\xi}{}^{1k} = (\delta p_{1\xi}{}^{1k})_{1\xi} + C\{\alpha\gamma_1, \beta\gamma_1\} + C\{\alpha^2\gamma_1, \alpha\beta\gamma_1, \beta^2\gamma_1, \gamma^2\gamma_1\} + C\{\alpha^3\gamma_1, \alpha^2\beta\gamma_1, \alpha\beta^2\gamma_1, \beta^3\gamma_1, \alpha\gamma^2\gamma_1, \beta\gamma^2\gamma_1, \alpha(\gamma_1)^3, \beta(\gamma_1)^3\} + \cdots\cdots \quad (74)$$

$$P_{1\xi}{}^{ql} = C\{(\gamma_q)^2\gamma_1\} + C\{\alpha(\gamma_q)^2\gamma_1, \beta(\gamma_q)^2\gamma_1\} + \cdots\cdots \qquad (q = 2, 3, \cdots\cdots, h) \quad (75)$$

As for the total π electronic energy an equation similar to Eq. 66, as for the total bond order (and the electron density) one similar to Eq. 67, and as for the total bond order of a newly formed bond one similar to Eq. 75 may be obtained.

Thus it has become clear to what order of perturbation terms the additivity rule applies, and what kinds of terms appear in several molecular quantities. If it is necessary, one could formulate cross terms in reference to the results of two perturbations.

Degenerate System

In the previous section it was assumed that no molecular orbital is degenerate with any other molecular orbital in the same molecule, not with molecular orbitals in any other system to be subjected to conjugation.

Even if some levels in the non-perturbed systems are degenerate, so far as they are chosen mutually orthogonal, the perturbed orbital energy and the perturbed separate bond order (and electron density) corresponding to non-degenerate orbitals are not affected at all, that is, equations derived in the preceding section, giving separate quantities, are valid also in this case.

As for degenerate levels, on the other hand, the sum of the perturbed orbital energies or of the perturbed bond orders over all the degenerate levels is easily obtained by taking a limit of the corresponding sum which is derived as if they were not degenerate. For instance, in Case I, when the lth and the $(l+1)$th levels are degenerate,

$$\varepsilon_l' + \varepsilon_{l+1}' = \lim_{\varepsilon_{l+1}\to\varepsilon_l} [\varepsilon_l', \text{nondeg} + \varepsilon_{l+1}', \text{nondeg}] = 2\varepsilon_l + [\delta(\varepsilon_l + \varepsilon_{l+1})]_r + [\delta(\varepsilon_l + \varepsilon_{l+1})]_s + 2\sum_{k(\neq l,l+1)}^{\text{all}} \frac{c_r{}^k c_s{}^k (c_r{}^l c_s{}^l + c_r{}^{l+1} c_s{}^{l+1})}{\varepsilon_l - \varepsilon_k} (\alpha_r'\alpha_s') + \cdots\cdots \quad (76)$$

where

$$[\delta(\varepsilon_l + \varepsilon_{l+1})]_r = [(c_r{}^l)^2 + (c_r{}^{l+1})^2]\alpha_r' + \sum_{k(\neq l,l+1)}^{\text{all}} \frac{(c_r{}^k)^2[(c_r{}^l)^2 + (c_r{}^{l+1})^2]}{\varepsilon_l - \varepsilon_k} (\alpha_r')^2 + \cdots\cdots \quad (77)$$

and ε_l', nondeg is given by Eq. 27, which is derived for non-degenerate system. Explicit formulae for other various degenerate cases are omitted here for the sake of brevity, but one

might write them down without difficulty according to the above principle. The total π electronic energy and the bond order (or the electron density) being represented as the sums of orbital energies and separate orders (or densities) over the occupied orbitals, it is concluded that, even in the degenerate cases, if all the degenerate levels are occupied, the degeneracy does not affect the additivity rule, though concrete formulae involved may differ from the case of no degeneracy.

Discussion

By the results obtained in the preceding sections the additivity rule concerning multiple perturbations and its limits of use have been clarified.

When a hetero-substitution of an atom in a conjugated system causes changes of the Coulomb integral of the atom and of the resonance integrals between neighboring atoms, their effects as a whole may be additively estimated in the first order perturbation treatment. When introduction of a conjugable group into a conjugated system at its certain atom gives rise simultaneously to a change of the Coulomb integral of the atom, the additivity rule applies to the first order terms.

Further, for the introduction of many substituents and hetero-substitutions, the additivity of these effects are materialized, and various examples are seen in experiments. The additivity of shift of absorption sprctra would be explained by the additivity in the orbital energy. The vector additivity of dipole moment would be understood as the additivity in the electron density or in the amount of charge transfer. Aono and Higuchi[4] interpreted the additivity of hyperfine splitting in the electron spin resonance spectrum of substituted semiquinones in terms of the additivity in the unpaired electron density.

Speaking of reactivity indices, i. g. the frontier electron density, P_{uu}^{r}, localization energy, ε^{r}(localized state)$-\varepsilon^{r}$(non-localized state), total π electron density, P_{uu}, free valence, $\sqrt{3}-\sum_{v}^{\prime}P_{uv}$, and most other indices, the additivity rule is applicable to a certain order of perturbation terms. Superdelocalizability is also proved to fulfil the additivity rule.

If one practically evaluates the cross terms appearing in the formulae, one would be able to discuss the deviation from the additivity rule, which is also often realized in experiments.

The authors are much indebted to Mr. Shigeyuki Aono for his helpful suggestions.

Faculty of Engineering
Kyoto University
Sakyo-ku, Kyoto

4) S. Aono, J. Higuchi, *Busseiron Kenkyu*, 7, 197 (1960).

The Adsorption of Dye Mixtures by Cellophane Sheet. II[1]. *A Quantitative Discussion of the Adsorption of Dyes*

By Yukio Horiki

(Received November 27, 1959)

In the previous work[1], a method of quantitative discussion of the interaction between dyes in a binary mixture dyebath has been discussed on the assumption that the decrease in adsorption of dyes from mixture dyeing is due to interaction. Further, the behavior of dyes in mixture dyeing has been qualitatively explained from those of single dyeings, taking account of the interaction obtained by the above method.

In this paper, the single dyeings of Chlorazol Sky Blue FF and Chrysophenine G and their mixture dyeing have been carried out in detail, to discuss quantitatively their behavior in mixture dyeing. In the single dyeing, the surface layer volume in Vickerstaff's theoretical equation for adsorption[2] has been discussed to obtain constant values of the standard affinity. In the mixture dyeing, the observed amounts of adsorption of the dyes have been compared with those calculated on the basis of the information both about the single dyeing particularly discussed and about the interaction obtained from the single and the mixture dyeings by the method reported before[1].

Experimental and Results

The single dyeings of Chlorazol Sky Blue FF (shortly called Blue dye) and Chrysophenine G (Yellow dye) and the mixture dyeing of them follow a method quite similar to that in the previous work[1].

In the single dyeings, the initial concentration ranged from 1×10^{-6} to 1.5×10^{-5} mol./l. for Blue dye and 1.25×10^{-6} to 1×10^{-4} mol./l. for Yellow dye, and in the mixture dyeing, that of Blue dye was fixed at about 1×10^{-5} mol./l. and that of Yellow dye varied from 2.5×10^{-6} to 1×10^{-4} mol./l.

Each dyeing was carried out for three, two and one day* at 50°, 70° and 90°C, respectively. The concentration of sodium chloride (2 g./l.) was the same as that in the previous work.

Results for single dyeings are shown in Figs. 1 (Blue dye) and 2 (Yellow dye) in terms of the relation between logarithms of the final dyebath concentration (Blue dye, F_σ mol./l.; Yellow dye, G_σ mol./l.) and those of the amount of adsorption (Blue dye, F_ϕ mol./kg.; Yellow dye, G_ϕ mol./kg.) of the dyes. The affinities of Blue dye and Yellow dye ($-\Delta\mu^0_F$ cal./mol.; $-\Delta\mu^0_G$ cal./mol.) were calculated by Vickerstaff's equation with $V=0.45$ l./kg. These results are shown in Figs. 3 (Blue dye) and 4 (Yellow dye) in terms of the relation between

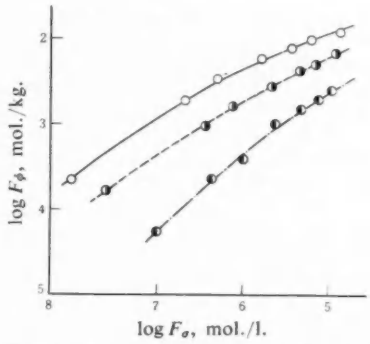

Fig. 1. Adsorption isotherms of Chlorazol Sky Blue FF on 'Cellophane' sheet at various temperatures: logarithmic plot of dyebath concentration and adsorption on the fiber.
—○— 50°C --◑-- 70°C -·-◐-·- 90°C

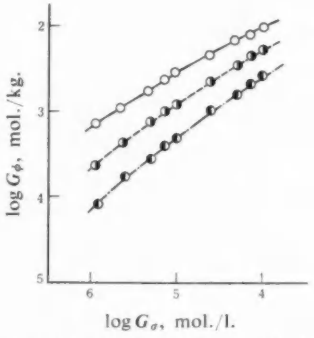

Fig. 2. Adsorption isotherms of Chrysophenine G on 'Cellophane' sheet at various temperatures: logarithmic plot of dyebath concentration and adsorption on the fiber.
—○— 50°C --◑-- 70°C -·-◐-·- 90°C

1) Part I of this series, Y. Horiki, Y. Tanizaki and N. Ando, This Bulletin, 33, 163 (1960).
2) R. H. Peters and T. Vickerstaff, *Proc. Roy. Soc.* (*London*) **A192**, 292 (1948).
* The dyeing time was ascertained to be sufficient to reach equilibrium at each temperature.

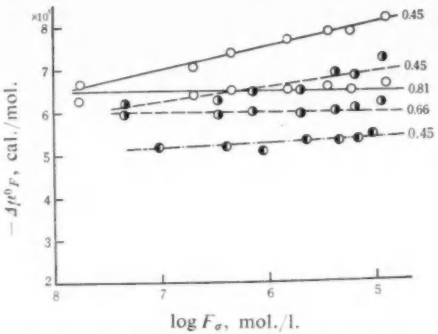

Fig. 3. Dependence of the standard affinity on dyebath concentration of Chlorazol Sky Blue FF at each temperature: plot of the standard affinity for logarithm of final dyebath concentration. The figures on each line indicate the surface layer volume (l./kg.) used in calculation.
—○— 50°C --◑-- 70°C -·-◐-·- 90°C

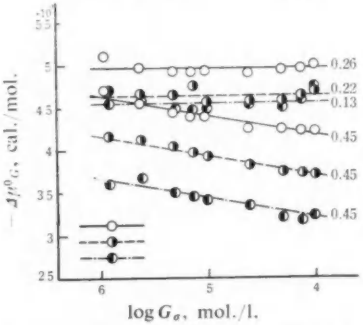

Fig. 4. Dependence of the standard affinity on dyebath concentration of Chrysophenine G at each temperature: plot of the standard affinity for logarithm of final dyebath concentration. The figure on each line indicates the surface layer volume (l./kg.) used in calculation.

the affinity and the logarithm of the final dyebath concentration. The relations of ($\log F_\phi\,Na^4{}_\phi - \log F_\sigma\,Na^4{}_\sigma$) and of ($\log G_\phi\,Na^2{}_\phi - \log G_\sigma\,Na^2{}_\sigma$) are shown in Figs. 5 and 6, respectively. It is recognized that they are nearly linear. Results of mixture dyeing, that is, the adsorptions of Blue dye (F_ϕ mol./kg.) and Yellow dye (G_ϕ mol./kg.), their effective dyebath concentrations obtained by the method reported before[1] (F_σ' mol./l.; G_σ' mol./l.), their dyebath concentrations which contributed to the interaction (F_c mol./l.; G_c mol./l.), and the ratios G_σ/F_σ and G_c/F_c are shown in Table I, together with the instability constant K (mol./l.) calculated in the region where $G_\sigma/F_\sigma = 0.8 \sim 1.1$, according to

$$K = \frac{F_\sigma' \cdot G_\sigma'}{\frac{F_c - G_c}{2}} = \frac{2F_\sigma' \cdot G_\sigma'}{F_c + G_c} = \frac{2(F_\sigma - F_c)(G_\sigma - G_c)}{F_c + G_c} \quad (1)$$

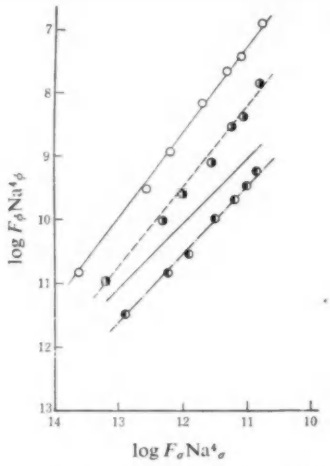

Fig. 5. Adsorption of Chlorazol Sky Blue FF on 'Cellophane' sheet at each temperature: plot of logarithm of ionic products in the fiber and in dyebath.

		α
———		1.00
—○—	50°C	1.32
--◑--	70°C	1.20
-·-◐-·-	90°C	1.05

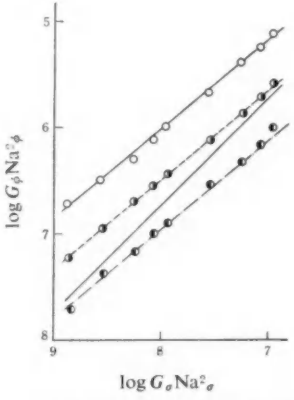

Fig. 6. Adsorption of Chrysophenine G on 'Cellophane' sheet at each temperature: Plot of logarithm of ionic products in the fiber and in dyebath.

		α
———		1.00
—○—	50°C	0.85
--◑--	70°C	0.84
-·-◐-·-	90°C	0.82

Table I

T°C	Exp. No.	F_ϕ mol./kg. $\times 10^3$	F_σ mol./l. $\times 10^6$	F_σ' mol./l. $\times 10^6$	F_c mol./l. $\times 10^6$	G_ϕ mol./kg. $\times 10^3$	G_σ mol./l. $\times 10^6$	G_σ' mol./l. $\times 10^6$	G_c mol./l. $\times 10^6$	G_σ/F_σ	G_c/F_c	K mol./l.
	1	10.36	9.46	7.5	2.0	0.03	2.53	?	?	0.27	?	
	2	8.98	9.30	4.9	4.4	0.25	4.94	?	?	0.53	?	
	3	7.76	9.64	3.2	6.4	0.45	6.91	?	?	0.72	?	
	4	6.37	9.72	1.8	7.9	0.78	8.88	1.1	7.9	0.91	1.0	2.5×10^{-7}
50	5	4.87	9.78	0.91	8.9	1.00	10.92	1.8	9.1	1.12	1.0	$1.8\times$ 〃
	6	1.82	9.74	0.19	9.6	2.36	19.79	7	12.8	2.03	1.3	
	7	0.56	10.01	0.04	10.0	4.46	39.66	23	16.7	3.96	1.7	
	8	0.27	10.04	0.01	10.0	5.96	59.10	36	23.1	5.89	2.3	
	9	0.14	10.11	0.01	10.0	7.47	79.21	56	23.2	7.83	2.3	
	10	0.05	10.09	?	≒10	9.33	98.90	83	15.9	9.80	1.6	
	1	5.33	9.82	6.8	3.0	0.07	2.53	?	?	0.26	?	
	2	4.53	9.83	4.8	5.0	0.19	5.05	0.9	4.2	0.51	0.8	9.4×10^{-7}
	3	3.94	9.73	3.7	6.0	0.25	6.96	1.3	5.7	0.72	1.0	$8.2\times$ 〃
	4	3.40	9.78	2.9	6.9	0.40	8.90	2.2	6.7	0.91	1.0	$9.4\times$ 〃
70	5	2.87	9.91	2.0	7.9	0.51	10.91	2.9	8.0	1.10	1.0	$7.3\times$ 〃
	6	1.56	9.75	0.66	9.1	1.32	19.95	10	10.0	2.05	1.1	$6.9\times$ 〃
	7	0.72	9.92	0.25	9.7	2.34	39.61	25	14.6	3.99	1.5	
	8	0.44	9.92	0.14	9.8	3.18	59.77	43	16.8	6.02	1.7	
	9	0.29	10.01	0.09	9.9	3.92	79.75	61	18.8	7.97	1.9	
	10	0.20	9.97	0.06	9.9	5.47	99.33	100	?	9.96	?	
	1	1.96	9.64	6.8	2.8	0.09	2.51	1.3	1.2	0.26	0.4	
	2	1.87	9.74	6.2	3.5	0.10	4.98	1.5	3.5	0.51	1.0	2.7×10^{-6}
	3	1.72	9.77	5.4	4.4	0.18	7.48	2.8	4.7	0.77	1.1	$3.3\times$ 〃
	4	1.63	9.64	4.9	4.7	0.30	10.02	5.2	4.8	1.04	1.0	$5.4\times$ 〃
90	5	1.14	9.79	2.8	7.0	0.52	20.08	10.5	9.6	2.05	1.4	
	6	0.71	10.01	1.3	8.7	1.02	39.83	25	14.8	3.98	1.7	
	7	0.51	9.94	0.87	9.1	1.53	59.63	45	14.6	6.00	1.6	
	8	0.37	9.90	0.58	9.3	1.94	79.60	64	15.6	8.04	1.7	
	9	0.30	10.05	0.45	9.6	2.35	99.11	86	13.1	9.86	1.4	

Discussion

The standard affinity of dye anions for the fiber in the single dyeing can be calculated theoretically by[2]

$$\log \frac{D_\phi \mathrm{Na}^z{}_\phi}{V^{z+1}} = \log D_\sigma \mathrm{Na}^z{}_\sigma + \left(\frac{-\Delta\mu^0}{RT}\right) \qquad (2)$$

$$\mathrm{Na}_\phi = D_\phi\left\{\frac{z}{2}+\left(\frac{z^2}{4}+\frac{V^2\mathrm{Na}_\sigma\cdot\mathrm{Cl}_\sigma}{D^2{}_\phi}\right)^{1/2}\right\} \qquad (2')$$

where D_ϕ is the amount of adsorbed dye anions on the fiber at equilibrium (mol./kg.), D_σ, the dyebath concentration of dye anions at equilibrium (mol./l.), Na_ϕ, the concentration of the sodium ion in the fibre phase at equilibrium (mol./kg.), Na_σ, Cl_σ, the concentrations of the sodium and the chloride ions in the dyebath at equilibrium (mol./l.), $-\Delta\mu^0$, the standard affinity of dye anions for the fiber (cal./mol.), z, the valency of dye anions, R, T, the gas constant and the absolute temperature, and V, the surface layer volume of the fiber (l./kg.). However, the relation of Eq. 2 does not always come into being, depending on values employed as the surface layer volume, and it forms the following relations usually:

$$\log \frac{D_\phi \mathrm{Na}^z{}_\phi}{V^{z+1}} = \alpha \log D_\sigma \mathrm{Na}^z{}_\sigma + \left(\frac{-\Delta\mu^{0\prime}}{RT}\right) \qquad (3)$$

Hence, $-\Delta\mu^{0\prime}$ corresponding to the affinity in this equation does not show a constant value. This was also seen in the present results; the value of α obtained from the results of the single dyeing of Blue dye or Yellow dye by using $V=0.45$ l./kg. does not become unity, as is shown clearly by the relations of $\log F_\phi \mathrm{Na}_\phi{}^4 - \log F_\sigma \mathrm{Na}^4{}_\sigma$ and of $\log G_\phi \mathrm{Na}^2{}_\phi - \log G_\sigma \mathrm{Na}^2{}_\sigma$ in Figs. 5 and 6. Consequently, $-\Delta\mu^{0\prime}$ does not show constant values as shown in Figs. 3 and 4. Theoretically the affinity should remain constant. In order to discuss quantitatively the behavior of dyes in the mixture dyeing, it is desirable that $-\Delta\mu^{0\prime}$ obtained from the single dyeing should be constant. Now, let us assume simply that the reason why α is not unity is due to the improper value of V. If

V' is put as the surface layer volume corresponding to $\alpha=1$, V should be replaced by V' in Eq. 2, and then Na_ϕ by Na_ϕ' (mol./kg.) corresponding to V'. Thus we obtain

$$\frac{1}{\alpha}\log\frac{D_\phi Na_\phi^z}{V^{z+1}}=\log\frac{D_\phi Na_\phi'^z}{V'^{z+1}} \tag{4}$$

Then, Eq. 3 becomes

$$\log\frac{D_\phi Na_\phi'^z}{V'^{z+1}}=\log D_\sigma Na_\sigma^z+\frac{1}{\alpha}\left(\frac{-\Delta\mu^0}{RT}\right) \tag{5}$$

Thus we shall obtain constant affinities by putting

$$\frac{1}{\alpha}\left(\frac{-\Delta\mu^{0\prime}}{RT}\right)=\frac{-\Delta\mu^0}{RT} \tag{6}$$

Such a surface layer volume V' can be calculated as follows: from a graph of $\log D_\phi Na_\phi^z-\log D_\sigma Na_\sigma^z$ drawn by using any seemingly adequate value of V (e. g. 0.45 l./kg.), we obtain a value of α, and then putting it into Eq. 4 together with any two pairs of the results of single dyeing (D_{ϕ_1}, Na_{ϕ_1}) (D_{ϕ_2}, Na_{ϕ_2}), we have

$$\frac{1}{\alpha}\log\frac{D_{\phi_1}Na_{\phi_1}^z}{V^{z+1}}=\log\frac{D_{\phi_1}Na_{\phi_1}'^z}{V'^{z+1}} \tag{7}$$

$$\frac{1}{\alpha}\log\frac{D_{\phi_2}Na_{\phi_2}^z}{V^{z+1}}=\log\frac{D_{\phi_2}Na_{\phi_2}'^z}{V'^{z+1}} \tag{7'}$$

Thus the following equation is obtained,

$$\frac{Na'_{\phi_1}}{Na'_{\phi_2}}=\left(\frac{D_{\phi_1}}{D_{\phi_2}}\right)^{\left(\frac{1}{\alpha}-1\right)/z}\cdot\left(\frac{Na_{\phi_1}}{Na_{\phi_2}}\right)^{\frac{1}{\alpha}} \tag{8}$$

On the other hand, if each of (D_{ϕ_1}, Na'_{ϕ_1}) and (D_{ϕ_2}, Na'_{ϕ_2}) satisfies Eq. 2', we obtain from Eqs. 8 and 2'

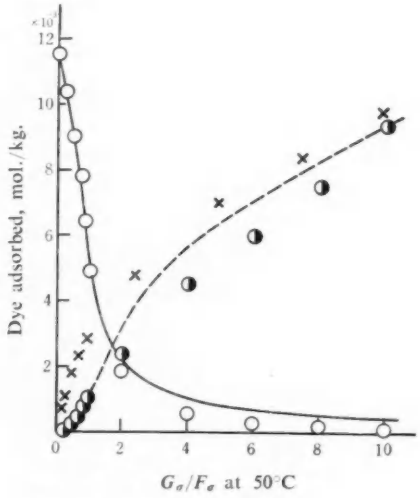

Fig. 7.

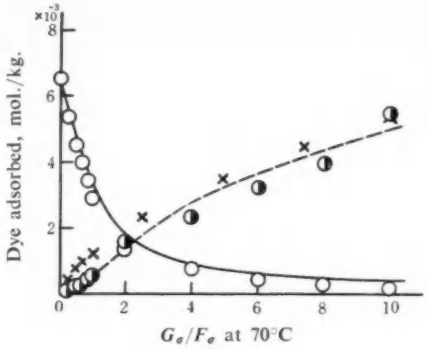

Fig. 8.

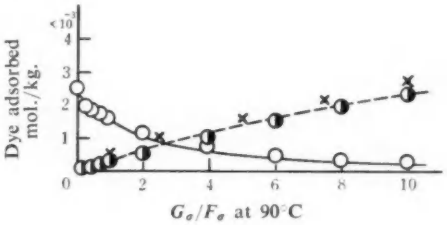

Fig. 9.

Figs. 7, 8 and 9. Adsorption isotherms of Chlorazol Sky Blue FF and Chrysophenine G in mixture dyeing at various temperatures: plot of adsorption on the fibre and ratio G_σ/F_σ; solid line, the curve of adsorption predicted theoretically of Chlorazol Sky Blue FF in mixture dyeing; broken line, the curve of adsorption predicted theoretically of Chrysophenine G in mixture dyeing.

○: The adsorption observed of Chlorazol Sky Blue FF in mixture dyeing.

◑: The adsorption observed of Chrysophenine G in mixture dyeing.

×: The adsorption observed of Chrysophenine G in single dyeing.

$$\frac{Na'_{\phi_1}}{Na'_{\phi_2}}=\frac{D_{\phi_1}\left\{\frac{z}{2}+\left(\frac{z^2}{4}+\frac{V'^2Na_{\sigma_1}\cdot Cl_{\sigma_1}}{D^2_{\phi_1}}\right)^{1/2}\right\}}{D_{\phi_2}\left\{\frac{z}{2}+\left(\frac{z^2}{4}+\frac{V'^2Na_{\sigma_2}\cdot Cl_{\sigma_2}}{D^2_{\phi_2}}\right)^{1/2}\right\}} \tag{9}$$

where Na_{σ_1}, Cl_{σ_1}, etc. denote the concentrations of the sodium and the chloride ion in the dyebath at equilibrium (mol./l.) respectively. When we solve Eq. 9 with respect to V' and put it into Eq. 5, we may be able to obtain constant values of the standard affinity.

Now in practice, values of the surface layer volume V' for the single dyeings of Blue dye and Yellow dye are obtained by use of α resulting from $V=0.45$ l./kg. and the affinities

are calculated from Eqs. 5 and 6 by use of this V'. These results are shown in Table II, Figs. 3 and 4. "$-\Delta\mu^0_{\text{mean}}$" in the table denotes the mean values of adjusted affinities of Blue dye and Yellow dye. They give rather constant values**. Such adjustment of the surface layer volume so as to obtain a constant affinity means to treat V as a parameter.

The observed amounts of adsorption of the dyes from the mixture dyeing are compared with those calculated by using the adjusted $-\Delta\mu^0_{\text{mean}}$ (Table II) and the instability constant K (Table I), which was obtained from the results of the single and the mixture dyeings as mentioned before[1], on the assumption

Table II

Dye	T°C	α	V' l./kg.	$-\Delta\mu^0_{\text{mean}}$ cal./mol.
Blue dye	50	1.32	0.81	6500
	70	1.20	0.66	6000
	90	1.05	0.45	5300
Yellow dye	50	0.85	0.26	4970
	70	0.84	0.22	4640
	90	0.82	0.13	4550

that the reduction in amounts of adsorption from mixture dyeing is mainly due to an interaction between both dyes in the dyebath. These results are shown in Figs 7, 8 and 9. However, on the supposition that only a one to one complex is formed over the whole concentration region of the dyes and that dye molecules which contribute to the complex formation have no relation to adsorption, the effective dyebath concentration of Blue dye $F'_{\sigma\text{cal}}$ (hereafter "cal" is suffixed to calculated values) is obtained from Eq. 10

$$F'_{\sigma\text{cal}} = 1/2\{(G_\sigma - a)^2 + (b^2 - a^2)\}^{1/2} + 1/2(a - G_\sigma) \tag{10}$$

where $a = F_\sigma - K$ and $b = F_\sigma + K$, and the mean value of the instability constant shown in Table I is used as K, i.e. 2×10^{-7}, 8×10^{-7} and 4×10^{-6} (mol./l.) at 50°, 70° and 90°C, respectively. The final dyebath concentration of Blue dye and Yellow dye in Table I are used as F_σ and G_σ in Eq. 10.

The effective dyebath concentration of Yellow dye $G'_{\sigma\text{cal}}$ is obtained from

$$G'_{\sigma\text{cal}} = G_\sigma - G_{c\text{cal}} = G_\sigma - (F_\sigma - F'_{\sigma\text{cal}}) = G_\sigma - F_{c\text{cal}} \tag{11}$$

The amount of adsorption of both dyes are calculated by the following equations, on the assumption that the affinity of each dye does not change in the mixture dyeing.

$$F_{\phi\text{cal}} = F'_{\sigma\text{cal}}\mathrm{Na}^{-4}_{F\phi\text{cal}}\mathrm{Na}^{4}_{\sigma}V_F'^{5} \times\exp\left(\frac{-\Delta\mu^0_{F\text{mean}}}{RT}\right) \tag{12}$$

$$G_{\phi\text{cal}} = G'_{\sigma\text{cal}}\mathrm{Na}^{-2}_{G\phi\text{cal}}\mathrm{Na}^{2}_{\sigma}V_G'^{3} \times\exp\left(\frac{-\Delta\mu^0_{G\text{mean}}}{RT}\right) \tag{12'}$$

where the values for $\mathrm{Na}_{F\phi\text{cal}}$ and $\mathrm{Na}_{G\phi\text{cal}}$ are approximately obtained from the equations derived by eliminating D_ϕ in Eqs. 2 and 2',

$$\mathrm{Na}^{3}_{F\phi\text{cal}}(\mathrm{Na}^{2}_{F\phi\text{cal}} - V_F'^{2}\mathrm{Na}_\sigma\cdot\mathrm{Cl}_\sigma) = 4\mathrm{Na}_\sigma{}^{-4}F'_{\sigma\text{cal}}V_F'^{5}\exp\left(\frac{-\Delta\mu^0_{F\text{mean}}}{RT}\right) \tag{13}$$

$$\mathrm{Na}_{G\phi\text{cal}}(\mathrm{Na}^{2}_{G\phi\text{cal}} - V_G'^{2}\mathrm{Na}_\sigma\cdot\mathrm{Cl}_\sigma) = 2\mathrm{Na}_\sigma{}^{-2}G'_{\sigma\text{cal}}V_G'^{3}\exp\left(\frac{-\Delta\mu^0_{G\text{mean}}}{RT}\right) \tag{13'}$$

where the values of V_F', V_G', $-\Delta\mu^0_{F\text{mean}}$ and $-\Delta\mu^0_{G\text{mean}}$ are obtained from the respective values at the various temperatures shown in Table II.

It is brought out from these results that the observed amounts of adsorption of the dyes agree well with those calculated over the whole range of concentration at 90°C (Fig. 9); this means that the behavior of the dyes in mixture may be explained quantitatively by the formation of a 1:1 complex in the dyebath. Though both values calculated and observed show considerably good agreement at 70 and 50°C, too, some deviation is recognized at these temperatures in the range where $2 \lesssim G_\sigma/F_\sigma \lesssim 8$. It may be due to the fact that where $G_\sigma/F_\sigma \geqq 2$, the dyes form not only one to one complex, but higher complexes richer in Yellow dye (may be one to two), which promote the reduction of adsorption***. In the region $G_\sigma/F_\sigma \approx 10$, the observed adsorption of Yellow dye tends to approach that in the single dyeing. This will be explained by the thought that even if the composition of complexes becomes completely one to two, Yellow dye may behave as in the single dyeing, because of its comparatively higher concentration than

** Standing has discussed the value of V for Chrysophenine G ($z=2$) using the so-called p-q equation (*J. Text. Inst.*, **45**, T 21 (1954)). With his method, however, the calculation for Chlorazol Sky Blue FF ($z=4$) becomes complicated. Hence in this work, V was adjusted as above. The results for Chrysophenine G are considerably approximated to his result.

*** It has been recognized by spectral measurements that a 1:2 complex richer in Yellow dye is also formed in the mixture of Blue and Yellow dye at room temperature (T. Kobayashi, Y. Tanizaki and N. Ando., This Bulletin, **33**, 661 (1960)). On the other hand, it has been concluded that only a one to one complex is formed at 60°C (A. N. Derbyshire and R. H. Peters, *J. Soc. Dyers Col.*, **72**, 268 (1956)).

However, the spectral measurements for the mixture solution in the presence of sodium chloride at high temperature has not yet been carried out, so the composition of complexes may be open to discussion.

that of Blue dye. On the other hand, since F_a is almost constant, the formation of complexes and their compositions may have considerable influence on the adsorption of Blue dye with an increase of Yellow dye. In fact, the observed values of adsorption of Blue dye shown in Figs. 7 and 8 are small compared with those calculated on the basis of the formation of only a one to one complex.

Thus the behavior of dyes in the mixture dyeing may be well explained quantitatively by the method mentioned above if both dyes interact with each other (complex formation) in the dyebath. If further information on these matters, i.e. on the single dyeing and the interaction, is obtained hereafter, this problem will be treated more clearly.

Summary

1. The single dyeings of Chlorazol Sky Blue FF and Chrysophenine G and the mixture dyeing of them were carried out at 50, 70 and 90°C.

2. In the single dyeing, the surface layer volume in Vickerstaff's equation was adjusted so as to obtain constant values of the standard affinity.

3. In the mixture dyeing, the behavior of dyes was explained quantitatively on the basis of the information of the single dyeing and the interaction between both dyes in the dyebath.

The author is greatly indebted to Professor Noboru Ando and Mr. Yoshié Tanizaki for their valuable advice and encouragement throughout this work.

Laboratory of Physical Chemistry
Tokyo Institute of Technology
Meguro-ku, Tokyo

Dichroism of Dyes in the Stretched PVA Sheet. III[1]. *Direction of Absorption of Pinacyanol Iodide*[*1]

By Yoshié TANIZAKI

(Received December 18, 1959)

In the previous paper[1], a theoretical expression was derived concerning the relation between the optical density ratio $R_d(=D_{\parallel}/D_{\perp})$ and the stretch ratio R_s of the sample sheet, for the analysis of the relative absorption direction of dye molecules in the stretched PVA (polyvinyl alcohol) sheet. It was also proved experimentally that the adopted assumption in the derivation of the distribution function and accordingly the above R_d expression are adequate[2]. A parameter r in the R_d expression, which determines the R_d-R_s curve practically, is a particular one to each absorption band. Also this r-value determines the angle between the transition direction and the orientation axis of the molecule. Therefore, the greater the number of the absorption band in the observable region, the easier would be the discussion on the correspondence between the relative transition direction and the molecular structure.

In this paper, turning our attention to the fact that the pinacyanol cation reveals a number of absorption bands from the visible to the near ultraviolet region, we determined the relative transition direction of some absorptions from the quantitative analysis. We also deduced the directions of other absorptions.

Experimental

The pinacyanol iodide used was synthesised and purified in the Laboratory of Fuji Photo Film Co., Ltd.

The experiment was carried out in the same way as before[1,3]. When a quantitative test is required, the correction of absorption and reflection by the substrate of the sheet becomes important, especially in the ultraviolet region.

Resultant optical density D from the absorption and/or the reflection of the PVA sheet itself in the visible region is as small as less than 0.05, almost

1) Part II of this series, Y. Tanizaki, This Bulletin, 32, 75 (1959).

*1 Presented at the 12th Annual Meeting of the Chemical Society of Japan, Kyoto, April, 1959.

2) Y. Tanizaki, T. Kobayashi and N. Ando, This Bulletin, 32, 1362 (1959).

3) Y. Tanizaki and N. Ando, *J. Chem. Soc. Japan, Pure Chem. Sec.* (*Nippon Kagaku Zasshi*), **78**, 542 (1957).

independent of the stretch ratio R_s, and the difference of $D_\parallel$ and $D_\perp$ is negligible because it is of the order of 0.001. In the near ultraviolet region, however, with decrease in wavelength, not only $D_\parallel$ and $D_\perp$ but their differences increases gradually, and these are all dependent on R_s. Accordingly, in the dichroic measurement the error arising from the incongruity in the stretch directions of the sample sheet and the correction sheet with each other (in the same R_s-value) becomes considerably large in general in the ultraviolet region. For this reason, the correction in the ultraviolet region, especially for the comparatively small density absorption, is of importance. So it was taken into consideration that the specific directions—the stretch directions—of the stained and the unstained sheet must be kept parallel with each other. An example of the observed relation between angle θ and optical density D_θ is illustrated in Fig. 1, in which θ

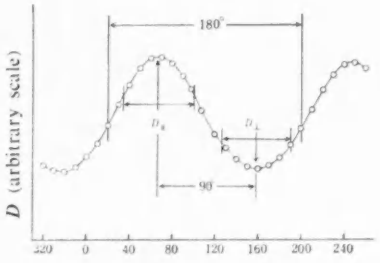

Fig. 1. Relation of optical density of pinacyanol in the stretched PVA sheet to the angle θ graduated on the disk of the sheet rotation apparatus. $R_s=5.4$, $\lambda=284$ mμ.

means the angle graduated on the disk of the sheet-rotation apparatus (see Figure 1 of Ref. 1). In Fig. 1, D_θ for a given angle θ coincides with $D_{(\theta+180°)}$ for $(\theta+180°)$. When the angle of the middle point of equivalent densities on both sides of the maximum is denoted as $\parallel$ and that for the minimum as $\perp$, the angle scale difference between $\parallel$ and $\perp$ is equal to just 90°. The optical densities for $\parallel$ and $\perp$ are indicated by $D_\parallel$ and $D_\perp$, respectively. A revolution of the disk gives two $D_\parallel$'s and two $D_\perp$'s. Two $D_\parallel$'s ought to be equivalent to each other, and the same must be said with two $D_\perp$'s, but sometimes they were not. These differences, however, were small, so that the mean value of each was used for the purpose of analysis.

Results

Absorption spectra of pinacyanol in the non-stretched PVA sheet are shown by solid lines in Figs. 2 and 3. In these figures, spectra in ethanol are also shown by broken lines for the comparison. Pinacyanol reveals absolutely corresponding absorption bands in both media, where every band in the sheet only shifts more or less to the longer side (200~300 cm^{-1}) compared with that in ethanol.

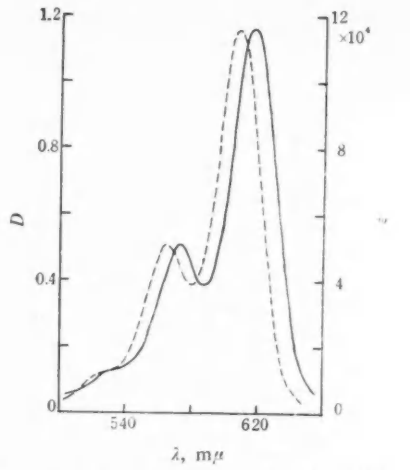

Fig. 2. Absorption spectra both in visible region of pinacyanol in the non-stretched ($R_s=1.0$) PVA sheet (solid line) and in an ethanolic solution of 2.79×10^{-5} mol./kg. (broken line).

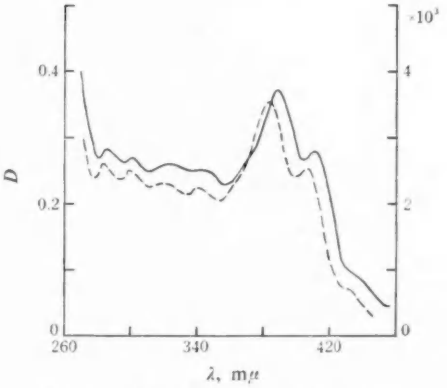

Fig. 3. Absorption spectra both in the near ultraviolet region of pinacyanol in the non-stretched ($R_s=1.0_4$) PVA sheet (solid line) and in ethanolic solution of 2.79×10^{-5} mol./kg. (broken line).

Curves indicated in Figs. 4 and 5 corresponding to respective ones of Figs. 2 and 3 are obtained by stretching the sheet and then observing it with polarized light. None of the bands in Fig. 4 nor those around 400 mμ in Fig. 5 have any change either in shape or in maximum position, with the change of angle θ, and they have the same order of the optical density ratio R_β, with a considerably large value compared with the rest of the bands.

The rest, on the other hand, change in shape and maximum position, together with θ. The behavior with θ of the absorption curves near

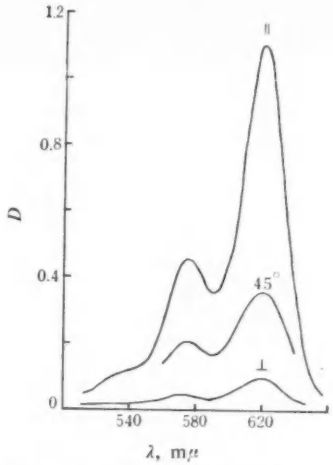

Fig. 4. Dichroism of pinacyanol in the stretched sheet at $R_s=8.2$, corresponding to Fig. 2. The sheet reflection is already corrected. ∥, 45° and ⊥ mean the absorptions for the polarized light of which the direction of the electric vector is parallel, 45° and right angles to the stretch direction of the sheet, respectively.

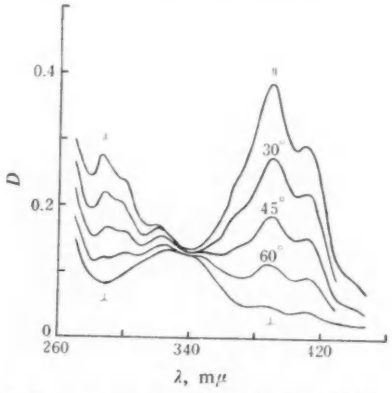

Fig. 5. Dichroism of pinacyanol in the stretched sheet at $R_s=8.0$, corresponding to Fig. 3. Corrected as for the absorption and reflection of the sheet. ∥, 30°, 45°, etc. have the same meaning as these in Fig. 4.

340 mμ is especially noticeable in the point that the absorption intensity has no great change with θ.

Expansion of observation from the first bands to the long wavelength found out a weak but single band at 700 mμ. This is as shown in Fig. 6 and has similar behavior as other visible bands. Moreover, there were noticed weak absorptions at about 470 mμ and at 440 mμ,

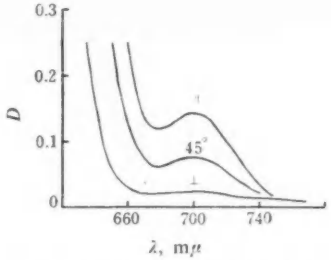

Fig. 6. Dichroism of the pinacyanol weak band at 700 mμ. $R_s=11$.

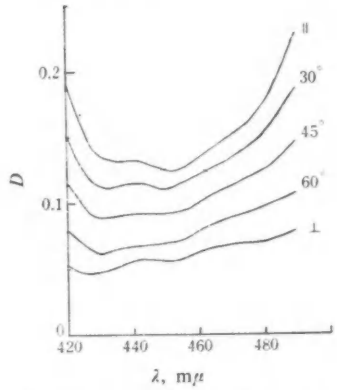

Fig. 7. Dichroism of the Pinacyanol weak band at about 470 mμ and at 440 mμ. $R_s=6.0$.

but their properties could not be judged owing to the nearby strong absorptions (Fig. 7).

The polarization degree of the polaroid used decreases in short region of 300 mμ and follows a curve as shown in Fig. 8. That is to say, the incident light in this region is a partially polarized light. Absorption spectra by this light are indicated by solid lines in Fig. 8. Curves in this figure show an obvious absorption band at 240 mμ and a shoulder at 260 mμ. The absorption at 240 mμ becomes more indistinct as it moves from $D_\parallel$ to $D_\perp$ curve, and that of 260 mμ stands just on the reverse.

All the absorption bands that could be recognized by the measurement are summarized in Table I, being numbered in order from high to low wavelength. These bands in Table I were distinguished by their shape in this way as follows. The number, wavelength and wavenumber of a band have no mark when it indicated a distinct maximum at least in one of $D_\parallel$ and $D_\perp$ (in general D_θ) curve, are put in parentheses when it indicated distinct shoulder, and are put in brackets when it showed indistinct shoulder or curvature.

Experimental relations between each R_I and

TABLE I. *r*-VALUES, DIRECTIONS AND CLASSIFICATION OF THE ABSORPTION BANDS OF PINACYANOL RECOGNIZED IN THE PVA SHEET BY DICHROIC MEASUREMENTS

Band No.	λ mμ	ν cm^{-1}	*r*-Value	Angle	Direction	Classification
I	700	14280			longi.	
II	620	16120	2.60～2.00	21.0～26.5	longi.	First group
III	575	17380	2.60～2.00	21.0～26.5	longi.	(strong)
(IV)	(530)	(18860)			longi.	
[V]	[470]	[21270]			longi. ?	
(VI)	(440)	(22710)			longi.	Second group
VII	410	24380	2.60～2.00	21.0～26.5	longi.	(weak)
VIII	388	25760	2.60～2.00	21.0～26.5	longi.	
[IX]	[365]	[27400]			longi. ?	
(X)	(345)	(29000)	0.75	53.1	⊥	
XI	328	30500	0.85	49.6	⊥	Third group
(XII)	(300)	(33300)	1.15	41.0	∥	(weak)
XIII	286	35000	1.30	37.6	∥	
(XIV)	(275)	(38900)			⊥	Fourth group
XV	240	41650			∥	(strong)
[XVI]	[230]	[43500]			⊥	

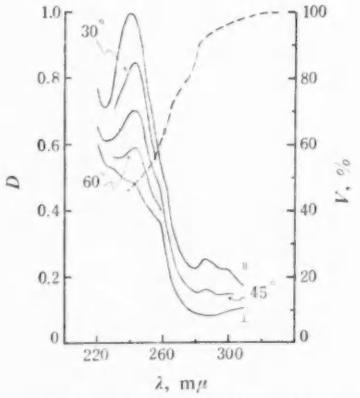

Fig. 8. Dichroism in the ultraviolet region of pinacyanol at R_s=5.4. The broken line represents the polarization degree of the polaroid used. Taken from Y. Tanizaki, This Bulletin, **30**, 935 (1957).

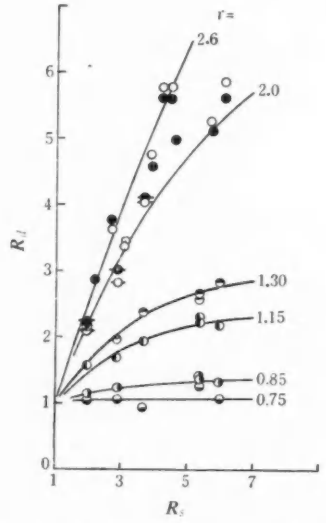

Fig. 9. Relations of R_d to R_s of absorption bands. Circles represent the observed values; ○: 620 mμ (Band II), ●: 570 mμ (III), -○-: 410 mμ (VII), -●-: 388 mμ (VIII), ◓: 286 mμ (XIII), ◒: 344 mμ (X), ◐: 300 mμ (XII), ◑: 328 mμ (XI). Curves are the calculated ones for respective *r*-value from the R_d expression of Ref. 1.

R_s of Bands II, III, VII, VIII and X—XIII are shown in Fig. 9. Curves in the figure are theoretical ones corresponding to respective *r*-values[1)*2]. Observed values of each Band II, III, VII and VIII approximately fall between these curves which have peculiar *r*-values. Angles between transition directions and an orientation axis of the molecule are evaluated from the *r*-values and indicated in Table I.

Assignment of Transition Direction.—As shown in Figs. 2—8, all the absorption bands in visible region and around 400 mμ had so large R_d values that they were distinguished from others. It is considered that the double bond system which runs through over the molecular axis responsible for the first band of cyanines of this kind (here Band II)[4]. If

*2) $\cot^{-1}r$ gives the angle between the direction of orientation and that of transition of the absorption.

4) For example, H. Kuhn, *J. Chem. Phys.*, **17**, 1198 (1949); G. S. Levinson, W. T. Simpson and W. Curtis, *J. Am. Chem. Soc.*, **79**, 4314 (1957).

this is the case, it must be expected that such an absorption band gives the maximum R_d when the longitudinal axis of the molecule meets the stretching direction of the sheet. In effects, the fact that the R_d-value of the first band is always larger than that of any band in the region below 360 mμ, means that this molecular axis approaches most completely its orientation axis. Accordingly, it is concluded that a group of bands, of which r-values fall between 2.0~2.6, as indicated in Fig. 9, is all due to transitions parallel to the long axis of molecule.

When two transition directions are at right angles to each other in a molecule, a product of these r-values must be unity. Namely,

$$r_{\parallel} \times r_{\perp} = 1 \quad (1)$$

According to Table I, the following two pairs are approximately unity*3.

$$r_{X} \times r_{XIII} = 0.975 \quad (2)$$

$$r_{XI} \times r_{XII} = 0.978 \quad (3)$$

Moreover, Table I indicates $r_{X} < r_{XI}$ and $r_{XIII} > r_{XII}$. If they lie in a common absorption plane[1] (made of an orientation axis and a transition direction) and if Relation 1 is held, relations $r_{\perp} = r_{X} = r_{XI}$ and $r_{\parallel} = r_{XIII} = r_{XII}$ must be kept. These disagreements would be due to the following reason. Because there are two bands XI and XII of opposite character existing close to each other, as is clarified in Fig. 5, R_d of Band XI might be elevated by might be elevated by XII, while that of XII might be lowered by XI. For this reason, concerning r-values in this case, r_{X} and r_{XIII} are believed to be a most reliable $r_{\perp}$ and $r_{\parallel}$ respectively. From the above discussion, it may be concluded that the product of each pair of r-values in Relations 2 and 3 is in fact unity and therefore satisfies Relation 1 in itself, and that the relations $r_{\perp} = r_{X} = r_{XI}$ and $r_{\parallel} = r_{XII} = r_{XIII}$ should come into existence.

If Bands XV (240 mμ) and XIV (260 mμ) in Fig. 8 were measured by perfect polarized light*4, R_d for XV would perhaps be found to be larger and for XIV smaller. Consequently, it can be expected that r-values for these bands approach r_{XIII} and r_{X}, respectively. In this case, therefore, r_{XV} presumably corresponds to $r_{\parallel}$ and r_{XIV} to $r_{\perp}$. Moreover, the weak band XVI (230 mμ) is not thought of conclusively.

According to the above discussion, the absorptions of Pinacyanol will be distinguished into the following three groups. One of these groups is such that the transition direction runs along the molecular axis. And to this groups Bands I—IX belong, although it is not certain regarding Bands V and IX. The other two groups contain the bands of which any two transition directions taken from each group separately are orthogonal. Let us decide to make "$\parallel$" represent those near to the molecular axis and make "$\perp$" represent the others; then Bands XII, XIII and XV become "$\parallel$" and X, XI, XIV and XVI become "$\perp$".

The transition direction assigned above was based on an analysis of the observed R_d—R_s relation. However, when we compare again the dichroic behavior of the band in the curves of Figs. 4—8 with their transition directions indicated in Table I, we see that the direction can well be decided only by an inspection of the dichroic behavior without the help of the R_d—R_s relation: for instance, absorption bands which have the maximum R_d for the same R_s in the whole region with no change in shape and in λ_{max} can be decided as "longi." (bands shown in Fig. 2 and around 400 mμ in Fig. 3). Others in general change in their shape of absorption and in λ_{max} for D_θ: this fact suggests the superposition of absorptions with different directions. R_d-values of these bands are so small as to be easily distinguished from "longi.". This absorption group is considered to be formed of $\parallel$ $\perp$ absorptions. Accordingly, of these absorptions the ones with the larger R_d may be decided as $\parallel$ and the others with the smaller R_d as $\perp$.

Discussion

It is evident from Figs. 2 and 3 that pinacyanol shows the identical absorption both in PVA sheet and in ethanol. Therefore, the following discussion on the light absorption in PVA sheet may be thought to apply to that in ethanol.

In the last section, the absorption bands have been classified only from the standpoint of their transition directions. Now, turning attention to the absorption position and intensity, we can roughly divide them again into four groups (Table I and Figs. 2—8): the first group includes Bands I—IV, the second group Bands V*5—IX, the third group Bands X—XIII,

*3 In fact, however, these products are slightly smaller than unity. This may be interpreted by the following reason. From the polarization degree curve in Fig. 8, it is noticed that Bands XIII and XII were observed by the light of 93% and 97% polarization respectively. In this case, therefore, R_d becomes smaller than when observed by 100% polarization light, and r-value might be estimated to be exceedingly small.

*4 From Fig. 8, it is estimated, R_d(XV)=2.0 and R_d(XIV)=1.5 at R_s=5.4. As for r-values, r_{XV}=1.1 and r_{XIV}=0.9, and the former is smaller than 1.3 of r_{XIII} and latter is larger than 0.75 of r_{X}. But the product is again approximately unity.

*5 According to the apparent shape of the curve in Fig. 7, it seems plausible that Band V belongs to the Ist group. But, from the standpoint of band distance, as will be seen later, it will reasonably be put into the 2nd group.

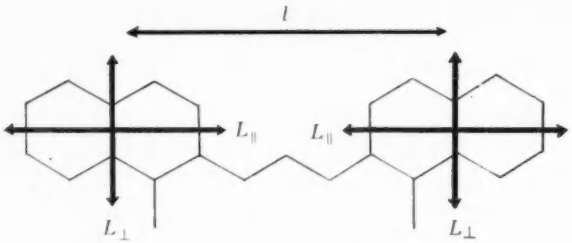

Fig. 10. The molecular skeleton of pinacyanol.

and the fourth groups Band XIV~XVI.

As already mentioned, the absorptions of the first and the second group lie on the long axis of the molecule. Accordingly, if the molecular skeleton of Pinacyanol cation is just as shown in Fig. 10, the direction of these absorptions may correspond to *l*-direction of the figure. And again as mentioned, the $\parallel$ and the $\perp$ transition are normal to each other in the same plane. This is visually understood from the fact that the sum of angles between the transition direction and orientation axis in Table I, for example, Band X($\perp$) and XIII ($\parallel$), is approximately 90 degrees. Thus, it may conclusively be said that the $\parallel$ and the $\perp$ transition coinside with the long and the short axis of the quinoline nucleus, respectively.

The absorption bands of the 3rd and the 4th groups, therefore, are attributed to the localized π electron system in the quinoline nuclei: those of the 3rd group would be derived, for example, from the weak 320 and 310 mμ absorption of 2-methyl-*N*-ethyl-quinolinium cation, and those of the 4th group from the strong 240 and 220 mμ absorption.

Now, if the molecule is planar in the shape of Fig. 10, the direction of the long axis ($L_{\parallel}$) of quinoline nucleus and *l*-direction become parallel, hence these two directions must take any identical angle toward the orientation axis of the molecule. Table I actually shows, however, rather great difference between the two angles*6. This means that two quinolines are to a large extent off the common plane*7.

Absorptions of the 1st and the 2nd group apparently resemble each other in shape (cf. Figs. 2 and 3). Further, the fact that the latter is weaker than the former in intensity and that their directions are the same suggests that the 2nd goup corresponds to an overtone of the 1st group. In this connection, the following fact is of interest: the distances of the adjacent bands in the 1st group are $1500\pm300\,cm^{-1}$ and those in the 2nd group are also $1500\pm200\,cm^{-1}$, indicating a constant space of band-distribution. It is from the standpoint of band distance that we have put Band V into the 2nd group, in the above group classification.

As is already well known, the first group absorption is very sensitive to the solvent nature[5,6]. A correspondence of complexes of monomer, dimer, etc. with absorptions were attempted[6], with the help of the fact that the pinacyanol cation is easily aggregated. At the present stage, however, it can not be decided whether respective absorption bands correspond to those intrinsic to respective complexes possibly considered, e. g. such new absorptions as revealed by a Davidov splitting[7], or transitions originally existing are intensified by coupling with vibration[8] on some account involving complex formation.

Summary

1. Dichroism of pinacyanol iodide in the PVA sheet was observed in the region higher than 220 mμ, and at least sixteen absorption bands were recognized.

2. The relation of R_d to R_s was analyzed concerning some absorption bands, and it was verified that there are two groups of transitions,

*6 Namely, if two absorption planes of "longi", and "$\parallel$" (Band XIII) were coincident, the angle between these transitions would be about 64 degrees. The difference is about 14 degrees, indicating that the molecule is almost planar. That this is not correct would be shown by constructing the structural model corresponding to Fig. 10. Besides, the assumption that the absorption planes coincide with each other has no grounds.

*7 Concerning the double bond character, this is not inconsistent with the concept of the usual planar molecule. Because, if the rotation of quinoline planes is equally shared by the polymethine bonds (here 4 bonds) the double bond character of each bond will be roughly lowered only by about 10 percent of that in case of planar, even though the inclined angle of the planes is 80 degrees.

5) I. M. Klotz, *Chem. Revs.*, **41**, 382 (1947); S. E. Sheppard and A. L. Geddes, *J. Chem. Rhys.*, **13**, 63 (1945).

6) R. C. Merrill and R. W. Spencer, *J. Am. Chem. Soc.*, 72, 2894 (1950).

7) For instance, J. W. Weigl, *J. Chem. Rhys.*, **24**, 364 (1956).

8) S. E. Sheppard and G. R. Brigham, *J. Am. Chem. Soc.*, **66**, 380 (1944); S. E. Sheppard and A. L. Geddes, ibid., **66**, 2003 (1944).

one existing along the long axis of the molecule, the other being at right angles to one another in geometry.

3. The absorption group at right angles to one another appears in the shorter wavelength region than about 340 mμ, and it was shown that this is due to the two orthogonal electronic transitions localized in the quinoline nuclei of the molecule.

4. The absorptions of the long axis of the pinacyanol molecule consist of two groups, each involving several bands and it was pointed out that the bands are distributed with nearly constant distance of 1500 cm^{-1} between adjacent one.

5. It was deduced that the molecule is not a planar and both quinoline planes are far from planar.

6. Sixteen absorptions mentioned above were reasonably classified in their relation to the transition direction or in their correspondence to the molecular structure.

The author wishes to express his thanks to Professor N. Ando and I. Tana kain this laboratory for their encouragement throughout this work, also to Mr. Y. Mori in our laboratory for his useful discussion and helpful advice, and to Mr. H. Ono of the Laboratory of Fuji Photo Film Co. for his kind supply of the dye sample used in this investigation.

Laboratory of Physical Chemistry
Tokyo Institute of Technology
Meguro-ku, Tokyo

*On Some Dark-colored Chlorocuprates(I, II) and Related Compounds. I. The Method of Preparation and Some Properties**

By Masayasu MORI

(Received September 14, 1959)

A considerable amount of data has now been accumulated concerning the characteristic properties of "mixed valence" compounds, i.e. compounds containing atoms of the same element in different valence states. Mixed valence compounds having a comparatively covalent character have been fairly well studied and are now utilized in the field of semiconductors. One of the most characteristic features of such mixed valence semiconductors is that the ratio of atoms in two valence states can often be changed arbitrarily, thus resulting in a change in the properties of the substance, as if the valence of the metal could take a continuous non-integral number. Such a technique of preparing semiconductors, termed *valence control*, is often useful for giving desired electrical properties to these substances[1]. On the other hand the properties of the mixed valence compounds of ionic character containing halometallate ions have scarcely ever been elucidated. Most of these mixed valence halometallates show an "interaction color" due to an abnormal light absorption[2].

The interaction color of copper(I) and copper(II) chlorides in hydrochloric acid solution has been known from an early date. Doehlemann and Fromherz measured the absorption spectrum of this system and found a broad interaction absorption in the visible region[3]. However, the present-day knowledge of the structure of chlorocuprate ions is very meager, and it is not known what kinds of chlorocuprate ion are responsible for the interaction color. This is mainly due to the fact that the phenomenon has hitherto been observed only in aqueous solution. It occurred, therefore, to the present author that an investigation on crystalline compounds showing an interaction color of copper(I) and copper(II) might be helpful in throwing light on the nature of this problem and he succeeded in obtaining dark brown chlorocuprates(I, II) of hexamminechromium(III) and hexamminecobalt(III) cations. For comparison the chlorocuprates(I) and chlorocuprates(II) of these

1) E. J. W. Verwey, *Philips Research Repts.*, **5**, 173 (1950).

* A part of this study was presented at the Symposium on Coordination Chemistry, Tokyo, November, 1958.

2) The paper of J. E. Whitney and N. Davidson [*J. Am. Chem. Soc.*, **71**, 3809 (1949)] contains a survey of the literature up to that time.

3) E. Doehlemann and H. Fromherz, *Z. physik. Chem.*, **171A**, 353 (1934).

complex cations were also prepared and they were found to form yellow or orange crystals. In the following paragraphs the methods of preparation and some properties of these compounds will be described.

Experimental

Methods of Preparation.—*Hexamminechromium(III) Chlorocuprate(I, II) and Hexamminecobalt(III) Chlorocuprate(I, II).*—Five tenths grams of copper(I) chloride was dissolved in 100 ml. of hot water containing 15 g. of ammonium chloride and 40 ml. of concentrated hydrochloric acid. When the color of the solution was found to be greenish yellow, a dilute solution of titanium(III) chloride was added dropwise, until the very moment when the yellow color disappeared. The solution was quickly filtered and the filtrate was poured into a solution of 2.7g. of hexamminechromium(III) chloride mono-hydrate and 3 g. of copper(II) chloride di-hydrate in 100 ml. of water. The same amount of hexamminecobalt(III) chloride was used in preparing the corresponding cobalt compound. It seemed preferable to heat both solutions to about 60°C before mixing, for the precipitate formed in the cold solution was very fine and liable to decomposition. The mixture was cooled in a cold water bath for 30 min. with occasional stirring. The dark brown or almost black crystalline precipitate thus formed was filtered off, washed with 2 N hydrochloric acid and then with ethanol, and dried in air. (Samples No. 3 and 8 in Table I.)

Found for the chromium compound: Cr, 14.2, 13.8, 13.6; N, 21.5, 21.7, 21.8; total Cu, 16.8, 15.7; Cl, 42.3; loss in wt. at 110°C, 1.05, 1.23. Calcd. for $[Cr(NH_3)_6]_2Cu_2Cl_9(H_2O)_{1/2}$: Cr, 13.6; N, 22.0; Cu, 16.6; Cl, 41.8; H_2O, 1.14%.

Found for the cobalt compound: Cu, 15.2; N, 21.3; total Cu, 16.5, 16.9; Cl, 41.1; loss in wt. at 110°C, 1.15. Calcd. for $[Co(NH_3)_6]_2Cu_2Cl_9(H_2O)_{1/2}$: Co, 15.2; N, 21.6; Cu, 16.4; Cl, 41.1; H_2O, 1.13%.

The total copper content in the above analytical data was determined gravimetrically. The content of bivalent copper was determined iodometrically in 3 N acetic acid using finely powdered sample. The chromium compound gave a fairly sharp end point of titration and it was found to contain about a half of the total copper in the bivalent state (Found, 8.4; calcd., 8.3). In the cobalt compound the end point of the iodometric titration was very obscure, and the results were less reproducible (Found, 8.7, 9.0, 9.1, 9.3. Calcd., 8.2). It was found, however, that the composition of the chlorocuprate(I, II) depends on the quantity of copper(I) and copper(II) chlorides and used in the preparation. An outline of this relationship is given in Table I. Samples Nos. 1—6 are chromium compounds and Nos. 7—11 cobalt compounds. The procedure adopted in preparing these samples was the same as that given above except the difference in the quantities of the copper chlorides used.

Hexamminechromium(III) Chlorocuprate(I) and Hexamminecobalt(III) Chlorocuprate(I).—One gram of copper(I) chloride and 15 g. of ammonium chloride were dissolved in a mixture of 100 ml. of hot water, 20 ml. of 15% titanium(III) chloride solution in hydrochloric acid and 40 ml. of concentrated hydrochloric acid. The solution was quickly filtered and the filtrate was poured into a solution at 60°C of 2.7 g. of hexamminechromium(III) chloride mono-hydrate in 100 ml. of water. The same amount of hexamminecobalt(III) chloride was used in preparing the corresponding cobalt compound. The mixture was cooled in a cold water bath for 30 min. with occasional stirring. The yellow or orange precipitate was filtered off and washed with 2 N hydrochloric acid and ethanol, and then it was

TABLE I. THE RELATIONSHIP BETWEEN THE QUANTITIES OF THE STARTING MATERIALS AND THE CHEMICAL COMPOSITION OF THE CHLOROCUPRATE

Sample No.	Starting Material[a]		Product		
	CuCl (in g.)	$CuCl_2 \cdot 2H_2O$ (in g.)	Total Cu (in %)	Bivalent Cu (in %)	Color
1	0	3	16.1	16.1	yellow
2	0.2	3	17.0	12.7	brownish black
3	0.5	3	16.8	8.4	black
4	1	3	19.5	2.0	grayish brown
5	1	1	20.0	1.0	brown
6	1	0	20.4	0	yellow
7	0	3	15.8	16.8[b]	orange
8	0.5	3	16.4	9.2[b]	black
9	1	3	19.0	2.3[b]	dark brown
10	1	1	19.8	1.6[b]	brown
11	1	0	19.8	0	orange

a) For samples Nos. 1—6 the complex cation used was hexamminechromium(III) ion and for samples Nos. 7—11 hexamminecobalt(III) ion.

b) The end point of the iodometry of the cobalt compound is very obscure.

dried in vacuo over potassium hydroxide. (Samples No. 6 and No. 11 in Table I.)

Found for the chromium compound: Cr, 13.6; N, 21.7; Cu, 20.4; Cl, 39.2. Calcd. for $[Cr(NH_3)_6]_4$-Cu_3Cl_{17}: Cr, 13.5; N, 21.9; Cu, 20.7; Cl, 39.2%.

Found for the cobalt compound: Co, 15.4; N, 20.8; Cu, 19.8; Cl, 38.5. Calcd. for $[Co(NH_3)_6]_4$-Cu_3Cl_{17}: Co, 15.1; N, 21.5; Cu, 20.3; Cl, 38.5%.

Hexamminechromium(III) Chlorocuprate(II).—Two grams of hexamminechromium(III) chloride monohydrate and 2 g. of copper(II) chloride di-hydrate were dissolved in 60 ml. of water. The solution was filtered and the filtrate was heated to 60°C and mixed with 20 ml. of concentrated hydrochloric acid. The mixture was cooled in a cold water bath for 30 min. with occasional stirring and the precipitated complex was filtered and washed with ethanol. (Sample No. 1, Table I.)

Found: Cr, 13.8; N, 21.5; Cu, 16.1; Cl, 44.9. Calcd. for $[Cr(NH_3)_6]CuCl_5$: Cr, 13.2; N, 21.3; Cu, 16.1; Cl, 44.5%.

The corresponding cobalt compound had already been prepared by Levi[4]. (Sample No. 7, Table I).

Hexamminechromium(III) Bromocuprate(II).—Two grams of hexamminechromium(III) bromide, 2.4 g. of copper(II) sulfate penta-hydrate, 10 g. of sodium bromide, 20 ml. of water and 20 ml. of 48% hydrobromic acid were mixed and the mixture was occasionally stirred. After 1 hour the resulting black crystals were filtered off through a glass filter under strong suction, washed quickly with fuming hydrobromic acid (ca. 66%) and dried in vacuo over sulfuric acid.

Found: Cr, 9.0; N, 13.9; Cu, 9.6; Br, 65.1. Calcd. for $[Cr(NH_3)_6]CuBr_5$: Cr, 8.4; N, 13.6; Cu, 10.3; Br, 64.7%.

An attempt to prepare the corresponding cobalt compound was unsuccessful.

Absorption Spectrum Measurement.—The absorption spectrum of copper sulfate dissolved in 48% hydrobromic acid was measured with a Beckman spectrophotometer, model DU. The result is given in Fig. 1. The concentration of copper sulfate was 0.0000870 M and the extinction coefficient is expressed on the basis of g. ion of copper.

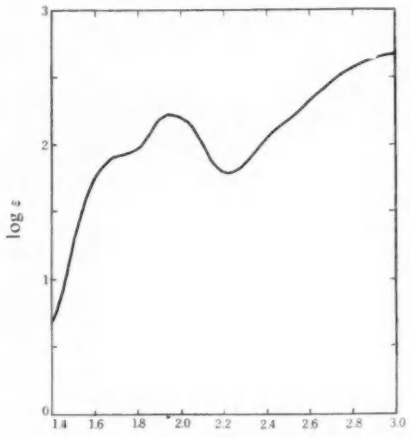

Fig. 1. Absorption spectrum of copper(II) sulfate in 48% hydrobromic acid.

Measurement of Magnetic Susceptibility.—Dr. Saburo Fujii* of the Tokyo Institute of Technology kindly measured the magnetic susceptibility of hexamminecobalt(III) chlorocuprate(I, II) by Weiss-Foex's zero point compensation method.

Results and Discussion

All the foregoing chlorocuprates crystallize in regular octahedra. As has been pointed out in the preceding section, the composition of the chlorocuprate(I, II) depends on the quantities of copper(I) and copper(II) chlorides used in the preparation (Table I). Observation under a microscope as well as with the naked eye shows that the color changes from sample to sample as the chemical composition changes, although it is uniform in a given sample. This fact indicates that the product is not a mixture of two chemical species, but a nearly uniform chemical compound whose composition can change continuously. As far as is known to the present author, this series of chlorocuprates form the only known typical ionic crystals consisting of well-defined cations and anions in which the valence control is possible.

From the total copper content given in Table I it will be seen that the atomic ratio of chromium to copper is 1:1 when more than a half of the total copper is bivalent, and that this ratio gradually decreases to the limiting value of 4:5 when the bivalent copper is less than a half. In this extreme case the product is a pure chlorocuprate(I) (samples No. 6 and No. 11 in Table I). The reason why compounds having such different chemical formulae belong to one series of compounds would be made clear only by a crystallographic investigation with X-rays. A research along this line is now in progress and the results will be published shortly.

An interesting phenomenon is observed when crystals of hexamminecobalt(III) chlorocuprate-(I, II) are digested in the mother liquor at 30~40°C for many hours. The crystals reach 0.1~1 mm. in size and often present a tortoise-shell appearance. The black or dark brown crystals are spotted with yellow transparent portions although the crystals as a whole are well developed octahedra. This may be explained as follows. By the oxidation of the mother liquor in the air the quantity of univalent copper therein is gradually decreased. The portions of the crystals that grow at later stages, therefore, have a poorer content of

4) G. R. Levi, *Atti Accad. Lincei*, (5) 32 I, 633 (1923).

* The present address: Toho Rayon Co., Ltd., Kitajima-cho, Itano-gun, Tokushima-ken.

univalent copper and consequently the interaction color is feeble in these portions.

Hexamminechromium(III) bromocuprate(II) is black in contrast to yellow chlorocuprate(II). This difference of color is probably due to the strong absorption band of bromocuprate(II) ion with a peak at 1.95×10^{4} cm^{-1} as is observed in the spectrum of copper(II) sulfate in hydrobromic acid in Fig. 1. An investigation of hexamminechromium(III) bromocuprate(II) may give some information about the ionic species to which this absorption band belongs.

Magnetic study on $[Co(NH_3)_6]_2Cu_2Cl_6(H_2O)_{1/2}$ showed, after a correction being made for the presence of diamagnetic groups, a magnetic moment of 1.9 Bohr magnetons per each formula unit. This value may be considered quite reasonable as the magnetic moment ascribed to the bivalent copper atom present in the crystals. The magnetic moment of the bivalent copper atom, therefore, seems to be little affected even when an interaction color is observed.

Summary

A series of dark-colored chlorocuprates(I, II) of hexamminechromium(III) and hexamminecobalt(III) have been prepared. The chemical composition and the color of these compounds have been found to change continuously with the composition of the mother liquor in which they were crystallized.

The author wishes to express his sincere thanks to Professor Yuichi Nakatsuka under whose kind guidance the present work was carried out. He is also grateful to Dr. Saburo Fujii for the magnetic measurement. A part of the expenses of the present study was defrayed by a grant-in-aid of the Ministry of Education.

Institute of Polytechnics
Osaka City University
Kita-ku, Osaka

Diffusion Coefficients for Amorphous Polymer and Water Systems

By Akira KISHIMOTO, Etsuji MAEKAWA and Hiroshi FUJITA

(Received December 29, 1959)

Recent studies of absorption and desorption of low-molecular-weight substances in amorphous polymers olids have demonstrated a sharp distinction between organic solvents and water. In systems of amorphous polymer + organic vapor the processes are of the Fickian type[1-4], usually with a diffusion coefficient which depends appreciably on penetrant concentration, when the systems are well above the glass transition temperatures, T_g, of respective polymers. At temperatures below T_g they exhibit various non-Fickian features[5-8]. No definite information has as yet been obtained about the behavior at temperatures slightly above T_g[9]. On the other hand, the processes of water are Fickian both above and below T_g, if in the latter region the system is not greatly removed from T_g[10]. In addition, the diffusion coefficients for amorphous polymer +water systems are practically independent of water concentration at any given temperature in the region mentioned above[10-13]. It is also reported that while the apparent activation energies, ΔH_d, for diffusion of organic solvents in amorphous polymers increase as the temperature is lowered toward T_g[3,4], the ΔH_d for aqueous systems are constant in the corresponding temperature region[10-12]. Furthermore, there are some experimental data[13] which show that plots of $\log D$ vs. $1/T$ for a water system

1) S. Prager and F. A. Long, *J. Am. Chem. Soc.*, **73**, 4072 (1951).
2) S. Prager, E. Bagley and F. A. Long, ibid., **75**, 1255 (1953).
3) M. J. Hayes and G. S. Park, *Trans. Faraday Soc.*, **51**, 1134 (1955).
H. Fujita, A. Kishimoto and K. Matsumoto, ibid. **56**, 438 (1960).
5) R. J. Kokes, F. A. Long and J. L. Hoard, *J. Chem. Phys.*, **20**, 1711 (1952).
6) F. A. Long and R. J. Kokes, *J. Am. Chem. Soc.*, **75**, 2232 (1953).
7) G. S. Park, *J. Polymer Sci.*, **11**, 97 (1953).
8) A. Kishimoto, H. Fujita, H. Odani, M. Kurata and M. Tamura, *J. Phys. Chem.*, **64**, 594 (1960).
9) A. Kishimoto and K. Matsumoto, ibid., **63**, 1529 (1959); A. Kishimoto and K. Matsumoto, unpublished results.
10) F. A. Long and L. J. Thompson, *J. Polymer Sci.*, **15**, 413 (1955).
11) A. M. Thomas, *J. Appl. Chem.*, **1**, 141 (1951).
12) F. Bueche, *J. Polymer Sci.*, **14**, 414 (1954).
13) K. Kawasaki and Y. Sekita, *J. Appl. Phys. Japan, (Oyo Butsuri Gakkaishi)*, **26**, 678 (1957).

are represented by two straight lines intersecting at T_g, where D is the mutual diffusion coefficient of the system and T is the absolute temperature. This implies that the ΔH_d of such a system changes discontinuously to another constant value when the temperature is lowered through T_g. These features suggest that the molecular mechanism responsible for the diffusion of water in amorphous polymers must be different from that for the diffusion of organic solvents in the same polymers. No adequate explanation has yet been presented concerning this problem.

In a recent publication[1] we have shown that the dependence on temperature and also on concentration of diffusion coefficients for systems of amorphous polymer + organic solvent above T_g can be interpreted quite satisfactorily in terms of a simple theory based on the free volume model of polymer network. One will find it natural that in view of this previous success we were interested in examining the extent to which our free volume theory can account for data of diffusion coefficients for polymer + water systems. One of the purposes of the study reported in this paper is to obtain experimental data pertinent to this problem. The other purpose is concerned with the re-examination of the previously reported variation of D for polymer + water systems with temperature. This arose from a close inspection of existing data and also from the prediction that if the free volume of the polymer network is the controlling factor for the diffusion of water, the linear relation between $\log D$ and $1/T$ should be only approximate.

Experimental

Materials.—Two amorphous polymers, polyvinyl acetate (PVAc) and polymethyl acrylate (PMA), were chosen for the present study. These were purified, unfractionated materials obtained from the Institute for Chemical Research, University of Kyoto. The number-average molecular weight of the PVAc, determined osmotically in a mixture of methanol (80) and ethanol (20) at 17°C, was 8.3×10^4. According to Naito[14], this is a thata solvent for PVAc. In fact, our osmotic measurements gave a second virial coefficient which was zero within the accuracy of the experiment. The films for sorption experiments were prepared in the same manner as described previously[15]. Their thicknesses were varied from 1.0×10^{-2} to 4.1×10^{-2} cm., depending upon the rate of absorption or desorption in respective cases.

The PMA used was identical to that used for obtaining the data reported in reference (4) and had a number-average molecular weight of 3.1×10^5 (determined osmotically in acetone at 25°C). Films of this polymer prepared for sorption measurements were 1.1×10^{-2} to 4.9×10^{-2} cm. thick.

Apparatus and Procedure.—Our sorption apparatus has been described previously[15]. Integral absorption from and integral desorption to zero pressure were measured for several external pressures of water vapor at a number of temperatures in the range 10 to 60°C for PMA and in the range 5 to 60°C for PVAc. In each experiment the temperature of the system was controlled to within ±0.1°C. According to the literature[16], the glass transition temperatures, T_g, of dry PMA and PVAc are about 3°C and about 28°C, respectively. Thus the present study for PVAc covered the temperature range both above and below T_g, and that for PMA treated the range above T_g only. Pressures of water vapor in the sorption tube were measured to ±1 mm. on a dioctyl phthalate manometer. This corresponded to an accuracy of ±0.07 mmHg. At every temperature studied, especially at temperatures below T_g, it was essential to use well-annealed specimens in order to obtain reproducible results.

For PVAc we performed steady-state permeation measurements at three temperatures, 10, 30 and 40°C, by using the cup method.

Results and Discussion

Diffusion Coefficients.—It was found that for both PVAc and PMA the equilibrium water concentrations, Q_∞ (grams of water sorbed per gram of dry polymer), at given relative humidities are independent of the temperature, over the ranges studied, within the accuracy of the present measurements. Those isotherm data are not shown here.

All the absorption and desorption data obtained were plotted in the form of Q_t/Q_∞ against $(t)^{1/2}$, where Q_t denotes the amount (in grams) of water absorbed or desorbed per gram of dry polymer for a time t from the start of a particular run. For all the external pressure and temperature measured, these plots had shapes expected from the normal Fickian diffusion mechanism. Furthermore, in each case, the absorption curve and the corresponding desorption curve coincided with each other over the entire range of time-scale of the experiment. According to theory[17], these features indicate that the mutual diffusion coefficient, D, of such a system should be independent of the penetrant concentration and may be evaluated from the initial slope, I, of the coincident absorption-desorption plot by means of the equation:

$$D=\pi I^2X^2/16 \qquad (1)$$

where X is the thickness of the sample film.

14) R. Naito, *Chem. High Polymers (Tokyo)* (*Kobunshi Kagaku*), **16**, 7 (1959).
15) H. Fujita and A. Kishimoto, *J. Polymer Sci.*, **28**, 547 (1958).
16) M. L. Williams, R. F. Landel and J. D. Ferry, *J. Am. Chem. Soc.*, **77**, 3701 (1955).
17) J. Crank, "The Mathematics of Diffusion", Oxford Univ. Press, Oxford (1956).

Fig. 1 illustrates how well a pair of absorption and desorption curves coincided with each other. The solid line in the figure represents the curve which has been calculated from the Fick diffusion equation by using for D the value determined by Eq. 1. A similar agreement between observed and calculated values was found for almost all the experimental data obtained. In Fig. 2 the values of D calculated by Eq. 1 from the data for the PVAc system are semi-logarithmically plotted against the equilibrium water concentration Q_∞. It is seen that the D values for each temperature are independent of Q_∞, and hence of the penetrant concentration, within errors of experiment. In the figure the filled circles give results from the steady-state permeation measurements. There are good agreements between the D values from the two different types of measurement at all temperatures where comparison can be made. It is of interest to note that this agreement was obtained even at 10°C, a tempetature about 20°C below T_g of PVAc. The indication from these results is that the diffusion of water into PVAc is controlled by the purely Fickian mechanism not only above T_g but also below T_g, provided that in the latter region the temperature is not too low from T_g. In this connection it is of significance to recall that the sorption processes of organic vapors in amorphous polymers generally exhibit marked deviations from the behavior expected from the normal Fickian mechanism when the systems are studied at temperatures below T_g of respective polymers.

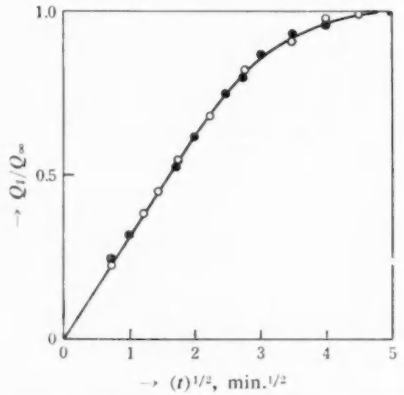

Fig. 1. Absorption and desorption curves for water in PMA. Water vapor pressure = 17.2 mmHg; thickness of film = 1.83×10^{-2} cm; temperature = 30°C; concentration of water at sorption equilibrium = 0.99×10^{-2} g./g. Open circles, absorption; filled circles, desorption; solid line, theoretical.

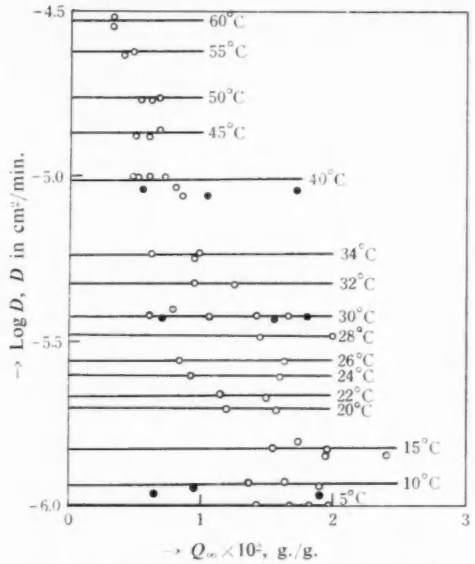

Fig. 2. Mutual diffusion coefficient vs. concentration relations on the system PVAc+water.
○ sorption studies;
● steady-state permeation studies.

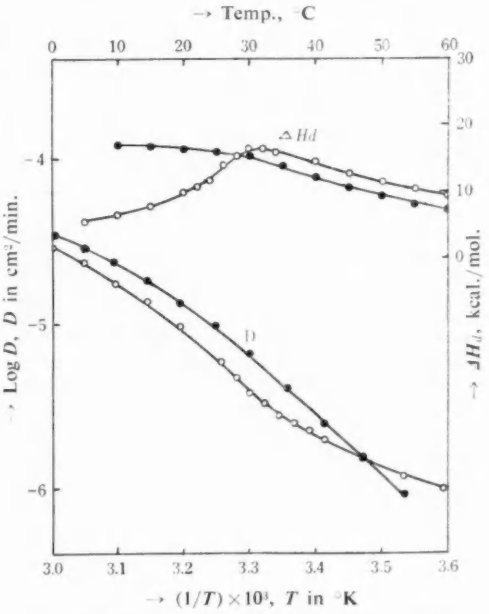

Fig. 3. Mutual diffusion coefficient vs. reciprocal absolute temperature (lower part); Apparent activation energies for diffusion, ΔH_d, vs. temperature (upper part).
○ PVAc; ● PMA.

The data for the PMA system were exactly similar to those for the PVAc system described above, although the behavior below T_g could not be studied on this polymer in the present work.

In Fig. 3 the values of D for the two systems are semi-logarithmically plotted against the reciprocal of absolute temperature T. First it will be seen that the plots for the two systems are not linear but curved. Of special interest is the inflection point which appeared on the plot for PVAc at a temperature near T_g of the polymer. Values of ΔH_d, the activation energy for diffusion of water in a polymer, were calculated from the smooth $\log D$ vs. $1/T$ curves drawn in Fig. 3, and are plotted against T in the upper part of the same figure. One finds that for both systems ΔH_d increases as the temperature is lowered toward T_g of respective polymers, and for PVAc it reaches a maximum at a temperature near T_g and then decreases gradually with further decrease in temperature. This appearance of a maximum ΔH_d is the reflection of the fact that the corresponding $\log D$ vs. $1/T$ plot has an inflection point. We wish to emphasize that this is the first experimental demonstration of a ΔH_d vs. T curve which goes through a maximum at a temperature in the vicinity of which the system undergoes glass transition. It should also be mentioned that our data for PVAc do not conform to the previous finding[13] for the system polymethyl methacrylate + water where the plots for $\log D$ vs. $1/T$ were represented by two straight lines intersecting at a temperature near T_g.

By employing the steady-state permeation method Meares[18,19] measured diffusion coefficients of several gases in PVAc and found that the slope of the plots for $\log D$ vs. $1/T$ showed distinct discontinuities at two temperatures, about 10°C apart from one another, in the region encompassing T_g of the polymer. Then he suggested that the glass transition of PVAc must take place over a range of temperature, rather than at a particular temperature. Although our PVAc data do not show any break in the temperature region studied, it appears that the occurrence of a broad maximum in ΔH_d has some correlation with Meares' suggestion on the "glass transition region". Recently, there are similar arguments from measurements of viscoelastic properties of dry polymers[20].

Comparison with Amorphous Polymer + Organic Solvent Systems.—Fig. 4 compares the temperature dependence of D_0 (the value of D at the limit of zero penetrant concentration) for systems PMA + ethyl acetate, PMA + methanol, and PMA + water. The data for the first two systems were taken from our previous publication[4]. The graph shows that with increasing molecular size as well as chemical affinity to PMA of the penetrant the values of $\log D_0$ at fixed temperatures decrease and their temperature dependence becomes more pronounced. This latter fact implies that more activation energy for diffusion into PMA is required at any given temperature (above T_g) for organic solvents than for water.

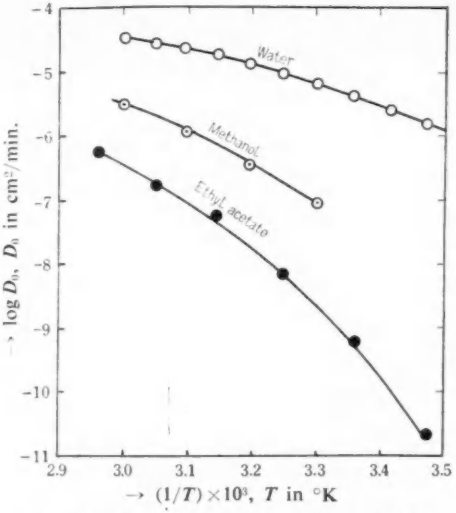

Fig. 4. Mutual diffusion coefficients at the limit of zero penetrant concentration as a function of reciprocal absolute temperature.

As noted in the introduction to this article, we have recently shown that the dependence on temperature and also on penetrant concentration of diffusions coefficients for amorphous polymer + organic solvent systems (above T_g of respective polymers) can be accounted for satisfactorily by a simple free volume theory[4]. According to this theory, the thermodynamic diffusion coefficient, $\mathfrak{D}_T$, of a penetrant in an amorphous polymer at a temperature T is represented by the equation:

$$\ln\ (\mathfrak{D}_T/\mathfrak{D}_0) = B_d\hat{\beta}'(T)/[f(T,0)^2 + \hat{\beta}'(T)f(T,0)v_1] \qquad (2)$$

Here $\mathfrak{D}_0$ is the value of $\mathfrak{D}_T$ at the limit of zero penetrant concentration, $f(T,0)$ is the average fractional free volume in the dry polymer at temperature T, v_1 is the volume fraction of the penetrant in the mixture, B_d is

18) P. Meares, *J. Am. Chem. Soc.*, **76**, 3415 (1957).
19) P. Meares, *Trans. Faraday Soc.*, **53**, 101 (1957).
20) e. g. T. Hideshima, *Sci. Pap. Inst. Phys. & Chem. Research (Tokyo)*, **53**, 36 (1959).

a constant characteristic of the system, and $\beta'(T)$ is a parameter representing the plasticizing effect of the penetrant. The value of $\mathfrak{D}_T$ can be calculated from D when the corrections for the volume expansion of the polymer by the addition of penetrant and for the thermodynamic non-ideality of the mixture are applied. The former correction can be made under the assumption that no volume change on mixing occurs and the latter correction may be derived from the analysis of the isotherm curve of the system.

We examined the applicability of Eq. 2 to the present data, by assigning to $\beta'(T)$ the values which we had previously deduced from measurements of stress-relaxation on these systems[15]. It was found that in order that Eq. 2 may fit the concentration dependence data obtained, the values of B_d have to be chosen as almost equal to zero for both PVAc and PMA systems. On the other hand, as shown previously[4], the constant B_d may also be determined from the ratio of ΔH_d to ΔH_v, where ΔH_v is the apparent activation energy for the steady-flow viscosity of the pure polymer. Comparison of the ΔH_d data given in Fig. 3 with the ΔH_v values calculated from the equation of Williams, Landel and Ferry[16] yielded $B_d = 0.16$ for PVAc and 0.25 for PMA. These B_d values are inconsistent with those derived above from the analysis of concentration dependence data, indicating that Eq. 2 is no longer applicable to the polymer+water systems investigated here. This result leads us to the conjecture that the amount of free volume must not be a major controlling factor for the diffusion of small molecules, such as water, through amorphous polymers. Previously we have inferred[4] that for penetrants very small in size and less soluble in the given polymer only a very local cooperation of the solid-like vibrations of two or three monomer units on the polymer chain would be sufficient to give a cross-section for the penetrant molecules to pass. This cooperative motion is so local that the probability of its occurrence, and hence the rate of diffusion of the penetrant molecule in the mixture, may be, in a first approximation, independent of how large the free volume in the mixture is. This will explain why the D values for the polymer+water systems studied did not exhibit measurable variation with water content. If the above is the case, then we would have to ascribe the observed temperature dependence of D for these systems to a temperature variation of solid-like vibration of monomer units, rather than to the temperature dependence of the free volume which is thought to be associated with larger-scale cooperative motions of several polymer segments.

We wish to thank Mr. Kinya Matsumoto of this Laboratory who carried out the steady-state permeation experiments on PVAc.

Physical Chemistry Laboratory
Department of Fisheries
University of Kyoto
Maizuru, Kyoto-fu

On the Assignment of a Band at 727 cm^{-1} in Polyethylene Terephthalate

By Akihisa MIYAKE

(Received December 17, 1959)

Some controversy surrounds the assignment of a strong band at 727 cm^{-1} in polyethylene terephthalate. It was first assigned to a C–O–C bending mode[1]. This assignment is now believed to be incorrect[2,3] because it seems much too high for a C–O–C bending mode. The most generally favored explanation is that the band arises from an aromatic C–H out-of-plane bending mode[4-6] and therefore that it is similar in origin to a band at 875 cm^{-1}. The removal of the band in question, on going from polyethylene terephthalate to polyethylene deuteroterephthalate[2,5], has been considered as strong evidence for this explanation. On the other hand, the present author has proposed an alternative interpretation that two bands at

1) R. G. J. Miller and H. A. Willis, *Trans. Faraday Soc.*, **49**, 433 (1953).
2) D. Grime and I. M. Ward, ibid., **54**, 959 (1958).
3) A. Miyake, *J. Polymer Sci.*, **38**, 497 (1959).
4) C. Y. Liang and S. Krimm, *J. Chem. Phys.*, **27**, 327 (1957).
5) W. W. Daniels and R. E. Kitson, *J. Polymer Sci.*, **33**, 161 (1958).
6) M. C. Tobin, *J. Phys. Chem.*, **61**, 1392 (954).

875 cm^{-1} and 727 cm^{-1} arise from coupled C–H out-of-plane bending and CO_2 out-of-plane bending vibrations[3].

This problem is of interest because the band mentioned above is in close relation with the so-called extra-bands[7] present in aromatic acids, esters, amides and nitro compounds, the origin of which has yet been unexplained. In order to ascertain whether the author's interpretation is correct or not, some additional observations have been carried out, infrared investigations of polyethylene terephthalate below NaCl region and examinations of thiol esters as model compounds.

Experimental

Material. — 1) *Polyethylene Terephthalate, Polyethylene-d_4 Terephthalate.*—The film samples used are the same as those used in previous researches[3,5].

2) *1,2-Ethanedithiol Dibenzoate.* — Benzoyl chloride (20 g.) was added dropwise with agitation to an ice-cooled solution of 1,2-ethanedithiol (7.5 g.) in pyridine (40 g.). The reaction mixture was allowed to stand overnight and poured into cold dilute sulfuric acid. The solid resulted was collected by filtration and washed successively with aqueous sodium carbonate and water. Repeated recrystallization from ethanol gave white crystals, m. p. 94.5°.

Found: C, 63.18; H, 4.61; O, 10.72. Calcd. for $C_{16}H_{14}O_2S_2$: C, 63.59; H, 4.64; O, 10.59%.

3) *1,2-Ethanedithiol Bis-(4-methoxycarbonylbenzoate).* — A solution of 4-methoxycarbonylbenzoyl chloride (10 g.) in chloroform (50 ml.) was added dropwise with agitation to an ice-cooled solution of 1,2-ethanedithiol (3 g.) in pyridine (40 g.). The reaction mixture, after standing overnight, was poured into cold dilute sulfuric acid with stirring. The solid product obtained as a suspension in the chloroform layer was recrystallized after the addition of ethanol. The resulting crystals were collected by filtration and washed with aqueous sodium hydroxide. Recrystallization from a mixture of ethanol and benzene (1 : 2) gave white crystals, m. p. 208~210°.

Found: C, 57.20; H, 4.35; O, 22.68. Calcd. for $C_{20}H_{18}O_6S_2$: C, 57.40; H, 4.33; O, 22.94%.

Infrared Spectra*. — The infrared spectra were obtained by means of Perkin-Elmer spectrometers model 21, 13 and 321 with NaCl, KBr and CsBr prisms respecively.

The polymer films were investigated in the KBr and CsBr regions. The two thiol esters were investigated in the NaCl and KBr regions as Nujol mulls and KBr disks. Dichroic measurements for the polymer were made in the KBr region on drawn films. Dichroic measurements for 1,2-ethanedithiol dibenzoate were made in the NaCl region on oriented crystal film obtained by differential cooling of a melt between rock-salt plates.

Results

Polyethylene Terephthalate.—Infrared spectra of polyethylene terephthalate and polyethylene-d_4 terephthalate in the range 10~32 μ are shown in Fig. 1. The frequencies of the bands observed below 750 cm^{-1} together with those reported by Tobin[6] are listed in Table I. Two bands at 575 and 422 cm^{-1} reported by Tobin were not observed though a band at 631 cm^{-1} which was reported as a weaker band than the above two was detected. None of the bands between 700~400 cm^{-1} showed perpendicular dichroism. Tentative assignments for some of the bands are given in the last column of Table I. The assignment of the CO_2 rocking vibrations is supported by the fact that corresponding bands are found in ethylene glycol dibenzoate (480 cm^{-1}) and 1,2-ethanedithiol bis-(4-methoxycarbonylbenzoate) (488 cm^{-1}) but not in 1,2-ethanedithiol dibenzoate.

Table I. Infrared frequencies (cm^{-1}) of polyethylene terephthalate

P. E. T.		P. E.-d_4. T.	Mode
Tobin	This work		
727(s) σ	727(s) σ	725(s) σ	
670(m)	680(w)		
628(w)[c]	631(w) π	631(w) π	aromatic vibration
575(m)			
508(s)[a] π	506(m)[c] π	502(m)[c] π	CO_2 rocking
500(s)[a]	500(m)[a]	530(m)[a]	
437(c) π	437(m)[c] π		C–C–O deformation
422(s)[a]			
382(s)[c]	379(s)[c]	364(s)[c]	C–O–C deformation

s: strong, m: medium, w: weak, a: amorphous band, c: crystalline band, σ: perpendicular dichroism, π: parallel dichroism.

7) M. Margoshes and V. A. Fassel, *Spectrochim. Acta*, 7, 14 (1955).
8) A. Miyake, *J. Polymer Sci.*, 38, 479 (1959).
* The author is indebted to Dr. Y. Mashiko et al. of the Government Chemical Industrial Research Institute, Tokyo, for the measurement in the CsBr region and to Dr. H. Tadokoro of Osaka University for the dichroic measurement for 1,2-ethanedithiol dibenzoate.

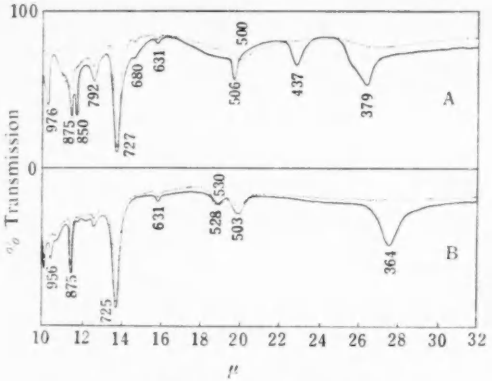

Fig. 1. Infrared spectra of polyethylene terephthalate (A) and polyethylene-d_4 terephthalate (B). ····· quenched sample; —— annealed sample.

Thiol Esters. — Infrared spectra of the two thiol esters in the NaCl region are shown in Fig. 2 together with that of ethylene glycol bis-(4-methoxycarbonylbenzoate) previously reported[2]. It is apparent that the strong band at 727 cm^{-1} observed in ethylene glycol bis-(4-methoxycarbonylbenzoate) disappears in 1,2-ethanedithiol bis-(4-methoxycarbonylbenzoate), while the bands at 1502, 1408 and 1021 cm^{-1} in the former which are attributable to the vibrations of *p*-phenylene group by analogy with polyethylene terephthalate[3] also appear in the latter at substantially the same frequencies (1502, 1403, and 1016 cm^{-1}). Most of the strong bands observed in the latter can be attributed to the ester or thiol ester groups (Table II). The bands which arise from the thiol ester group are easily identified by their distinguished intensities in 1,2-ethanedithiol dibenzoate. The assignments for the vibrations of the thiol ester group given in Table II are consistent with the results of dichroic measurement which will be described next.

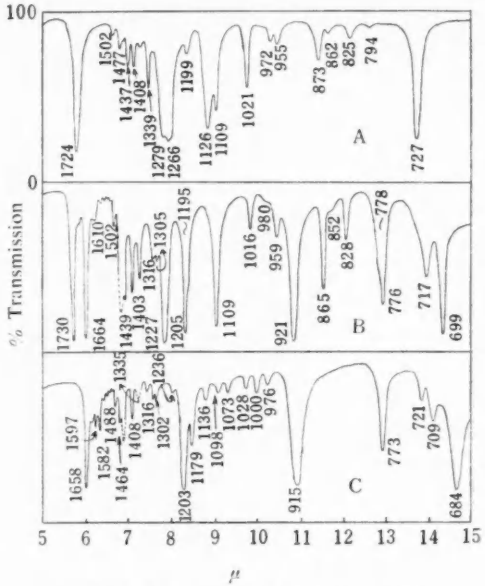

Fig. 2. Infrared spectra of ethylene glycol bis-(4-methoxycarbonylbenzoate) (A), 1,2-ethanedithiol bis-(4-methoxycarbonylbenzoate) (B) and 1,2-ethanedithiol dibenzoate (C).

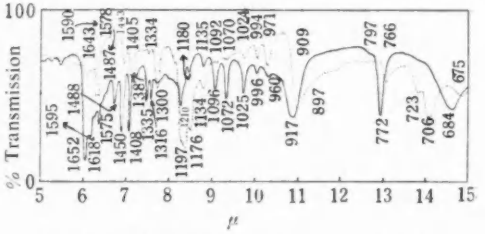

Fig. 3. Polarized infrared spectra of 1,2-ethanedithiol dibenzoate.

Dichroic Measurement for 1, 2-Ethanedithiol Dibenzoate. — Fig. 3 shows the spectra of an oriented crystalline film of 1,2-ethanedithiol dibenzoate. The solid curve was run with the polarizer setting so that the electric vector of the polarized beam was perpendicular to the direction of the crystal growth of the sample.

TABLE II. VIBRATION OF ESTER AND THIOL ESTER GROUPS (cm^{-1})

$(CH_3O_2CC_6H_4CO_2CH_2\text{-})_2$	$(CH_3O_2CC_6H_4COSCH_2\text{-})_2$	$(C_6H_5COSCH_2\text{-})_2$	Assignment
1724	1730		C=O stretching
	1664	1658	C=O stretching
1279, 1266	1277		C–O–C asym. stretching
	1205	1203	C–S–C asym. stretching
972	1109		C–O–C sym. stretching
	921	915	C–S–C sym. stretching
	776	773	COS out-of-plane bending
	717		CO_2 in-plane bending
	699	684	COS in-plane bending

The dotted curve was run with the sample in the same position but with the polarizer rotated 90° from the first position. The C=O stretching (1652 cm^{-1}) and C–S–C antisymmetric stretching (1197 cm^{-1}) bands whose assignments are certain, show perpendicular and parallel dichroisms respectively. Further, a band at 1450 cm^{-1} attributable to CH_2 bending vibrations shows perpendicular dichroism and a band at 1300 cm^{-1} attributable to CH_2 wagging vibrations shows parallel dichroism. From these facts, it follows that the chain CO–S–CH_2–CH_2–S–CO is essentially parallel to the direction of crystal growth. On the other hand, bands attributable to in-plane vibrations of the phenyl group by analogy with toluene and monodeutero benzene show perpendicular dichroism, while bands attributable to out-of-plane vibrations show parallel dichroism (Table III). This indicates that the plane of the phenyl group is approximately normal to the direction of crystal growth. Based on these results, the probable configuration and arrangement of the molecule** are shown in Fig. 4. The dichroisms observed for the three strong bands at 917, 772 and 684 cm^{-1} which were assigned, respectively, to the C–S–C symmetric stretching, COS out-of-plane bending, and COS in-plane bending vibrations are in agreement with those expected from the above arrangement.

TABLE III. VIBRATION OF PHENYL GROUP (cm^{-1})

Mode[a]		C_6H_5D[9]	$C_6H_5CH_3$[10]	$(C_6H_5COSCH_2-)_2$
In-plane	8 b	1574	1586	1575 (σ)
	19 a	1480	1483	1488 (σ)
	19 b	1450	1310	1316 (σ)
	15	1076	1070	1072 (σ)
	18 a	1031	1030	1025 (σ)
Out-of-plane	5	995	943	994 (π)
	17 a	970	(985)	971 (π)
	17 b	922	890	890 (π)
	10 b	850	730	723 (π)
	4	698	695	706 (π)

a) We owe the numbering of vibrational modes to Wilson [E. B. Wilson, Jr., *Phys. Rev.*, **45**, 706 (1934)].

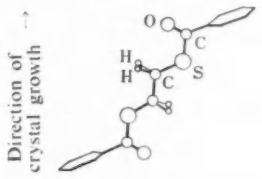

Fig. 4. Probable configuration of 1,2-ethane dithiol dibenzoate.

Discussion

Although a good deal of work has been done on the characteristic stretching frequencies of the ester group, no systematic study of the deformation frequencies has been carried out. Our knowledge of the factors influencing the frequency and intensity of the deformation vibrations is still relatively meager. Nevertheless, it is possible to predict the approximate position for some of them. Thompson and Torkington[11] have found two characteristic bands of fair intensities at about 600 cm^{-1} for acetates and propionates (612 and 640 cm^{-1} for acetates and 590 and 610 cm^{-1} for propionates). Later, Wilmshurst[12] has assigned the bands at 639 and 615 cm^{-1} in methyl acetate to CO_2 in-plane bending and CO_2 out-of-plane bending vibrations, respectively. In a number of α,β-unsaturated esters, Walton and Hughes[13] have found strong bands at 850~750 cm^{-1}, which have been reasonably assigned to the CO_2 out-of-plane vibration by their dichroic behaviors. A band of similar nature falls at 781 cm^{-1} in methyl oxalate[13]. In the light of these results, the CO_2 out-of-plane bending vibration of aromatic esters is reasonably expected to appear above 600 cm^{-1}.

In either polyethylene terephthalate or polyethylene-d_4 terephthalate, however, no band attributable to the CO_2 out-of-plane bending vibration is observed in the range 700~550 cm^{-1}. The bands at 680 and 631 cm^{-1} are too weak to be assigned to a CO_2 out-of-plane vibration, and moreover their dichroisms are inconsistent with that expected for an out-of-plane vibration. The polymer chain in a drawn sample of polyethylene terephthalate has been known to orient parallel to the direction of drawing[1,4,14] and hence an out-of-plane vibration is expected to exhibit perpendicular dichroism. Since the absorption bands above 750 cm^{-1} in this polymer have been assigned with fair certainty[3] to vibrations other than the CO_2 out-of-plane bending vibration, the only band left assignable to it is the strong and perpendicular band at 727 cm^{-1}.

There are three infrared-active out-of-plane

9) C. K. Ingold et al., *J. Chem. Soc.*, **1946**, 299, 316.
10) K. S. Pitzer and D. W. Scott, *J. Am. Chem. Soc.*, **65**, 817 (1943).
** The crystal structure of this compound is not known. It is assumed that all the molecules take the same arrangement with respect to the direction of crystal growth. Configurations obtained from that shown in Fig. 4 by rotating the S-CO bond are also possible, but this does not affect the following discussions.
11) H. W. Thompson and P. Torkington, *J. Chem. Soc.*, **1945**, 640.
12) J. K. Wilmshurst, *J. Mol. Spectroscopy*, **1**, 201 (1957).
13) W. L. Walton and R. B. Hughes, *J. Am. Chem. Soc.*, **79**, 3985 (1957).
14) W. J. Dulmage and A. L. Geddes, *J. Polymer Sci.*, **31**, 499 (1958).

TABLE IV. INFRARED-ACTIVE OUT-OF-PLANE VIBRATIONS (cm^{-1})

Mode	C_6H_6[15]	p-$C_6H_4D_2$[16]	p-$C_6H_2D_4$[16]	C_6D_6[15]	p-$C_6H_4(CH_3)_2$[16]
16 b	405	367	383	350	389
11	673	597	548	496	(170)
17 b	975	876	925	793	796

vibrations for p-disubstituted benzenes (point group V_h). Some authentic frequencies for these vibrations are listed in Table IV together with those of benzene. Based on these frequencies, modes 16b and 11 in polyethylene terephthalate can be reasonably assumed to appear below 500 cm^{-1}. Hence, the only aromatic out-of-plane vibration expected to appear above 700 cm^{-1} is the mode 17b. It is unlikely that both the perpendicular bands (875 and 727 cm^{-1}) observed in polyethylene terephthalate can be assigned to aromatic out-of-plane vibrations.

It thus seems logical to consider that the band at 727 cm^{-1} is related to the CO_2 out-of-plane bending vibration. It should be noted that similar bands called the extra bands[7] are found in aromatic esters, acids, amides, and nitro compounds, all of which have out-of-plane bending vibrations of the substituents.

The band at 727 cm^{-1}, however, cannot be described as a pure CO_2 out-of-plane bending vibration, because it is removed by the deuteration of terephthalic acid residue[2,3]. This removal can be explained by assuming that the CO_2 out-of-plane bending mode and the 17b mode referred to above couple between each other. These two modes are similar in their frequencies and symmetry types. Therefore it is very probable that the perpendicular band at 875 and 727 cm^{-1} in polyethylene terephthalate arise from these coupled vibrations. The assumption of the coupling between the CO_2 and aromatic C–H out-of-plane bending vibration can also explain the anomalous shift of the latter in certain aromatic esters[7]. For example, the appearance of two bands at 809 and 711 cm^{-1} in methyl benzoate[5] may be explained as a consequence of this coupling, considering that pure frequencies for phenyl C–H and ester CO_2 out-of-plane bending vibrations fall at 770~730 cm^{-1} and 800~750 cm^{-1}, respectively. Furthermore, similar anomalies of C–H out-of-plane bending frequencies in some α, β-unsaturated esters seem also to result from an analogous coupling. The ethylenic C–H out-of-plane bending frequencies of acrylates and methacrylates fall outside the normal range, while those of crotonates lie close to the normal range (Table V). Based on the assumption that the ethylenic C–H and ester CO_2 out-of-plane bending vibrations in crotonates are substantially free of coupling and hence that the frequency of a pure out-of-plane vibration of an ester group attached to an ethylenic bond falls at about 840 cm^{-1}, the shifts in acrylates and methacrylates can be easily explained as the result of coupling between the ethylenic C–H and ester CO_2 out-of-plane bending vibrations. The frequency difference between the two pure modes is about 50 cm^{-1} in acrylates and methacrylates, while it amounts to about 120 cm^{-1} in crotonates.

TABLE V. C–H AND CO_2 OUT-OF-PLANE BENDING FREQUENCIES (cm^{-1}) FOR α, β-UNSATURATED ESTERS

Compound	π(C–H)	π(CO_2)	Normal position[17] for π(C–H)
Crotonates[13]	982~970	842~833	970~960
Acrylates[13,15]	988~981 967~960	813~808	995~985 915~905
Methacrylates[13,15]	943~935	817~813	895~885

All these facts indicate the general occurrence of the coupling between CO_2 and C–H out-of-plane bending vibrations in aromatic esters. This coupling is, of course, destroyed when any one of the following conditions is not satisfied; first, similarity of frequencies of pure vibrations for the two modes, and second, coplanarity of the aromatic ring and the ester group.

1, 2-Ethanedithiol dibenzoate and 1, 2-ethanedithiol bis-(4-methoxycarbonylbenzoate) investigated in the present work provide further evidence for the interpretation developed above. As was shown in the section of experimental results, phenyl and thiol ester groups of the former compound are not present in the same plane, and hence no coupling is expected between the out-of-plane vibrations of the two groups. Therefore the perpendicular band at 773 cm^{-1} can be considered as an essentially pure COS out-of-plane bending vibration. Since the out-of-plane bending frequency of an ester group is expected not to be very different from that of a thiol ester group, the appearance of the latter at 773 cm^{-1} supports

15) F. A. Miller, *J. Chem. Phys.*, **24**, 996 (1956).
16) S. C. Carson, R. R. Gordon and C. K. Ingold, *J. Chem. Soc.*, **1946**, 288.
17) L. J. Bellamy, "The Infrared Spectra of Complex Molecules", 2nd Ed., Methuen, London (1958), p. 34.
18) W. H. T. Davison and G. R. Bates, *J. Chem. Soc.*, **1953**, 2607.

the assumption adopted in the foregoing discussion that a pure out-of-plane bending vibration of an aromatic ester group falls at about 800 cm^{-1}. The aromatic out-of-plane vibration of this compound (721 and 709 cm^{-1}) falls close to the normal positions for phenyl groups (see Table III). In ethylene glycol dibenzoate[8], however, three bands were observed at 804, 695 and 683 cm^{-1}, but no band was observed in the normal range (770~720 cm^{-1}) for the mode 10b. This difference between the thiol ester and the ester can be again explained by the coupling between the out-of-plane vibrations. If one assumes that the CO_2 vibration couples with phenyl vibration, the lowering of the phenyl out-of-plane frequency in ethylene glycol dibenzoate is readily explained.

Two bands at 873 and 727 cm^{-1} in ethylene glycol bis-(4-methoxycarbonylbenzoate) undoubtedly correspond to the two perpendicular bands at 875 and 727 cm^{-1} in polyethylene terephthalate. The latter disappears and the former shifts to 865 cm^{-1} on going from ethylene glycol bis-(4-methoxycarbonylbenzoate) to 1, 2-ethanedithiol bis-(4-methoxycarbonylbenzoate). This change seems also to be accounted for by assuming that the aromatic ring and thiol ester group in the latter are not coplanar. The C–H out-of-plane vibration of the *p*-phenylene group and the CO_2 out-of-plane vibrations of the two ester groups in the former compound couple amoung each other giving rise to two bands at 873 and 727 cm^{-1}. On the other hand, in the latter compound, at least the vibration of the thiol ester group may not be coupled with the aromatic vibration, and hence their frequencies are different from those of the former compound. It is not known whether the ester and *p*-phenylene groups in 1, 2-ethanedithiol bis-(4-methoxycarbonylbenzoate) are coplanar or not, but in any case the bands at 865 and 778 cm^{-1} (shoulder) are attributable to the out-of-plane vibrations of these two groups. It is difficult to explain the spectral difference between the two model compounds on the basis of assigning both the bands at 873 and 727 cm^{-1} cited above to aromatic out-of-plane vibrations.

In conclusion, the bands at 875 and 727 cm^{-1} in polyethylene terephthalate can be reasonably assigned to coupled vibrations of aromatic C–H and ester CO_2 out-of-plane bending modes which provide a consistent explanation for several aromatic esters and thiol esters.

Finally, mention should be made of the CO_2 in-plane bending frequency. Since this is expected not to be very different from that of the COS in-plane bending vibration, that band at 717 cm^{-1} in 1, 2-ethanedithiol bis-(4-methoxycarbonylbenzoate) can probably be assigned to this mode. It is possible that this vibration in polyethylene terephthalate lies buried under the band at 727 cm^{-1}.

Summary

Infrared spectra of polyethylene terephthalate and polyethylene-d_4 terephthalate were investigated in the KBr and CsBr regions. No band attributable to a CO_2 out-of-plane bending vibration was found below 700 cm^{-1}. The only band assignable to this mode is a strong and perpendicular band at 727 cm^{-1}. This fact together with the disappearance of the 727 cm^{-1} band in polyethylene deuteroterephthalate, indicates that two bands at 875 and 727 cm^{-1} in polyethylene terephthalate can be assigned to coupled vibrations of aromatic C–H and ester CO_2 out-of-plane bending modes. This interpretation provides a consistent explanation for the spectral differences between ethylene glycol dibenzoate and 1, 2-ethanedithiol dibenzoate and between ethylene glycol bis-(4-methoxycarbonylbenzoate) and 1, 2-ethanedithiol bis-(4-methoxycarbonylbenzoate) as well as for the anomalous shifts of C–H out-of-plane frequencies and the appearances of "extra bands" in several aromatic esters.

Central Research Laboratories
Toyo Rayon Co.
Otsu, Shiga

Note Added in Proof:

Recently, perpendicular bands at about 820 cm^{-1} have been found in polyethylene terephthalate-d_4 and polyethylene d_4 terephthalate-d_4 [C. Y. Liang and S. Krimm, *J. Mol. Spectroscopy*, **3**, 554 (1959).]. These bands can be assigned to the CO_2 out-of-plane vibration in these deuteroterephthalates. If this assingnment is correct, it seems better to consider that the 17b vibration of the terephthalates has a lower frequency than the CO_2 out-of-plane vibration. Then, for the band at 727 cm^{-1} in polyethylene terephthalate, the contribution of the 17b vibration may exceed that of the CO_2 vibration, and vice versa for the band at 875 cm^{-1}).

Application of the Theory of Regular Solutions to Binary Phase Equilibria. I. Method of Application to Binary Liquid Equilibria

By Kiyoharu ISHIDA

(Received January 7, 1960)

Accurate prediction of phase relationships over a wide range of temperatures from some data determined at several temperatures is difficult in general. It seems that if the theory of strictly regular solutions developed by Guggenheim[1] is applicable to mixtures for most binary systems, the behavior of solutions may be more satisfactorily interpreted by the theory than by the semi-empirical equations according to van Laar or Margules. However, exceedingly few systems satisfy all the conditions for forming regular mixtures in which the molecules are assumed to be sufficiently alike in size and shape to be interchangeable on a lattice or quasi-lattice.

The author has shown that the theory of regular solutions can apply to a much wider class of mixtures by assuming the formation of stable 'clusters' consisting of each component in its liquid phases[2]. This paper will be concerned with the derivation of the relationship between the compositions in two conjugate liquid phases on which the application of the theory of regular solutions is based and with the method of representing the solubility curves for most binary systems symmetrically. Detailed consideration referring to the estimation of interchange energy from mutual solubility data and its dependency upon temperature will be given in a subsequent paper.

1. Thermodynamic Aspects on the Coexistence Curve of Binary Liquid Mixtures

The rigorous thermodynamic equations of the form

$$\ln(a_{\mathrm{I}}/a_{\mathrm{II}}) = \ln(x_{\mathrm{I}}/x_{\mathrm{II}}) + \ln(\gamma_{\mathrm{I}}/\gamma_{\mathrm{II}}) \qquad (1,1)$$

are applicable to any binary mixtures, where a's, x's and γ's denote activities, mole fractions and activity coefficients of the component designated by subscripts I and II at a given temperature, respectively. (The pure component is taken as standard state). When the solution is separated into two liquid phases by the increase of the deviation from Raoult's law, designating the I-component rich phase by one prime and the II-component rich phase by two primes,

$$a_{\mathrm{I}}' = a_{\mathrm{I}}'', \; a_{\mathrm{II}}' = a_{\mathrm{II}}'' \text{ and } x_{\mathrm{I}}' = 1 - x_{\mathrm{II}}'.$$

It therefore follows

$$\ln\{(1-x_{\mathrm{II}}')/x_{\mathrm{II}}'\} - \ln\{(1-x_{\mathrm{II}}'')/x_{\mathrm{II}}''\} = \ln(\gamma_{\mathrm{I}}''\gamma_{\mathrm{II}}'/\gamma_{\mathrm{I}}'\gamma_{\mathrm{II}}'') \qquad (1,2)$$

In cases where mutual solubilities are not so great, both values of γ_{I}' and γ_{II}'' are near unity.

The temperature dependence of the activity coefficient can be related to the heat of mixing by the following equation

$$\frac{\mathrm{d}\ln\gamma_{\mathrm{I}}}{\mathrm{d}T} = -\frac{\Delta\bar{H}_{\mathrm{I}}}{RT^2} \qquad (1,3)$$

where $\Delta\bar{H}_{\mathrm{I}}$ is the partial molal heat of solution of component I, R the gas constant and T the absolute temperature. Then, Eq. 1,2 may be transformed into

$$\frac{\mathrm{d}\ln\{(1-x')/x'\}}{\mathrm{d}T} - \frac{\mathrm{d}\ln\{(1-x'')/x''\}}{\mathrm{d}T} = -\frac{\Delta H}{RT^2} \qquad (1,4)$$

where

$$\Delta H = \Delta\bar{H}_{\mathrm{I}}'' - \Delta\bar{H}_{\mathrm{II}}'' - (\Delta\bar{H}_{\mathrm{I}}' - \Delta\bar{H}_{\mathrm{II}}') \qquad (1,5)$$

In Eq. 1,4 x_{II} is represented as x for the sake of simplicity.

For most binary liquid mixtures with a few exceptions, it is observed that the solubilities of one component in one phase increase as the corresponding values in the other conjugate phase decrease with changing temperatures, and then the signs of $(\Delta\bar{H}_{\mathrm{I}}'' - \Delta\bar{H}_{\mathrm{II}}'')$ and $(\Delta\bar{H}_{\mathrm{I}}' - \Delta\bar{H}_{\mathrm{II}}')$ are opposite. The absolute values of these two quantities are equal in particular systems where the solubility curves are symmetrical with respect to the mole fraction as it is for a regular mixture. If the absolute value of the latter of these two quantities is m times the former and m is assumed to be independent of temperature, then

$$\Delta\bar{H}_{\mathrm{I}}' - \Delta\bar{H}_{\mathrm{II}}' = -m(\Delta\bar{H}_{\mathrm{I}}'' - \Delta\bar{H}_{\mathrm{II}}'') \qquad (1,6)$$

1) E. A. Guggenheim, "Mixtures", Oxford University Press, London (1952).
2) K. Ishida, *Nature*, **184**, 814 (1959).

Using these assumptions, Eq. 1,4 may be written in the form

$$\frac{\mathrm{d}\ln\{(1-x')/x'\}}{\mathrm{d}T} - \frac{\mathrm{d}\ln\{(1-x'')/x''\}}{\mathrm{d}T} = (1+m)\frac{\mathrm{d}\ln(\gamma_{\mathrm{I}}''/\gamma_{\mathrm{II}}'')}{\mathrm{d}T} \qquad (1,7)$$

In the following Eq. 1,8, which is obtained by setting the value of the first derivative of the molal free energy of mixing at a given temperature and pressure, $g(x)$, with respect to x equal to zero,

$$\ln(\gamma_{\mathrm{I}}/\gamma_{\mathrm{II}}) = -\ln\{(1-x)/x\} \qquad (1,8)$$

values of x represent the mole fractions of component II along the coexistence curve in cases of symmetrical systems. However, in cases of ordinary unsymmetrical systems, values of x do not represent the mole fractions along the consolute curve, but they represent those at the extreme values on the $g(x)$ curve in the neighborhood of the compositions in mutual equilibrium of two phases such as x' and x'', which are the two points of contact of the common tangent on the $g(x)$ curve. If the dependency of the logarithms of mole ratio of two components at the compositions in two coexisting phases upon temperature is assumed to be scarcely different from that at the compositions corresponding to the extreme values on the $g(x)$ curve, the following simple relation can be obtained

$$\ln\{(1-x')/x'\} = -m\ln\{(1-x'')/x''\} + B \qquad (1,9)$$

for the values of x' and x'' on the coexistence curves, where B is a constant independent of temperature.

As will be clear from Figs. 1—3* in which plots are made of the logarithms of the mole ratios of two components in one phase against the corresponding values in the other conjugate phase for several systems described in the literature, fair straight lines whose slopes are near minus unity are obtained from these plots over the considerably wide range of temperatures not only for systems with virtually symmetrical solubility curves, but also for systems with extremely unsymmetrical ones. Even for the systems showing the closed solubility curve, the linear relationships between the functions $\log\{(1-x')/x'\}$ and $\log\{(1-x'')/x''\}$ hold for temperatures within 30° of a critical solution temperature, T_c. This fact indicates that the value of m is near unity for most systems and the deviations due to two assumptions involved in the derivation of Eq. 1,9 from actual behavior of solutions are almost cancelled, and that when the logarithm of the mole ratio of two components in one phase increases with the change in temperature, the corresponding value in the other phase decreases in proportion to the increase of that in the former phase and the proportional factor is a constant over a wide range of temperature. It is clear that the form of Eq. 1,9 is independent of whether weight, mole or volume fractions are used for the unit of concentration.

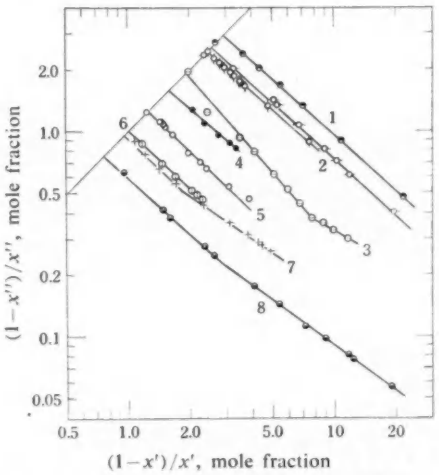

Fig. 1. Plot on double logarithmic coordinates of $(1-x'')/x''$ against $(1-x')/x'$.

No.	Symbol	Component I	Component II	Ref.
1	◓	Benzene—	Perfluoromethylcyclohexane	3
2	-○-	Carbon tetrachloride—	Perfluoromethylcyclohexane	3
	○	〃	〃	4
3	⊖	*n*-Butane—	Perfluoro-*n*-butane	5
4	●	Silicon tetrachloride—	Stannic iodide	6
5	○	Cyclohexane—	Aniline	7
6	①	Isooctane—	Stannic iodide	8
7	+	Cyclohexane—	Methanol	9
8	◒	*n*-Heptane—	Furfural	10

* Estimated values of the compositions in coexisting phases from solubility curves are also included as points in these figures.

3) J. H. Hildebrand and D. R. F. Cochran, *J. Am. Chem. Soc.*, **71**, 22 (1949).
4) B. H. Zimm, *J. Phys. & Colloid Chem.*, **54**, 1306 (1950).
5) J. H. Simons and J. W. Mansteller, *J. Chem. Phys.*, **20**, 1516 (1952).
6) J. H. Hildebrand and G. R. Negishi, *J. Am. Chem. Soc.*, **59**, 339 (1937).
7) D. Atack and O. K. Rice, *J. Chem. Phys.*, **22**, 382 (1954); *Disc. Faraday Soc.*, **15**, 210 (1953).
8) M. E. Dice and J. H. Hildebrand, *J. Am. Chem. Soc.*, **50**, 3023 (1928).
9) E. L. Eckfeldt and W. W. Lucasse, *J. Phys. Chem.*, **47**, 164 (1934).
10) E. N. Pennington and S. J. Marwil, *Ind. Eng. Chem.*, **45**, 1371 (1953).

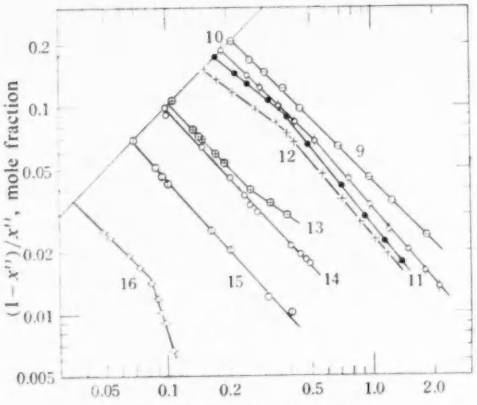

Fig. 2. Plot on double logarithmic coordinates of $(1-x'')/x''$ against $(1-x')/x'$.

No.	Symbol	Component I — II	Ref.
9	⊖	Ethylbenzene—Liquid ammonia	11
10	○	Mesitylene—Liquid ammonia	11
11	●	Propylbenzene—Liquid ammonia	11
12	+	1-Methylnaphthalene—Liquid ammonia	11
13	⊕	Methyldiethylamine—Water	12
14	○	Phenol—Water	13
15	ⓘ	2,6-Dimethylpyridine—Water	14
16	-○-	Palmitic acid—Liquid propane	15

It is reasonable that Eq. 1, 9 holds for temperatures within 30°C of a critical solution temperature for most binary liquid systems, since this formula is immediately derived from the empirical relations 1, 10 shown by Cox and Herington[14].

$$T-T_c=[A'\log\{(1-x')/x'\}+B']^3 \qquad (1,\ 10a)$$

$$T-T_c=[A''\log\{(1-x'')/x''\}+B'']^3 \qquad (1,\ 10b)$$

2. Method of Representing the Solubility Curve Symmetrically

At the critical solution temperature T_c, the two coexisting phases become identical having the composition $x'=x''=x_c$. Eq. 1, 9 may be transformed into

$$\frac{1-x'}{x'}\cdot\frac{x_c}{1-x_c}=\left[\frac{1-x''}{x''}\cdot\frac{x_c}{1-x_c}\right]^{-m} \qquad (2,\ 1)$$

11) K. Ishida, This Bulletin, **31**, 143 (1958).
12) J. L. Copp, *Trans. Faraday Soc.*, **51**, 1056 (1955).
13) A. E. Hill and W. M. Malisoff, *J. Am. Chem. Soc.*, **48**, 918 (1926).
14) J. D. Cox and E. F. G. Herington, *Trans. Faraday Soc.*, **52**, 926 (1956).
15) D. A. Drew and A. N. Hixson, *Trans. Am. Inst. Chem. Engrs.*, **40**, 675 (1944).

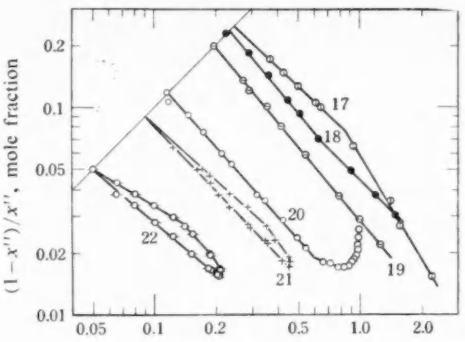

Fig. 3. Plot on double logarithmic coordinates of $(1-x'')/x''$ against $(1-x')/x'$.

No.	Symbol	Component I — II	Ref.
17	ⓘ	Octene—Liquid sulfur dioxide	16
18	●	*m*-Xylene—Liquid ammonia	11
19	⊖	Isopropylbenzene—Liquid ammonia	11
20	○	*n*-Butanol—Water	13
21	+	1-Propoxypropane-2-ol—Water	17
22	-○-	Ethylene glycol *n*-butyl ether—Water	18

It is possible to represent the solubility curve for a binary liquid system symmetrically with respect to the composition by plotting properly selected units. When the following units φ, which are the variation of volume fractions, are used for the concentrations, the resulting solubility curve will be symmetrical with respect to φ as for regular binary mixtures, since $\varphi'+\varphi''=1$.

$$\varphi'=\frac{x'/x_c}{x'/x_c+(1-x')/(1-x_c)}$$

$$\varphi''=\frac{(x''/x_c)^m}{(x''/x_c)^m+\{(1-x'')/(1-x_c)\}^m} \qquad (2,\ 2)$$

Therefore, the interchange energy w between two kinds of cluster may be obtained from the theory of regular solutions by assuming that each component forms clusters consisting of each component in its liquid phase, the number of moles being $(1-x')x_c$ and $x'(1-x_c)$ respectively, and that two kinds of cluster are stable and sufficiently alike in size and shape to satisfy all the conditions for forming strictly regular solutions on mixing[2]. In this case, by the definition of Eq. 2, 2 the molecular

16) W. F. Seyer and L. Hodnett, *J. Am. Chem. Soc.*, **58**, 996 (1936).
17) H. L. Cox, W. L. Nelson and L. H. Cretcher, ibid., **49**, 1080 (1927).
18) H. L. Cox and L. H. Cretcher, ibid., **48**, 451 (1926).

ratio, r', becomes

$$r'=\frac{1-\varphi'}{\varphi'}=\frac{1-x'}{x'}\cdot\frac{x_c}{1-x_c} \qquad (2,3)$$

Sometimes values of the interchange energy estimated from the compositions in one phase, x', differ a little from those estimated by the use of the compositions in the other phase, x'', since a constant m is not always exactly equal to unity as shown in Figs. 1—3. Of course, both values should coincide with each other when they are calculated by φ' and φ'' using the value of m estimated from the mutual solubility data determined at two temperatures by Eq. 1, 9, but calculations are considerably tedious.

It is convenient to introduce a variable x_k defined by

$$\frac{x_k}{1-x_k}=\left(\frac{x'}{1-x'}\cdot\frac{x''}{1-x''}\right)^{1/2} \qquad (2,4)$$

and to use the variable x_k instead of critical composition x_c setting the value of m equal to unity. Then,

$$\varphi'=\frac{\{x'/(1-x')\}^{1/2}}{\{x'/(1-x')\}^{1/2}+\{x''/(1-x'')\}^{1/2}}$$
$$=\frac{\{(1-x'')/x''\}^{1/2}}{\{(1-x')/x'\}^{1/2}+\{(1-x'')/x''\}^{1/2}}\equiv\varphi$$

and Eq. 2, 3 is replaced by Eq. 2, 6

$$r=\frac{1-\varphi}{\varphi}=\left(\frac{x''}{1-x''}\cdot\frac{1-x'}{x'}\right)^{1/2} \qquad (2,6)$$

Thus, by using x_k instead of x_c and putting $m=1$, the solubility curve can always be represented symmetrically with respect to φ and the molecular ratio and the interchange energy at a given temperature can be evaluated by simpler calculation.

The value of x_k may be dependent of the temperature and different from x_c to a certain extent when m is not unity, but x_k corresponds to x_c at the critical solution temperature. It may be easily proved by further algebraic arguments that there are straight line relationships between the functions $\log\{x_k/(1-x_k)\}$ and $\log\{x'/(1-x')\}$ and between the functions $\log\{x_k/(1-x_k)\}$ and $\log\{x''/(1-x'')\}$, and that x_c is given by the following equation

$$\log\frac{x_c}{1-x_c}=\left[\log\frac{1-x_2'}{x_2'}\log\frac{x_1''}{1-x_1''}-\log\frac{1-x_1'}{x_1'}\log\frac{x_2''}{1-x_2''}\right]\Big/\left[\log\left(\frac{x_1'}{1-x_1'}\cdot\frac{1-x_2'}{x_2'}\right)-\log\left(\frac{x_1''}{1-x_1''}\cdot\frac{1-x_2''}{x_2''}\right)\right] \qquad (2,7)$$

where subscripts 1 and 2 denote the values at temperatures T_1 and T_2, respectively.

Thus it should be possible to predict the solubility relationships of the system from mutual solubility data, determined at more than one temperature, when the dependence of the interchange energy estimated from mutual solubility data in terms of φ-fractions upon temperature is known.

Summary

The same expression for the correlation of compositions in mutual equilibrium of two liquid phases as that which is immediately obtained from the empirical relations used by Cox and Herington was derived thermodynamically. The method has been given in such a manner as to represent the solubility curve for a binary liquid system symmetrically and to estimate the interchange energy from the mutual solubility data by applying the theory of regular solutions.

The Chemical Research Institute of Non-Aqueous Solutions
Tohoku University
Katahira-cho, Sendai

Application of the Theory of Regular Solutions to Binary Phase Equilibria. II. Dependency of the Interchange Energy upon Temperature

By Kiyoharu ISHIDA

(Received January 7, 1960)

A few examples[1] have been shown for the comparison of the theories of strictly regular solutions with experiments, since there are few suitable systems for which measurements necessary to adequate comparison have been made. In cases of many systems in which mixtures of two components show so great deviations from Raoult's law that the solutions separate into two liquid phases, the solutions are generally formed from chemically dissimilar constituents which are different in molecular size, chemical structure, polarity and so on, these conditions being far from those for forming regular mixtures. It, therefore, was impossible that the comparisons of the theories with experimental results obtained for such mixtures with great deviations from ideal behavior were made in order to verify the validity of theories and to extend their application to the field of the chemical engineering design, but now the application of the theories of strictly regular solutions to most partially miscible liquid systems and the estimation of the interchange energy from the mutual solubility data have become possible as described in the previous paper[2]. It is interesting and desirable from a practical viewpoint to study what relations are obtained between the interchange energy or the co-operative energy and the temperature for such systems.

3. Theoretical Expressions for Estimating Co-operative Energy from Compositions in Two Coexisting Phases

It has been shown that the problem of the phase transition for the regular mixtures of two components is mathematically identical with that of the so-called Ising model of ferromagnetism and that there is an equivalent relation between the compositions in mutual equilibrium of two liquid phases and the intensity of spontaneous magnetization in the absence of a magnetic field[3,4]. No exact results for the three-dimensional problems are available at present that could be applied to phase equilibria, but exact closed form expressions of the free energy in the absence of a magnetic field[5], which corresponds to the theory of regular solutions with equal ratio of constituents, and of the spontaneous magnetization[6] are available for the two-dimensional model, particularly the square net, though it has been found that there is a marked difference in behavior between two- and more realistic three-dimensional model[7].

The intensity of spontaneous magnetization per spin at zero magnetic field for a two-dimensional ferromagnetic Ising square lattice is given by

$$I=\left[\frac{1+\zeta^2}{(1-\zeta^2)^2}\,(1-6\zeta^2+\zeta^4)^{1/2}\right]^{1/4} \quad \text{for } \zeta\leqq\sqrt{2}-1 \tag{3,1}$$

$$\zeta=\exp(-\varepsilon/\boldsymbol{k}T) \tag{3,2}$$

where ε is the interaction energy between each pair of nearest neighbor antiparallel spins assuming the interaction energy between pairs of parallel spins to be zero, and $\boldsymbol{k}$ is the Boltzmann constant.

By the correspondence of the theory of regular solutions to the Ising model, the interchange energy or one half of the energy increase of the whole system when a pair of two molecules of type I and a pair of two molecules of type II are converted into two pairs of a molecule of type I and a molecule of type II, w, will be obtained in terms of the mole fractions of component II in two coexisting phases, x, by the relation

$$\exp(w/\boldsymbol{k}T)=\left[\frac{1+[1+\{1-(1-2x)^8\}^{1/2}]^{1/2}}{\{1-(1-2x)^8\}^{1/4}}\right]^{-1} \tag{3,3}$$

for the square lattice. At the critical solution temperature,

1) E. A. Guggenheim, "Mixtures", Oxford Press, (1952).
2) K. Ishida, *Nature*, **184**, 814 (1959). See also the preceding paper.
3) R. Peierls, *Proc. Cambridge Phil. Soc.*, **32**, 477 (1936). G. F. Newell and E. W. Montroll, *Rev. Mod. Phys.*, **25**, 353 (1953).
4) C. Domb, *Proc. Roy. Soc.*, A **199**, 199 (1949).
5) L. Onsager, *Phys. Rev.*, **65**, 117 (1944).
6) C. N. Yang, ibid., **85**, 808 (1952).
7) C. Domb and M. F. Sykes, *Proc. Roy. Soc.*, A235, 247 (1956).

$$x=1/2, \qquad \exp(w/\boldsymbol{kT})_c=[1+\sqrt{2}]^4 \quad (3,4)$$

The information on the behavior of the model has been provided by exact series expansion of the partition function to any desired degree of accuracy[4,7-9]. In the rigorous expansion of the partition function by Bethe-Kirkwood's method of moments[8], the molar free energy of mixing in the notation used by Guggenheim[1] is given by

$$\frac{\Delta mF}{\boldsymbol{RT}}=(1-x)\ln(1-x)+x\ln x+x(1-x)\frac{w}{\boldsymbol{kT}}-\frac{z}{2}\left[\frac{l_2}{2!}\left(\frac{2w}{z\boldsymbol{kT}}\right)^2+\frac{l_3}{3!}\left(\frac{2w}{z\boldsymbol{kT}}\right)^3+\frac{l_4}{4!}\left(\frac{2w}{z\boldsymbol{kT}}\right)^4+\cdots\right] \quad (3,5)$$

where z is the coordination number and

$$l_2=x^2(1-x)^2 \quad (3,6)$$

$$l_3=x^2(1-x)^2(1-2x)^2 \quad (3,7)$$

$$l_4=x^2(1-x)^2(1-6x+6x^2)^2+6\left(\frac{y}{z}-1\right)x^4(1-x)^4 \quad (3,8)$$

$$l_5=x^2(1-x)^2(1-2x)^2(1-12x+12x^2)^2+60\left(\frac{y}{z}-1\right)x^4(1-x)^4(1-2x)^2 \quad (3,9)$$

$$l_6=x^2(1-x)^2\{1-60x(1-x)(1-2x)^2\}+30\left(13\frac{y}{z}+17\right)x^4(1-x)^4+120\left(\frac{\gamma_1}{z}-30\frac{y}{z}-28\right)x^5(1-x)^5+120\left(\frac{\gamma_2}{z}-4\frac{\gamma_1}{z}+66\frac{y}{z}+42\right)x^6(1-x)^6 \quad (3,10)$$

y, γ_1 and γ_2 are parameters depending on the lattice and defined by

$$y=\sum_{a'}z^2_{aa'}-z(z-1) \quad (3,11)$$

$$\gamma_1=\sum_{a'}z^3_{aa'}-3\sum_{a'}z^2_{aa'}+2z(z-1) \quad (3,12)$$

$$\gamma_2=\sum_{a}\sum_{a'}{}'z_{aa'}z_{a'a''}z_{a''a}-3(z-2)\sum_{a'}z^2_{aa'}+2z(z-1)(z-2) \quad (3,13)$$

where $z_{aa'}$ is another coordination number denoting the number of first neighbors common to the sites a and a'.

The compositions in two coexisting phases are given by the points where the value of the first derivative of the free energy of mixing is zero, owing to the symmetry of the solubility curve. To obtain the value of $w/\boldsymbol{kT}$ it is convenient to introduce an abbreviation u defined by

$$u=\ln\frac{1-x}{x}\Big/(1-2x) \quad (3,14)$$

Differentiating Eq. 3,5 with respect to x and setting $\mathrm{d}(\Delta_mF/\boldsymbol{RT})/\mathrm{d}x$ equal to zero, the expression for u/z as a power series in $2w/z\boldsymbol{kT}$ is obtained, which can be inverted into an expression for $2w/z\boldsymbol{kT}$ as a power series in u/z as follows:

$$\begin{aligned}\frac{w}{\boldsymbol{kT}}=u\Bigg[&1+x(1-x)\frac{2u}{z}+\frac{x(1-x)}{3}\left(\frac{2u}{z}\right)^2\\&+\frac{x(1-x)}{12}\left\{1+2x(1-x)+12x^2(1-x)^2\frac{y}{z}\right\}\left(\frac{2u}{z}\right)^3\\&+\frac{x(1-x)}{60}\left\{1+8x(1-x)+120x^2(1-x)^2(1-2x+2x^2)\frac{y}{z}\right\}\left(\frac{2u}{z}\right)^4\\&+\frac{x(1-x)}{360}\left\{1+22x(1-x)+4x^2(1-x)^2\left(4+195\frac{y}{z}\right)+30x^3(1-x)^3\left(10\frac{\gamma_1}{z}-104\frac{y}{z}\right)+360x^4(1-x)^4\left(\frac{\gamma_2}{z}-4\frac{\gamma_1}{z}+10\frac{y}{z}\right)\right\}\left(\frac{2u}{z}\right)^5+\cdots\cdots\Bigg]\end{aligned} \quad (3,15)$$

And

$$(w/\boldsymbol{kT})_c=2\left[1+\frac{1}{z}+\frac{4}{3}\frac{1}{z^2}+\left(2+\frac{y}{z}\right)\frac{1}{z^3}+\left(\frac{16}{5}+4\frac{y}{z}\right)\frac{1}{z^4}+\left(\frac{16}{3}+10\frac{y}{z}-\frac{2}{3}\frac{\gamma_1}{z}+\frac{\gamma_2}{z}\right)\frac{1}{z^5}+\cdots\cdots\right] \quad (3,16)$$

The evaluation of the series of coefficients is increasingly tedious and complicated as the series is ascended.

Since the series converges to the exact value extremely slowly, and the presence of a magnetic field, which corresponds to regular solutions of varying concentrations, is difficult to deal with by an exact method even in

8) J. G. Kirkwood, *J. Chem. Phys.*, **6**, 70 (1938); *J. Phys. Chem.*, **43**, 97 (1939); H. A. Bethe and J. G. Kirkwood, *J. Chem. Phys.*, **7**, 578 (1939); T. S. Chang, ibid., **9**, 169 (1941).

9) G. S. Rushbrooke, *Nuovo cimento*, **6**, (suppl. 2), 251 (1949); A. J. Wakefield, *Proc. Cambridge Phil. Soc.*, **47**, 419, 799 (1951); C. Domb, *Proc. Roy. Soc.*, **A196**, 36 (1949); J. E. Brooks and C. Domb, ibid., **A207**, 343 (1951); T. Tanaka, H. Katsumori and S. Toshima, *Prog. Theoret. Phys.*, **6**, 17 (1951); etc.

two-dimensions, several approximate solutions have been derived in closed form[1,10,11].

In the first (pairs) approximation[1] treated according to the quasi-chemical equilibrium conditions which is equivalent to Bethe approximation, w is given by

$$\exp(w/zkT)=(1-r)/(r^{1/z}-r^{(z-1)/z}) \qquad (3,17)$$

where r is the molecular ratio. At the critical solution temperature

$$\exp(w/zkT)_c=\frac{z}{z-2} \qquad (3,18)$$

In the zeroth approximation[1] which corresponds to the limiting form taken by the first approximation when the coordination number is made infinite, and is equivalent to Bragg-Williams approximation,

$$\frac{w}{kT}=\ln\frac{1-x}{x}\Big/(1-2x)=u \qquad (3,19)$$

Eq. 3,19 is only the first term in the Eq. 3,15 of rigorous series expansion. At the critical solution temperature

$$(w/kT)_c=2 \qquad (3,20)$$

Several methods which are capable of yielding successively higher approximations in the quasi-chemical method have been developed[1,10,12], but the use of a large group introduces troublesome calculations in practical applications of these higher approximations. In the higher approximation for the case of the simple square lattice with the tetrahedra as basic figure[1,10], which is the simplest case treated by the method of a logical extention to larger groups of the quasi-chemical approximation for pairs, the method being equivalent to an approximation developed by Kikuchi, w/kT is obtained from

$$\exp\left(\frac{w}{kT}\right)=\left[\frac{(\sqrt{r}+1)^2+\{(\sqrt{r}+1)^4+4r\}^{1/2}}{2\sqrt{r}}\right]^2 \qquad (3,21)$$

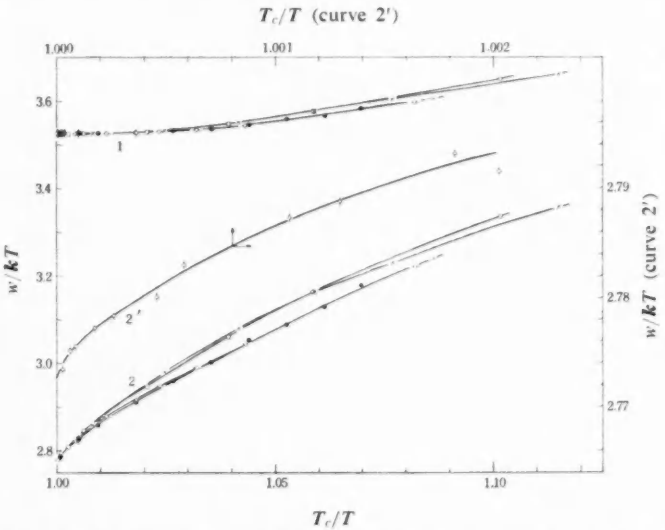

Fig. 4. Relations between w/kT and T_c/T for several systems. Values of w/kT along curve 1 are obtained from Eq. 3,3. Corresponding values along curves 2 and 2' are obtained from Eq. 3,17 assuming $z=4$.

Symbol	System	Ref.
○	Ethylbenzene—Liquid ammonia	13
-○-	Carbon tetrachloride—Perfluoromethylcyclohexane	14
◌	〃 — 〃	15
●	*n*-Butane—Perfluoro-*n*-butane	16
×	*n*-Hexane—Methanol	17

10) J. A. Barker, *Proc. Roy. Soc.*, **A216**, 45 (1953).
11) I. Prigogine, L. S. Mathot and L. van Hove, *Trans. Faraday Soc.*, **48**, 485 (1952).
12) Y. Y. Li, *Phys. Rev.*, **76**, 972 (1949); C. N. Yang, *J. Chem. Phys.*, **13**, 66 (1945).
13) K. Ishida, This Bulletin, **31**, 143 (1958).
14) J. H. Hildebrand and D. R. F. Cochran, *J. Am. Chem. Soc.*, **71**, 22 (1949).
15) B. H. Zimm, *J. Phys. & Colloid Chem.*, **54**, 1306 (1950).
16) J. H. Simons and J. W. Mansteller, *J. Chem. Phys.*, **20**, 1516 (1952).
17) "International Critical Tables", III, McGraw-Hill Book Company, Inc., New York (1928), p. 386.

At the critical solution temperature

$$\exp(w/kT)_c = (2+\sqrt{5})^2 \qquad (3,22)$$

When the value of w/kT is less than the value given by Eqs. 3, 4, 3, 16, 3, 18, 3, 20 or 3, 22, the separation into two liquid phases does not occur.

4. Dependency of w/kT upon Temperature

All formulae described in the above section contain the co-operative energy w in the form of the ratio w/kT or in particular $\exp(w/kT)$. It is convenient to compare the theories with the experiment, regarding either of these quantities as a single parameter whose value determines all the thermodynamic properties at a given temperature. Using φ defined by Eq. 2,5 in the preceding paper instead of x, similar results between the functions w/kT according to each theoretical formula and T_c/T were obtained from the mutual solubility data for most binary liquid systems described in the literature as shown in Fig. 4. Accordingly, it may be sufficiently shown by the results for some representative systems how values of w/kT are affected by such various theoretical

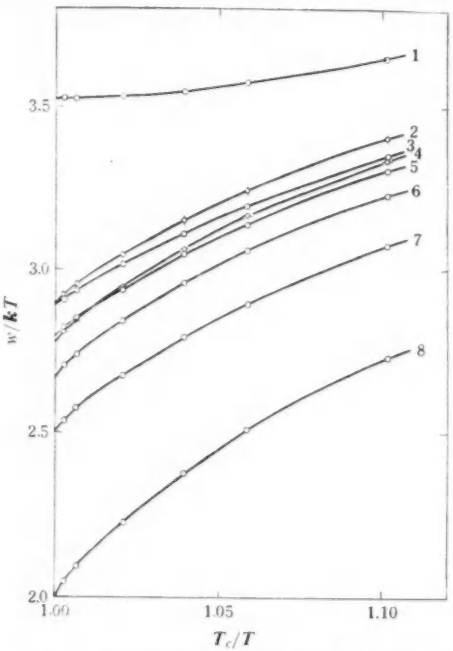

Fig. 5. Plot of values of w/kT obtained from several theoretical expressions against T_c/T for the system ethylbenzene—liquid ammonia.

Curve 1 is obtained from Eq. 3,3; curve 2 is obtained from Eq. 3,21; curve 3 is the expansion to terms of order $(2u/z)^4$ as given by Eq. 3,15 assuming $z=4$; curve 4 corresponds to Eq. 3,17 assuming $z=4$; curves 5, 6 and 7 are the expansions to terms of order $(2u/z)^3$, $(2u/z)^2$ and $(2u/z)$ as given by Eq. 3,15 assuming $z=4$, respectively; curve 8 is obtained from Eq. 3,19.

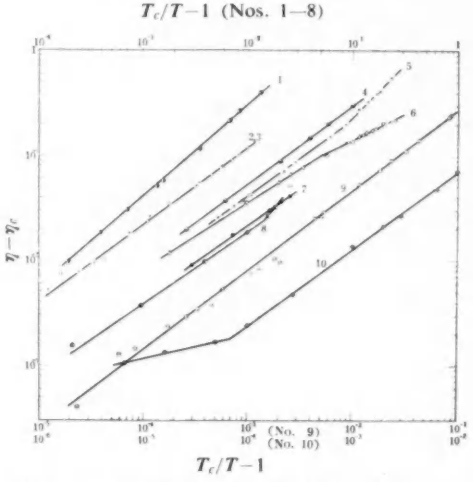

Fig. 6. Plot on logarithmic coordinates $\eta-\eta_c$ against $|T_c/T-1|$ for several systems.

No.	Symbol	System	Ref.
1	◑	Octene—Liquid sulfur dioxide	18
2	+	Methyldiethylamine—Water	19
3	○	Palmitic acid—Liquid propane	20
4	◒	Ethylbenzene—Liquid ammonia	13
5	×	*n*-Heptane—Furfural	21
6	⊙	Phenol—Water	22
	-⊙-	Phenol—Water	17
7	●	Isooctane—Stannic iodide	23
8	◐	Silicon tetrachloride—Stannic iodide	24
9	ⓘ	Carbon tetrachloride—Perfluoromethylcyclohexane	14
	⊖	Carbon tetrachloride—Perfluoromethylcyclohexane	15
10	⊕	Cyclohexane—Aniline	25

18) W. F. Seyer and L. Hodnett, *J. Am. Chem. Soc.*, **58**, 996 (1936).
19) J. L. Copp, *Trans. Faraday Soc.*, **51**, 1056 (1955).
20) D. A. Drew and A. N. Hixson, *Trans. Am. Inst. Chem. Engrs.*, **40**, 675 (1944).
21) E. N. Pennington and S. J. Marwil, *Ind. Eng. Chem.*, **45**, 1371 (1953).
22) A. E. Hill and W. M. Malisoff, *J. Am. Chem. Soc.*, **48**, 918 (1926).
23) M. E. Dice and J. H. Hildebrand, ibid., **50**, 3023 (1928).
24) J. H. Hildebrand and G. R. Negishi, ibid., **59**, 339 (1937).
25) D. Atack and O. K. Rice, *J. Chem. Phys.*, **22**, 382 (1954); Idem., *Disc. Faraday Soc.*, **15**, 210 (1953).

TABLE I. COMPARISON OF ESTIMATED VALUES FOR CRITICAL SOLUTION POINT WITH OBSERVED VALUES

System		T_1	T_2	Observed value		Eq. 2,7	Eq. 5,1	Eq. 1,10	Ref.
				T_c	x_c	x_c	ΔT_c	ΔT_c	
Component I	Component II	°C	°C	°C	Mole fraction	Mole fraction	°C	°C	
Cyclohexane	Methanol	31.30	39.05	45.14	0.507	0.537	0.46	1.18	26
Cyclohexane	Aniline	27.459	29.339	29.422	0.447	0.445	0.007	0.023	25
n-Heptane	Furfural	37.4	48.8	93.7	0.56	0.596	11.7	17.2	21
n-Butane	Perfluoro-*n*-butane	−53.2	−45.2	−41.0	0.37	0.365	0.5	1.0	16
Methyldiethylamine	Water*	51.28	50.52	49.42	0.902	0.922	0.10	−0.01	19
Carbon tetrachloride	Perfluoromethylcyclohexane	4.0	14.4	26.8	0.30	0.301	2.3	3.7	14
〃	〃	27.92	28.232	28.310	0.290	0.289	−0.010	0.000	15
Benzene	Perfluoromethylcyclohexane	61.1	81.6	85.3	0.27	0.255	1.3	1.8	14
Phenol	Water	25.0	35.0	65.85	0.910	0.924	−2.75	3.39	22
Octene	Liquid sulfur dioxide	−47.1	−32.8	−16.4	0.801	0·749	4.0	6.0	18
Butanol	Water	80.0	90.0	125.15	0.895	0.915	−4.23	4.64	17
Isooctane	Stannic iodide	185.4	191.6	195.4	0.501	0.506	0.2	0.6	23
Silicon tetrachloride	Stannic iodide	133.4	138.2	139.8	0.432	0.389	0.1	0.3	24
Cetylstearate	Liquid propane*	99.5	97.0	95.2	0.979	0.972	−0.4	−1.2	20
Palmitic acid	Liquid propane*	100.5	98.5	96.9	0.966	0.936	−0.2	−0.4	20
n-Hexane	Methanol	25.0	30.0	42.6	0.548	0.573	0.2	1.6	17
Ethylbenzene	Liquid ammonia	0.0	10.0	10.7	0.827	0.823	0.1	0.2	13
Isopropylbenzene	Liquid ammonia	0.0	10.0	20.0	0.835	0.839	1.9	3.0	13
Mesitylene	Liquid ammonia	0.0	20.0	33.9	0.841	0.826	3.6	5.4	13
1-Methylnaphthalene	Liquid ammonia	0.0	20.0	28.8	0.861	0.846	1.8	3.1	13
Aniline	Water	80.0	100.0	167.5	0.844	0.862	0.8	15.9	17

ΔT_c indicates the difference between observed and calculated values.
* These are systems which show a lower critical solution temperature.

expressions. Fig. 4. shows the relations between $w/\boldsymbol{kT}$ by Eqs. 3, 3 and 3, 17 in which z is assumed to be 4 and T_c/T for systems of ethylbenzene—liquid ammonia[13], carbon tetrachloride—perfluoromethylcyclohexane[14,15], *n*-butane—perfluoro-*n*-butane[16] and *n*-hexane—methanol[17]. Plots are made of values of $w/\boldsymbol{kT}$ obtained from formulae according to several approximations for square lattice against T_c/T for the system ethylbenzene—liquid ammonia in Fig. 5, compared with results obtained from Eq. 3, 3. As will be clear from these figures, simple uninflected curves convex downward are obtained by exact solution for the two dimensional model, while similar curves convex upward by several approximate solutions, and it is observed that w can be represented by neither a linear function of T nor a constant since no linear relationships are observed in these figures.

Inspection of literature data on partially miscible binary liquid systems reveals that $w/\boldsymbol{kT}$ is satisfactorily expressed by the following exponential functions

$$w/\boldsymbol{kT}-(w/\boldsymbol{kT})_c=K(|T_c/T-1|)^n \qquad (4,1)$$

where K and n are constants. When values of $|T_c/T-1|$ are small, using the abbreviation η for the quantity $\exp(w/z\boldsymbol{kT})$, this formula may be transformed into

$$\eta-\eta_c=K\eta_c(|T_c/T-1|)^n/z \qquad (4,2)$$

by expanding η/η_c in terms of $K(T_c/T-1)^n/z$ and neglecting higher than square.

Plots of $\log(\eta-\eta_c)$ against $\log(|T_c/T-1|)$ for several binary liquid systems are shown in Fig. 6 where values of η are evaluated from the mutual solubility data described in the literature according to Eqs. 3, 17 and 3, 18 assuming $z=4$. It will be seen from Fig. 6 that fair straight lines are obtained from these plots over a wide range of temperatures.

26) E. L. Eckfeldt and W. W. Lucasse, *J. Phys. Chem.*, 47, 164 (1943).

5. Prediction of the Critical Solution Temperature

It has been observed that the quasi-chemical approximation is considerably more accurate than the zeroth approximation and the results given by the first approximation differ little from those given by the higher approximations. Considering the possibility of the application of the theory of regular solutions to the vapor-liquid equilibria, it will be convenient at present to estimate $w/\boldsymbol{kT}$ by the Eqs. 3, 17 and 3, 18 according to the first approximation.

Since two empirical constants K and n, besides the critical solution temperature T_c, are involved in Eqs. 4, 1 or 4, 2, three pairs of data are required for the estimation of the critical solution temperature. However, it is observed in Fig. 6 that the average value of n for many systems is about 5/7 in the first approximation when z is assumed to be 4. When the approximate value of five seventh is used for n in Eq. 4, 2, it is possible to estimate the critical solution temperature and the solubility relationships at any other temperature from two pairs of the mutual solubility data.

In Table 1 are given critical compositions estimated by Eq. 2, 7 from the solubility data at temperatures T_1 and T_2 and critical solution temperatures calculated according to the expression

$$T_c=\frac{T_1T_2\{(\eta_1-\eta_c)^{7/5}-(\eta_2-\eta_c)^{7/5}\}}{T_1(\eta_1-\eta_c)^{7/5}-T_2(\eta_2-\eta_c)^{7/5}} \qquad (5,1)$$

which is derived from Eq. 4, 2 by the use of approximate value of five seventh for n and the notation of η_1 and η_2 for the respective values of $\exp(w/z\boldsymbol{kT})$ at temperatures T_1 and T_2, compared with experimental values and the calculated values of critical solution temperature according to Eq. 1, 10.

It will be seen that with few exceptions in which m in Eq. 1, 9 is not a constant over a wide range of temperatures, showing two straight lines having different slopes on plots of $\log\{(1-x')/x'\}$ against $\log\{(1-x'')/x''\}$ such as shown in Figs. 1—3 in the preceding paper, the agreement between the experimental and calculated values of T_c by Eq. 5, 1 is about as good as the experimental accuracy even though the approximation of $n=5/7$ is used, better than the results given by Eq. 1, 10 which has been proposed by Cox and Herington[27].

Summary

Theoretical expressions for estimating the interchange energy w were given in such form as to be obtained from the mutual solubility data. It has been found that the dependency of the interchange energy estimated from mutual solubility data in terms of φ-fractions upon temperature is satisfactorily expressed by the form of equations $w/\boldsymbol{kT}-(w/\boldsymbol{kT})_c=K(|T_c/T-1|)^n$. The method of predicting the critical solution point was described as an example of the application of the theory of regular solutions.

The Chemical Research Institute of Non-Aqueous Solutions
Tohoku University
Katahira-cho, Sendai

27) J. D. Cox and E. F. G. Herington, *Trans. Faraday Soc.*, 52, 926 (1956).

Normal Vibrations and Thermodynamic Properties of Chromium and Molybdenum Hexacarbonyls

By Kiyoyasu KAWAI and Hiromu MURATA

(Received December 4, 1959)

Hawkins, Mattraw, Sabol and Carpenter[1] have observed successfully infrared spectra of chromium and molybdenum hexacarbonyls in gaseous state and have made an attempt to obtain Raman spectra of molybdenum hexacarbonyl. Recently, Danti and Cotton[2] have reported Raman spectra of those and tungsten hexacarbonyls using chloroform as solvent. The molecular structure by electron diffraction has been reported by Brockway, Evens and Lister[3], and by X-ray diffraction by Rudorf and Fofmann[4], and it has been clear for the molecule to have O_h-symmetry. The assignments of the observed frequencies have been made by these investigators and the thermodynamic properties have been calculated by Hawkins, Mattraw, Sabor and Carpenter[1].

Out of thirteen fundamental vibrations resulting from the O_h-symmetry of the $M(XY)_6$ type of molecule only four fundamental vibrations are infrared active, and the lowest frequency of them, which has considerably great contribution to thermodynamic properties is out of the region of the observation by a usual spectrometer. In connection with the other metal carbonyls previously reported[5] and now proceeding*, the present paper** deals with a normal coordinate analysis for chromium and molybdenum hexacarbonyls to establish the more reliable assignments of vibrational frequencies and to compute the potential constants which may afford some information concerning the nature of the metal-carbonyl and carbonyl bonds in those compounds. The thermodynamic properties based on these assignments were calculated.

1) N. J. Hawkins, H. C. Mattraw, W. W. Sabol and D. R. Carpenter, *J. Chem. Phys.*, **23**, 2422 (1955).
2) A. Danti and F. A. Cotton, ibid., **28**, 736 (1958).
3) L. O. Brockway, R. V. G. Evens and M. W. Lister, *Trans. Faraday Soc.*, **34**, 1350 (1938).
4) W. Rudorf and U. Fofmann, *Z. physik Chem.*, **B28**, 351 (1935).
5) H. Murata and K. Kawai, *J. Chem. Phys.*, **26**, 1355 (1957); K. Kawai and H. Murata, *J. Chem. Soc. Japan, Pure Chem. Sec.* (*Nippon Kagaku Zasshi*), **78**, 496 (1957).
* A normal coordinate treatment of iron pentacarbonyl is being carried out in our laboratory. A part of the study has already been reported by H. Murata and K. Kawai, *J. Chem. Phys.*, **28**, 516 (1958).
** A part of this work has been reported by H. Murata and K. Kawai, *J. Chem. Phys.*, **27**, 605 (1957).

Normal Coordinate Treatment

The method of group theory shows that, as explained by Hawkins, Mattraw, Sabol and Carpenter[1], thirty-three normal modes of vibration of the octahedral $M(XY)_6$ type molecule are reduced to two of a_{1g}, two of e_g, one of f_{1g}, four of f_{1u}, two of f_{2g} and two of f_{2u}, and a_{1g}, e_g and f_{2g} species are active in Raman and f_{1u} species in infrared. The f_{1g} and f_{2u} species are inactive in both.

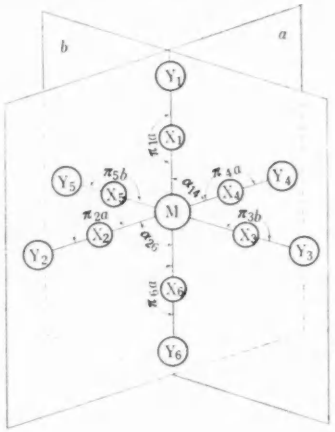

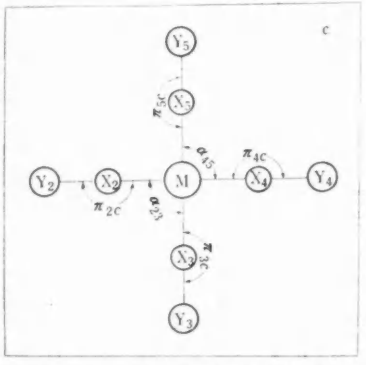

Fig. 1. Internal coordinates of $M(XY)_6$ molecule.

The general secular equation may be obtained by means of the Wilson's method[6]. The internal coordinates of $M(XY)_6$ molecule of this type are as follows:

$$d(M-X_i)=x_i \qquad d(X_i-Y_i)=y_i$$
$$\angle(M-X_i-Y_i)_{\text{lying in } j\text{th plane}}=\pi_{ij}$$
$$\angle(X_i-M-X_j)=\alpha_{ij}$$

Fig. 1 illustrates the above internal coordinates.

The symmetry coordinates were set up from these internal coordinates as follows:

For a_{1g} species:

$$R_1=1/\sqrt{6}\,(\Delta y_1+\Delta y_2+\Delta y_3+\Delta y_4+\Delta y_5+\Delta y_6)$$
$$R_2=1/\sqrt{6}\,(\Delta x_1+\Delta x_2+\Delta x_3+\Delta x_4+\Delta x_5+\Delta x_6)$$

For e_g species:

$$R_{3a}=1/\sqrt{12}(2\Delta y_1-\Delta y_2-\Delta y_3-\Delta y_4-\Delta y_5+2\Delta y_6)$$
$$R_{4a}=1/\sqrt{12}(2\Delta x_1-\Delta x_2-\Delta x_3-\Delta x_4-\Delta x_5+2\Delta x_6)$$

For f_{1g} species:

$$R_{5a}=1/2(\Delta\pi_{1a}-\Delta\pi_{2a}+\Delta\pi_{4a}-\Delta\pi_{6a})$$

For f_{1u} species:

$$R_{6a}=1/2(\Delta y_1+\Delta y_2-\Delta y_4-\Delta y_6)$$
$$R_{7a}=1/\sqrt{8}\,(\Delta\pi_{1a}+\Delta\pi_{2a}+\Delta\pi_{3b}-\Delta\pi_{3c}+\Delta\pi_{4a}+\Delta\pi_{5b}+\Delta\pi_{5c}+\Delta\pi_{6a})$$
$$R_{8a}=1/2(\Delta x_1+\Delta x_2-\Delta x_4-\Delta x_6)$$
$$R_{9a}=1/4(2\Delta\alpha_{12}+\Delta\alpha_{13}+\Delta\alpha_{15}+\Delta\alpha_{23}+\Delta\alpha_{25}-\Delta\alpha_{34}-\Delta\alpha_{36}-\Delta\alpha_{45}-\Delta\alpha_{56}-2\Delta\alpha_{46})$$

For f_{2g} species:

$$R_{10a}=1/2(\Delta\pi_{1a}+\Delta\pi_{2a}-\Delta\pi_{4a}-\Delta\pi_{6a})$$
$$R_{11a}=1/2(\Delta\alpha_{12}-\Delta\alpha_{14}-\Delta\alpha_{26}+\Delta\alpha_{46})$$

For f_{2u} species:

$$R_{12a}=1/\sqrt{8}\,(\Delta\pi_{1a}+\Delta\pi_{2a}-\Delta\pi_{3b}+\Delta\pi_{3c}+\Delta\pi_{4a}-\Delta\pi_{5b}-\Delta\pi_{5c}+\Delta\pi_{6a})$$
$$R_{13a}=1/4\,(2\Delta\alpha_{12}-\Delta\alpha_{13}-\Delta\alpha_{15}-\Delta\alpha_{23}-\Delta\alpha_{25}+\Delta\alpha_{34}+\Delta\alpha_{36}+\Delta\alpha_{45}+\Delta\alpha_{56}-2\Delta\alpha_{46})$$

Using the table of Decius[7] and for the M−X−Y bending the method by Ferigle and Meister[8] **G** matrices were evaluated. In therms of the abbreviations ρ and τ for reciprocal of the bond lengths x and y, respectively, and μ_M, μ_X and μ_Y for the reciprocals of the atomic masses, the following **G** matrix elements were obtained***:

For a_{1g} species:

$$\boldsymbol{G}_{11}=\mu_X+\mu_Y,\quad \boldsymbol{G}_{12}=-\mu_X,\quad \boldsymbol{G}_{22}=\mu_X$$

For e_g species:

$$\boldsymbol{G}_{33}=\boldsymbol{G}_{11}(a_{1g}),\quad \boldsymbol{G}_{34}=\boldsymbol{G}_{12}(a_{1g}),$$
$$\boldsymbol{G}_{44}=\boldsymbol{G}_{22}(a_{1g})$$

For f_{1g} species:

$$\boldsymbol{G}_{55}=(\rho+\tau)^2\mu_X+\tau^2\mu_Y$$

For f_{1u} species:

$$\boldsymbol{G}_{56}=\boldsymbol{G}_{11}(a_{1g}),\quad \boldsymbol{G}_{67}=\boldsymbol{G}_{69}=0,$$
$$\boldsymbol{G}_{68}=\boldsymbol{G}_{12}(a_{1g}),$$
$$\boldsymbol{G}_{77}=4\rho^2\mu_M+(\rho+\tau)^2\mu_X+\tau^2\mu_Y,$$
$$\boldsymbol{G}_{78}=\sqrt{8}\,\rho\mu_M,$$
$$\boldsymbol{G}_{79}=-\sqrt{2}\,\{4\rho^2\mu_M+(\rho^2+\rho\tau)\mu_X\},$$
$$\boldsymbol{G}_{88}=2\mu_M+\mu_X,\quad \boldsymbol{G}_{89}=-4\rho\mu_M,$$
$$\boldsymbol{G}_{99}=2\rho^2(4\mu_M+\mu_X)$$

For f_{2g} species:

$$\boldsymbol{G}_{1010}=\boldsymbol{G}_{55}(f_{1g}),$$
$$\boldsymbol{G}_{1011}=-2(\rho^2+\rho\tau)\mu_X,\quad \boldsymbol{G}_{1111}=4\rho^2\mu_X$$

For f_{2u} species:

$$\boldsymbol{G}_{1212}=\boldsymbol{G}_{55}(f_{1g}),$$
$$\boldsymbol{G}_{1213}=-\sqrt{2}\,(\rho^2+\rho\tau)\mu_X,$$
$$\boldsymbol{G}_{1313}=2\rho^2\mu_X$$

Following the method of Shimanouchi[9], the Urey-Bradley type quadratic potential energy function for octahedral $M(XY)_6$ molecule may be written as:

$$2V=\sum_{i=1}^{6}\{K(M-X)+2[F(X\cdots X)+F'(X\cdots X)]\}(\Delta x_i)^2+\sum_{i=1}^{6}K(X-Y)(\Delta y_i)^2+\sum_{i<j=1}^{6}\{H(X-M-X)+1/2[F(X\cdots X)-F'(X\cdots X)]\}(x_0\Delta\alpha_{ij})^2+\sum_{i=1}^{6}\sum_{l=a}^{c}H(M-X-Y)(\sqrt{x_0y_0}\Delta\pi_{il})^2+2\sum_{i<j=1}^{6}1/2[F(X\cdots X)$$

6) E. B. Wilson, Jr., *J. Chem. Phys.*, **7**, 1047 (1939), **9**, 76 (1941).
7) J. C. Decius, ibid., **16**, 1025 (1948).
8) S. M. Ferigle and A. G. Meister, ibid., **19**, 982 (1951).

*** There is one misprint in the **G** matrix elements presented by H. Murata and K. Kawai, *J. Chem. Phys.*, **26**, 605 (1957), *viz* $\boldsymbol{G}_{34}$ in f_{1u} species which corresponds to $\boldsymbol{G}_{79}$ of this paper.
9) T. Shimanouchi, *J. Chem. Phys.*, **17**, 245, 734, 848 (1949).

$$-F'(X\cdots X)](\Delta x_i)(\Delta x_j)$$
$$-2\sum_{i<j}^{6}1/2[F(X\cdots X)$$
$$+F'(Y\cdots X)](\Delta x_i)(x_0\Delta\alpha_{ij})$$
$$-2\sum_{i=j=k-1}^{6}1/(2x_0^2)\kappa(x_0\Delta\alpha_{ij})(x_0\Delta\alpha_{ik})$$

where x_0 and y_0 are the equilibrium M−X and X−Y bond distances respectively; K, H, F and F' are the potential constants and κ the intramolecular tension whose definition and physical meaning were expressed by Shimanouchi[9].

The intra-molecular tension for the octahedral MX_6 type molecule can easily be derived from the following relation obtained for the octahedral geometrical structure

$$\Sigma(\Delta\alpha_{ij})+1/2\Sigma(\Delta\alpha_{ij})(\Delta\alpha_{ik})=0$$

where the first summation extends for all of the twelve angles and the second for all the forty-eight sets of adjacent angles.

The potential energy matrix elements evaluated from the above potential function are as follows:

For a_{1g} species:

$$\boldsymbol{F}_{11}=K(X-Y),\quad \boldsymbol{F}_{12}=0,$$
$$\boldsymbol{F}_{22}=K(M-X)+4F(X\cdots X)$$

For e_g species:

$$\boldsymbol{F}_{33}=\boldsymbol{F}_{11}(a_{1g}),\quad \boldsymbol{F}_{34}=0,$$
$$\boldsymbol{F}_{44}=K(M-X)+0.7F(X\cdots X)$$

For f_{1g} species:

$$\boldsymbol{F}_{55}=x_0y_0H(M-X-Y)$$

For f_{1u} species:

$$\boldsymbol{F}_{66}=\boldsymbol{F}_{11}(a_{1g}),\quad \boldsymbol{F}_{77}=\boldsymbol{F}_{55}(f_{1g}),$$
$$\boldsymbol{F}_{88}=K(M-X)+1.8F(X\cdots X),$$
$$\boldsymbol{F}_{89}=0.9x_0F(X\cdots X),$$
$$\boldsymbol{F}_{99}=x_0^2[H(X-M-X)+0.55F(X\cdots X)]+\kappa,$$
$$\boldsymbol{F}_{67}=\boldsymbol{F}_{68}=\boldsymbol{F}_{69}=\boldsymbol{F}_{78}=\boldsymbol{F}_{79}=0$$

For f_{2g} species:

$$\boldsymbol{F}_{1010}=\boldsymbol{F}_{55}(f_{1g}),\quad \boldsymbol{F}_{1011}=0,$$
$$\boldsymbol{F}_{1111}=x_0^2[H(X-M-X)+0.55F(X\cdots X)]$$

For f_{2u} species:

$$\boldsymbol{F}_{1212}=\boldsymbol{F}_{55}(f_{1g}),\quad \boldsymbol{F}_{1213}=0,$$
$$\boldsymbol{F}_{1313}=x_0^2[H(X-M-X)+0.55F(X\cdots X)]-\kappa$$

In the above elements it was assumed experimentally that $F'=-1/10F$, and consequently six potential constants are used here.

TABLE I. MOLECULAR CONSTANTS FOR $Cr(CO)_6$ AND $Mo(CO)_6$[a]

Bond	$Cr(CO)_6$	$Mo(CO)_6$
M[b]—C	1.92 Å	2.08 Å
C—O	1.16 Å	1.15 Å

Symmetry number……24 for all fundamentals

a From Ref. 3.
b M denotes Cr or Mo.

TABLE II. POTENTIAL CONSTANTS FOR $Cr(CO)_6$ AND $Mo(CO)_6$ (mdyn./Å)

Type	$Cr(CO)_6$	$Mo(CO)_6$
K(C—O)	16.2	16.02
K(M—C)	1.83	1.77
H(M—C—O)	0.41	0.34
H(C—M—C)	0.03	0.02
F(C···C)	0.15	0.12
$\kappa(MC_6)$	0.02 Å^2	0.02 Å^2

TABLE III. COMPARISON OF OBSERVED AND CALCULATED FUNDAMENTALS FOR $Cr(CO)_6$ AND $Mo(CO)_6$

Assignment			$Cr(CO)_6$		$Mo(CO)_6$	
Type	Fundamental	Description	Calc.	Obs.	Calc.	Obs.
a_{1g}:	σ_1	ν(C—O)	2042	2108	2037	2131
	σ_2	ν(M—C)	374	393	361	379
e_g:	σ_3	ν(C—O)	2031	2019	2029	2022
	σ_4	ν(M—C)	336	373	329	334
f_{1g}:	σ_5	δ(M—C—O)	564	539	524	477
f_{1u}:	σ_6	ν(C—O)	1992[c]	2000	1992[c]	2000
	σ_7	δ(M—C—O)	636	661	560	595
	σ_8	ν(M—C)	475	436	422	368
	σ_9	δ(C—M—C)	113	102	95	80
f_{2g}:	σ_{10}	δ(M—C—O)	608	598[b]	560	557[b]
	σ_{11}	δ(C—M—C)	111	90	101	80
f_{2u}:	σ_{12}	δ(M—C—O)	586	570[b]	541	517[b]
	σ_{13}	δ(C—M—C)	81	80	72	70

a Obtained from the values of the **L** matrix elements.
b Inferred from combination or overtone bands.
c Obtained by the method of high-frequency separation.

To evaluate numerically the above elements, the bond lengths listed in Table I and the atomic masses on a physical scale were used.

Discussion

A comparison of the normal frequencies calculated from the set of potential constants in Table II with those observed by Hawkins, Mattraw, Sabol and Carpenter[1] are summarized in Table III. The numbering of the frequencies is the same as that used by Hawkins et al.[1]

The agreement between the calculated and the observed frequencies is satisfactory except for the M—C—O bending vibrations. The present results from the Urey-Bradley type potential function in which all the M—C—O bending interaction constants are not included indicated that 213 and 310 cm^{-1} bands assigned to σ_{10} and σ_{12} respectively by Hawkins, Matraw, Sabol and Carpenter[1] and 137.1 cm^{-1} band to σ_{10} by Danti and Cotton[2] for chromium hexacarbonyl and 230 and 327 cm^{-1} bands by the former[1] and 135.7 cm^{-1} band by the latter[2] for molybdenum hexacarbonyl are too small for M—C—O bending vibrational frequencies. Based on this point of view, all of the observed bands by Hawkins, Matraw, Sabol and Carpenter[1] except for only three strong bands which may be designated as fundamentals, were reassigned as shown in Table IV for chromium hexacarbonyl and Table V for molybdenum hexacarbonyl.

In order to obtain better agreement with the observed frequencies of a_{1g} and e_g species some other sets of values of diagonal terms in **F** matrix were used, but as long as proper values with physical meaning were used the calculated values were not close to the observed ones. This, therefore, may suggest that the

Table IV. Infrared bands of gaseous $Cr(CO)_6$

Frequency (cm^{-1})	Intensity	Assignment	Calc. (cm^{-1})
4098	m	$\sigma_1+\sigma_6$	4108
4000	m	$\sigma_3+\sigma_6$	4019
2688	w	$\sigma_3+\sigma_7$	2680
2554	w	$\sigma_1+\sigma_8$, $\sigma_5+\sigma_6$	2544, 2539
2466	m	$\sigma_3+\sigma_8$	2455
2393	s	$\sigma_2+\sigma_6$	2393
2336	sh	q	
2212	w	$\sigma_1+\sigma_9$	2210
2174	w	q	
2121	s	$\sigma_3+\sigma_9$	2121
2090	s	$\sigma_6+\sigma_{11}$, $\sigma_3+\sigma_{13}$	2090, 2099
2033	sh	q	
2000	vs	σ_6	
1970	sh	q	
1912	m	$\sigma_3+\sigma_9$, $\sigma_6+\sigma_{11}$	1917, 1910
1631	w	$\sigma_6+\sigma_4$	1627
1196	s	$\sigma_5+\sigma_7$	1200
1055	sh	$\sigma_2+\sigma_7$	1054
1032	s	$\sigma_4+\sigma_7$, $\sigma_8+\sigma_{10}$	1034, 1034
963	m	$\sigma_5+\sigma_9$	975
875	s	q	
811	s	$\sigma_4+\sigma_9$	809
755	m	$\sigma_7+\sigma_{11}$	751
673	sh	$\sigma_{10}+\sigma_{13}$	678
661	vs	σ_7	
635	s (sh)	$\sigma_5+\sigma_9$	641
595	sh	q	
522	mb	$\sigma_5+\sigma_{11}$, $\sigma_{10}-\sigma_{13}$	526, 518
513	mb	$\sigma_{10}-\sigma_{13}$, $\sigma_2+\sigma_9$	518, 495
477	mb	$\sigma_4+\sigma_9$, $\sigma_{12}-\sigma_{11}$	475, 480
465	wb	q	
449	wb	$\sigma_4+\sigma_{13}$	453
436	s	σ_8	

vs Very strong; s Strong; m Medium; w Weak; b Broad; sh Shoulder; q More than binary combination or questionable band.

Table V. Infrared bands of gaseous $Mo(CO)_6$

Frequency (cm^{-1})	Intensity	Assignment	Calc. (cm^{-1})
4150	m	$\sigma_1+\sigma_6$	4131
4050	m	$\sigma_3+\sigma_6$	4022
2600	w	$\sigma_3+\sigma_7$	2617
2480	w	$\sigma_1+\sigma_8$, $\sigma_5+\sigma_6$	2499, 2477
2380	s	$\sigma_3+\sigma_8$, $\sigma_2+\sigma_6$	2390, 2379
2330	w	$\sigma_4+\sigma_6$	2334
2210	m	$\sigma_1+\sigma_9$	2211
2115	s	$\sigma_3+\sigma_9$	2102
2085	s	$\sigma_6+\sigma_{11}$, $\sigma_3+\sigma_{13}$	2080, 2092
2000	vs	σ_6	
1985	sh	q	
1955	m (sh)	$\sigma_3-\sigma_{13}$	1952
1925	m (sh)	$\sigma_6-\sigma_{11}$	1920
1650	w	$\sigma_3-\sigma_8$	1654
1615	w	$\sigma_6-\sigma_2$	1621
1070	s	$\sigma_5+\rho_7$, $\sigma_{10}+\sigma_{12}$	1072, 1074
980	s	$\sigma_2+\sigma_7$	974
927	s	$\sigma_4+\sigma_7$, $\sigma_8+\sigma_{10}$	929, 925
905	w	q	
845	s	$\sigma_5+\sigma_8$, $\sigma_4+\sigma_{12}$	845, 851
740	m	$\sigma_2+\sigma_8$	747
705	m	$\sigma_4+\sigma_8$	702
670	m	$\sigma_7+\sigma_{11}$	675
661	w	q	
595	vs	σ_7	
563	s	$\sigma_5+\sigma_9$	557
386	s	σ_8	

vs Very strong; s Strong; m Medium; w Weak; b Broad; sh Shoulder; q More than binary combination or questionable band.

TABLE VI. L MATRICES FOR $Cr(CO)_6$

		Q_1	Q_2	Q_3	Q_4	Q_7	Q_8	Q_9	Q_{10}	Q_{11}	Q_{12}	Q_{13}
a_{1g}:	R_1	0.381	0.017									
	R_2	−0.226	0.187									
e_g:	R_3			0.380	0.012							
	R_4			−0.224	0.169							
f_{1u}:	R_7					0.453	−0.113	0.028				
	R_8					0.120	0.242	−0.007				
	R_9					−0.258	−0.029	0.128				
f_{2g}:	R_{10}								0.452	0.034		
	R_{11}								−0.274	0.123		
f_{2u}:	R_{12}										0.453	0.017
	R_{13}										−0·191	0.094

TABLE VII. L MATRICES FOR $Mo(CO)_6$

		Q_1	Q_2	Q_3	Q_4	Q_7	Q_8	Q_9	Q_{10}	Q_{11}	Q_{12}	Q_{13}
a_{1g}:	R_1	0.382	0.015									
	R_2	−0.225	0.180									
e_g:	R_3			0.382	0.012							
	R_4			−0.224	0.182							
f_{1u}:	R_7					0.451	−0.044	−0.021				
	R_8					0.054	0.229	0.008				
	R_9					−0.021	−0.034	0.110				
f_{2g}:	R_{10}								0.445	0.031		
	R_{11}								−0.251	0.118		
f_{2u}:	R_{12}										0.446	0.016
	R_{13}										−0.175	0.090

TABLE VIII. HEAT CONTENT, FREE ENERGY, AND HEAT CAPACITY OF $Cr(CO)_6$ AND $Mo(CO)_6$ FOR THE IDEAL GASEOUS STATE AT 1 ATOMOS PRESSURE (cal. deg^{-1} mol^{-1})

	$Cr(CO)_6$				$MO(CO)_6$			
T(°K)	$(H^0-E_0^0)/T$	$-(F^0-E_0^0)/T$	S^0	C_p^0	$(H^0-E_0^0)/T$	$-(F-E_0^0)/T$	S^0	C_p^0
273.15	28.99	78.68	107.67	45.01	30.77	82.65	113.42	48.24
298.15	30.48	81.16	111.64	46.94	32.28	85.43	117.71	49.08
300	30.58	81.35	111.93	47.06	32.38	85.65	118.00	49.20
400	35.52	90.76	126.28	52.65	37.25	95.63	132.88	54.17
600	42.48	106.49	148.97	59.20	43.95	112.12	156.07	60.00
800	47.24	119.34	166.58	63.26	48.49	125.45	173.94	63.74
1000	50.73	130.36	181.09	65.98	51.78	136.77	188.55	66.28

interaction terms between X−Y and M−X or X−Y stretching internal coordinates in the Urey-Bradley type potential function are not negligibly small.

Though, as explained above, there are contained a few quetionable points and the limits of error are uncertain, we may be allowed to conclude that the assignments in Table III and the potential constants in Table II are reasonable.

As the carbon-oxygen stretching potential constant K(C−O), that of nickel carbonyl[5], 16.02 mdyn./Å, was employed. For this selection the metal-carbon stretching potential constants K(M−X) were obtained to be 1.83 and 1.77 mdyn./Å for chromium and molybdenum hexacarbonyls respectively. These metal-carbon stretching potential constants are a little smaller than that of nickel carbonyl[5], 2.12 mdyn./Å, and this fact is in agreement with the study by Giacometti[10] who suggested that the shortening of chromium-carbon bond is smaller than that of nickel-carbon bond in the metal carbonyls. The values of the metal-carbon stretching potential constant, although many authors[10,11] have discussed the evidence of partial double bond caracter in such coordination compounds of various symmetry as these metal carbonyls, are nearly equal to those of Si—C and Cr—Cl bonds of tetramethylsilane[12] and chromyl

10) G. Giacometti, ibid., 23, 2068 (1955).
11) See e. g., L. Pauling, "The Nature of the Chemical Bond", Cornell University Press. Ithaca. New York (1939), p. 251.
12) K. Shimizu and H. Murata, private communication.

chloride[13] (2.72 and 2.56 mdyn./Å respectively), which are considered as single bonds.

The **L** matrices, whose components give the transformation from normal to symmetry coordinates, were calculated and listed in Table VI for chromium hexacarbonyl and Table VII for molybdenum hexacarbonyl.

Thermodynamic Properties

The heat content, free energy, entropy and heat capacity at constant pressure were calculated for seven temperatures from 273.15 to 1000°K in the rigid rotator-harmonic oscillator approximation using the probable values of the observed wave numbers listed in Table III. The molecular constants used in these computation and the symmetry number are given in Table I, while Table VIII lists the thermodynamic properties.

The authors express their sincere appreciation to Professor R. Tsuchida of Osaka University for helpful suggestions and valuable advice.

Osaka Municipal
Technical Research Institute
Kita-ku, Osaka

13) H. Stammreich, K. Kawai and Y. Tavares, *Spectrochim. Acta*, **1959**, 438.

SHORT COMMUNICATIONS

*Glumamycin, A New Peptide-type Antibiotic**

By Michitaka INOUE, Hiroshi HITOMI, Komei MIZUNO, Masahiko FUJINO, Akira MIYAKE, Koiti NAKAZAWA, Motoo SHIBATA and Toshihiko KANZAKI

(Received May 13, 1960)

A Streptomyces strain isolated in March, 1954 from a sample collected in Osaka Prefecture resembled the Zaomycin producing strain, S. zaomyceticus[1], in morphological and cultural characteristics and the utilization of carbon source, and therefore it was named S. zaomyceticus No. 7548 tentatively. The strain, when cultivated on a medium containing 3.0% of starch, 1.0% of polypepton, 0.2% of potassium phosphate 0.3% of soybean oil, and 2.0% of rice bran for 96 hr., produced an antibiotic, but the potency lowered abruptly thereafter.

The antibiotic inhibited the growth of Gram-positive bacteria such as Micrococcus aureus 209p and B. subtilis and was especially active against the bacteria resistant to known antibiotics. Although this antibiotic was similar to Amphomycin[2,3], Zaomycin[1] and Crystallomycin[4,5], it differed from them clearly. The authors, having found it to be a new antibiotic, named it Glumamycin and investigated its constituents.

The antibiotic was isolated pure from the broth by Craig's counter current distribution method 300 plates; chloroform- methanol-0.02 N hydrochloric acid (2:2:1), and it gave only one spot in paper chromatography and paper ionophoresis at various pH's. M. p. 230°C (decomp.). Found: C, 51.71; H, 7.20; N, 12.99%. From its dissociation constant, the molecular weight was estimated to be about 1800. The antibiotic had its isoelectric point at pH 3.4, and though it showed the typical infrared-spectrum characteristic of peptides, it exhibited no peculiar absorption in the ultraviolet-region.

The antibiotic was not hydrolized by any hydrolyrase such as pepsin, trypsin and carboxypeptidase, but it was completely hydrolized by heating with 6 N hydrochloric acid at 110°C for 20 hr. When the hydrolysate was subjected to two dimensional paper chromatography *n*-butanol-acetic acid-water (4:1:5) or 80% phenol containing 0.5 N ammonia, six amino acids were detected, four of which were aspartic acid, glycine, valine and proline and the other were unknown. Of the two unknown amino acids, one was a basic amino acid differing from lysine, histidine and arginine on paper chromatogram, and the other was a neutral amino acid which was characterized by a violet blue color with ninhydrin and a blue color with isatin. The six amino acids were separated from each other in crystalline form when chromatographed first on ion-exchange resin (IR-4B, Dowex 50×8) and then on cellulose powder.

After recrystallization from 75% methanol, the unknown basic amino acid showed m. p. 202°C (decomp.), $[\alpha]_D^{22}=+16°$ (c, 1:H_2O), Pk <2, 6.6, 9.6, and gave the values of 1.0 mol. of C-CH_3 (Kuhn-Roth) and 1.8 mol. of amino nitrogen (Van Slyke), and it was different from authentic α,γ-diaminobutyric acid on paper chromatogram. From these facts it was presumed to be α,β-diaminobutyric acid. On the other hand, the unknown neutral amino acid, when recrystallized from methanol·ether, melted at 240°C (decomp.), showed $[\alpha]_D^{21}=+10°$ (c, 1:H_2O) and accorded with $C_6H_{11}O_2N$·HCl, but no amino nitrogen (Van Slyke) and C-CH_3 (Kuhn-Roth) were detected. This compound was in complete agreement with synthetic DL-pipecolic acid in paper chromatography with various solvent systems, and the optical rotations of its hydrochloride and tartarate were $[\alpha]_D^{25}=+10°$ (c, 1:H_2O) and $[\alpha]_D^{25}=+20°$ (c, 1:H_2O), respectively. As the sign of optical activity of the neutral amino acid was opposite to that of the natural pipecolic acid it belongs to the D-series; the aspartic acid, valine, and proline derived from the antibiotic belong to the L-series.

The hydrolysate mentioned before contained about 10% of a substance soluble in ether, which was found to ba a monobasic unsaturated fatty acid, b. p. 139°C (1 mmHg), $[\alpha]_D^{21}=+4°$

* Presented at the 119th Monthyl Meeting of Japan Antibiotic Association, March 25, 1960.

1) Y. Hinuma, *J. Antibiotics*, ser. A **7**, 134 (1954).
2) B. Heinemann, M. A. Kaplan, et al., *Antib. & Chemoth.*, **3**, 1239 (1953).
3) G. Giolitti, G. Corti et al., *Giorn. Microbiol.*, **3**, 70 (1957).
4) G. F. Game et al., *Antibiotiki*, **2**, (6) 14 (1957).
5) N. N. Lomakina and M. G. Branzhnikova, *Biokhimiya* **24**, 425 (1959).

(c, 1 : C_2H_5OH), $C_{13}H_{24}O_2$. Oxidation of the substance with ozone afforded a compound $C_9H_{18}O_2$, b. p. 154°C (25 mmHg), $[\alpha]_D^{21} = +12°$ (c. 1 : C_2H_5OH), and from this and other results, a 4-isotridecenoic acid structure, $C_8H_{17}CH=CHC_2H_4COOH$, was assigned to the unsaturated fatty acid.

Thus Glumamycin was assumed to be composed of 4-isotridecenoic acid, L-aspartic acid, glycine, L-valine, L-proline, D-pipecolic acid, and α, β-diaminobutyric acid combined through peptide linkages. Full details of this work will be reported shortly.

The authors are grateful to Dr. Satoru Kuwada, Dr. Kikiti Sato and Dr. Sueo Tatsuoka for their guidance and encouragement in this work.

Research Laboratories, Takeda Pharmaceutical Industries, Ltd.
Juso, Higashiyodogawa-ku, Osaka
(M.I., H.H., K.M., M.F. and A.M.)
Institute for Fermentation
Juso, Higashiyodogawa-ku, Osaka
(K. N., M. S. and T. K.)

Eine Neue Synthese des cis- und trans D, L-Desmethylmuscarins

Von Takeshi MATSUMOTO
und Akitami ICHIHARA

(Eingegangen am 4. Juni, 1960)

In früheren Mitteilungen[1,2] haben wir die Synthese und pharmakologische Wirkung von stereoisomeren Muscarinen beschrieben. Hier soll nun über die Synthese der einfacher gebauten Desmethylmuscarine berichtet werden. Zu ihrer Herstellung haben wir die Reaktionsfolge, die bei der Durcharbeitung der Muscarinsynthesen erprobt wurde, übertragen.

Als Ausgangsmaterial bot sich Allylmalonsäure-äthylester (I). Durch Hydroxylierung dieses Esters mittels Perameisensäure und darauf folgende Ammonolyse wurde Dihydroxydiamid (II)[3] erhalten. Das letztere wurde dann nach der bekannten Methode von W. Traube[3] über Bromlacton (III) in Tetrahydrofurandicarbonsäure (IV) übergeführt. Erhitzte man die wässrige Lösung von Dicarbonsäure (IV) auf 150～160°C, so entstanden erwartungsgemäss zwei stereoisomere Monocarbonsäuren (V) (α, Schmp. 143.5°C, Ber. C 45.45 H 6.10 Gef. C 45.59 H 5.99%; β, Schmp. 129°C, Ber. C 45.45 H 6.10 Gef. C 45.50 H 6.10, die sich durch Chromatographie an Alumina-Säule

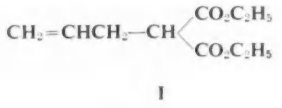

I

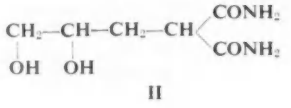

II

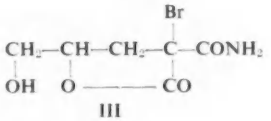

III

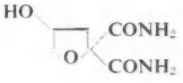

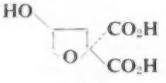

IV

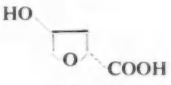

V

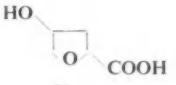

V

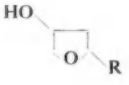

VI α R = ···CO_2CH_3
β R = —CO_2CH_3

VII α R = ···$CON(CH_3)_2$
β R = —$CON(CH_3)_2$

VIII α R = ···$CH_2N(CH_3)_2$
β R = —$CH_2N(CH_3)_2$

IX α R = ···$CH_2\overset{+}{N}(CH_3)_3\ I^-$
β R = —$CH_2\overset{+}{N}(CH_3)_3\ I^-$

1) T. Matsumoto und H. Maekawa, *Angew. Chem.*, **70** 507, (1958).

2) T. Matsumoto und A. Ichihara, *Biochem. Z.*, **331**, 580 (1959).

3) W. Traube, *Ber.*, **37**, 4540 (1904).

trennen liessen, in Mengenverhältnisse von um 1 : 1. Veresterung dieser beiden Säuren mittels Diazomethans ergab Methylester (VI) (α, Sdp. 115°C/7 Torr. IR. 3410 (OH) 1735 ($-COOCH_3$) 1075 cm^{-1} (tetrahydrofuran) ohne Lösungsmittel; β, Sdp. 110°C/7 Torr. IR. 3420 (OH) 1740 ($COOCH_3$) 1080 cm^{-1} (Tetrahydrofuran) ohne Lösungsmittel), die mittels Dimethylamin in Dimethylamide VII (α, IR. 3400 (OH) 1635 ($CONMe_2$) 1077 cm^{-1} (Tetrahydrofuran) ohne Lösungsmittel; β, IR. 3400 (OH) 1640 ($CONMe_2$) 1075 cm^{-1} (Tetrahydrofuran) ohne Lösungsmittel) umgesetzt wurden. Aus diesen Amiden erhielt man mit Hilfe von Lithium Alanat D, L-Nordesmethylmuscarine (VIII) (α, IR. 3410 (OH) 1066 cm^{-1} (Tetrahydrofuran) in Tetrachlorkohlenstoff; β, IR. 3194 (OH) 1085 cm^{-1} (Tetrahydrofuran) in Tetrachlorkohlenstoff). Die OH Valenzschwingung der β-Norbase in Tetrachlorkohlenstoff bleibt beim genügenden Verdünnen (0.0072 Mol) konstant. Es liegt also bei der β-Norbase die Wasserstoffbrücke vor. Es kommt daher den Verbindungen der β-Reihe cis- Konfiguration zu. Die quarternären Ammonium Iodide IX wurden kristallisiert erhalten (α, Schmp. 120°C β, Schmp. 117°C, Ber. C 33.47 H 6.32 Gef. C 33.70 H 6.59). Die IR. Spektren der beiden Desmethylmuscarine stimmen mit denjenigen der Eugsters Präparate[4] gut überein. Gegen Krötenherzen zeigen Desmethylmuscarine schwächere, aber charakteristische Muscarin wirkung. Von den beiden Isomeren wirkte *trans*-Desmethylmuscarin stärker[5].

Chemische Abteilung
Naturwissenschaftliche Fakultät
Universität Hokkaido
Sapporo

4) C. H. Eugster, *Helv. Chim. Acta*, **42**, 1177 (1959).

5) Herrn Prof. Dr. Akira Ooga an dem Pharmakologischen Institut der Universität Hokkaido möchten wir fur seine Prüfung bestens danken.

Formation of Isoxazolecarboxylic Acids from α, β-Unsaturated α-Nitroesters[1]

By Sumio Umezawa and Shōnosuke Zen

(Received April 15, 1960)

We wish to report the synthesis of new members of isoxazolecarboxylic acids. When treated with *n*-butylamine (2.0 g.) in ligroin at room temperature overnight, diethyl α-nitroglutaconate[2] (I) (1.0 g.) produced 3, 5-bis(*n*-butylcarbamoyl) - 4 - (*n*-butylcarbamoylmethyl)-isoxazole (III) (crude product 0.6 g.). We have found that the cyclization is generaily applicable to the synthesis of 4-substituted isoxazole-3, 5-dicarboxylic acids. Thus, 4-phenyl-3, 5-bis(*n*-butylcarbamoyl)isoxazole (VI) (crude product 0.22 g.) and 4-methyl-3, 5-bis (*n*-butylcarbamoyl)isoxazole (IX) have been obtained from ethyl α-nitrocinnamate[3] (V) (1.0 g.) and ethyl α-nitrocrotonate[4] (VIII) by refluxing with *n*-butylamine in absolute ethanol for three hours, respectively (Tables I and II).

By mild alkaline hydrolysis with 10% sodium hydroxide in 50% aqueous ethanol at about 60°C for two hours, III (1.12 g.) and VI (1.0 g.) were converted into isoxazole-3, 5-dicarboxylic-4-acetic acid (IV) (crude product 0.56 g.) and 4-phenylisoxazole-3, 5-dicarboxylic acid (VII) (crude product 0.45 g.), respectively (Table I).

Drastic alkaline hydrolysis of VI by refluxing with 28% potassium hydroxide in 50% aqueous ethanol resulted in the formation of phenylacetic acid and oxalic acid, the fact indicating that the above-mentioned cyclization forms a 4-substituted isoxazole-3, 5-dicarboxylic acid derivative.

It seems reasonable to suggest that the initial step involves base-catalyzed cleavage of α, β-unsaturated α-nitroester to liberate nitroacetic ester moiety which may be in equilibrium

1) Presented in part at the Division of Organic Chemistry of the Annual Meeting of the Chemical Society of Japan, Kyoto, April 2, 1959.

2) Prepared by the condensation of sodium salt of ethyl formylacetate with ethyl nitroacetate in the presence of diethylamine or *n*-butylamine; b. p. 125–130°C/0.2 mmHg.

3) Prepared by the method of A. Dornow and H. Menzel, [*Ann.*, **580**, 43 (1952)]. They obtained carbethoxydiethylcarbamoyl-4-phenylisoxazoline *N*-oxide by refluxing an ethanol solution of diethylamine and diethylamine salt of ethyl 1,3-dinitro-2,3-diphenylbutyrate which was prepared from ethyl α-nitrocinnamate and phenylnitromethane. This result is closely related to the method reported in the present paper, whereby, however, isoxazole derivatives are obtained.

4) Prepared from ethyl α-nitro-β-acetoxybutyrate by heating with anhydrous sodium carbonate in dry benzene by a variation of the method of H. B. Hass, A. G. Susie and R. L. Heider, (*J. Org. Chem.*, **15**, 8 (1950)).

TABLE I. 4-SUBSTITUTED 3,5-BIS(*n*-BUTYLCARBAMOYL)ISOXAZOLES AND ISOXAZOLE-3,5-DICARBOXYLIC ACIDS

Compounds	M.p. °C	Formula	Analyses						Neutralization equivalent	
			Calcd.			Found				
			C, %	H, %	N, %	C, %	H, %	N, %	Calcd.	Found
III	179~179.5[a]	$C_{19}H_{32}O_4N_4$	59.97	8.48	14.73	60.41	8.22	15.15	—	—
VI	160~162[a]	$C_{19}H_{25}O_3N_3$	66.45	7.34	12.24	66.86	6.90	12.55	—	—
IX	84~ 86[b]	$C_{14}H_{23}O_3N_3$	59.76	8.24	14.94	60.32	7.95	15.18	—	—
IV	108~110 (hydrate)[c]	$C_7H_5O_7N$	39.08	2.34	6.51	39.02	2.42	6.57	71.7	72.3
VII	183~183.5[d] (decomp.)	$C_{11}H_7O_5N$	56.66	3.03	6.01	56.87	2.97	6.08	116.6	115.7

a) Recrystallized from ethanol.
b) Recrystallized from ligroin.
c) Recrystallized from dioxane-chloroform; the anhydrous sample melted at 177~178°C (decomp.).
d) Recrystallized from a mixture of dioxane and ethylenedichloride-ligroin.

TABLE II. ABSORPTION SPECTRA OF 4-SUBSTITUTED 3,5-BIS(*n*-BUTYLCARBAMOYL)ISOXAZOLES

Compounds	U.V. absorption λ_{max}, mμ (ε)	Infrared absorption γ_{max}^{Nujol}, cm^{-1}		
III	245 (10500)[a]	3299 (NH),	1682 (CO),	1537 (secondary, non-cyclic amide)
VI	—[b]	3338,	1678,	1535
IX	246 (10100)[c]	3290,	1664,	1555

a) Methanol solution.
b) No characteristic maximum in the range of 220~340 mμ.
c) Ethanol solution.

with the original unsaturated nitroester, followed by the addition of the former to the latter to give a key intermediate II, which may cyclize by elimination of water and nitrous acid to form isoxazole derivatives, as outlined in the following scheme:

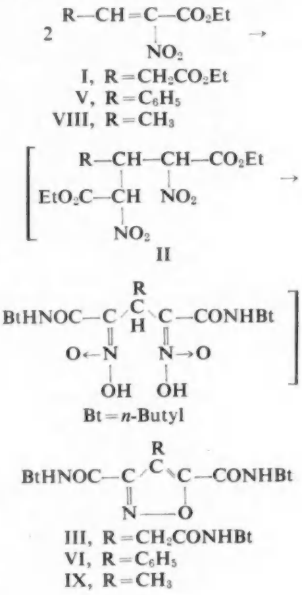

The validity of the above mechanism has been supported by the experimental observation that, if ethyl nitroacetate is added to the above-mentioned reaction system as an external source of nitroacetate moiety, the yield of isoxazole derivative is significantly increased. As a typical result: When a mixture of ethyl α-nitrocinnamate (5.0 g.) and ethyl nitroacetate (3.0 g.) was caused to react with *n*-butylamine (10 g.) under similar conditions, VI (crude product 4.7 g.) was obtained in a 60% yield.

Further studies on the related reactions are in progress.

The authors are grateful to Mr. S. Nakada and Miss S. Taguchi for helping their experiments.

Department of Applied Chemistry
Faculty of Engineering
Keio University, Tokyo

Electrolytic Reduction of Benzaldehyde at a Mercury Cathode—Preparation of Dibenzyl Mercury

By Toshio Arai and Tsuneto Oguri

(Received February 12, 1960)

Many studies have already been carried out on the electrolytic reduction of aldehydes, with the result that usually their reduction tends to form resinous materials. There is no doubt that the formation depends upon electrolytic conditions employed. In the case of lead or mercury cathode which has a high hydrogen overvoltage, resinous materials are easily formed.

It has been reported that the electrolytic reduction of ketones in sulfuric acid solution at a mercury cathode produces organomercury compounds[1-3]. The present investigation was undertaken to prepare organomercury compounds from aldehydes which have the carbonyl radical as ketones. Consequently, a way was found to produce dibenzyl-mercury from benzaldehyde. However, other aldehydes such as vanillin, piperonal, anisaldehyde, furfural and salicyl aldehyde were not reduced to their mercury compounds under the same conditions, and resinous materials were easily formed.

The experiment was carried out according to the procedures described previously[3]. Benzaldehyde was shaken with 5% sodium carbonate solution several times, dried and distilled prior to use. The electrolysis was carried out under following conditions: cathode, mercury 15.2 cm^2; cathodic solution, 50% sulfuric acid in which 15 g. of benzaldehyde was suspended; electric current, 3 A. (current density 19.7 A./dm^2); time of electrolysis, 7.5 hr. A 50% sulfuric acid served as anodic solution and cylindrical lead was employed as anode. The anolyte was separated from the catholyte by a porous pot.

As the electrolysis proceeded, a pale yellow material floated on the surface. After the electrolysis, the product was collected on a funnel and sucked as much as possible to give solid residue. It was recrystallized from ethanol several times to give needle crystals, m. p. 110°C (the reported value, 111°C)[4], yield being about 2.4 g., 8.5% of theoretical amount.

Found: Hg, 52.56. Calcd. for $C_{14}H_{14}Hg$: Hg, 52.40%.

When the compound in the product was heated with ethanol solution of mercuric chloride, mercuric bromide and mercuric acetate, benzylmercuric chloride (m. p. 103°C. plates from ethanol-xylene), benzylmercuric bromide (m. p. 118°C, plates from ethanol) and benzylmercuric acetate (m. p. 126°C, needles from ethanol) were obtained respectively.

Found for benzylmercuric chloride: Hg, 61.69. Calcd. for C_7H_7HgCl: Hg, 61.31%.

In this reduction under the conditions described above, hydrobenzoin was also obtained, but it was separated completely by recrystallizing several times with ethanol.

The temperature of reduction was found to have influence on the yield of dibenzyl mercury. Temperatures below 25°C gave the favorable dibenzyl mercury yields, but at 50°C only oily material and hydrobenzoin were obtained.

In an attempt to compare the influence of concentration of sulfuric acid on the yield of dibenzyl mercury, experiments were made at several concentrations. It was found that 50% sulfuric acid was the most efficient catholyte and a lower acidity resulted in the decrease of the yield.

It was also found that the current density had no effect between 20 and 40 A./dm^2.

The authors express their sincere thanks to Professor Buhei Sakurai for his kind guidance and encouragement throughout the present experiment.

Department of Chemistry
Faculty of Liberal Arts and Science
Shinshu University
Matsumoto

1) J. Tafel, *Ber.*, **39**, 3626 (1906).
2) C. J. Haggerty, *Trans. Am. Electrochem. Soc.*, **56**, 421 (1929).
3) T. Arai, This Bulletin, **32**, 184 (1959).
4) P. Wolff, *Ber.*, **46**, 64 (1913).

Genesis of Sulfate in Acid Hot Spring

By Iwaji Iwasaki and Takejiro Ozawa

(Received March 18, 1960)

Acid hot springs contain generally large amounts of sulfate ion, and it has been usually considered that most of them are formed by the oxidation of hydrogen sulfide or other sulfides with oxygen from the air at or near the ground surface[1].

However, this explanation is not always acceptable, when their high discharges and the chemical composition of gases accompanied with the acid hot springs are taken into consideration.

Fumarolic gases from active volcanoes contain usually hydrogen sulfide, sulfur dioxide,

1) E. T. Allen and A. L. Day, "Hot Springs of the Yellowstone National Park" Carnegie Inst. Washington Pub. (1935); D. E. White, *Bull. Geol. Soc. Am.*, **68**, 1637 (1957) etc.

TABLE I

Silicate rock	Condition	H_2SO_3(mM) Residual	H_2SO_4(mM) Found	S(mM) Found	H_2SO_4/S
None	A	6.51	2.36	1.10	2.1
	B	3.43	3.79	1.80	2.1
Basalt	A	0.69	5.96	2.38	2.5
	B	0.36	5.68	2.69	2.1
Andesite	A	0.26	5.89	2.75	2.1
	B	0.14	5.25	2.95	2.1
Granite	A	1.03	5.60	2.70	2.1
	B	2.68	3.89	1.72	2.3

hydrogen chloride and carbon dioxide in the same order of amounts, and nitrogen in a smaller amount, but scarcely any oxygen and sulfur trioxide.

On the other hand, gases from region of the acid hot springs consist of carbon dioxide and hydrogen sulfide as the major components, and of nitrogen as the minor components, and of sulfur dioxide, hydrogen chloride and oxygen as the trace components. Therefore, the most important chemical species for the formation of sulfate would not be hydrogen sulfide, but sulfur dioxide.

When volcanic gases are condensed by cooling under the ground, hydrogen chloride and sulfur dioxide would dissolve into the condensed water to form hydrochloric and sulfurous acids. Then sulfuric acid may be formed from this sulfurous acid, liberating sulfur by the following self oxidation-reduction reaction.

$$3H_2SO_3 = 2H_2SO_4 + S + H_2O \qquad (1)$$

In order to confirm this new hypothesis, some experiments were carried out as follows. Two grams of the powdered silicate rock were taken into an ampoule (50 ml.) and 20 ml. of 0.5 M sulfurous acid solution (condition A) or 20 ml. of the mixed solution consisting of 0.5 M sulfurous acid and 0.5 M hydrochloric acid (condition B) were added. Then each ampoule was sealed in the atmosphere of carbon dioxide and kept at 105°C. After about three days, some droplets of sulfur were observed on the surface of the solution into which andesite or granite was added. After a week, all ampoules were cooled to room temperature and the amount of each reaction product was determined (Table I).

It is clear that, as shown in Table I, the self oxidation-reduction reaction of sulfurous acid is mainly based on Eq. 1 under these conditions and this reaction proceeds easily in the presence of hydrochloric acid or silicate rock. Under natural circumstances where higher pressure and temperature are expected, this reaction would proceed more easily and the sulfur formed may contribute to the formation of some ores such as pyrite and native sulfur impregnated with wall rocks.

It is concluded that the principal source of sulfate in the acid hot spring may be sulfur dioxide from volcanic gas and the formation of sulfate may be based on the self oxidation-reduction of sulfurous acid.

Laboratory of Analytical Chemistry and Geochemistry
Tokyo Institute of Technology
Ookayama, Meguro-ku, Tokyo

A Research on Isotopic Composition of Evolved Hydrogen Molecules with Special Reference to the Mechanism of Nickel Cathode

By Kozo HIROTA and Takeo HISANO*

(Received May 2, 1960)

Although a number of research has been published on the separation factor of hydrogen evolved at the electrolysis of aqueous solutions, no attention has been paid on the composition of isotopically different molecules, i.e., H_2 HD and D_2. However, by the following reasoning, it seems very important to investigate if the composition coincides with the one expected by the gaseous equilibrium:

$$H_2 + D_2 \rightleftarrows 2HD \qquad (1)$$

In the case of the discharge mechanism (A), evolved hydrogen must be equilibrated by the practical equilibrium of the recombination step of statistically independent hydrogen atoms formed by the rate-determining step $H^+ + e \rightarrow H$ of this mechanism. On the other hand, in the case of the catalytic (B) or the electrochemical (C) mechanism the evolved hydrogen need not be equilibrated, inasmuch

* Research fellow from the Engineering Faculty, Tokushima University (1959-1960).

TABLE I. SEPARATION FACTOR AND ISOTOPIC COMPOSITION EVOLVED AT THE NICKEL ELECTRODE AT 0°C

Exp. no.	Current density mA/cm²	D atom%	Separation factor α	$K(\text{obs}) = \frac{[HD]^2}{[H_2][D_2]}$
41	25.3	30.3	4.3	2.8
42	50.6	25.1	5.6	2.7
43	84.3	21.6	6.6	2.7
44	147.3	20.5	7.3	2.7
45	190	21.4	7.4	2.8

* a) All the data of the columns 3,4 and 5 are the means of two measurements except for No. 41.

b) D atom% of the original solution: 65.2%.

as the rate is governed in either case by the step of formation of the hydrogen molecule itself, which is not of course in equilibrium.

It is interesting therefore to demonstrate the above consideration experimentally on some cathode. As the first example, nickel electrode has been taken up, because the mechanism of this electrode is not yet determined in spite of the effort of many researchers. The electrolysis was carried out on 1 N sodium carbonate solution with the cathode of nickel plate (surface area, 0.48 cm²) and the anode of platinum wire. Deuterium content in the original solution was 65.2% (atom%). The ratio H_2: HD: D_2 of the hydrogen evolved at the cathode as well as the separation factor α, defined by $(H/D)_{gas}/(H/D)_{sol}$, were determined mass-spectrometrically.

The result obtained at 0°C is summarized in Table I. It is shown that α increases with current density and approaches to the value of 7.4 which is nearly equal to that hitherto obtained by the electrolysis of aqueous solution of low deuterium concentration in the case of nickel cathode[1]. It is noteworthy on the other hand that the factor $K(\text{obs.}) = [HD]^2/[H_2][D_2]$ is 2.7 or 2.8 which is less than the K (equil.), i.e., 3.25 at 0°C[2].

Such being the situation, the discharge mechanism (A) can not be accepted so far as nickel cathode is concerned. Although the mechanism (B) or (C) is reasonable, some other experimental fact must be resorted to for the discussion between the mechanisms. From the reason that no positive proof for the mechanism (C) has been found until now, the catalytic mechanism (B)[1,3] may be accepted.

Detailed research on other electrodes is now in progress.

We express sincere thanks to Professor J. Horiuti, Hokkaido University, for his kind advice and discussions on this research.

Department of Chemistry
Faculty of Science
Osaka University
Nakanoshima, Osaka
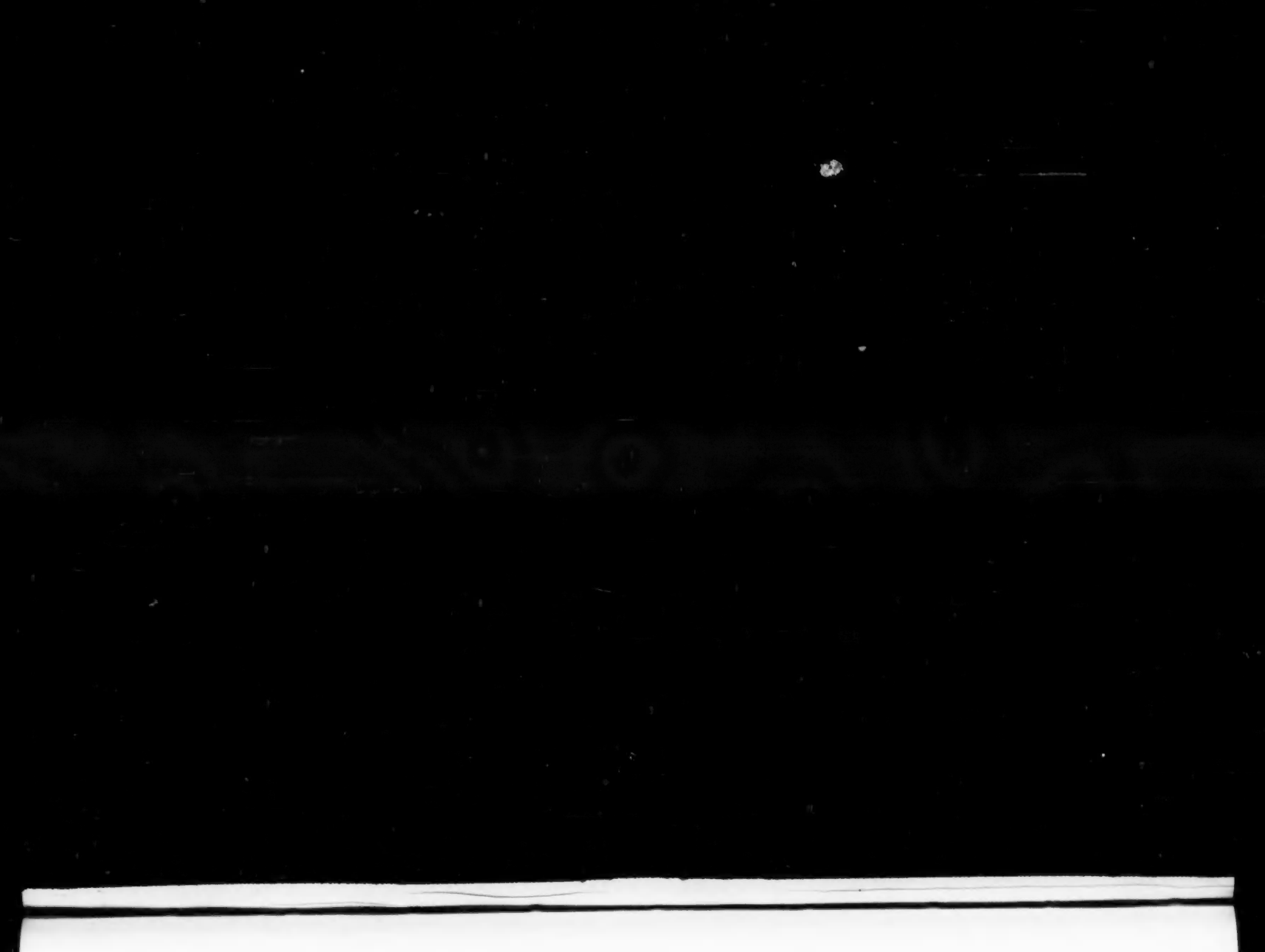
1) G. Okamoto and J. Horiuti, *Sci. Pap. Inst. Phys. Chem. Res.* (Tokyo), **28**, 231 (1936).
2) H. Urey, *J. Chem. Soc.*, **1947**, 562.
3) J. Horiuti, G. Okamoto and K. Hirota, *Sci. Pap. Inst. Phys. Chem. Res.* (Tokyo), **29**, 223 (1936).